INVESTIGATION OF THE ADSORPTION OF DITHIOPHOSPHATE AND DITHIOPHOSPHINATE ON CHALCOPYRITE AS A FUNCTION OF PULP POTENTIAL AND pH

A THESIS SUBMITTED TO
THE GRADUATE SCHOOL OF NATURAL AND APPLIED SCIENCES
OF
THE MIDDLE EAST TECHNICAL UNIVERSITY

BY

TAKİ GÜLER

IN PARTIAL FULFILMENT OF THE REQUIREMENTS FOR THE DGREE OF
DOCTOR OF PHILOSOPHY
IN
THE DEPARTMENT OF MINING ENGINEERING

JUNE 2002

Approval of the Graduate School of Natural and Applied Sciences

Prof.Dr. Tayfur ÖZTÜRK
Director

I certify that this thesis satisfies all the requirements as a thesis for the degree of Doctor of Philosophy.

Prof.Dr. Tevfik GÜYAGÜLER
Head of Department

This is to certify that we have read this thesis and that in our opinion it is fully adequate, in scope and quality, as a thesis for the degree of Doctor of Philosophy.

Assoc.Prof.Dr. Gülsün GÖKAĞAÇ
Co-Supervisor

Prof.Dr. Cahit HİÇYILMAZ
Supervisor

Examining Committee Members

Prof.Dr. Cahit HİÇYILMAZ

Assoc.Prof.Dr. Ali İhsan AROL

Assoc.Prof.Dr. Zafir EKMEKÇİ

Assoc.Prof.Dr. Gülsün GÖKAĞAÇ

Assoc.Prof.Dr. Özcan Yıldırım GÜLSOY

ABSTRACT

INVESTIGATION OF THE ADSORPTION OF DITHIOPHOSPHATE AND DITHIOPHOSPHINATE ON CHALCOPYRITE AS A FUNCTION OF PULP POTENTIAL AND pH

Güler, Taki

Ph.D., Department of Mining Engineering

Supervisor: Prof.Dr. Cahit Hiçyılmaz

Co-Supervisor: Assoc.Prof.Dr. Gülsün Gökağaç

June 2002, 204 pages

Pulp potential and pH play important roles on flotation of sulphide ores. These parameters define the redox products formed on sulphide mineral surface. Therefore, it is essential to investigate electrochemical behaviour of sulphide minerals under different conditions.

In this research, electrochemical behaviour of chalcopyrite from Artvin-Murgul deposit were investigated in the presence and absence of dithiophosphate (DTP) and dithiophosphinate (DTPI) by cyclic voltammetry and Diffuse Reflectance Infrared Fourier Transform (DRIFT) spectroscopy. Microflotation tests were performed by using a modified Hallimond tube to determine the effect of pulp potential (Eh), pH and collectors.

Cyclic voltammetry studies showed that iron preferentially dissolves from chalcopyrite surface and would cause iron-deficient, S^{o}-rich surface in acid

solution, and iron-hydroxide precipitation on chalcopyrite in neutral and alkaline solutions. DTP and DTPI caused surface passivation and did not form any redox peak on voltammograms.

Compounds, which adsorbed on the surface of chalcopyrite electrode, were identified by DRIFT spectroscopy: Adsorbed dithiophosphate (DTP^o) would be the major surface compound of chalcopyrite at reducing and mildly oxidising potentials, whereas at oxidising potentials, CuDTP+$(DTP)_2$ may be in acid solutions in DTP induced condition. However, hydrophobic DTP species could not be defined in neutral and alkaline pH. On the other hand, in DTPI induced condition, CuDTPI formed in acid and neutral solutions. In alkaline conditions, CuDTPI formation at reducing potentials and $Cu(DTPI)_2$ and/or $(DTPI)_2$ formation on mineral surface at oxidising potentials would be possible.

Microflotation tests demonstrated that maximum recovery could be obtained in acid solutions possibly due to iron-deficient surface. It decreased with increasing pH because of hydrophilic surface hydroxides. Recovery increased up to mildly oxidising potentials (100-300 mV) and then decreased. Recovery was low in reducing (<0 mV) and highly oxidising potentials (>300 mV) possibly due to unoxidised surface and surface coverage by hydrophilic oxy/hydroxy species, respectively. Although DTP and DTPI improved flotation recovery, their effect decreased at higher pH values. DTPI displayed higher recoveries than DTP.

Keywords: Chalcopyrite, Electrochemistry of Chalcopyrite Flotation, Pulp Potential, Cyclic Voltammetry, Microflotation, DRIFT Spectroscopy, Dithiophosphate, Dithiophosphinate.

ÖZ

KALKOPİRİT ÜZERİNE DİTHİOFOSFAT VE DİTHİOFOSFİNİN ADSORPSİYONUNUN PÜLP POTANSİYELİ VE pH DEĞERİNİN BİR FONKSİYONU OLARAK İNCELENMESİ

Güler, Taki
Doktora, Maden Mühendisliği Bölümü
Tez Yöneticisi: Prof.Dr. Cahit Hiçyılmaz
Ortak Tez Yöneticisi: Doç.Dr. Gülsün Gökağaç

Haziran 2002, 204 sayfa

Pülp potansiyeli ve pH, sülfür cevherlerinin flotasyonunda önemli rol oynar. Bunlar sülfürlü mineral yüzeyinde oluşan redoks ürünlerini belirler. Bu nedenle farklı koşullarda sülfürlü minerallerin elektrokimyasal davranımının incelenmesi gerekmektedir.

Bu araştırmada Artvin-Murgul cevher yatağı kalkopiritinin elektrokimyasal davranımı dithiofosfat (DTP) ve dithiofosfinin (DTPI) var ya da yok olduğu ortamlarda dönüşümlü voltmetre ve Diffuse Reflectance Infrared Fourier Transform (DRIFT) spectroskopi ile araştırıldı. Pülp potansiyeli (Eh), pH ve kollektörlerin etkisini belirlemek için modifiye edilmiş Hallimond tüp ile mikroflotasyon deneyleri yapılmıştır.

Dönüşümlü voltmetre çalışmaları, asitli çözeltilerde kalkopirit yüzeyinden demirin öncelikli olarak çözündüğünü ve demirce eksik, kükürtçe zengin yüzey oluşturduğunu, nötür ve alkali çözeltide ise kalkopirit yüzeyinde demir hidroksit çökelmesine neden olduğunu göstermiştir. DTP ve DTPI yüzey pasifizasyonuna neden olmuş ve voltamogramlarda herhangi bir sinyal oluşturmamışlardır.

Kalkopirit elektrodu yüzeyinde adsorplanan bileşikler DRIFT spektroskopi ile belirlenmiştir: Asit çözeltide kalkopirit DTP ile şartlandırıldığında indirgen ve orta yükseltgen potansiyellerde, adsorbe olmuş dithiofosfat temel yüzey bileşiği iken, yükseltgen potansiyellerde ise muhtemelen CuDTP+$(DTP)_2$'dir. Bununla birlikte, nötür ve alkali pH degerlerinde kalkopirit yüzeyinde oluşan hidrofobik DTP bileşikleri tanımlanamamıştır. Kalkopirit DTPI ile şartlandırıldığında asitli ve alkali ortamlarda CuDTPI oluştuğu gözlenmiştir. Alkali ortamda, indirgen potansiyelde CuDTPI oluşumu, yükseltken potansiyelde ise $Cu(DTPI)_2$ ve/veya $(DTPI)_2$ oluşumu tahmin edilmiştir.

Mikroflotasyon deneyleri, asit çözeltide, muhtemelen demirce eksik yüzeyden dolayı en yüksek verimin elde edildiğini göstermiştir. Hidrofilik yüzey hidroksitlerinden dolayı verim pH'nın artırılması ile azalmıştır. Verim orta yükseltgen potansiyele (100-300 mV) kadar artmış ve daha yüksek potansiyellerde (>300 mV) düşmüştür. Verim, indirgen potansiyellerde (<0 mV) muhtemelen oksitlenmemiş yüzeyden dolayı ve yükseltgen potansiyellerde (>300 mV) ise muhtemelen hidrofilik bileşenlerin yüzeyi kaplamasından dolayı düşük çıkmıştır. DTP ve DTPI'nin verimi artırmalarına rağmen, etkileri yüksek pH değerlerinde düşmüştür. DTPI, DTP'a oranla daha iyi sonuç vermiştir.

Anahtar Kelimeler: Kalkopirit, Kalkopirit Flotasyonunun Elektrokimyası, Pülp Potansiyeli, Dönüşümlü Voltmetre, Mikroflotasyon, DRIFT Spectroskopi, Dithiofosfat, Dithiofosfin.

To my wife and my son

ACKNOWLEDGEMENTS

I would like to express my sincere appreciation and greatest thanks to my supervisor Prof.Dr. Cahit HİÇYILMAZ and co-supervisor Assoc.Prof.Dr. Gülsün GÖKAĞAÇ for their endless support, patience, concern and friendship throughout this tidy study. Their encouragement, guidance and suggestions during the very critical stage of my work made this study possible. Assoc.Prof.Dr. Zafir EKMEKÇİ (Hacettepe University) is gratefully acknowledged whose comments and assistance was very important for my study. Thanks to Assoc.Prof.Dr. Gürkan KARAKAŞ (Chemical Engineering Department) and Assoc.Prof.Dr. Özdemir DOĞAN (Department of Chemistry) who helped me in DRIFT and NMR spectroscopy studies, respectively. Turkish Scientific and Technical Research Association (TÜBİTAK) (Project No. YDABÇAY 198Y 024) and Research Foundation of Middle East Technical University (Project No. 98-03-05-03) are also gratefully acknowledged for their financial support.

Dr. Ali H. ERCAN (England), my sister Sevgi AYYILDIZ and her husband Muharrem AYYILDIZ (Germany) were generous in supplying some of the very important literature sources from abroad. I wish to express my gratitude to technical staff of Mining Engineering Department and Metin YANIK (Department of Chemistry) for their technical support in various stages of my thesis. I would like to forward my special thanks to my friend research assistant N. Emre ALTUN for his support and encouragement during my hard days.

Finally, I wish to express my dearest thanks to my wife, Güngör, for her very valuable patience, help, support, and especially for her endless tolerance throughout this long and tiring study which made me feel that I was never alone.

TABLE OF CONTENTS

Page

ABSTRACT iii

ÖZ v

DEDICATION vii

ACKNOWLEDGEMENTS viii

TABLE OF CONTENTS ix

LIST OF TABLES xiv

LIST OF FIGURES xv

CHAPTER

1. INTRODUCTION 1

2. LITERATURE REVIEW 5

2.1 Surface Properties of Sulphides 5

2.2 Electrochemistry of Sulphides 7

2.2.1 Electrochemical Potential 7

2.2.2 Pulp Potential Measurement 9

2.2.3 Pulp Potential Control 12

2.2.4 Voltammetry 12

2.3 Electrochemistry of Sulphide Flotation 16

2.3.1 Collectorless Flotation 16

2.3.2 Collector Induced Flotation 19

2.3.2.1 Dithiophosphate 24

2.3.2.2 Dithiophosphinate 28

2.4 Eh-pH Diagrams and Application to Sulphide Flotation 30

2.5 Surface Spectroscopy 32

2.5.1 Infrared spectroscopy 33

3. MATERIALS AND METHODS 37

3.1 Material Preparation and Analysis 37
3.2 Equipment and Procedure 41
3.2.1 Voltammetry Experiments 41
3.2.2 DRIFT Study 43
3.2.3 Microflotation 44
4. RESULTS 47
4.1 Cyclic Voltammetry 47
4.1.1 pH 4.67 47
4.1.1.1 Cyclic Voltammograms of Chalcopyrite in Collectorless Condition in pH 4.67 47
4.1.1.2 Cyclic Voltammograms of Chalcopyrite in the Presence of DTP in pH 4.67 53
4.1.1.3 Cyclic Voltammograms of Chalcopyrite in the Presence of DTPI in pH 4.67 55
4.1.2 pH 6.97 58
4.1.2.1 Cyclic Voltammograms of Chalcopyrite in Collectorless Condition in pH 6.97 58
4.1.2.2 Cyclic Voltammograms of Chalcopyrite in the Presence of DTP in pH 6.97 64
4.1.2.3 Cyclic Voltammograms of Chalcopyrite in the Presence of DTPI in pH 6.97 66
4.1.3 pH 9.2 69
4.1.3.1 Cyclic Voltammograms of Chalcopyrite in Collectorless Condition in pH 9.2 69
4.1.3.2 Cyclic Voltammograms of Chalcopyrite in the Presence of DTP in pH 9.2 74
4.1.2.3 Cyclic Voltammograms of Chalcopyrite in the Presence of DTPI in pH 9.2 76
4.1.4 pH 11 79
4.1.4.1 Cyclic Voltammograms of Chalcopyrite in Collectorless Condition in pH 11 79

4.1.4.2 Cyclic Voltammograms of Chalcopyrite in the Presence of DTP in pH 11 84
4.1.4.3 Cyclic Voltammograms of Chalcopyrite in the Presence of DTPI in pH 11 87
4.2 DRIFT Study 89
4.2.1 DRIFT Study with DTP 90
4.2.2 DRIFT Study with DTPI 101
4.3 Flotation 112
4.3.1 Flotation Studies in Collectorless Condition 113
4.3.2 Flotation Studies with DTP 116
4.3.3 Flotation Studies with DTPI 119
4.3.4 Effect of Eh an pH on Flotation 123
5. DISCUSSIONS 126
5.1 Cyclic Voltammetry 126
5.1.1 pH 4.67 127
5.1.1.1 Cyclic Voltammetry Study in Collectorless Condition in pH 4.67 127
5.1.1.2 Cyclic Voltammetry Study in the Presence of DTP in pH 4.67 132
5.1.1.3 Cyclic Voltammetry Study in the Presence of DTPI in pH 4.67 133
5.1.2 pH 6.97 135
5.1.2.1 Cyclic Voltammetry Study in Collectorless Condition in pH 6.97 135
5.1.2.2 Cyclic Voltammetry Study in the Presence of DTP in pH 6.97 138
5.1.2.3 Cyclic Voltammetry Study in the Presence of DTPI in pH 6.97 139
5.1.3 pH 9.2 140
5.1.3.1 Cyclic Voltammetry Study in Collectorless Condition in pH 9.2 140

5.1.3.2 Cyclic Voltammetry Study in the Presence of DTP in pH 9.2 141
5.1.3.3 Cyclic Voltammetry Study in the Presence of DTPI in pH 9.2 142
5.1.4 pH 11 143
5.1.4.1 Cyclic Voltammetry Study in Collectorless Condition in pH 11 143
5.1.4.2 Cyclic Voltammetry Study in the Presence of DTP in pH 11 144
5.1.4.3 DTPI Induced Condition 144
5.2 DRIFT Study 145
5.2.1 DRIFT Spectroscopy Study in the Presence of DTP . . . 146
5.2.1.1 DRIFT Spectroscopy Study in the Presence of DTP in pH 4.67 148
5.2.1.2 DRIFT Spectroscopy Study in the Presence of DTP in pH 6.97 150
5.2.1.3 DRIFT Spectroscopy Study in the Presence of DTP in pH 9.2 151
5.2.1.4 DRIFT Spectroscopy Study in the Presence of DTP in pH 11 151
5.2.1.5 Effect of Eh and pH on Chalcopyrite in the Presence of DTP 153
5.2.2 DRIFT Spectroscopy Study in the Presence of DTPI . . 153
5.2.2.1 DRIFT Spectroscopy Study in the Presence of DTPI in pH 4.67 156
5.2.2.2 DRIFT Spectroscopy Study in the Presence of DTPI in pH 6.97 157
5.2.2.3 DRIFT Spectroscopy Study in the Presence of DTPI in pH 9.2 158
5.2.2.4 DRIFT Spectroscopy Study in the Presence of DTPI in pH 11 160

5.2.2.5 Effect of Eh and pH on Chalcopyrite in the Presence of DTPI 161
5.3 Flotation Study 162
5.3.1 Collectorless Flotation 162
5.3.2 DTP Induced Flotation 164
5.3.3 DTPI Induced Flotation 166
5.3.4 Effect of Eh and pH on Flotation 168
6. CONCLUSIONS AND RECOMMENDATIONS 170
6.1 Conclusions 170
6.2 Recommendations 173
REREFENCES 174
APPENDICES
A. SCANNING ELECTRON MICROSCOPY RESULT 199
B. NUCLEAR MAGNETIC RESONANCE SPECTROSCOPY RESULTS 200
VITA 204

LIST OF TABLES

TABLE		Page
2.1	Typical properties of AEROPHINE 3418A promoter (Rickelton, 1998)	28
3.1	Chemical analysis of –212+150 μm chalcopyrite sample	37
3.2	Chemical analysis of massive specimens of chalcopyrite	38
3.3	The composition of the buffer solutions	38
3.4	Analysis of nitrogen gas (BOS Co.)	39

LIST OF FIGURES

FIGURES Page

2.1 Gradation between ionic and covalent bonding (Tolun, 1987) . . 6

2.2 Current-potential curve for a galena electrode in pH 9.3 buffer solution containing $9.5x10^{-3}$ M ethyl xanthate (Woods, 1971) . . 14

2.3 Schematic representation of the interaction of a chelating agent (X) with copper ions from the mineral surface by chemisorption, surface reaction, or by bulk precipitation (bulk precipitation may occur in the region during adjacent to the mineral surface). In the case of chemisorption and surface reaction, the charge on the various species is not shown 23

2.4 Reversible potentials for the $Fe^{+2}/Fe(OH)_2/Fe(OH)_3$ (----), $S/H_2S/HS^{-1}$ (———) and $CuFeS_2/CuS$, $Fe(OH)_3$, S (—•—) systems as a function of pH (Gardner and Woods, 1979) 31

3.1 Three-electrode system for electrochemical investigations 41

3.2 Counter and working electrodes used in electrochemical and flotation experiments: (a) Platinum (counter) electrode; (b) Chalcopyrite (working) electrode 42

3.3 Polarisation cell for DRIFT study 43

3.4 Modified Hallimond tube 45

3.5 Experimental setup for microflotation tests 46

4.1 Cyclic voltammogram of chalcopyrite (pH 4.67, v = 50 mV/s) . . 48

4.2 Controlled sweep voltammogram of chalcopyrite (pH 4.67, v = 50 mV/s) 49

4.3 Cyclic voltammogram of chalcopyrite (pH 4.67, v = 20 mV/s) . . 50

4.4 Cyclic voltammogram of chalcopyrite (pH 4.67, v = 10 mV/s) . . 50

4.5 Cyclic voltammogram of chalcopyrite for different scan rates at pH 4.67 51
4.6 Relationship between formation potentials of peaks and scan rate 52
4.7 Relationship between current density of peaks and square-root of scan rate 52
4.8 Cyclic voltammogram of chalcopyrite (pH 4.67, DTP = 10^{-4} M, v = 50 mV/s) 53
4.9 Cyclic voltammogram of chalcopyrite (pH 4.67, DTP = 10^{-3} M, v = 50 mV/s) 54
4.10 Cyclic voltammogram of chalcopyrite (pH 4.67, DTP = 10^{-2} M, v = 50 mV/s) 54
4.11 Cyclic voltammograms of chalcopyrite for 0 M, 10^{-4} M, 10^{-3} M and 10^{-2} M DTP (pH 4.67, v: 50 mV/s) 55
4.12 Cyclic voltammogram of chalcopyrite (pH 4.67, DTPI = 10^{-4} M, v = 50 mV/s) 56
4.13 Cyclic voltammogram of chalcopyrite (pH 4.67, DTPI = 10^{-3} M, v = 50 mV/s) 56
4.14 Cyclic voltammogram of chalcopyrite (pH 4.67, DTPI = 10^{-2} M, v = 50 mV/s) 57
4.15 Cyclic voltammograms of chalcopyrite for 0 M, 10^{-4} M, 10^{-3} M and 10^{-2} M DTPI (pH 4.67, v: 50 mV/s) 57
4.16 Cyclic voltammogram of chalcopyrite (pH 6.97, v = 50 mV/s) . . 58
4.17 Controlled sweep voltammogram of chalcopyrite (pH 6.97, v = 50 mV/s) 59
4.18 Cyclic voltammogram of chalcopyrite (pH 6.97, v = 20 mV/s) . . 61
4.19 Cyclic voltammogram of chalcopyrite (pH 6.97, v = 10 mV/s) . . 61
4.20 Cyclic voltammogram of chalcopyrite for different scan rates at pH 6.97 62
4.21 Relationship between formation potential of peaks and scan rate . 63
4.22 Relationship between current density of peaks and square-root of scan rate 63

4.23 Cyclic voltammogram of chalcopyrite (pH 6.97, DTP = 10^{-4} M, v = 50 mV/s) 64
4.24 Cyclic voltammogram of chalcopyrite (pH 6.97, DTP = 10^{-3} M, v= 50 mV/s) 65
4.25 Cyclic voltammogram of chalcopyrite (pH 6.97, DTP = 10^{-2} M, v = 50 mV/s) 65
4.26 Cyclic voltammograms of chalcopyrite for 0 M, 10^{-4} M, 10^{-3} M and 10^{-2} M DTP (pH 6.97, v: 50 mV/s) 66
4.27 Cyclic voltammogram of chalcopyrite (pH 6.97, DTPI = 10^{-4} M, v = 50 mV/s) 67
4.28 Cyclic voltammogram of chalcopyrite (pH 6.97, DTPI = 10^{-3} M, v = 50 mV/s) 67
4.29 Cyclic voltammogram of chalcopyrite (pH 6.97, DTPI = 10^{-2} M, v = 50 mV/s) 68
4.30 Cyclic voltammograms of chalcopyrite for 0 M, 10^{-4} M, 10^{-3} M and 10^{-2} M DTPI (pH 6.97, v: 50 mV/s) 68
4.31 Cyclic voltammogram of chalcopyrite (pH 9.2, v = 50 mV/s) . . 70
4.32 Controlled sweep voltammogram of chalcopyrite (pH 9.2, v = 50 mV/s) 70
4.33 Cyclic voltammogram of chalcopyrite (pH 9,2, v = 20 mV/s) . . 71
4.34 Cyclic voltammogram of chalcopyrite (pH 9,2, v = 10 mV/s) . . 72
4.35 Cyclic voltammograms of chalcopyrite for different scan rates at pH 9.2 72
4.36 Relationship between formation potentials of peaks and scan rate 73
4.37 Relationship between current density of peaks and square-root of scan rate 73
4.38 Cyclic voltammogram of chalcopyrite (pH 9.2, DTP = 10^{-4} M, v = 50 mV/s) 74
4.39 Cyclic voltammogram of chalcopyrite (pH 9.2, DTP = 10^{-3} M, v = 50 mV/s) 75
4.40 Cyclic voltammogram of chalcopyrite (pH 9.2, DTP = 10^{-2} M, v = 50 mV/s) 75

4.41 Cyclic voltammograms of chalcopyrite for 0 M, 10^{-4} M, 10^{-3} M and 10^{-2} M DTP (pH 9.2, v: 50 mV/s) 76
4.42 Cyclic voltammogram of chalcopyrite (pH 9.2, DTPI = 10^{-4} M, v = 50 mV/s) 77
4.43 Cyclic voltammogram of chalcopyrite (pH 9.2, DTPI = 10^{-3} M, v = 50 mV/s) 77
4.44 Cyclic voltammogram of chalcopyrite (pH 9.2, DTPI= 10^{-2} M, v = 50 mV/s) 78
4.45 Cyclic voltammograms of chalcopyrite for different scan rates at pH 9.2 for 0 M, 10^{-4} M, 10^{-3} M and 10^{-2} M DTPI 78
4.46 Cyclic voltammogram of chalcopyrite (pH 11, v = 50 mV/s) . . . 79
4.47 Controlled sweep voltammogram of chalcopyrite (pH 11, v = 50 mV/s) 80
4.48 Cyclic voltammogram of chalcopyrite (pH 11, v = 20 mV/s) . . . 81
4.49 Cyclic voltammogram of chalcopyrite (pH 11, v = 10 mV/s) . . . 82
4.50 Cyclic voltammogram of chalcopyrite for different scan rates at pH 11 83
4.51 Relationship between formation potential of peaks and scan rate 83
4.52 Relationship between current density of peaks and square-root of scan rate 84
4.53 Cyclic voltammogram of chalcopyrite (pH 11, DTP = 10^{-4} M, v = 50 mV/s) 85
4.54 Cyclic voltammogram of chalcopyrite (pH 11, DTP = 10^{-3} M, v = 50 mV/s) 85
4.55 Cyclic voltammogram of chalcopyrite (pH 11, DTP = 10^{-2} M, v = 50 mV/s) 86
4.56 Cyclic voltammograms of chalcopyrite for 0 M, 10^{-4} M, 10^{-3} M and 10^{-2} M DTP (pH 11, v: 50 mV/s) 86
4.57 Cyclic voltammogram of chalcopyrite (pH 11, DTPI = 10^{-4} M, v = 50 mV/s) 87
4.58 Cyclic voltammogram of chalcopyrite (pH 11, DTPI = 10^{-3} M, v = 50 mV/s) 88

4.59 Cyclic voltammogram of chalcopyrite (pH 11, DTPI = 10^{-2} M, v = 50 mV/s) 88
4.60 Cyclic voltammograms of chalcopyrite for 0 M, 10^{-4} M, 10^{-3} M and 10^{-2} M DTPI (pH 11, v: 50 mV/s) 89
4.61 DRIFT spectra of a) DTP, b) $(DTP)_2$, c) Pt-powder polarised with 10^{-1} M DTP in pH 4.67 buffer at 750 mV, and d) Cu-DTP precipitate 91
4.62 DRIFT spectra of chalcopyrite samples interacted with 10^{-1} M DTP in pH 4.67 buffer solution at c) –100 mV, d) +150 mV and e) +400 mV. Spectra of a) DTP and b) $(DTP)_2$ are given as references 93
4.63 DRIFT spectra of chalcopyrite samples interacted with 10^{-1} M DTP in pH 6.97 buffer solution at c) –100 mV, d) +150 mV and e) +400 mV. Spectra of a) DTP and b) $(DTP)_2$ are given as references 94
4.64 DRIFT spectra of chalcopyrite samples interacted with 10^{-1} M DTP in pH 9.2 buffer solution at c) –100 mV, d) +150 mV and e) +400 mV. Spectra of a) DTP and b) $(DTP)_2$ are given as references 96
4.65 DRIFT spectra of chalcopyrite samples interacted with 10^{-1} M DTP in pH 11 buffer solution at c) –100 mV, d) +150 mV and e) +400 mV. Spectra of a) DTP and b) $(DTP)_2$ are given as references 97
4.66 DRIFT spectra of chalcopyrite samples interacted with 10^{-1} M DTP at –100 mV in c) pH 4.67, d) pH 6.97, e) pH 9.2 and f) pH 11 buffer solutions. Spectra of a) DTP and b) $(DTP)_2$ are given as references 98
4.67 DRIFT spectra of chalcopyrite samples interacted with 10^{-1} M DTP at +150 mV in c) pH 4.67, d) pH 6.97, e) pH 9.2 and f) pH 11 buffer solutions. Spectra of a) DTP and b) $(DTP)_2$ are given as references 99

4.68 DRIFT spectra of chalcopyrite samples interacted with 10^{-1} M DTP at +400 mV in c) pH 4.67, d) pH 6.97, e) pH 9.2 and f) pH 11 buffer solutions. Spectra of a) DTP and b) $(DTP)_2$ are given as references 100

4.69 DRIFT spectra of a) DTPI, b) $(DTPI)_2$, c) Pt-powder polarised with 10^{-1} M DTPI in pH 4.67 buffer at 1250 mV, and d) Cu-DTPI precipitate 102

4.70 DRIFT spectra of chalcopyrite samples interacted with 10^{-1} M DTPI in pH 4.67 buffer solution at c) –100 mV, d) +150 mV and e) +400 mV. Spectra of a) DTPI and b) $(DTPI)_2$ are given as references 104

4.71 DRIFT spectra of chalcopyrite samples interacted with 10^{-1} M DTPI in pH 6.97 buffer solution at c) –100 mV, d) +150 mV and e) +400 mV. Spectra of a) DTPI and b) $(DTPI)_2$ are given as references. 105

4.72 DRIFT spectra of chalcopyrite samples interacted with 10^{-1} M DTPI in pH 9.2 buffer solution at c) –100 mV, d) +150 mV and e) +400 mV. Spectra of a) DTPI and b) $(DTPI)_2$ are given as references 107

4.73 DRIFT spectra of chalcopyrite samples interacted with 10^{-1} M DTPI in pH 11 buffer solution at c) –100 mV, d) +150 mV and e) +400 mV. Spectra of a) DTPI and b) $(DTPI)_2$ are given as references 108

4.74 DRIFT spectra of chalcopyrite samples interacted with 10^{-1} M DTPI at –100 mV in c) pH 4.67, d) pH 6.97, e) pH 9.2 and f) pH 11 buffer solutions. Spectra of a) DTPI and b) $(DTPI)_2$ are given as references 109

4.75 DRIFT spectra of chalcopyrite samples interacted with 10^{-1} M DTPI at +150 mV in c) pH 4.67, d) pH 6.97, e) pH 9.2 and f) pH 11 buffer solutions. Spectra of a) DTPI and b) $(DTPI)_2$ are given as references 110

4.76 DRIFT spectra of chalcopyrite samples interacted with 10^{-1} M DTPI at +400 mV in c) pH 4.67, d) pH 6.97, e) pH 9.2 and f) pH 11 buffer solutions. Spectra of a) DTPI and b) $(DTPI)_2$ are given as references 111
4.77 Change of quartz recovery with gas flowrate (Flotation time: 10 min; pH 5.5 (distilled water)) 113
4.78 Flotation time vs. recovery relationship in collectorless condition at pH 9.2 (conditioning: 15 min) 114
4.79 Rest potential change of chalcopyrite with respect to pulp pH . . 114
4.80 Pulp potential-recovery relationship in collectorless condition . . 115
4.81 Three-dimensional relief map for collectorless flotation 116
4.82 Effect of DTP amount on flotation recovery (conditioning 15 min; pH 9.2) 117
4.83 Effect of DTP amount on pulp potential (pH 9.2) 118
4.84 Pulp potential-recovery relationship in DTP (50 g/t) induced flotation 118
4.85 Three-dimensional relief map for DTP induced flotation 119
4.86 Effect of DTPI amount on flotation recovery (conditioning 15 min; pH 9.2) 120
4.87 Effect of DTPI amount on pulp potential (pH 9.2) 121
4.88 Pulp potential-recovery relationship in DTPI (20 g/t) induced flotation 122
4.89 Three-dimensional relief map for DTPI induced flotation 122
4.90 Effect of collectors on recovery in pH 4.67 buffer solution 123
4.91 Effect of collectors on recovery in pH 6.97 buffer solution 124
4.92 Effect of collectors on recovery in pH 9.2 buffer solution 125
4.93 Effect of collectors on recovery in pH 11 buffer solution 125
5.1 Equilibrium distribution of sulphur species in water at 25°C and 1 atmosphere total pressure for activity dissolved sulphide = 0^{-1}. Under these conditions, native sulphur is a stable phase. Dashed line indicates equal values of dissolved species within sulphur field. (Garrels and Christs, 1965) 131

5.2 DRIFT spectra of chalcopyrite polarised in collectorless condition at a) –100 mV and b) +400 mV in pH 9.2 buffer solution and at c) –100 mV and d) +400 mV in pH 11 buffer solution 152
A1 Scanning electron microscopy spectrum of highly mineralised chalcopyrite rock specimen 199
B1 ^{1}H NMR spectrum of DTP (Solvent: Deuterated Water) 200
B2 ^{14}C NMR spectrum of DTP (Solvent: Deuterated Water) 200
B3 ^{31}P NMR spectrum of DTP (Solvent: Chloroform) 200
B4 ^{1}H NMR spectrum of $(DTP)_2$ (Solvent: Chloroform) 201
B5 ^{14}C NMR spectrum of $(DTP)_2$ (Solvent: Chloroform) 201
B6 ^{31}P NMR spectrum of $(DTP)_2$ (Solvent: Chloroform) 201
B7 ^{1}H NMR spectrum of DTPI (Solvent: Chloroform) 202
B8 ^{14}C NMR spectrum of DTPI (Solvent: Chloroform) 202
B9 ^{31}P NMR spectrum of DTPI (Solvent: Chloroform) 202
B10 ^{1}H NMR spectrum of $(DTPI)_2$ (Solvent: Chloroform) 203
B11 ^{14}C NMR spectrum of $(DTPI)_2$ (Solvent: Chloroform) 203
B12 ^{31}P NMR spectrum of $(DTPI)_2$ (Solvent: Chloroform) 203

CHAPTER 1

INTRODUCTION

Flotation has gradually moved to a predominant role in mineral separation since the first decade of last century. There are several reasons for this; the first reason is the continuing trend toward treatment of low grade and more finely disseminated ores being the major one. Not only has this been true for sulphides to which the process was first applied commercially, but also for most non-sulphide ores as well. The second reason is the broad applicability of the process with respect to particle size; it is effective from 8 to 10 mesh (2.36 to 1.65 mm) to below 10 μm. Finally, flotation has almost no limitation in separating minerals. Flotation can utilise the wide range of surface chemical differences among minerals, and an equally wide range of reagents (Arbiter et al., 1985; Fuerstenau, D.W., 1999).

Sulphide ores constitute the major economic source of nonferrous base metals (Marabini et al., 1993; Ralston, 1991) and are the largest groups of ores treated by flotation process (Aplan and Chander, 1987). In industrial practice, most sulphide minerals are floated with the aid of small quantities of a thiol collector. Some of the commercially used thiol collectors are xanthates (65 % of US market), dithiophosphates (15 %), and thionocarbonates plus xanthogen formates (15 %) (Aplan and Chander, 1987). Several other collectors, such as thiocarbamates, xanthic esters, dithiophosphinates, etc., are known to have collecting properties and sometimes are used commercially on a small scale (Chander, 1999).

Sulphide minerals are predominantly covalently bonded and do not form hydrogen bonds with water. Their solubilities in water are low. They are semiconductors. Therefore, they can act as an electron acceptor or donor, and so support electrode reactions, such as their surface oxidation (Kocabağ, 1983; 1992).

The key chemical step in the flotation process is the adsorption of the organic collector on the selected mineral surfaces. It is now well established that the interaction of thiol collectors with sulphide minerals is electrochemical in nature. An anodic process involving the collector is coupled with a cathodic process, which is usually the reduction of oxygen. The anodic process can be charge transfer chemisorption in which the collector becomes attached to the surface through bonding with metal atoms in the sulphide mineral, the development of a thiol compound with a metal component of the mineral, or the formation of the dimer of thiol collector (Fuerstenau, M.C., 1980; Woods, 1996).

The structure and composition of the surface layer formed on the mineral surface at the preparation stage is the central subject in the basic studies of sulphide flotation (Leppinen, 1991). A large number of investigations have been directed towards understanding sulphide mineral-thiol collector interactions. It is apparent from these studies that the oxidation of both sulphide mineral and collector play an important role in the collection process, but very little is known about the oxidation reactions, especially for dithiophosphates and dithiophosphinates.

Electrochemical, wetting and spectroscopic techniques are used to clarify the flotation and surface properties of sulphide minerals. Linear potential sweep voltammetry is the most important electrochemical technique and is particularly useful for studying surface reactions (Buckley et. al., 1985). Wetting techniques are contact angle measurement and flotation. Combination of electrochemical techniques and wetting measurements has been traditionally employed methods to investigate the surface composition of sulphide minerals in an aqueous solution.

By combining these techniques, hydrophobic species that might be present at the mineral surface could be achieved (Chander, 1988).

Although electrochemical investigations yield important information on the characteristics of adsorption, such techniques do not provide direct information on the chemical composition of the adsorbed layer (Buckley and Woods, 1992), and generally comparison of experimental results and theoretically calculated relations is required to elucidate the oxidation state of sulphide. Moreover, collectors do not always give rise to voltammetric current that are readily distinguished from background currents due to other surface processes (Chander, 1988). Therefore, electrochemical and surface spectroscopic techniques have been used together to characterise sulphide surfaces (Ralston, 1991).

Chalcopyrite ($CuFeS_2$) is the most abundant copper sulphide mineral and is the major commercial source of copper. The principal industrial extraction process involves crushing, grinding, and flotation, followed by pyrometallurgical treatment of the concentrate. However, falling of mined copper ore grades and strict environmental protection legislation has led to increase the interest in more selective and efficient froth flotation and in hydrometallurgical processes to recover copper from its minerals. This has been the motivation behind many studies of copper sulphide and copper iron sulphide oxidation and reduction mechanisms (Buckley and Woods, 1984; Cases et al., 1997; Fairthorne et al., 1997; Gómez et al., 1996; Kelsall et al., 1992; Klauber et al., 2001).

Electrochemistry of collectorless flotation and xanthate-chalcopyrite interaction has been studied extensively (Buckley et al., 1985; Cases et al., 1997; Chander, 1991; Ekmekçi, 1995; etc.). However, electrochemical and flotation behaviour of chalcopyrite in the presence of dithiophosphate (DTP) and dithiophosphinate (DTPI), which are more selective for pyrite rejection in complex sulphide ores than xanthate, have not been adequately clarified, yet.

Comparative investigation of the effect of DTP and DTPI on selective flotation of sulphide minerals has become necessary due to that DTPI has displayed better selectivity against pyrite and sphalerite as compared with DTP, and chemical formulas of DTPI and DTP are the same except the oxygen content of DTP. Therefore, in this thesis, it was aimed to establish the electrochemical and flotation behaviour of chalcopyrite in the absence, and presence of collectors (DTP and DTPI). Cyclic voltammetry, microflotation with Hallimond tube and surface spectroscopic studies (DRIFT) are the tools to establish the electrochemical and flotation behaviour of chalcopyrite.

CHAPTER 2

LITERATURE REVIEW

2.1 Surface Properties of Sulphides

Minerals may be classified according to their behaviour in the flotation process as follows (Tolun, 1987):

1- Non-polar, non-metallic minerals (graphite (C), sulphur (S), talc ($Mg_3Si_4O_{10}(OH)_2$), etc.)
2- Sulphides of heavy metals and native metals (galena (PbS), sphalerite (ZnS), chalcopyrite ($CuFeS_2$), etc.)
3- Oxidised minerals of non-ferrous metals (cerussite ($PbCO_3$), smithsonite ($ZnCO_3$), malachite ($CuCO_3.Cu(OH)_2$), etc.)
4- Polar salt-type minerals which contain cations of calcium magnesium, barium and strontium (calcite ($CaCO_3$), fluorite (CaF_2), apatite ($Ca_5(PO_4)_3(F_2Cl_2OH_2O)$), barite ($BaSO_4$), etc.)
5- Oxides, silicates and aluminosilicates (feldspars, hematite (Fe_2O_3), pyrolusite (MnO_2), etc.)
6- Soluble salts of alkali and alkaline earth metals (sylvite (KCl), gypsum ($CaSO_4.2H_2O$), colemanite ($Ca[(B_3O_4)(OH)_3].H_2O$), etc.)

The ease of flotability of these minerals decrease as the ionic character of the chemical bonding increases. The gradation between covalent and ionic bonding is simply presented in Figure 2.1 (Dennen, 1959; Rogers, 1962; Tolun, 1987).

As shown from Figure 2.1, sulphides, unlike oxides and silicates, are predominantly, covalently bonded, and do not form hydrogen bonds with water. Their solubilities in water are extremely low, reflecting in the solubility product values for PbS, CuS, ZnS and HgS of 10^{-28}, 10^{-45}, 10^{-23} and $10^{-52.4}$, respectively (Kocabağ, 1983). Such low solubility products suggest that sulphide minerals should be relatively inert in aqueous solutions. However, this is not the case, since they are characterised by their chemical reactivity with water and dissolved oxygen (Gaudin, 1974). They show electrical conductivity, but compared with metals they are extremely poor conductors (i.e. semiconductor, semimetallics). Due to semiconducting properties, their reactions, including the adsorption of collectors, are usually electrochemical in nature and dependent on the redox conditions in the flotation pulp (Buckley and Woods, 1982; Woods, 1984), which is determined not only by the oxygen but all the reducing and oxidising agents present (Kocabağ, 1994). In addition, sulphides are thermodynamically unstable in the presence of oxygen as surface oxidation to S_n^{-2}, S^0, $S_2O_3^{-2}$, SO_3^{-2}, SO_4^{-2} and metal ions or oxides/hydroxides occurs depending on the pH. The oxidation products are more soluble than the underlaying sulphides (Buckley and Woods, 1982; Kocabağ, 1983).

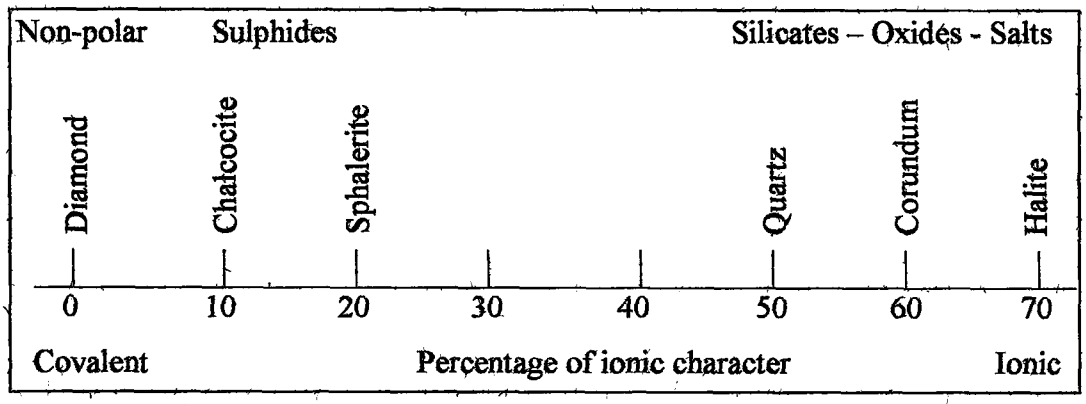

Figure 2.1: Gradation between ionic and covalent bonding (Tolun, 1987)

The mineral samples taken from different ores show differences with respect to both their physical and chemical characteristics. Even the minerals from the same ore body may different with respect to their crystal structures and compositions. Bulk electronic properties of sulphides can vary depending on

deviations from stoichiometric compositions, impurity contents, and a variety of lattice imperfections. That is as the stoichiometry of a sulphide mineral varies from metal-rich to sulphur-rich, its electronic conductivity changes from n-type to p-type, and therefore, mineral becomes more covalently bonded due to metal deficiency (Plaksin et al., 1968; Smith, 1942).

If a solid brought in contact with an aqueous solution, charged species will be transferred across the interface until equilibrium is established. The interface between the solid and solution phase may be treated as a semi-permeable membrane which allows only charged species common to both the solid and the solution to pass through. These species will be those ions which serve as the building blocks of the solid and are called potential determining ions (de Bruyn and Agar, 1962). The potential determining ions of base metal sulphides are expected to be metallic cations and sulphide ions; but S^{-2} ions are hydrolysed in aqueous solution and form compounds like SO_4^{-2}, S_2O_3, HS^- and H_2S depending on the potential of the medium. For any metal sulphide found in a solution, it is convenient to say that the changes in the chemical potential are related with the chemical equilibrium (Ralston, 1991). So it can be concluded that H^+ and OH^- ions are also potential determining ions for the sulphide-solution interface. This situation does not change the effect of metal (M^{+2}) and S^{-2} ions on the medium; but shows the importance of H^+ and OH^- ions (Kocabağ, 1983).

2.2 Electrochemistry of Sulphides

2.2.1 Electrochemical Potential

When charged species (ions or electrons) are major constituents of a material system, it is referred to as an electrochemical system. In addition to the chemical behaviour of such systems, the electrical effects produced by the presence of the charged particles must also be considered. A flotation pulp

represents such an electrochemical system because many of the reagents, organic and inorganic electrolytes, also the dissolved species derived from suspended solids are ionic in nature (de Bruyn and Agar, 1962). Therefore, when a solid comes into contact with an aqueous solution, a mixed potential will be created on the surface. A mixed potential may be defined as the steady-state open circuit potential observed with an electrode when more than one reaction is occurring at the surface (Natarajan and Iwasaki, 1974).

In an electrochemical system, electrochemical reactions are represented by oxidation and reduction reactions. In the case of anodic oxidation reaction, minerals donate electron, and for cathodic reduction, they accept electron. Each of oxidation and reduction reactions is named as half-reaction and it can be written as in equation 2.1:

$$\text{Reduced State} \rightleftharpoons \text{Oxidised State} + ne \qquad 2.1$$

and the corresponding half-cell potential is given by the Nernst equation:

$$Eh = E^{\circ} + \frac{RT}{nF} \ln \frac{|\text{oxidised state}|}{|\text{reduced state}|} \qquad 2.2$$

where R: Gas constant (0.001987 kcal/deg)

n: Number of electron

T: Temperature (298.15 °K)

F: Faraday constant (23.06 kcal/volt-gram)

[oxidised state] and [reduced state] are the activities of oxidised and reduced products, respectively. E° represents the standard formation potential and is measured at standard states (unit activity, 1 atmospheric pressure and 25°C temperature). Eh is the reversible potential of the reaction 2.1, and it shows the measured (or calculated) potential when standard hydrogen electrode is used as reference electrode.

2.2.2 Pulp Potential Measurement

The redox potential measurements in flotation systems are very useful for monitoring changes at the mineral/solution interface or in the liquid phase. The potential at a solid/solution interface is determined by the presence of oxidising and reducing species in solution. For the measurement of oxidation/reduction potentials, an electrode pair consisting of an inert indicator electrode and a reference electrode is commonly used.

The indicator electrode functions as an acceptor or a donor of electrons to the ions in solution. Three types of indicator electrodes are commonly used for measurement of redox potential: Noble metal electrodes, mineral electrodes and ion selective electrodes (Zhou and Chander, 1991). Noble metal electrode used most is platinum, although gold electrode has a fair number of applications (Garrels and Christ, 1965; Labonté and Finch, 1990; Rand and Woods, 1984). Mineral electrodes used for monitoring Eh include chalcopyrite, pyrite, chalcocite, etc. (Gebhardt and Shedd, 1988). Sulphide ion selective electrodes are most widely used in the sulphidisation process for the flotation of oxidised copper, lead and zinc ores (Jones and Woodcock, 1978a, b, 1979; Malghan, 1986).

A clean platinum surface is imperative in securing a reproducible potential on short conditioning. The behaviour of platinum electrode as a redox potential indicator was investigated in detail by Natarajan and Iwasaki (1970, 1973a, 1973b, 1974) and they stated that sulphide ions might result in poisoning of platinum electrodes. They concluded that the poisoning of platinum electrodes by organic and inorganic impurities present in the solution may lead to erratic results, since a platinum electrode is not inert as often thought to be. Therefore, there is a need for platinum electrodes to be cleaned before transferring from one system to another. There are several techniques for cleaning indicator electrode: Chemical treatment in acid solution (such as sulphuric, nitric and chromic acids), mechanical treatment, and electrochemical treatment (cathodic and anodic cleaning). The mechanical treatment of platinum electrodes can give a very short

response time in the Eh measurement. However, if an electrode is to be used for on-line monitoring of a flotation pulp, mechanical cleaning of the electrode is not very convenient. Although electrochemical activation by anodic/cathodic treatment is the most rigorous method for cleaning noble metal electrodes, dipping in chromic acid provides an effective and rapid means for obtaining clean reproducible surfaces (Natarajan and Iwasaki, 1970, 1974; Rand and Woods, 1984).

In flotation systems, the relevant Eh is the established potential at the mineral/solution interface. This suggests that an electrode constructed from the mineral being concentrated should be the most appropriate for Eh measurement (Woods, 1984). However, since oxidised surface layers form on mineral sulphide electrodes through reaction with dissolved species in the flotation pulp, such electrodes could rapidly reach a condition where they no longer respond rapidly to changes in the pulp environment (Rand and Woods, 1984).

Rand and Woods (1984) demonstrated how Eh depended on the nature of the indicator electrode by studying the behaviours of platinum, gold and galena electrodes in iron/oxygen and xanthate/oxygen systems. They found that pulp potentials in the same system can be different for different indicator electrodes because the rate of the electrode reaction is dependent on the nature of the electrode surface. They concluded that gold electrode could be a better material since it responded more electrode potential more closely.

Since the pyrite mineral has a higher rest potential than any other sulphide minerals, it is reported to be the noblest sulphide mineral. In oxygenated solutions containing ferric and ferrous ions, it was observed that the response of the pyrite electrode was identical to that of a platinum electrode (Sato, 1960; Natarajan and Iwasaki, 1972). This behaviour was verified by Gebhardt and Shedd (1988) when they investigated both platinum and pyrite electrodes in deoxygenated ferrous sulphate solutions, and showed that platinum electrode responded similarly to

pyrite electrode. However, it was observed that these two electrodes responded differently in deoxygenated copper sulphate solutions.

A study was made by Cheng and Iwasaki (1992) to investigate the flotation of chalcopyrite and pyrrhotite and their mixture using platinum, chalcopyrite and pyrrhotite electrodes as indicators. The results of this study showed that the electrodes responded to the system slowly and erratically, and the time needed for the mineral electrodes to reach a steady state was longer than for the platinum electrode. It was concluded, therefore, that platinum electrode was a better indicator that would be used in the flotation pulps.

Early in the development of electrochemical techniques, the standard hydrogen electrode (SHE) was accepted as a standard. For this reason, reference tables of standard potentials are given versus this electrode. In practice, the SHE is difficult to use. So, for the reference electrode, saturated calomel electrodes (SCE) and Ag/AgCl electrodes are widely used to make electric connection with the system to be measured (Hochstetler, and Wightman, 1998; Kounaves, 1997). When a platinum indicator electrode is connected to a calomel reference electrode, the platinum electrode can accept electrons from dissolved ionic species, or it can give them up, depending on whether the potential of the half-cell containing the dissolved species is greater or less than that of the calomel reference electrode. Potential is determined by the reaction

$$Hg_2Cl_{2(s)} + 2e \rightleftharpoons 2Hg_{(l)} + 2Cl^- \qquad 2.3$$

and the Eh may be calculated from the measured potential by

$$Eh = E_{measured} + 0.245 \text{ volt} \quad \text{at } 25°C \qquad 2.4$$

where the numerical value of 0.245 volt represents the potential of a saturated calomel electrode with respect to standard hydrogen scale (Garrels and Christ, 1965).

2.2.3 Pulp Potential Control

There are two methods of Eh control: potentiostatic and chemical. The potentiostatic method is intrinsically cleaner as it does not require the addition of redox agents to the flotation pulp as in chemical control. In the latter case, the possibility of specific interactions with mineral surface must be considered. With potentiostatic control, the Eh can be readily manipulated to any desired value, whereas chemical control is less flexible, particularly near Eh zero. Chemical control of Eh is more directly related to plant practice and produces a more uniform electrochemical environment around the sulphide particles in the flotation pulp, whereas potentiostatic control is very dependent on the efficiency of electrode/particle contact. In plant applications, since the potentiostatic control requires a high voltage application, it necessitates a great energy source and a very good isolation (Cheng and Iwasaki, 1992; Hayes and Ralston, 1988; Rao et al., 1992).

For chemical control, there are many redox reagents used to control pulp potential: For anodic oxidation potentials, $KMnO_4$, H_2O_2 and NaOCl are used; for cathodic reduction potentials, Na_2S, $Na_2S_2O_4$, $Na_2S_2O_5$, Na_2SO_3 and iron powder are used (Cheng and Iwasaki, 1992; Ekmekçi, 1995; Trahar, 1984; Yoon, 1981). Conventional steel mill grinding provides strongly reducing conditions compared with the non-reducing conditions that are obtained in the autogenous grinding or in a porcelain mill (Berglund and Forssberg, 1987).

In laboratory experiments, pulp potential can be controlled either by redox reagents (Heyes and Trahar, 1977) or by electrochemically (Gardner and Woods, 1979; Hayes and Ralston, 1988).

2.2.4 Voltammetry

Historically, the branch of electrochemistry, it is now called voltammetry, developed from the discovery of polarography in 1922 by the Czech chemist

Jaroslav Heyrovsky. The early voltammetric methods experienced a number of difficulties, making them less than ideal for routine analytical use. However, in the 1960s and 1970s significant advances were made in all areas of voltammetry (theory, methodology, and instrumentation) which enhanced the sensitivity and expanded the repertoire of analytical methods (Kounaves, 1997; Sturrock and Barringer, 1998).

Linear sweep and cyclic voltammetry techniques have been very popular among electrochemists (Chander and Fuerstenau, 1974; Ekmekçi, 1995; Kim, 1995; Kowal and Pomianowski, 1973; Woods, 1971, 1987). Cyclic voltammetry (CV) is widely used for the initial characterisation of electrochemically active systems. In addition to indicating the number of different oxidation states, and their relative energies, CV can also be used for mechanistic studies of systems in which the electron transfer reactions, due to the characteristic appearance of cyclic voltammograms associated with different mechanisms (Bott, 1999). A typical voltammogram is given in Figure 2.2 which shows the characteristic oxidation and reduction peaks.

This technique is based on varying the applied potential at a working electrode in both forward and reverse directions while monitoring the current. Oxidation occurs when the potential of the working electrode is sufficiently positive. Conversely, reduction occurs when the electromotive force (potential) of the working electrode is sufficiently negative. If oxidised product remains near the electrode surface (i.e., does not completely diffuse away) and is reducible, then a current will flow on the reverse scan when its redox potential is reached. In CV, depending on the analysis, one full cycle, a partial cycle, or a series of cycles can be performed.

The common characteristic of all voltammetric techniques is that they involve the application of a potential (E) to an electrode and the monitoring of the resulting current (i) flowing through the electrochemical cell. In many cases of the applied potential is varied or the current is monitored over a period of time (t).

Thus, all voltammetric techniques can be described as some function of E, i, and t (Kounaves, 1997).

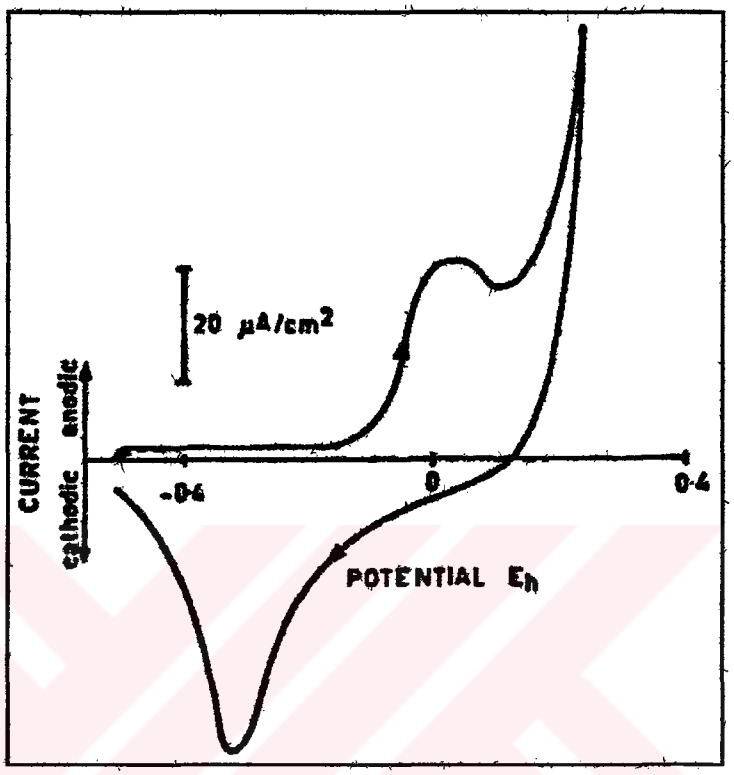

Figure 2.2. Current-potential curve for a galena electrode in pH 9.3 buffer solution containing $9.5x10^{-3}$ M ethyl xanthate (Woods, 1971)

The important parameters in a cyclic voltammogram are the peak potentials (E_{pc}, E_{pa}) and peak currents (i_{pc}, i_{pa}) of the cathodic and anodic peaks, respectively. If the electron transfer process is fast compared with other processes (such as diffusion), the reaction is said to be electrochemically reversible, and the peak separation is

$$\Delta E_p = E_{pa} - E_{pc} = 2.303RT/nF \qquad 2.5$$

Thus for a reversible redox reaction at 25°C with n electrons ΔE_p should be 0.0592/n V or about 60 mV for one electron. In practice this value is difficult to attain because of such factors as cell resistance. Irreversibility due to a slow

electron transfer rate results in $\Delta Ep > 0.0592/n$ V, greater, say than 70 mV for a one-electron reaction.

The coupling of chemisorption reactions to the electron transfer reactions can lead to changes in the peak potentials and/or the peak currents, and the effect of chemical reactions is often expressed in terms of changes in the peak current ratio and/or peak potentials (Bott, 1999; Chander and Briceno, 1987). Under linear diffusion conditions reversible charge transfer processes, in general, give peak potentials independent of sweep rate. Therefore, the large separation between the oxidation and reduction peaks is indicative of an irreversible process (Chander and Fuerstenau, 1974). So, for an irreversible process, E_{pa} and E_{pc} are much farther apart than 0.0592/n.

For a reversible process, peak current changes with a change in scan rate, but peak potential do not: The faster the scan rate, the greater the peak current as long as the reaction remains reversible. The increase in the peak current value is a function of the square root of the scan rate according to Randle-Sevcik equation,

$$i_p = 2.69 \times 10^5 n^{3/2} A c^\circ D^{1/2} v^{1/2}$$

where i_p is the peak current in amps, A is the electrode area (cm^2), D is the diffusion coefficient (cm^2/s), c° is the concentration in mol/cm^3, and v is the scan rate in V/s. If the peak current is a nonlinear increasing function of the square root of scan rate, it indicates an irreversible reaction (Bott, 1999; Chander and Briceno, 1987; Kounaves, 1997). In addition, larger peak separations at higher scan rates indicate that a slow electron transfer is involved. Shift in the formation potential of a peak at higher scan rates could also be associated with changes in the composition of the passivation layer (Cha and Park, 1996).

2.3 Electrochemistry of Sulphide Flotation

The flotation behaviour of minerals depends on the balance between the hydrophobic and hydrophilic species present at the surface of the minerals. Sulphide minerals exhibit different degrees of natural hydrophobicity, though few have sufficient hydrophobicity to ensure flotation (natural collectorless flotation). Generally organic reagents (collectors) are required to prepare a hydrophobic surface for flotation, although the hydrophobicity of some minerals can be changed through chemical reaction in the absence of conventional collectors (induced collectorless flotation).

Sulphides are semi-conductors, and can accept or donate electrons. So the nature and influence of electrochemical reactions which control the state of sulphide mineral surfaces has been the subject of many investigations (Woods, 1984). The exact nature of the hydrophobic surface species on sulphide minerals, which respond to natural or self induced flotation, is unclear, although the formation of a metal-deficient surface (Buckley et al., 1985), adsorption of polysulphides (Luttrell and Yoon, 1984a), or the presence of elemental sulphur (Gardner and Woods, 1979) was suggested. Trahar (1983, 1984) and Heyes and Trahar (1977) investigated the influence of pulp potential on the self-induced and collector-induced flotation of the various sulphide minerals and have substantiated that mineral flotability can be affected by changes in the pulp potential.

2.3.1 Collectorless Flotation

Numerous research works have been carried out on flotability of sulphide minerals without collector since it was recognised by Ravitz and Porter (1933) in the flotation of galena cleaned with ammonium salts in a de-oxygenated system. Some sulphides are naturally floatable, but others require special conditions for collectorless flotation. Therefore, it is important to distinguish between natural flotability and collectorless flotation.

Minerals such as molybdenite (MoS_2), orpiment (As_2S_3), realgar (AsS) and stibnite (Sb_2S_3) are easily floated without the need of collectors, or of special conditions for collectorless flotation, i.e. neither specific pulp potential is required for flotation, nor there is any display of variable flotability with Eh. Such minerals exhibit natural flotability. The origin of this behaviour is linked to the nature of the chemical bonding and the crystal structure of each mineral – a relatively non-polar surface is exposed after fracture (Arbiter et al., 1975).

Other common sulphide minerals, e.g. chalcopyrite ($CuFeS_2$), do not show natural flotability. For these minerals, collectorless flotation is possible only under specific Eh conditions in the flotation pulp. Work by Chander et al. (1975), Heyes and Trahar (1977), Luttrell and Yoon (1984a), Pang and Chander (1993) and Woods (1987) suggested that oxidation of surface sulphide under very mildly oxidising conditions to elemental sulphur, polysulphides or a metal-deficient layer is probably responsible for collectorless flotation. The fact that sulphide ion which does not form hydrogen bonding with water molecule may also contribute to this phenomena (Fuerstenau, M.C., 1999; Matabishi et al., 2000).

Interest in collectorless flotation has increased sharply in last few decades, and chalcopyrite is the most investigated sulphide mineral (Kocabağ and Smith, 1989). The collectorless flotation of chalcopyrite increases up to a pulp potential of approximately 250 mV (Fornasiero et al., 1996) but excessive oxidation has a depressing effect (Rao et al., 1992).

Collectorless flotation of chalcopyrite has been studied in detail (Buckley and Woods, 1984; Ekmekçi and Demirel, 1997, 1998; Gardner and Woods, 1979; Heyes and Trahar, 1977; Luttrell and Yoon, 1984a, b; Zachwieja et al., 1989, etc.) and is thought to occur due to superficial oxidation resulting in the formation of a sulphur-rich phase such as elemental sulphur, polysulphide or an iron deficient chalcopyrite. Bulk thermodynamic data coupled with the position for the peaks in the voltammograms led Gardner and Woods (1979) to conclude that oxidation reactions were as in reactions 2.6-2.7 for acid and alkaline solutions, respectively:

$$CuFeS_2 \rightleftharpoons CuS + S^{\circ} + Fe^{+2} + 2e \qquad 2.6$$

$$CuFeS_2 + 3H_2O \rightleftharpoons CuS + Fe(OH)_3 + S^{\circ} + 3H^{+} + 3e \qquad 2.7$$

In the subsequent studies, however, Hamilton and Woods (1984), Buckley et al. (1985) and Buckley and Woods (1984) maintained that the absence of any detectable elemental sulphur in the X-ray photoelectron spectrum (XPS) of galena and other sulphides indicated that the initial oxidation of chalcopyrite resulted in the formation of a copper sulphide with a stoichiometry close to that of CuS_2 viz.

$$CuFeS_2 + 3H_2O \rightleftharpoons CuS_2 + Fe(OH)_3 + 3H^{+} + 3e \qquad 2.8$$

despite the conflicting evidence of Biegler and Horne (1985) who claimed that the oxidation reaction is

$$CuFeS_2 \rightleftharpoons 0.75CuS + 0.25Cu^{+2} + Fe^{+2} + 1.25S^{\circ} + 2.5e \qquad 2.9$$

with a product layer containing CuS and elemental sulphur about 1 nm thick. Buckley et al. (1985) refuted Biegler and Horne's (1985) findings, arguing that voltammograms are not sufficiently discriminating to distinguish between the possible reactions and reiterating their confidence in the XPS spectra.

In addition, Pang and Chander (1993) investigated the surface films by different electrochemical techniques and proposed the reactions 2.10 and 2.11 for anodic oxidation of chalcopyrite. They stated that under certain conditions the iron oxides that form when chalcopyrite oxidises do not adhere to the surface.

$$CuFeS_2 \rightleftharpoons CuFe_{1-x}S_2 + xFe^{+3} + 3xe \qquad 2.10$$

$$CuFeS_2 \rightleftharpoons (CuS+S) + Fe^{+3} + 3e \qquad 2.11$$

2.3.2 Collector Induced Flotation

The basic condition for flotation is the hydrophobicity of the surface of the mineral to be floated. For sulphides, this condition usually requires treatment with a collector solution. The interaction between collectors and surfaces plays an important role in many aspects of mineral processing. Therefore, to understand the interaction between different reagents and the mineral surface is central concept to achieve selective flotation (Piantadosi et al., 2000; Arbiter and Gebhardt, 1992).

Taggart and co-workers (Taggart et al., 1930) developed a theory based on chemical reaction and wrote: "All dissolved reagents which, in flotation pulps, either by action on the to-be-floated or on the not-to-be-floated particles affects their flotability, by function of reasons of chemical reactions of well recognised types between the reagent and the particle affected".

In early papers of Gaudin and Wark, collector adsorption was considered to take place simply as the adsorption of collector ions or possibly molecular entities (metal xanthates or xantic acid molecules). For example, Gaudin (1927) wrote: "The mechanism by which xanthate float other sulphides than galena may involve an adsorption of xanthate ions without further reaction". In 1934, he still remained ambivalent about the chemical theory of flotation: "The oxidised coatings on galena react metathetically with alkali xanthates in solution in water to produce coatings of lead xanthate" (Gaudin et al., 1934). Wark (Wark, 1938; Sutherland and Wark; 1955) drew attention to the fact that this model was inconsistent with established values for the solubility products of the species involved. He believed that the interaction of thiols with sulphides should be considered as adsorption and wrote in 1934: "We find that there is a strong connection between adsorption of xanthates and the solubility of the heavy metal xanthates, but we are unable to decide if this is an identity" (Wark and Cox, 1934).

The idea that chemical interactions on the sulphide surface would occur by an electrochemical mechanism was first put forward by Salamy and Nixon (1953). It is now well established that the development of hydrophobicity of sulphide mineral particles arises from an anodic process involving the oxidation of mineral, coupled with the cathodic reduction of oxygen in collectorless flotation. In a collector flotation system, the anodic process is the charge transfer chemisorption of a thiol ion, and/or oxidation of thiol ion to its disulphide, and/or the formation of a thiol compound with a metal component of the mineral. So, the pulp potential has now been recognised to be another important factor in controlling flotation (Bahena et al., 2000).

Depending on the minerals involved, the electrochemical mechanisms can be subdivided into four classes (Yoon and Basilio, 1993): Chemisorption, catalytic oxidation, EC-mechanism and metathetical substitution.

The first mechanism involves the formation of a monolayer of the thiol oxidation product at potentials below the potential for the metal thiol compound formation. This is referred to as underpotential deposition or chemisorption (Woods, 1971) which is usually observed as prewaves on voltammograms. Systems in which such underpotential deposition has been investigated include ethyl xanthate on the metal sulphides galena (Richardson and O'Dell, 1985; Woods, 1971; Gardner and Woods, 1977), chalcocite (Basilio et al., 1985; Kowal and Pomianowski, 1973; O'Dell et al., 1984, 1986; Richardson et al., 1984; Woods et al., 1990), and silver sulphide (Woods et al., 1997) and silver (Buckley and Woods, 1995; Talonen et al., 1991; Woods et al., 1992). Underpotential deposition has also been reported for methyl and butyl xanthates on galena (Gardner and Woods, 1977) and diethyl dithiophosphate on chalcocite (Chander and Fuerstenau, 1974, 1975; Buckley and Woods, 1992).

In the catalytic oxidation mechanism, the mineral provides a passage for the transfer of electrons from the site where the collector is oxidised to the site where oxygen is reduced, but does not participate in the reaction itself. This

mechanism applies to the adsorption of xanthates on pyrite, pyrrhotite and gold to form dixanthogen (Majima and Takeda, 1968; Woods, 1971; Gardner and Woods, 1977).

In the third mechanism, the mineral participates in the adsorption process to form a metal thiol compound on the surface. The mechanism of metal thiol formation may be viewed as involving an electrochemical reaction (E):

$$MS \rightleftharpoons M^{+2} + S^{\circ} + 2e \qquad 2.12$$

and a chemical reaction (C),

$$M^{+2} + 2X^{-} \rightleftharpoons MX_2 \qquad 2.13$$

in which X represents a thiol collector. The overall adsorption mechanism can then be represented by an electrochemical reaction:

$$MS + 2X^{-} \rightleftharpoons MX_2 + S^{\circ} + 2e \qquad 2.14$$

In organic electrochemistry, this mechanism is recognised as a coupled electrochemical and chemical reaction of the EC-type (Nicholson and Shain, 1964). In the EC mechanism, the electrochemical reaction is controlled by the electrochemical potential (E) of the system, while the chemical step is controlled by its stability constant (pK), as suggested by the chemical theory of collector adsorption. It may be stated, therefore, that the adsorption of thiol collectors on sulphides is controlled by both the E and pK values of the system. The E determines the availability of metal ions, while the pK of the metal thiol complex determines whether this complex can be formed. Thus, metal-thiol compounds can be formed when the mineral is easily oxidised, and/or when the metal-collector compound has a very large pK value. (Kim, 1995).

The EC mechanism was employed to explain the adsorption of modified thiol type collectors including thiophosphate (Basilio et al., 1992a) and thiophosphinates (Kim, 1995; Basilio et al., 1992b) on precious metals and that of dithiophosphinate on copper and copper sulphides (Basilio et al., 1991). According to EC mechanism, copper-DTPI formation process on copper may be viewed as a two-step process, involving an initial electrochemical reaction (E):

$$Cu^{\circ} \rightleftharpoons Cu^{+} + e \qquad 2.15$$

followed by the chemical reaction (C),

$$Cu^{+} + DTPI^{-} \rightleftharpoons CuDTPI \qquad 2.16$$

The overall reaction then becomes:

$$Cu^{\circ} + DTPI^{-} \rightleftharpoons CuDTPI + e \qquad 2.17$$

The fourth mechanism involves metathetical substitution of the oxidation product on a mineral surface by a thiol collector, which constitutes the chemical theory proposed by Taggart et al (1930). Although this mechanism does not directly involve a charge transfer process, it may be included in this classification since the oxidation products are formed by an electrochemical process.

Fuerstenau et al. (2000) studied on the interaction of chelating collectors with Cu-minerals. They defined chelating agent as collectors, which must contain at least two donor atoms capable of bonding to the same metal atom. Elements that act as donors are the more electronegative ones on the right-hand side of the periodic table (sulphur, nitrogen, oxygen and, to a lesser extent, phosphorous). The chelating agents might behave as a collector because of formation of chelate complex at the surface or at the interface. The chelating complexes may be hydrophobic to promote the attachment of air bubbles. The reaction of a chelating reagent with copper ions at copper mineral surfaces may take place by several

distinct mechanisms, as outlined by Fuerstenau and Pradip (1984): chemisorption, surface reaction, and bulk precipitation (Figure 2.3).

Chemisorption involves covalent and coordinating bonding of surface metal cations that do not move from their crystal lattice position when bonding with the electron-donor atoms of the functional group of the chelating reagent adsorbed at the mineral surface (Figure 2.3.a). Since each surface metal site bonds to a single chelating reagent molecule, adsorption is limited to a monolayer.

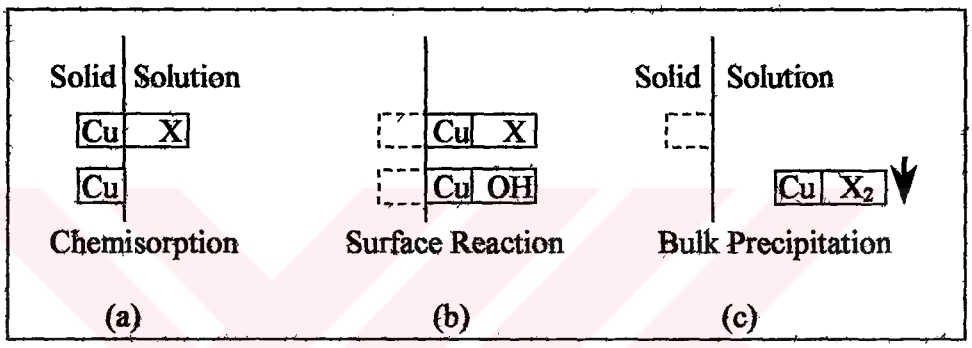

Figure 2.3. Schematic representation of the interaction of a chelating agent (X) with copper ions from the mineral surface by chemisorption, surface reaction, or by bulk precipitation (bulk precipitation may occur in the region during adjacent to the mineral surface). In the case of chemisorption and surface reaction, the charge on the various species is not shown.

Surface chemical reaction occurs when bonding with the chelating agent causes the metal cations to move out of their lattice position to the region directly adjacent to the surface (Figure 2.3.b). This process may involve or be assisted by hydrolysis of the metal cations at the surface. Such a hydrolysis reaction could cause the metal ion to be displaced from its lattice position and thereby susceptible to chelation with the added reagent. Fuerstenau and Hanson (1991) clearly demonstrated that hydroxamate will function as a collector on chalcocite only under oxidising conditions, which make the copper ions in the sulphide

mineral available for surface reaction. Finally, surface chemical reaction can by its nature lead to the formation of multilayers.

Bulk precipitation might occur if the solution chemistry of the mineral flotation system promotes the dissolution of the mineral surface such that the chelating collector can react chemically with the metal cations out in solution, forming metal chelate complexes and even metal chelate precipitates. Needless to say, this type of interaction between the chelating reagent and the mineral only depletes the collector available for reaction at the surface without rendering the mineral hydrophobic. Precipitation of a metal chelate at the interface seems to be a necessary condition for mineral flotation to take place. If the rate of metal dissolution and diffusion through the boundary layer is faster than diffusion of the collector to the mineral surface, precipitation of the metal chelate in the bulk may occur. Preferential partitioning of the chelating reagent in the form of bulk precipitate as opposed to surface precipitate appears to deleteriously affect the flotation of minerals (Nagaraj and Somasundaran, 1981).

2.3.2.1 Dithiophosphate

The dithiophosphate collector family is the second major class of sulphide collectors from a collector volume viewpoint. Its chemical formula is $(R_2O_2PS_2)^-$ and is presented as follows where R represents hydrocarbon chain:

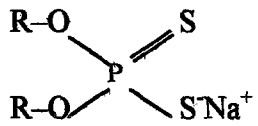

Dithiophosphates are generally water soluble, and if kept at sufficiently high pH, have reasonable shelf life. They have many chemical and flotation properties similar to those of the xanthates. They differ from xanthates principally in that they are more unstable in the presence of moisture and for this reason their

commercial forms are commonly stabilised with sodium carbonate (Crozier, 1978, 1984). They have a number of advantages over xanthates:

- Dithiophosphates only weakly interact with Fe(III) species at pH values greater than 4 (Fuerstenau et al., 1971) and, hence, adsorption of DTP onto chalcopyrite is likely to be strongly influenced by iron oxyhydroxide species.
- Dithiophosphates are relatively stable in mildly acid solution than xanthates (Leja, 1982)
- Dithiophosphates have high standard reduction potentials for dimerisation: 0.255 V for diethyl dithiophosphate (Kakowskii et al., 1959) relative to 0.060 V for ethyl xanthate (Winter and Woods, 1973).
- The dimer of dithiophosphates is more insoluble ($5x10^{-7}$M for diethyl dithiophosphate (Kakovskii and Areshkevitch, 1968)) compared to diethyl dixanthogen ($1.25x10^{-5}$M (Tipman and Leja, 1975)).

Yordanov and Ranguelova (2001) and Yordanov et al. (1998) studied the interaction between Cu^{+2} and DTP^- ions by EPR and stopped-flow spectrophotometer. They stated that after mixing the $CuSO4.5H_2O$ and ammonium salt of ethyl DTP, $[(C_2H_5O)_2P(S)S]NH_4$, a short-lived brown colour appears followed by the immediate precipitation of a pale yellow solid phase. It was found by EPR spectroscopy, magnetic susceptibility measurements and X-ray structure analysis (Hill, 1969; Rudzinski et al., 1980; Yordanov et al., 1983) to be the CuDTP and the other product was $(DTP)_2$. Yordanov (1997) investigated the appearance of brown colour with EPR spectrometer and concluded that Cu^{+2} and DTP^- react first to form $Cu(DTP)_2$ (brown colour) in accordance with reaction 2.18 and then immediately pale yellow precipitate occurs showing the formation of CuDTP+$(DTP)_2$ (pale yellow precipitate) by reaction 2.19.

$$2Cu^{+2} + 4DTP^- \rightleftharpoons 2Cu(DTP)_2 \qquad 2.18$$

$$2Cu(DTP)_2 \rightleftharpoons 2CuDTP + (DTP)_2 \qquad 2.19$$

Shubov et al. (1976) studied the interaction between dithiophosphate and chalcopyrite with UV spectrophotometer, and concluded that CuDTP, $Cu(DTP)_2$, as well as $(DTP)_2$ could be formed. They believed that $Cu(DTP)_2$ is formed initially by ion exchange with the oxidised surface (reaction 2.18) and then decomposes to form the cuprous compound and dithiolate (reaction 2.19). If pH is 7.5-9.5 $Cu(DTP)_2$ and, if less than 6.5 CuDTP and/or $(DTP)_2$ formed hydrophobic mineral surface. They also concluded that more higher hydrophobic surface could be obtained with $Cu(DTP)_2$ and aeration of pulp helped to the formation of $Cu(DTP)_2$. Goold and Finkelstein (1972) observed that the decomposition of $Cu(DTP)_2$ into CuDTP and $(DTP)_2$ (reaction 2.19) is very slow in alkaline solution.

Valli et al (1994) worked on the adsorption of DTP on chalcopyrite by using FTIR spectrometer equipped with a diffuse reflectance unit and a narrow range MCT detector. They deduced that copper is present as copper(I) on the surface of the oxidised copper containing minerals chalcocite, chalcopyrite and covellite, and copper(I) species are dissolved and solid CuDTP precipitate on the surface.

Leppinen (1991) also studied on chalcopyrite-DTP interaction by FTIR-ATR spectrometer equipped with narrow range MCT detector. Author stated that the IR spectrum of surface species on chalcopyrite is very similar to that of $Cu(DTP)_2$. Moreover, it was mentioned in the same study that the FTIR signal intensity decreases rapidly from pH 2 to 4, being close to zero at pH 8.

Chander and Fuerstenau (1974, 1975) have carried out a series of detailed investigations between DTP and chalcocite. They compared observations on the flotability and contact angles of the mineral with cyclic voltammetry studies and thermodynamic calculations. They considered CuDTP to be the product of reaction under flotation conditions and that the hydrophobicity of the surface by a

balance between the effects of this compound and cuprous oxide which can co-exist with it under some conditions. Their voltammograms indicate that DTP participates in a two-step irreversible oxidation on chalcocite, and that only the first step can take place at or below the rest potential in aerated solutions, and they suggest that CuDTP is present at the surface under such conditions. Their results indicate strongly that no $(DTP)_2$ can be present on chalcocite treated with DTP in aerated solution. They proposed that the following reactions take place:

$$DTP^- \rightleftharpoons DTP^o + e \qquad 2.20$$

$$Cu_2S + (2-y)DTP^o + yDTP^- \rightleftharpoons 2CuDTP + S + ye \qquad 2.21$$

$$Cu_2S + (4-m)DTP^o + mDTP^- \rightleftharpoons 2Cu(DTP)_2 + S + me \qquad 2.22$$

D.W. Fuerstenau (1980) presented the following results drawn from Eh-pH diagram of $Cu_2S/DTP/H_2O$ system in a paper related with thermodynamics of sulphide flotation:

- $(DTP)_2$ is stable at all pH values, and its stability domain is independent of the nature of the surface. For the equilibrium situation to be achieved, however, the surface must be capable of electron transfer, since it is recognised that $(DTP)_2$ does not form in bulk solutions.
- The maximum pH value below which CuDTP is stable, pH_s, is given by "$pH_s = 14.8 - p(DTP)$".
- The final oxidation product of the solid is Cu^{+2} in acid solutions and CuO in alkaline solutions.
- In acid solutions, where dissolved copper ions can normally form, precipitation of the metal-reagent salt can occur in the bulk solution rather than at the surface of the solid.
- In neutral and alkaline solutions, formation of CuDTP or $Cu(DTP)_2$ competes with the simultaneous formation of Cu_2O or CuO.

2.3.2.2 Dithiophosphinate

Dialkyl dithiophosphinates (DTPI), which are based on the phosphine chemistry, have recently become an important class of collectors for the flotation separation of galena, chalcopyrite and precious metals from complex and massive sulphide ores. The diisobutyl homologue is used commercially under the name AEROPHINE 3418A promoter (Cytec Technology Corp.). Some physical properties of DTPI is given in Table 2.1 (Rickelton, 1998). Its chemical formula is $(R_2PS_2)^-$ and is presented as follows where R represents hydrocarbon chain:

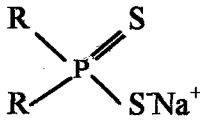

Table 2.1: Typical properties of AEROPHINE 3418A promoter (Rickelton, 1998)

Appearance	Colourless to light yellow mobile liquid
Assay	50-52 % active
pH	Slightly alkaline
Viscosity	23 cp at 24°C
Density	1.14 g/ml at 24°C
Freezing point	-12°C
Solubility in water	Complete
Flash point (closed cup)	>93°C
Autoignition temperature	437°C

DTPI is structurally similar to dithiophosphate but its collector properties are quite different from that of DTP. They are stronger in recovery capability than the dithiophosphates and are sometimes used like xanthates; they might be used instead of xanthates with better selectivity (Klimpel, 1999). In contrast to the xanthates and dithiophosphates, the dithiophosphinates are more resistant to the aqueous oxidation and they form more stable, insoluble complexes with

many transition metals and lead. They are expected to be stable even at elevated pulp temperatures. These characteristic properties of dithiophosphinates could partly explain the observed high collector strength, adsorption and flotation kinetics for Pb, Cu and precious metal values, and the improved selectivity against iron sulphides and sphalerite (Aslan, 2002; Gorken et al., 1992; Kim, 1995; Nagaraj and Avotins, 1988). Some of the advantages ultimately demonstrated by AEROPHINE 3418a promoter compared to traditional collectors include (Mingione, 1990):

- Improve selectivity and recovery in base metals flotation, particularly with complex polymetallic ores,
- Increase recovery of precious metals associated with base metal ores,
- Greater selectivity against iron-sulphide minerals,
- Rapid flotation kinetics and
- Decrease collector consumption.

Gorken et al (1992) investigated the influence of pulp potential on selective flotation of chalcopyrite from Cu-Zn-Ag-Fe ore. They found that mildly oxidising conditions, such as that achieved by aeration of the pulp, were necessary for obtaining selective flotation for chalcopyrite with DTPI.

Yordanov et al (1983) made a research to elucidate the reaction mechanism between Cu^{+2} and $DTPI^-$ similar to the work performed with DTP^- and Cu^{+2} as mentioned above. They observed similar behaviour with $DTPI^-$ as compared with DTP: Colour change and then precipitate formation. So they proposed the generation of $Cu(DTPI)_2$ and then formation of $CuDTPI+(DTPI)_2$ according to reactions 2.23 and 2.24. Similar behaviour was also observed for X^- and Cu^{+2} interaction (Alexiev et al., 1984; Yordanov and Velcheva, 1990).

$$2Cu^{+2} + 4DTPI^- \rightleftharpoons 2Cu(DTPI)_2 \qquad 2.23$$

$$2Cu(DTPI)_2 \rightleftharpoons 2CuDTPI + (DTPI)_2 \qquad 2.24$$

Hiçyılmaz et al (2001) studied the interaction between DTPI and platinum electrode by cyclic voltammetry. They obtained a voltammetric peak at about 1250 mV, and estimated the dimer formation consistent with the reaction 2.25.

$$2DTPI^- \rightleftharpoons (DTPI)_2 + 2e \qquad 2.25$$

2.4 Eh-pH Diagrams and Application to Sulphide Flotation

The discovery that charge transfer reactions are involved in the sulphide flotation systems has given rise to new methods of studying complex surface phenomena theoretically. A convenient way of summarising the thermodynamic information related to the stability of simple mineral systems in aqueous solutions is the Eh-pH diagram. The original diagrams of this kind were developed by Marcel Pourbaix (1963) for defining the thermodynamics of metal corrosion systems. Since then Garrells and Christ (1965) have calculated similar diagrams from the point of view of the geologist, who is concerned with the conditions under which minerals are formed and deposited from solutions or hydrothermal systems. Figure 2.4 presents a typical Eh-pH diagram for Cu-Fe-S system.

Several investigators have used this approach to study various flotation systems (Chander and Fuerstenau, 1975; Fuerstenau et al., 1968; Hepel and Pomianowski, 1977; Janetski et al., 1977; Wang et al., 1989). However, most of the thermodynamic calculations done were relatively simple and not comprehensive. Only the stable solid species were considered in these calculations and the soluble species were assumed to have fixed concentrations. This meant that mass-balance and kinetic effects were ignored. It has only been recently that more comprehensive thermodynamic calculations have been undertaken for sulphide flotation systems (Basilio et. al., 1985; Forssberg et. al., 1984; Palsson and Forssberg, 1988, 1989; Pritzker and Yoon, 1984, 1987; Pritzker et. al., 1985). A majority of these investigators considered metastable phases to

account for kinetic limitations caused by the relatively short time scales operative in flotation systems.

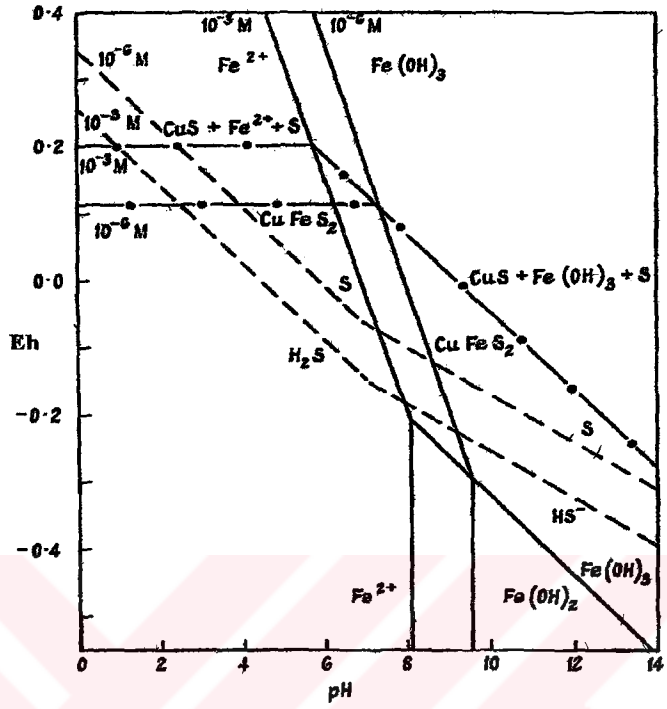

Figure 2.4. Reversible potentials for the $Fe^{+2}/Fe(OH)_2/Fe(OH)_3$ (– – – –), $S/H_2S/HS^{-1}$ (————) and $CuFeS_2/CuS$, $Fe(OH)_3$, S (—•—) systems as a function of pH (Gardner and Woods, 1979).

The usual approach taken in constructing Eh-pH diagrams is appropriate to natural systems of geological interest and geochemical concern, but has a number of limitations when mineral processing is concerned. It takes the total system to be essentially infinite whereas, in mineral processing, the system is closed with mass balance being maintained during the various reactions that take place. Also, Eh-pH diagrams usually portray only stable phases whereas, in the relatively short time scales operative in mineral processing, kinetic limitations may allow the development of metastable phases. The later situation is particularly relevant to the reactions of sulphide minerals due to the irreversibility of sulphate formation (Peters, 1984). In addition, Woods (1971) noted that in his investigation of the

adsorption of xanthate on galena the reaction took place at potentials lower than that the thermodynamically predicted reversible potential. He warns that the use of bulk thermodynamics should be approached with a great deal of cautions.

Since the introduction of Eh-pH diagrams by Pourbaix (1963), all methods of drawing these diagrams followed, basically, the same approach to resolve the competing equilibria. All methods consider the general reaction in which species A is converted to B, the reaction is:

$$aA + wH_2O \rightleftharpoons bB + hH^+ + ne \qquad 2.22$$

where a, w, b, h, and n are stoichiometric parameters. The reduction electrochemical potential is:

$$E_{rew} = \left(\frac{\Delta G^0}{nF}\right) - \left(\frac{2.303RT}{nF}h\right)pH + \frac{2.303RT}{nF}\log\frac{(a_B)^b}{(a_A)^a(a_{H_2O})^w} \qquad 2.23$$

where: ΔG° is the standard free energy charge of reaction 2.22, F is Faraday's constant, R is the gas constant, T is the absolute temperature.

2.5 Surface Spectroscopy

Surface chemistry plays an essential role in many aspects of mineral processing. In particular, an understanding of interaction of different reagents with the mineral surface in an aqueous medium is of crucial importance in achieving the desired beneficiation by flotation (Giesekke, 1983; Marabini et al., 1993).

Although electrochemical techniques provide valuable information on the nature of the surface reactions, they do not yield unequivocal identification of the products formed on the electrode surface. Because, collectors do not always give rise to voltammetric currents that are readily distinguished from background

currents due to other surface processes. For example, voltammetry was found (Yoon and Basilio, 1993) not to provide unequivocal information on the interaction of thionocarbamates at copper electrodes. To obtain information on the detailed nature of such collector/mineral interactions it is necessary to utilise spectroelectrochemical techniques (Piantadosi et al., 2000; Suoninen et al., 1992; Woods et al., 2000).

A number of spectroscopies have been applied to augment electrochemical approaches and provide information on the elemental and molecular composition, the atomic geometry, and the electronic structure of the interface. The spectroelectrochemical techniques that have been most widely applied to flotation systems have involved infrared spectroscopy or Fourier Transform infrared spectroscopy (FTIR). Beside this, there are many spectroscopic techniques to study the surfactant-mineral interaction in flotation: Secondary ion mass spectroscopy, Raman spectroscopy, Auger electron spectroscopy, X-ray photoelectron spectroscopy (XPS), etc.

2.5.1 Infrared spectroscopy

Infrared spectroscopy has found wide acceptance for characterising adsorption on mineral surfaces. An infrared spectrum represents a fingerprint of a sample with absorption peaks that correspond to the frequencies of vibrations between the bonds of the atoms making up the material. Because each different material is a unique combination of atoms, no two compounds produce the exact same infrared spectrum. Therefore, infrared spectroscopy can result in a positive identification of every different kind of material (Termes and Richardson, 1986; ThermoNicolet, 2002). This technique is, however, not sufficiently sensitive when adsorption is low and water interferes seriously with the analysis. Interpretation of the spectra is often difficult, especially when adsorbate orientation effects are involved. The external reflection technique requires a large, smooth, reflecting surface, which may be impossible to obtain for certain minerals. The problems are

accentuated when powdered particles are involved. Mixed mineral powders, such as an actual flotation concentrate from an ore, are almost impossible to investigate (Brinen et al., 1993).

Original infrared instruments were of the dispersive type. These instruments separate the individual frequencies of energy emitted from the infrared source. This was accomplished by the use of a prism or grating. An infrared prism works exactly the same as a visible prism, which separates visible light into its colours (frequencies). A grating is a more modern dispersive element, which better separates the frequencies of infrared energy. The detector measures the amount of energy at each frequency that has passed through the sample. This results in a spectrum, which is a plot of intensity vs. frequency. The dispersive type infrared instruments are time consuming, relatively insensitive and mechanically complex (Marabini et al., 1993; ThermoNicolet, 2002).

Fourier Transform Infrared (FTIR) spectrometry was developed in order to overcome these limitations encountered with dispersive instruments. The main difficulty was the slow scanning process. A method for measuring all of the infrared frequencies simultaneously, rather than individually, was needed. A solution was developed which employed a very simple optical device called an interferometer. The interferometer produces a unique type of signal which has all of the infrared frequencies encoded into it. The signal can be measured very quickly, usually on the order of one second or so. Thus, the time element per sample is reduced to a matter of a few seconds rather than several minutes. Because the analyst requires a frequency spectrum in order to make identification, the measured interferogram signal can not be interpreted directly. A means of decoding the individual frequencies is required. This can be accomplished via a well-known mathematical technique called the Fourier Transformation. This transformation is performed by the computer, which then presents the user with desired spectral information for analysis (Marabini et al., 1993; ThermoNicolet, 2002).

Different experimental techniques are used in the infrared spectroscopy of adsorbed species. The simplest is transmission infrared spectroscopy (KBr disc technique) that does not require a separate accessory. In this technique, the solid, which contains adsorbent (mineral) and adsorbate (collector or other reagent), are dried and mixed with KBr and pressed into a disc that is mounted in the sample beam of the spectrometer. The surfaces are of minerals recovered by flotation is relatively small. In order to increase the amount of reagent adsorbed on the mineral it is ground finer. Such fine minerals are not easily floated in practice but are necessary for recording infrared spectra with commercially available spectrometers, using their scale expansion facility (Giesekke, 1983).

The KBr disc technique is a useful means of studying adsorbed reagents on the mineral but remains an ex-situ technique, so that any detail about the adsorbate in an in-situ situation is lost. It is not possible to obtain in-situ measurements since the absorption spectrum of the water present in the solution would cover a good part of the analytical range of the experimental spectrum. In the case of chemisorption phenomena, one of the main drawbacks is that the solid residue may well contain not only the mineral and the surface-adsorbed species but also any agglomerated formed in solution and precipitated in bulk form. In order to get around this limitation, a method has been developed which involves double filtering of the treated mineral (Marabini and Cozza, 1988). Further, it is always assumed that the adsorbent and adsorbate do not interact with the KBr during the pressing of the disc (Giesekke, 1983; Marabini et al., 1993).

The Attenuated Total Reflection (ATR) method is the one most commonly used infrared spectroscopy technique for the surface study of mineral/aqueous-solution interactions. This method provides information on thin surface layers. An attenuated total reflection accessory operates by measuring the changes that occur in a totally internally reflected infrared beam when the beam comes into contact with a sample. An infrared beam is directed onto an optically dense crystal with a high refractive index at a certain angle. This internal reflectance creates an evanescent wave that extends beyond the surface of the crystal into sample held in

contact with the crystal. In regions of the infrared spectrum where the sample absorbs energy, the evanescent wave will be attenuated. The altered (attenuated) energy from each evanescent wave is passed back to the IR beam, which then exits the opposite end of the crystal and is directed at the detector in the IR spectrometer. The detector records the attenuated IR beam as an interferogram signal, which can then be used to generate an infrared spectrum. For FTIR-ATR, minimal sample preparation is required and samples can be analysed in their natural state. Cleaning the surface of the crystal is fast and easy (Giesekke, 1983; Marabini et al., 1993; ThermoNicolet, 2002).

Another technique is Diffuse Reflectance Infrared Fourier Transformation (DRIFT) spectroscopy. It requires almost always the sample as a powder. The quality of DRIFT spectra is enhanced with decreasing range of the particle size (Baulsir and Tague Jr., 2002; Persson, 1991). A diffused reflectance accessory operates by directing the infrared energy into a sample cup. The infrared radiation then interacts with the particles by interacting with them and reflecting off their surfaces, causing the light to diffuse, or scatter, as it moves throughout the sample. The detector records the altered IR beam as an interferogram signal, which can then be used to generate a spectrum (ThermoNicolet, 2002). DRIFT technique is applied with little or no sample preparation. Since there is no need for KBr pellets; only, sample is placed into a sample cup. Between each experiment, sample cup is carefully cleaned to prevent any contamination (Baulsir and Tague Jr., 2002).

FTIR spectroscopy has most widely been applied to investigate the xanthate adsorption on sulphide minerals (Leppinen et al., 1988; Bozkurt, 1998; Persson and Malmensten, 1991; Woods et al., 1995; Zhang et al., 1993; etc.). However, few studies have been made for DTP and DTPI (e.g. Goold and Finkelstein, 1972; Kim, 1995).

CHAPTER 3

MATERIALS AND METHODS

3.1 Material Preparation and Analysis

High purity chalcopyrite samples and highly mineralised chalcopyrite rock specimens were obtained from Artvin-Murgul deposit, Turkey. For infrared spectroscopy and microflotation experiments, high purity chalcopyrite samples were first ground in an agate mortar and pestle and screened in a size fraction of –212+150 μm. Then, sized samples were cleaned from its contaminated gangue (major gangue minerals are quartz and pyrite) with electrostatic separator (Boxmag-Rapid Ltd.) and dry magnetic separator (Carpco Research and Eng., Inc.). Cleaned chalcopyrite samples, having 96.07 % $CuFeS_2$ grade, were packaged into nylon bags, preventing direct contact with atmosphere. Chemical analysis of sample was made by atomic absorption spectroscopy (Table 3.1).

Table 3.1: Chemical analysis of –212+150 μm chalcopyrite sample

Element	Amount, %
Cu	33.24
Fe	31.55
Si	0.28

Highly mineralised chalcopyrite rock specimens were used to make working electrode. Analyses of specimens were made by different methods. At first specimens were examined under a mineral microscope. It was observed that these specimens were highly pure: Quartz and sphalerite in trace amounts as

gangue were seen on the surface of particle. Same samples were investigated with scanning electron microscopy (Appendix A), and only sphalerite could be seen in trace amount on the surface. Finally, chemical analyses were made by atomic absorption spectroscopy (Table 3.2) and its chalcopyrite content was calculated as 98.99 % $CuFeS_2$.

Table 3.2: Chemical analysis of massive specimen of chalcopyrite

Elements	Amount, %
Cu	34.25
Fe	30.21
Si	0.22
Zn	0.16

Cyclic voltammetry, microflotation and spectroscopic studies were conducted in four different buffer solutions. The compositions of buffers used were given in Table 3.3. All the chemicals used for buffer preparation were in analytical grade. Buffer solutions were used in order to prevent the changes that might occur in the pH of the solution as a result of the reactions that might take place between the mineral and the aqueous solution (Garrels and Christ, 1965).

Table 3.3: The composition of the buffer solutions

PH	Composition of the solution
4.67	0.5 M CH_3COOH + 0.5 M CH_3COONa
6.97	0.025 M KH_2PO_4 + 0.025 M Na_2HPO_4
9.20	0.05 M $Na_2B_4O_7$
11.00	0.025 M $NaHCO_3$ + 0.023 M NaOH

Buffer solution was de-oxygenated with high-purity nitrogen (Table 3.4) before each run. Intensive bubbling of nitrogen was applied for 15 minutes to eliminate the effects of dissolved oxygen on experimental results (Ekmekçi, 1995). During experiment, the flow of nitrogen was stopped and experimental

condition was completely sealed to prevent the diffusion of atmospheric oxygen into the cell.

Table 3.4: Analysis of nitrogen gas (BOS Co.)

Nitrogen (%)	99.998
Oxygen (vpm)	1.6
Moisture (vpm)	1.5

Collectors investigated were potassium diethyl dithiophosphate (DTP) and sodium diisobutyl dithiophosphinate (DTPI). DTP is a product of Aldrich Chem. Co. It is in analytical grade (97 % DTP) having a formula weight of 224.33 g. DTPI is a commercial product under the name of AEROPHINE 3418A of Cytec Technology Co. Its assay is 50-52 % DTPI and it has a formula weight of 232.326 g. Some physical properties of DTPI were given in Table 2.1. DTP and DTPI were analysed with Nuclear Magnetic Resonance (NMR) spectroscopy (Appendix B). Their chemical formulas would be written as follows according to NMR spectroscopy results:

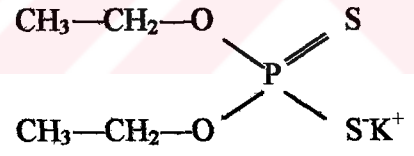

Potassium di-ethyl dithiophosphate

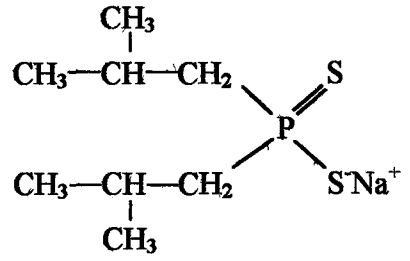

Sodium di-isobutyl dithiophosphinate

Dimers of DTP and DTPI were prepared applying the method cited in literature (Kakovskii et al, 1959): At first, I_3^- was prepared (reaction 3.1). Then, it

was mixed with collector solutions (DTP and DTPI) and dimer formation occurred (reaction 3.2).

$$I_2 + KI \rightleftharpoons I_3^- + K^+ \qquad 3.1$$

$$I_3^- + 2DTP^- \rightleftharpoons 3I^- + (DTP)_2 \qquad 3.2$$

When compared with the NMR spectra of monomer and dimer of DTP and DTPI, major shift is expected in the position of ^{31}P peak as shown in Appendix B. Therefore, this may shows us dimer formation.

In literature, it was stated that when Cu^{+2} and DTP^- ions are reacted, first $Cu(DTP)_2$ forms according to reaction 3.3 and then immediately CuDTP+$(DTP)_2$ precipitate is obtained consistent with the reaction 3.4 (Rudzinski et al., 1980; Yordanov et al., 1983, 1998; Yordanov and Ranguelova, 2001). Goold and Finkelstein (1972) proposed that decomposition of $Cu(DTP)_2$ into CuDTP and $(DTP)_2$ (reaction 3.4) is very slow in alkaline solution. Similar behaviour was also proposed for DTPI (Yordanov et al., 1983). Therefore, CuDTP+$(DTP)_2$ and CuDTPI+$(DTPI)_2$ precipitates were prepared in slightly acid solution (pH 4.67) by interacting 10^{-2} M collector solution with 10^{-2} M $CuSO_4$: A brownish yellow solid was precipitated in reddish brown solution in the case of DTP. On the other hand, a pale yellow precipitate was obtained from greenish yellow solution in the case of DTPI. The precipitates were washed with distilled water five times to remove possible contaminants.

$$2Cu^{+2} + 4DTP^- \rightleftharpoons 2Cu(DTP)_2 \qquad 3.3$$

$$2Cu(DTP)_2 \rightleftharpoons 2CuDTP + (DTP)_2 \qquad 3.4$$

3.2 Equipment and Procedure

3.2.1 Voltammetry Experiments

In order to determine the electrochemical reactions occurring on chalcopyrite surface depending on pH in an aqueous medium, cyclic voltammetry experiments were conducted. Voltammetry experiments were performed between +650 mV and –500 mV in pH 4.67 and pH 6.97 buffer solutions, and between +500 mV and –500 mV in pH 9.2 and pH 11 buffer solutions. Such scan limits were selected according to previous works (Ekmekçi, 1995; Gardner and Woods, 1979) to observe the $CuFeS_2$ oxidation peak to CuS and then oxidation of CuS in anodic region and to obtain clearly the reduction peaks of oxidation products in cathodic region. For voltammetry experiments, a conventional three-electrode system was employed (Figure 3.1).

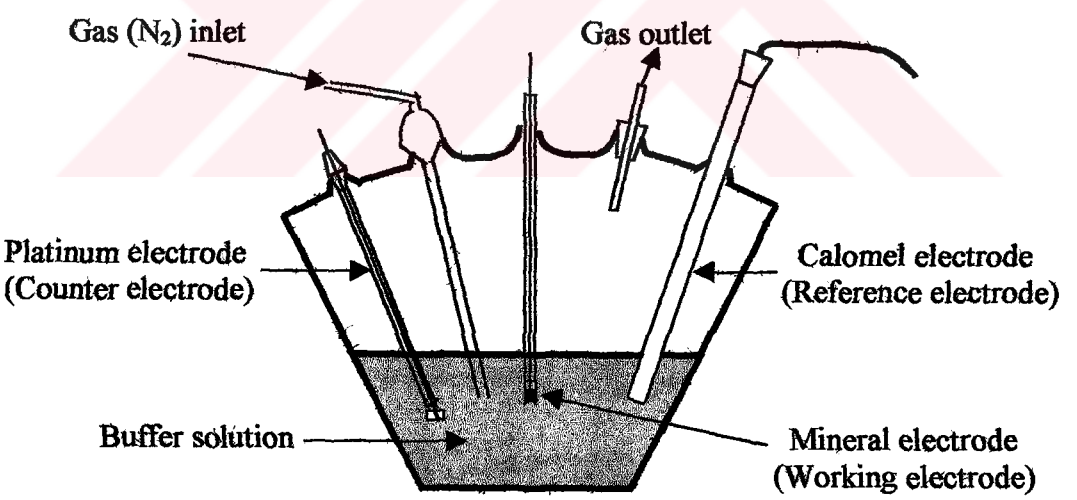

Figure 3.1. Three-electrode system for electrochemical investigations

Calomel, platinum and chalcopyrite electrodes were used as reference, counter and working electrodes, respectively. Pulp potential was controlled in the electrochemical, flotation and spectroscopic measurements with a Bank Elektronik Wenking PGS95 potentiostat/galvanostat and a Zyklo computer program.

Although a standard calomel electrode (SCE) was used as the reference electrode, the potentials reported here are all expressed on the standard hydrogen electrode (SHE) scale taking the potential of the SCE to be 0.245 V vs. SHE (Garrels and Christ, 1965):

$$E_{SHE} \rightleftarrows E_{SCE} + 245 \qquad 3.5$$

Platinum electrode was constructed from a glass tube, platinum wire of 0.5 mm in diameter, and a 1 cm^2 platinum plate having 0.5 mm thickness (Figure 3.2a). Platinum wire and plate were connected to each other with Ag welding. Before each experiment, platinum electrode was dipped into chromic acid to clean the surface. It was also cleaned in ultrasonic bath, by burning and by polishing with 1000 grid Si-carbide paper.

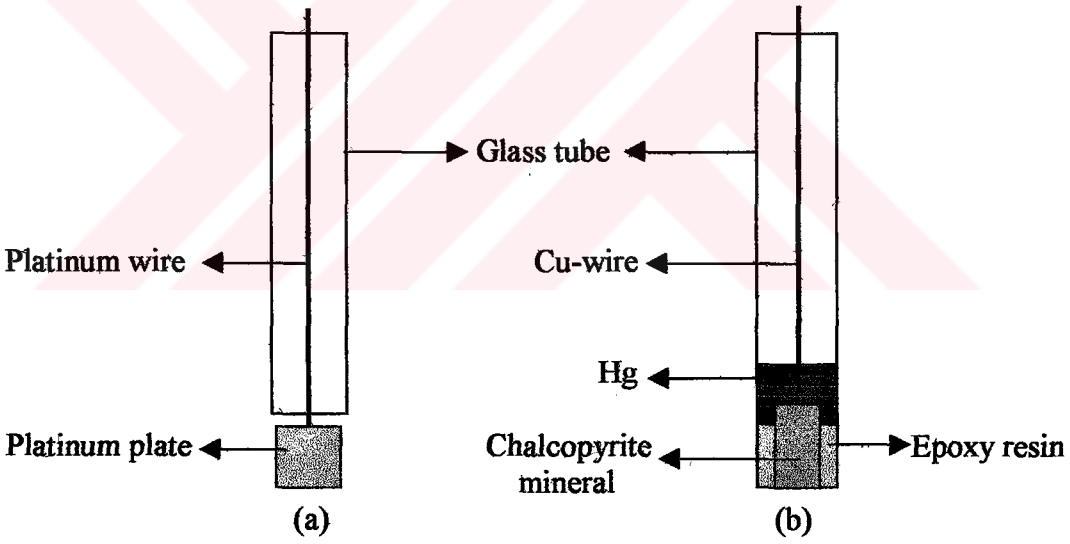

Figure 3.2. Counter and working electrodes used in electrochemical and flotation experiments: (a) Platinum (counter) electrode; (b) Chalcopyrite (working) electrode.

Working electrode was prepared from a massive specimen of chalcopyrite. The chalcopyrite specimen with a rectangular cross-section, having a cross-sectional area of 0.2346 cm^2, was cut from a larger piece. This specimen was mounted in a glass tube with an epoxy resin, namely Araldite, which has no

electrochemical activity (Figure 3.2b). Mineral electrode was connected to potentiostat with a Cu wire. Electrical conductivity between copper wire and mineral specimen was satisfied by using Hg. A cleaned surface was produced before each run by wet grinding on 800-grit silicon carbide paper and then by polishing with 1 μm diamond paste. After polishing the surface, the electrode was rinsed with distilled water and immediately transferred to the cell.

3.2.2 DRIFT Study

Cleaned chalcopyrite sample was used for DRIFT study. Sample was ground finely in an agate mortar just before each experiment. Then, 200 mg of it was put into a conditioning cell containing de-oxygenated buffer solution and collector (10^{-1} M) (Figure 3.3). In polarisation experiments, a platinum wire of 45 cm length and 0.5 mm diameter was used as working electrode. Also, calomel electrode and 1 cm^2 platinum plate were used as reference and counter electrodes, respectively.

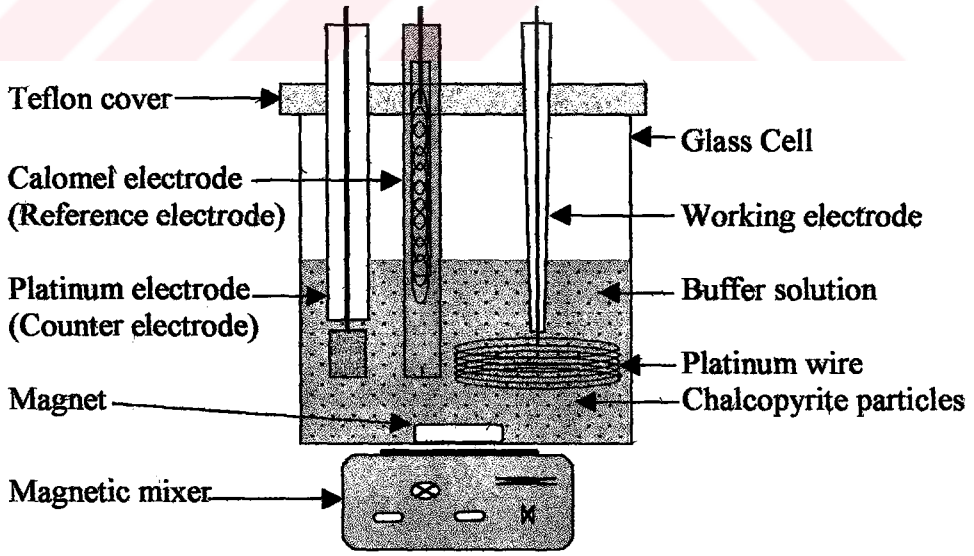

Figure 3.3. Polarisation cell for DRIFT study

Finely ground sample was conditioned for 15 minutes at predetermined potential. Then it was washed five times with distilled water to remove possible

contaminants coming from buffer solution and physically adsorbed species from mineral surface. After washing, it was dried for five hours at 35°C.

DRIFT spectra of dried samples were obtained on a Bruker Equinox 55 spectrometer equipped with a DTGS detector. The reflection and optical accessories were from Harrick Scientific Co. All spectra were recorded by averaging 100 scans at a resolution of 4 cm^{-1}. In collector adsorption study, non-treated finely ground chalcopyrite sample was used as background.

DRIFT spectra of monomer and dimer of collectors, CuDTP+$(DTP)_2$ and CuDTPI+$(DTPI)_2$ precipitates were obtained as reference. In these experiments, potassium bromide was used as non-absorbing matrix and background. For these spectra, 2-3 mg sample was mixed with ~100 mg KBr. DRIFT spectra of platinum polarised with 10^{-1} M DTP at 750 mV and with 10^{-1} M DTPI at 1250 mV in slightly acid solution (pH 4.67) were also measured. Collectors are expected to adsorb as dimer on platinum surface as depicted in literature (Hiçyılmaz et al., 2001; Shubov et al., 1976). For these spectra, untreated platinum was used as background.

3.2.3 Microflotation

Microflotation tests were conducted to investigate the effect of pulp potential at different pH values with DTP and DTPI on chalcopyrite recovery. For comparison, self-induced (without collector) flotation tests were also made. Flotation tests were made with 1 gram –212+150 μm size chalcopyrite samples.

A three electrode modified Hallimond tube (Ekmekçi, 1995) similar to that described by Fuerstenau et al. (1957) was used in microflotation tests (Figure 3.4). Tube had an effective volume of 125 ml. Reference and counter electrodes were connected with micro openings to the chamber where flotation occurred. Before

each experiment, hollows for reference and counter electrodes were filled with saturated NaCl solution to satisfy electrical conductivity between three electrodes.

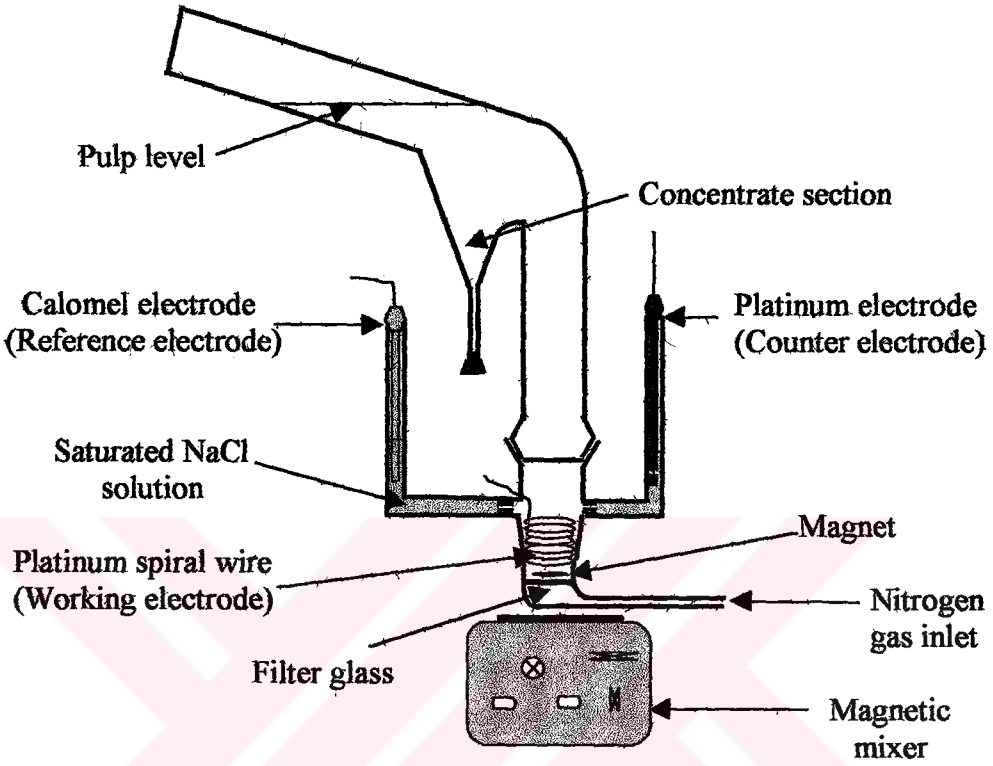

Figure 3.4. Modified Hallimond tube

Platinum and calomel electrodes were used as counter and reference electrodes, respectively. A platinum spiral wire having 0.5 mm diameter and 45 cm length was used as working electrode. The platinum wire was placed in a way that the maximum contact of the chalcopyrite particles with the platinum wire was ensured in order for the chalcopyrite particles to gain the same potential with that of the platinum wire during polarisation stage. To ensure the maximum contact of the chalcopyrite particles with the platinum wire, the polarisation was applied for 15 minutes. Pulp potential was controlled with a Bank Elektronik Wenking PGS95 potentiostat.

Flotation tests were conducted in pH 4.67, 6.97, 9.2 and 11 buffers solutions (Table 3.3). All the solutions were deoxygenated intensively for 15

minutes prior to each experiment. The feeding of buffer solution to the flotation cell was realised in a closed system to prevent the diffusion of the atmospheric oxygen into the cell (Figure, 3.5). After feeding buffer into flotation chamber, 15 minutes polarisation was applied, and then flotation was started. During polarisation and flotation, particles were kept in suspension by a magnetic stirrer. Nitrogen gas was used as the gaseous phase to carry the mineral particles to the collecting section. At the end of the experiment, gas flow was terminated and the magnetic stirrer was turned off. Concentrate and tailing products were taken from Hallimond tube and then dried and weighed. Concentrate recovery was calculated as the weight percentage of the concentrate to feed (1 g = concentrate + tailing).

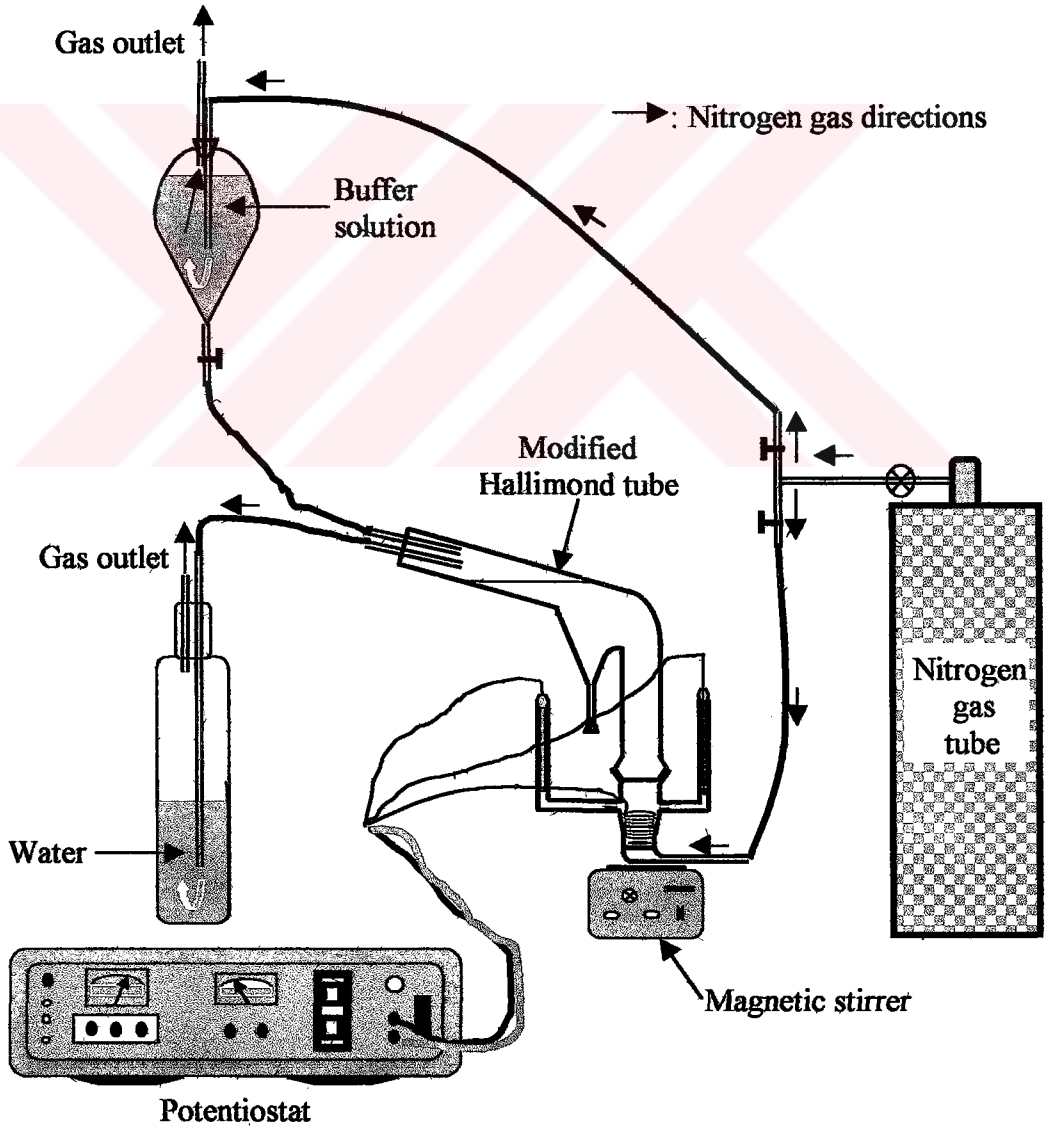

Figure 3.5. Experimental setup for microflotation tests

CHAPTER 4

RESULTS

4.1 Cyclic Voltammetry

Cyclic voltammograms were performed to determine the redox reactions taking place on the chalcopyrite surface. The electrochemical behaviour of the mineral was examined at different pH (4.67, 6.97, 9.2 and 11) and scan rates (5 mV/s, 10 mV/s, 20 mV/s and 50 mV/s) in the presence and absence of DTP and DTPI.

4.1.1 pH 4.67

4.1.1.1 Cyclic Voltammograms of Chalcopyrite in Collectorless Condition in pH 4.67

Cyclic voltammogram of chalcopyrite measured in pH 4.67 buffer solution at 50 mV/s scan rate (v) is given in Figure 4.1. Potential was cycled five times between initial potential (650 mV vs. SHE) and reverse potential (-500 mV vs. SHE) to show the effect of cycling.

The scan was started at +650 mV in cathodic direction. In anodic region, two small peaks appeared at ~190 mV (peak A1) and ~340 mV (peak A2). In cathodic region, a sharp peak (K1) appeared at ~ –380 mV. In the first cycle,

current densities of peaks were lower than second one. In the following cycles, current density decreased. Moreover, a different anodic peak (A3) started to occur above 400 mV in anodic direction and its current density increased with increasing the number of cycle.

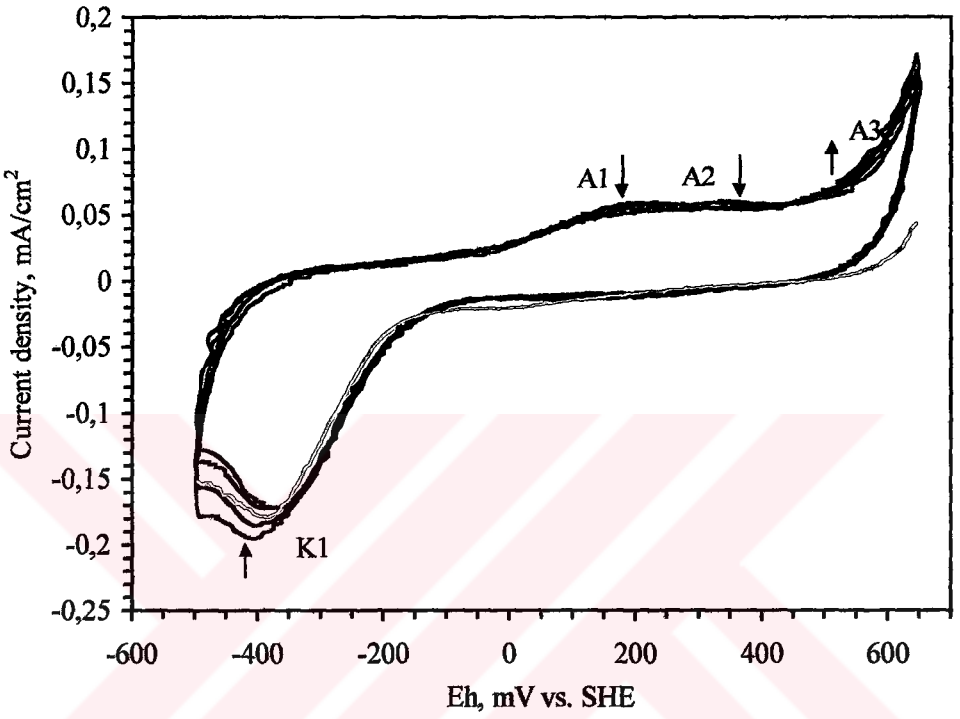

Figure 4.1. Cyclic voltammogram of chalcopyrite (pH 4.67, v = 50 mV/s)

In order to determine which anodic peak was related with which cathodic peak, a voltammogram was recorded by cycling from different set potentials (Figure 4.2). The scan was started at –100 mV in cathodic direction and voltammogram was obtained cutting the potential from 250 mV, 450 mV and 650 mV in anodic region and from –500 mV in cathodic region at subsequent cycles.

Current density increased with starting the scan initially in cathodic direction, but peak K1 did not appear. When cycling proceeded, peak A1 formed and in the reverse scan it resulted in peak K1. In the following cycle reversed from 450 mV, peak A2 developed. In the last cycle, peak A3 appeared in anodic scan and it resulted in a new broad peak K2 starting at about 380 mV in cathodic

region. The peak K2 was not clearly distinguished cyclic voltammogram in Figure 4.1.

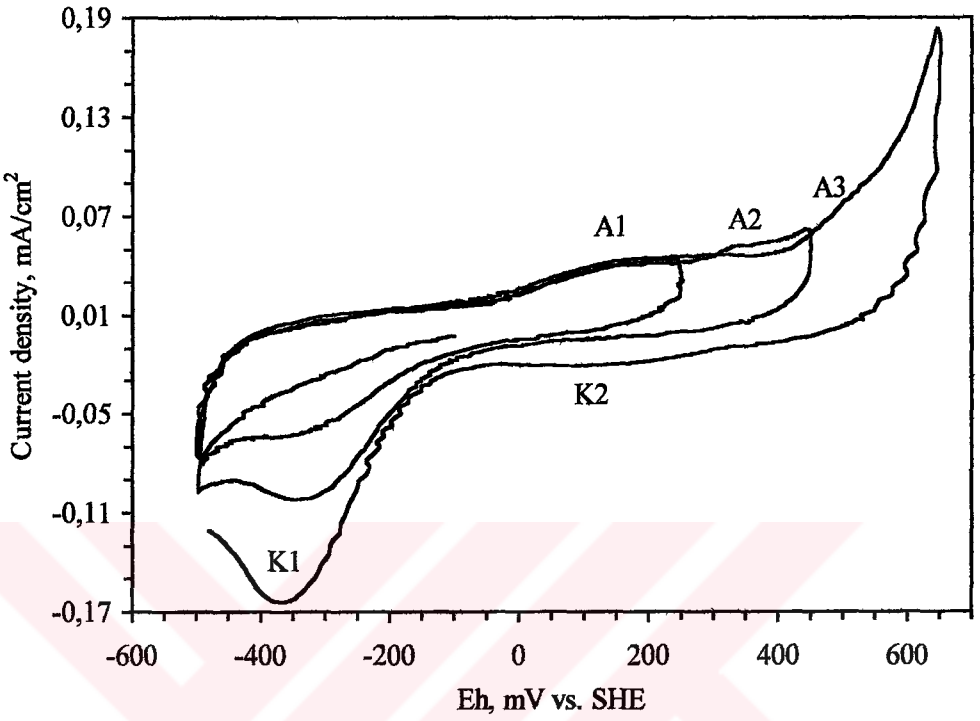

Figure 4.2. Controlled sweep voltammogram of chalcopyrite (pH 4.67, v = 50 mV/s)

Voltammograms were also drawn at 10 mV/s and 20 mV/s scan rates with cycling the potential five times to determine the effects of scan rate and number of cycles on peak potential and peak current density, (Figure 4.3-4.4). In the first cycles of these voltammograms, K1 appeared at higher cathodic potentials as compared with other cycles. Peak K2, which emerged only in controlled sweep voltammogram at 50 mV/s scan rate, formed as a shoulder and as a sharper peak at 20 mV/s and at 10 mV/s scan rates, respectively.

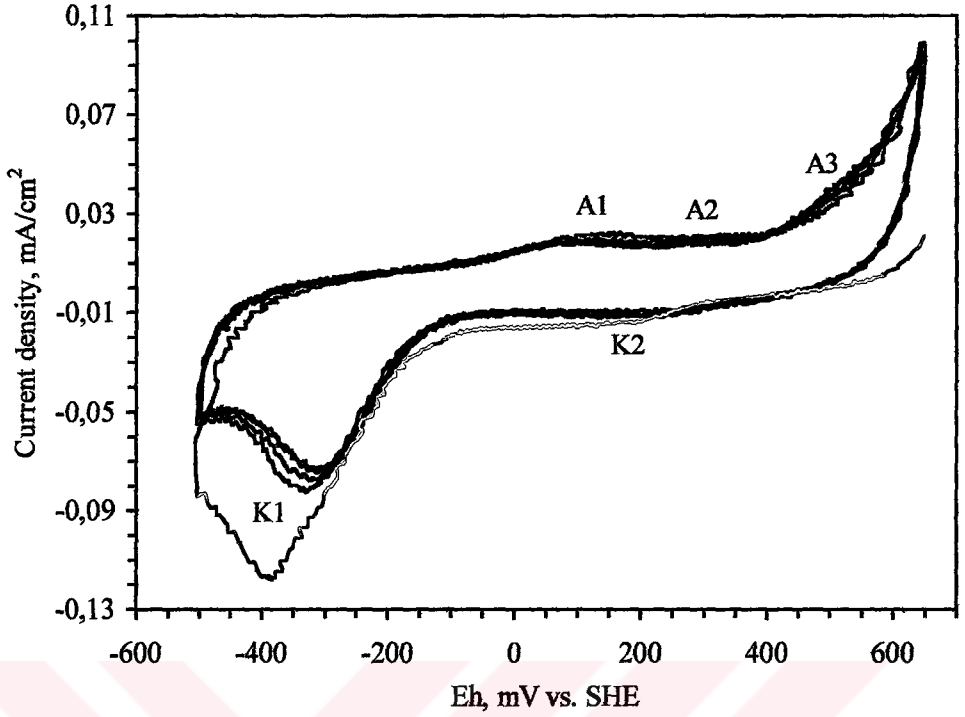

Figure 4.3. Cyclic voltammogram of chalcopyrite (pH 4.67, v = 20 mV/s)

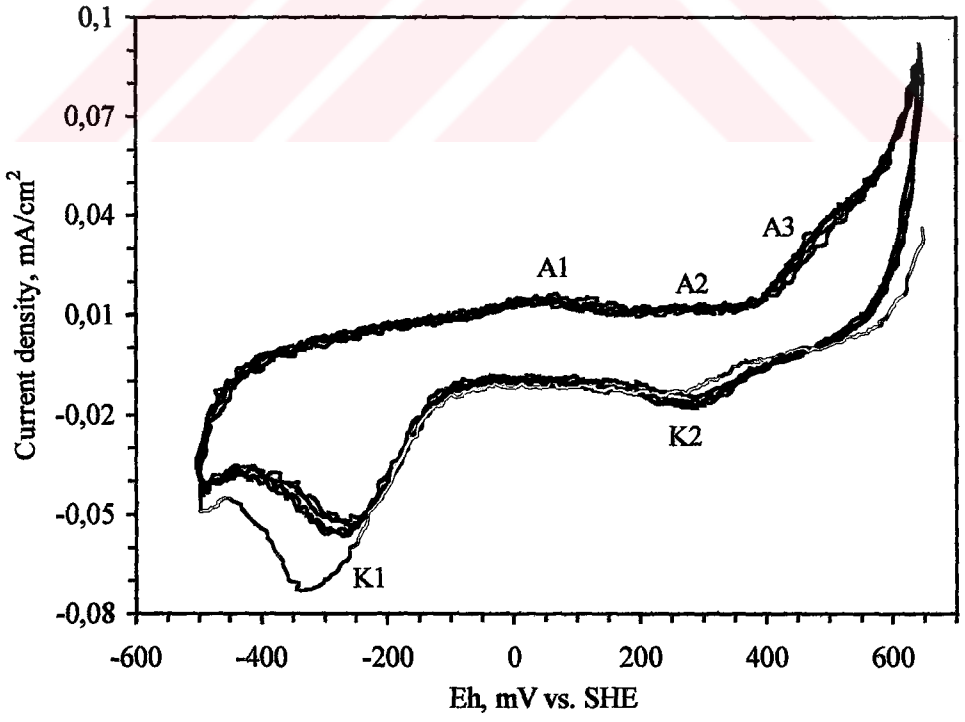

Figure 4.4. Cyclic voltammogram of chalcopyrite (pH 4.67, v = 10 mV/s)

The fifth cycles of all scan rates applied in the study are combined in Figure 4.5 for a clear demonstration of the effect of scan rate on peak potential and peak current density. The last cycle was chosen, because, with an increase in the number of cycle, experimental conditions come closer to equilibrium. In addition, Figures 4.6 and 4.7 were also drawn to show the effect of scan rate on formation potentials and current densities of redox peaks, respectively. Figures 4.5 and 4.6 show that peak positions of A1 and A2 were shifted to more oxidising potentials with increasing the scan rate, whereas that of K1 moved to more reducing potential. Moreover, increasing the scan rate resulted in the higher current densities for all oxidation and reduction peaks. It should be also mentioned here that there is a non-linear relationship between current density of anodic and cathodic peaks and square-root of scan rate as shown in Figure 4.7.

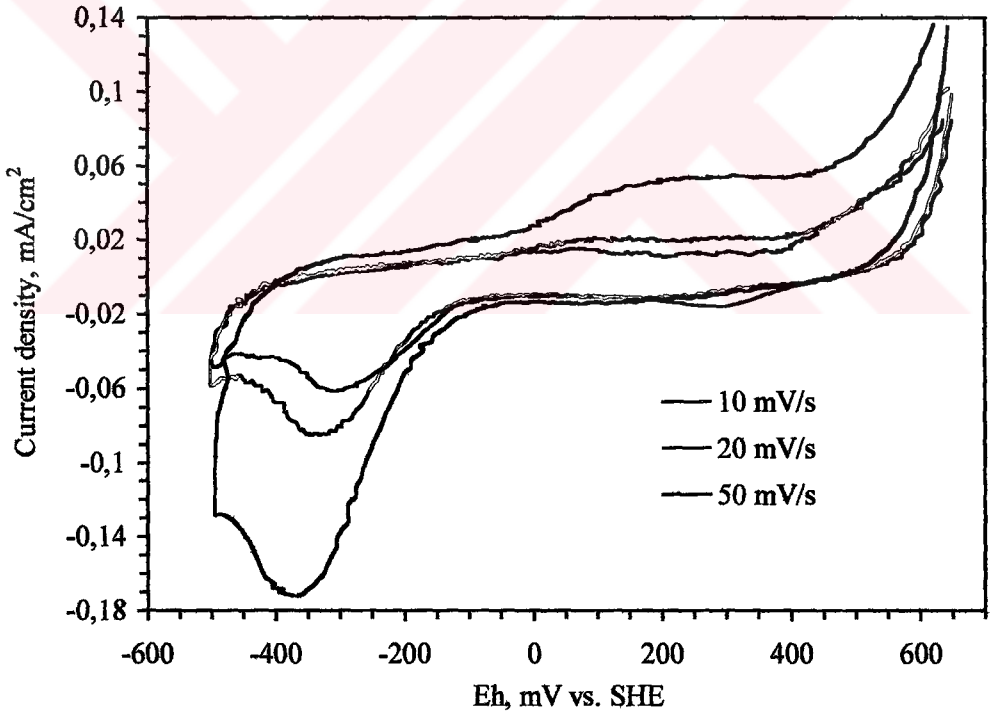

Figure 4.5. Cyclic voltammograms of chalcopyrite for different scan rates at pH 4.67

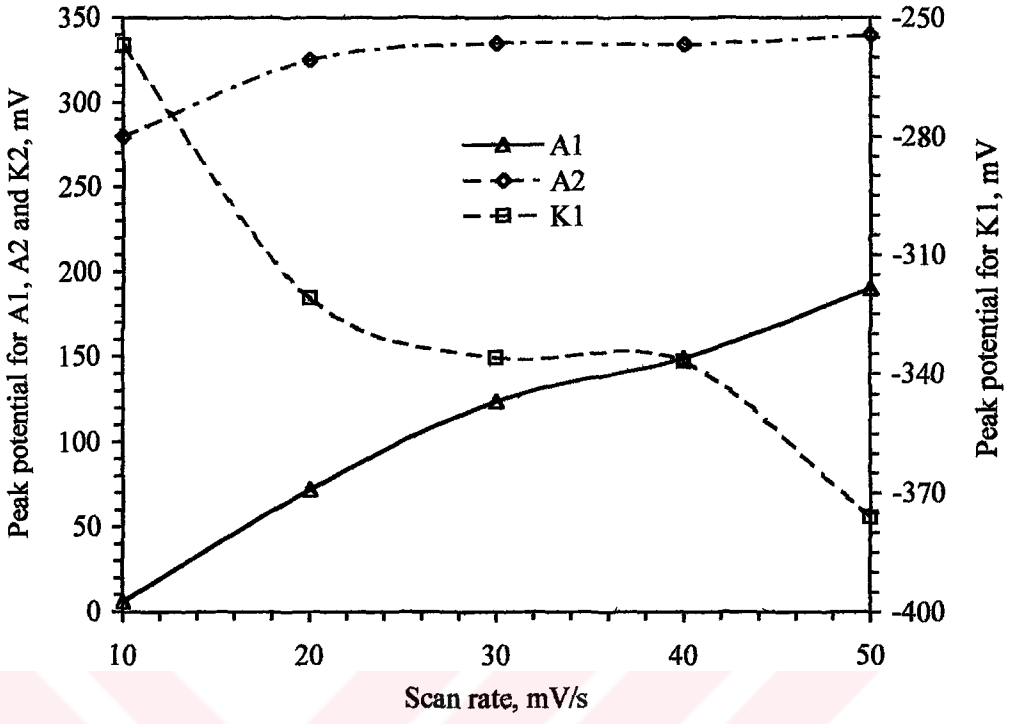

Figure 4.6. Relationship between formation potentials of peaks and scan rate

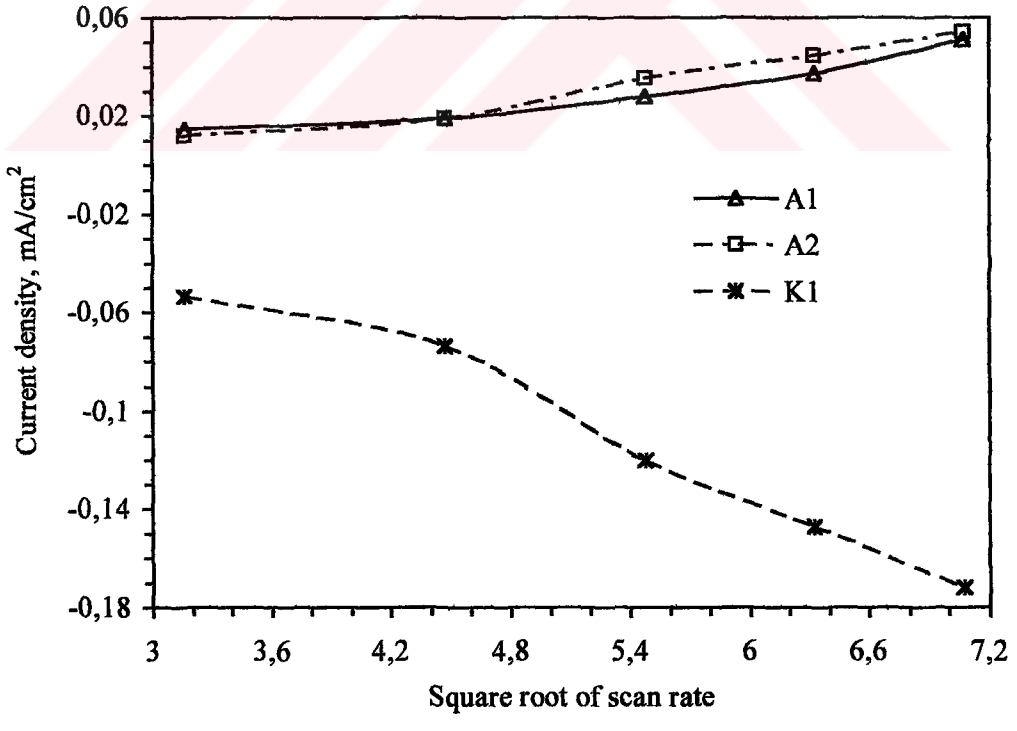

Figure 4.7. Relationship between current density of peaks and square-root of scan rate

4.1.1.2 Cyclic Voltammograms of Chalcopyrite in the Presence of DTP in pH 4.67

Chalcopyrite electrode surface was swept at 50 mV/s scan rate in the presence of DTP at 10^{-4} M, 10^{-3} M and 10^{-2} M concentrations (Figures 4.8-4.10). Surface scan was applied between +650-500 mV for five cycles. A new peak formation was not observed on the cyclic voltammograms performed in the presence of DTP as compared with collectorless condition (Figure 4.1). On the other hand, present peaks disappeared when collector concentration was increased. This situation can be seen clearly in Figure 4.11. This figure was drawn with the last cycles of voltammograms presented in Figures 4.1 and 4.8-4.10 to show the effect of DTP concentration on chalcopyrite electrode. As seen in the figure, current density decreased with increasing collector concentration.

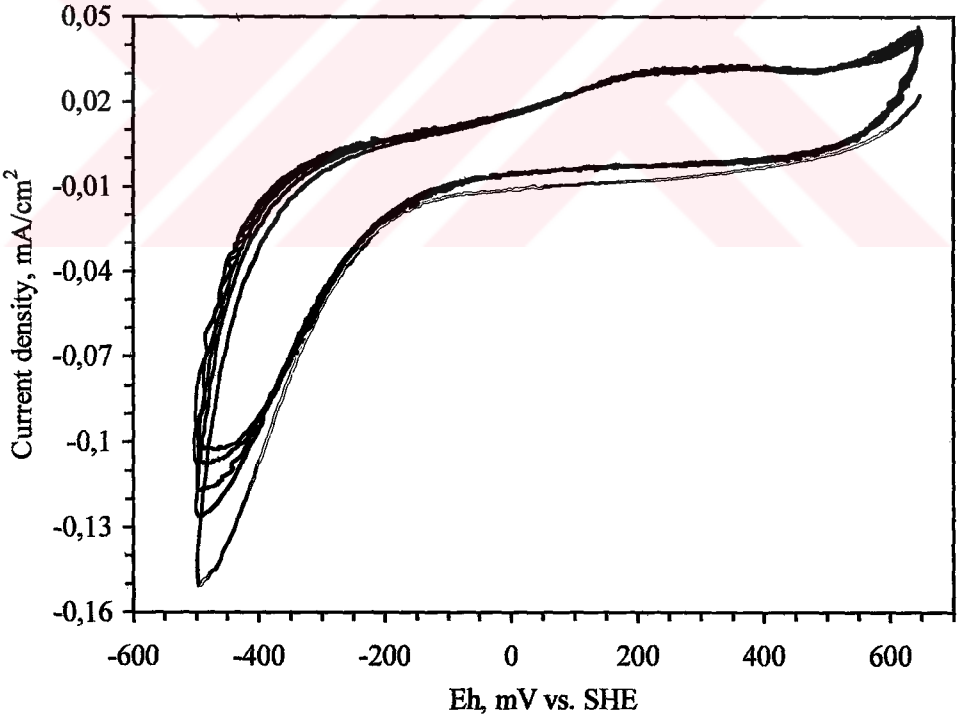

Figure 4.8. Cyclic voltammogram of chalcopyrite (pH 4.67, DTP = 10^{-4} M, v = 50 mV/s)

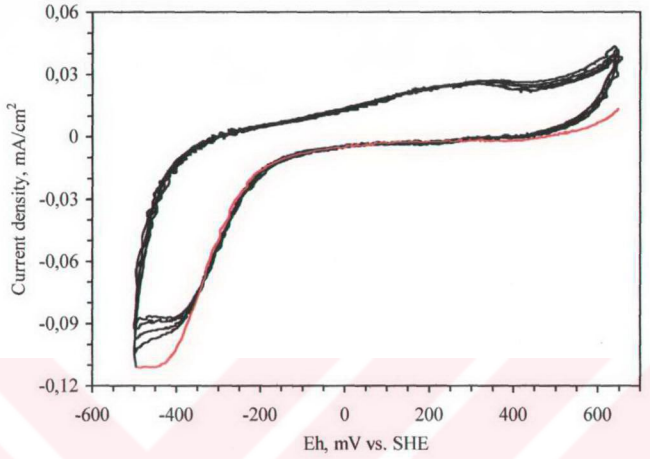

Figure 4.9. Cyclic voltammogram of chalcopyrite (pH 4.67, DTP = 10^{-3} M, v = 50 mV/s)

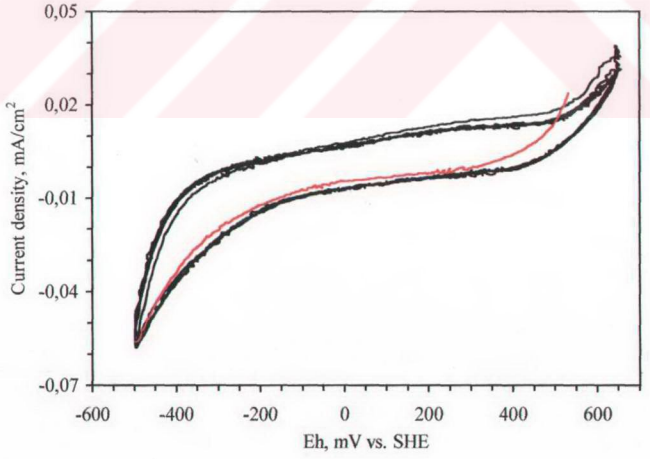

Figure 4.10. Cyclic voltammogram of chalcopyrite (pH 4.67, DTP = 10^{-2} M, v = 50 mV/s)

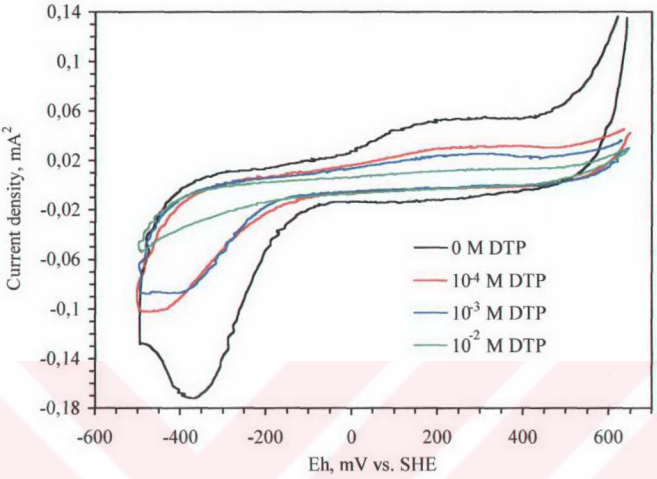

Figure 4.11. Cyclic voltammograms of chalcopyrite for 0 M, 10^{-4} M, 10^{-3} M and 10^{-2} M DTP (pH 4.67, v: 50 mV/s)

4.1.1.3 Cyclic Voltammograms of Chalcopyrite in the Presence of DTPI in pH 4.67

Figure 4.12-4.14 present the electrochemical spectra of chalcopyrite electrode obtained in pH 4.67 buffer solution containing 10^{-4} M, 10^{-3} M and 10^{-2} M DTPI. Surface scan was applied between +650-500 mV for five cycles at 50 mV/s scan rate. No new peak was observed on the voltammograms in the presence of DTPI as compared with collectorless condition (Figure 4.15). However, existing peaks with no collector disappeared with an increase in collector concentration. Figure 4.15 was drawn with the last cycles of voltammograms given in Figures 4.1 and 4.12-4.14 to clearly show the effect of DTPI concentration on chalcopyrite electrode. An increase in DTPI concentration resulted in a decrease in current density.

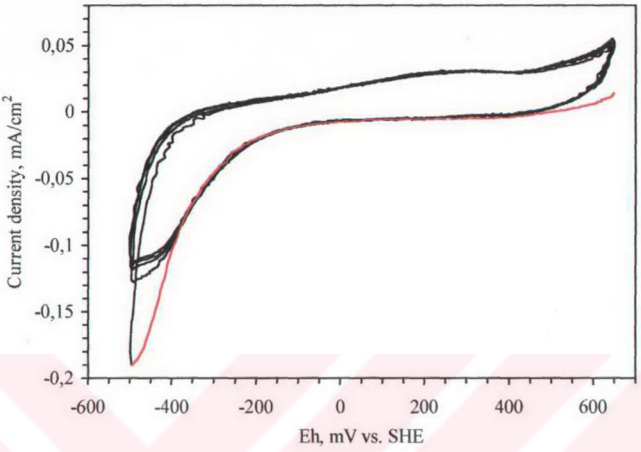

Figure 4.12. Cyclic voltammogram of chalcopyrite (pH 4.67, DTPI = 10^{-4} M, v = 50 mV/s)

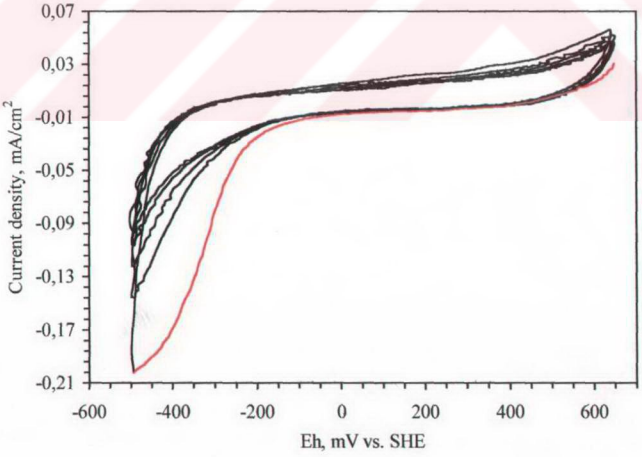

Figure 4.13. Cyclic voltammogram of chalcopyrite (pH 4.67, DTPI = 10^{-3} M, v = 50 mV/s)

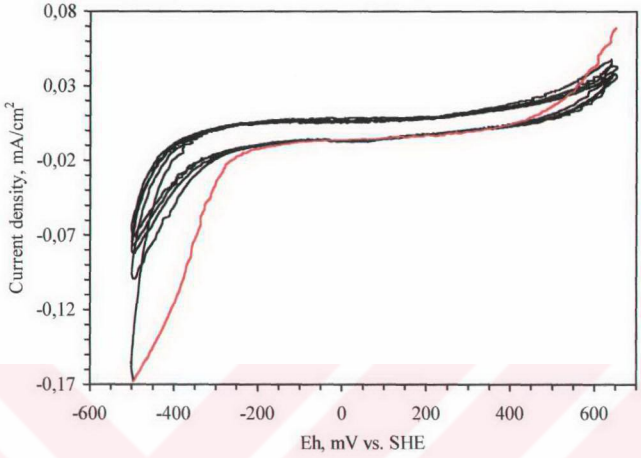

Figure 4.14. Cyclic voltammogram of chalcopyrite (pH 4.67, DTPI = 10^{-2} M, v = 50 mV/s)

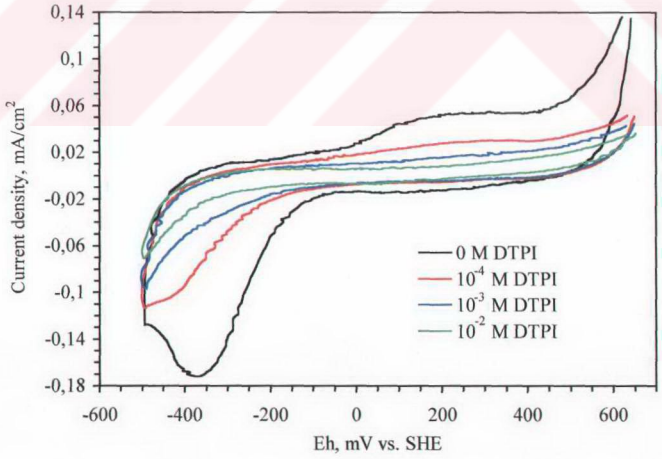

Figure 4.15. Cyclic voltammograms of chalcopyrite for 0 M, 10^{-4} M, 10^{-3} M and 10^{-2} M DTPI (pH 4.67, v: 50 mV/s)

4.1.2 pH 6.97

4.1.2.1 Cyclic Voltammograms of Chalcopyrite in Collectorless Condition in pH 6.97

The cyclic voltammogram of chalcopyrite in pH 6.97 buffer solution at 50 mV/s scan rate is shown in Figure 4.16. Potential was cycled five times between initial potential (650 mV) and reverse potential (-500 mV) to show the effect of cycling. Scan was started at +650 mV in cathodic direction. Three anodic (A1, A2 and A3) and three cathodic (K1, K2 and K3) peaks appeared at ~ –30 mV (peak A1), ~270 mV (peak A2), ~500 mV (peak A3), ~ –315 mV (peak K1), ~100 mV (peak K2) and ~275 mV (peak K3).

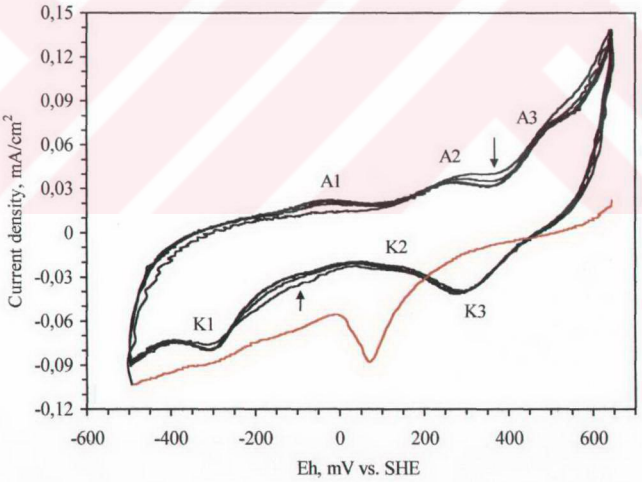

Figure 4.16. Cyclic voltammogram of chalcopyrite (pH 6.97, v = 50 mV/s)

In the first cycle, the peak K2 was very sharp at about 70 mV. In the following cycles, such a sharp peak was not observed at this potential. But, there

is a shoulder around 100 mV exhibiting that this reduction reaction sustains in the following cycles in a minor scale. In the succeeding cycles, current density of this peak did almost not change. Further, peak K1 and A1 can not be seen in the first cycle. In the latter cycles, they appeared clearly approximately at the same current densities. Peak A2 was observed at lower current densities with progress in the cycling.

In order to determine which anodic peak was related with which cathodic peak, a voltammogram was also measured at 50 mV/s scan rate by cycling from desired potentials (Figure 4.17). Scan was started at –200 mV in cathodic direction and voltammogram was measured cutting potential from 100 mV, 350 mV, 550 mV and 650 mV in anodic region and from –500 mV in cathodic region in sequencing cycles.

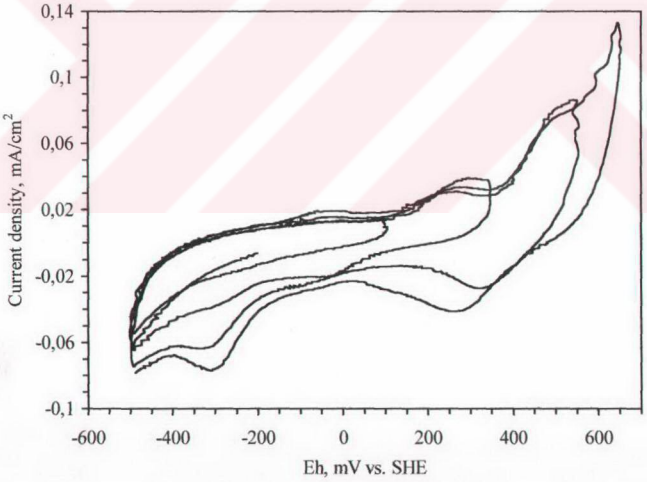

Figure 4.17. Controlled sweep voltammogram of chalcopyrite (pH 6.97, v = 50 mV/s)

When starting the scan initially in cathodic direction at –200 mV, no peak formation occurred. Again, when it was reversed from 100 mV, peaks A1 and K1 could not be seen clearly. Reversing scan from 350 mV resulted in the formation of peak A2 and K1. Additionally, a new peak also formed at ~ –40 mV in the cathodic sweep in this cycle. This new peak disappeared between cathodic peaks in the following cycles. However, as shown in Figure 4.16, a cathodic reduction reaction proceeded around –40 mV in cathodic scan and its peak could not be distinguished clearly due to larger cathodic peaks.

In the following cycle, reversed from 550 mV, peak A3 appeared at about 500 mV in anodic scan and, in the reverse sweep it caused the formation of K3 at about 330 mV in cathodic region. In the last cycle reversed from 650 mV, all cathodic and anodic peaks formed. However, peak K3 appeared at about 275 mV as a broad peak. This means that peak position of K3 was shifted from 330 mV to 275 mV. In addition, current densities of A1 and K1 increased with cycling, whereas that of A2 decreased.

Voltammograms were also performed at 10 mV/s and 20 mV/s scan rates with cycling the potential five times to determine the effects of scan rate and number of cycles on peak potential and peak current density, (Figure 4.18-4.19). Redox peaks displayed similar behaviour as compared with the peaks on the voltammogram drawn for 50 mV/s scan rate (Figure 4.16) except peaks A1, A2 and K2. These peaks disappeared at lower scan rates.

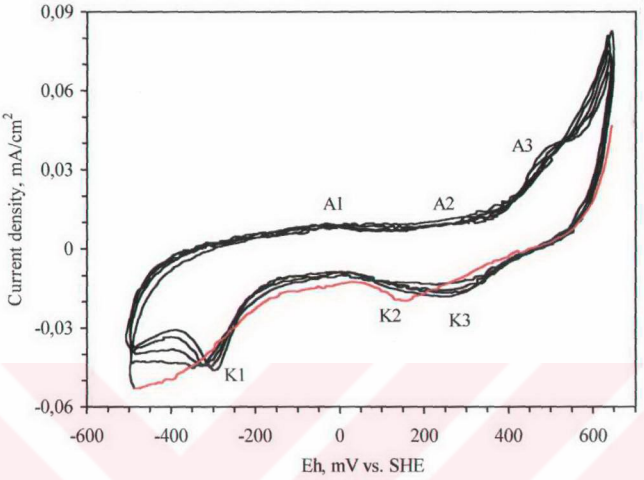

Figure 4.18. Cyclic voltammogram of chalcopyrite (pH 6.97, v = 20 mV/s)

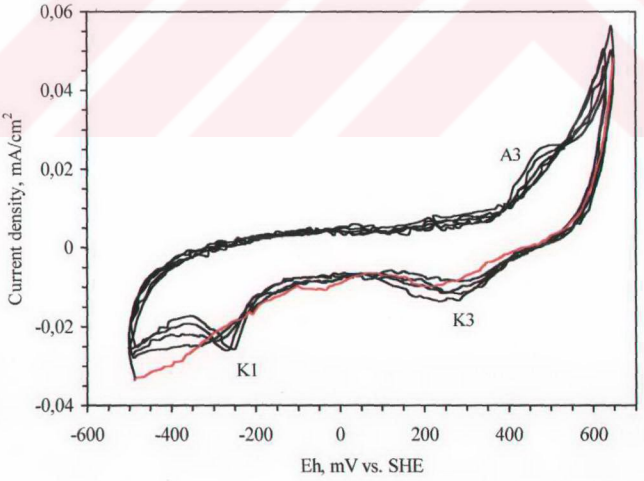

Figure 4.19. Cyclic voltammogram of chalcopyrite (pH 6.97, v = 10 mV/s)

Fifth cycles of voltammograms with a scan rate of 10 mV/s, 20 mV/s and 50 mV/s are given in Figure 4.20 for a clear presentation of the effect of scan rate on peak potential and peak current density. This figure shows that peaks A1 and A2 almost disappeared at smaller scan rates. In addition, formation potentials of peaks A3 and K3 shifted to more oxidising potentials at higher scan rates, while that of K1 shifted to more reducing potential (Figure 4.21). All the peaks occurred at higher current densities with the increased scan rates. Figure 4.22 demonstrates the relationship between current density of anodic and cathodic peaks and square-root of scan rates. As shown in Figure 4.22, there is almost a linear relationship between them.

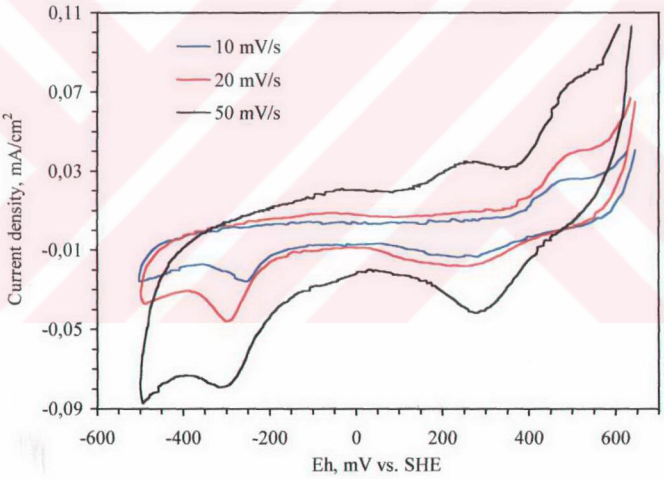

Figure 4.20. Cyclic voltammograms of chalcopyrite for different scan rates at pH 6.97

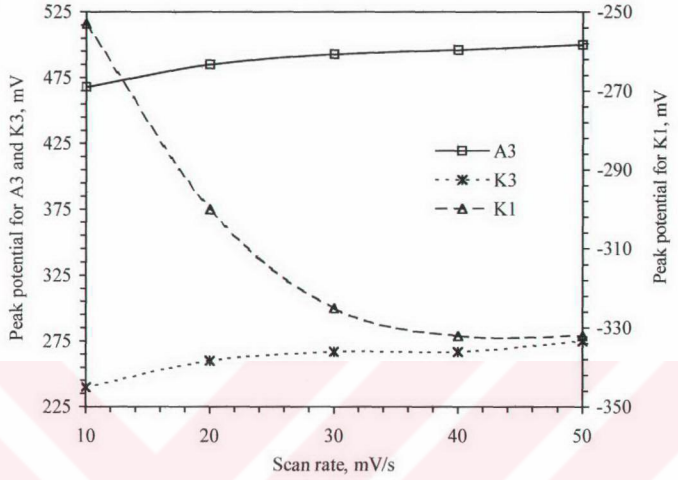

Figure 4.21. Relationship between formation potential of peaks and scan rate

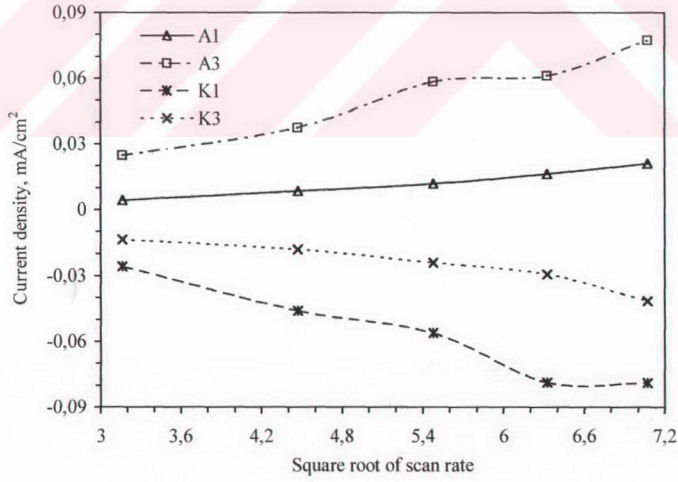

Figure 4.22. Relationship between current density of peaks and square-root of scan rate

4.1.2.2 Cyclic Voltammograms of Chalcopyrite in the Presence of DTP in pH 6.97

To determine the effect of DTP concentration on chalcopyrite surface, voltammograms were obtained at 50 mV/s scan rate in the presence of 10^{-4} M, 10^{-3} M and 10^{-2} M DTP (Figures 4.23-4.25). Electrode surface was scanned between +650-500 mV for five cycles. No new peak was observed in the presence of DTP as compared with collectorless condition (Figure 4.16). However, existing peaks disappeared when collector concentration is increased. Figure 4.26 shows the last cycles of voltammograms presented in Figures 4.16 and 4.23-4.25 to see clearly the effect of DTP concentration on chalcopyrite electrode. Furthermore, a sharp peak appeared at about 70 mV in cathodic region on voltammograms drawn at DTP induced condition like the peak K2 on voltammogram drawn in collectorless condition (Figure 4.16).

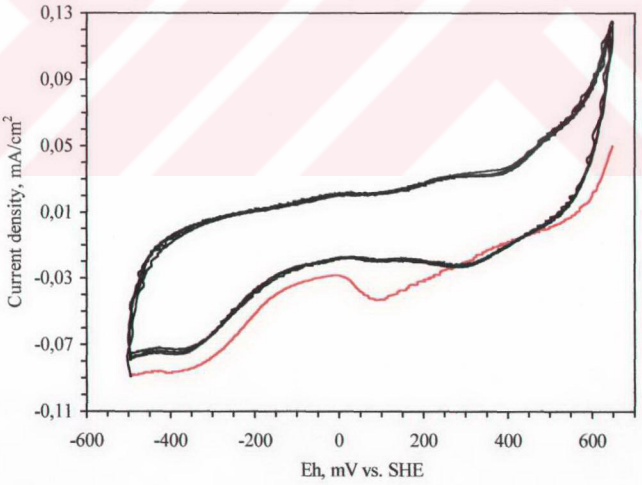

Figure 4.23. Cyclic voltammogram of chalcopyrite (pH 6.97, DTP = 10^{-4} M, v = 50 mV/s)

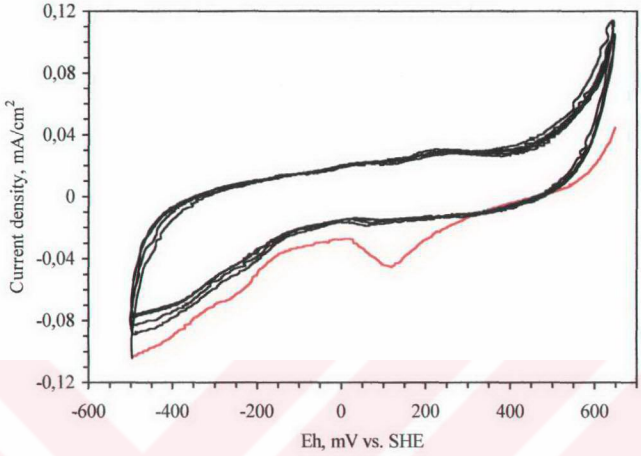

Figure 4.24. Cyclic voltammogram of chalcopyrite (pH 6.97, DTP = 10^{-3} M, v= 50 mV/s)

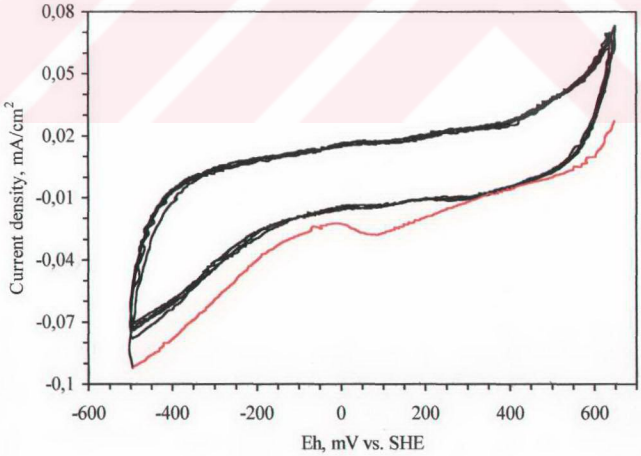

Figure 4.25. Cyclic voltammogram of chalcopyrite (pH 6.97, DTP = 10^{-2} M, v = 50 mV/s)

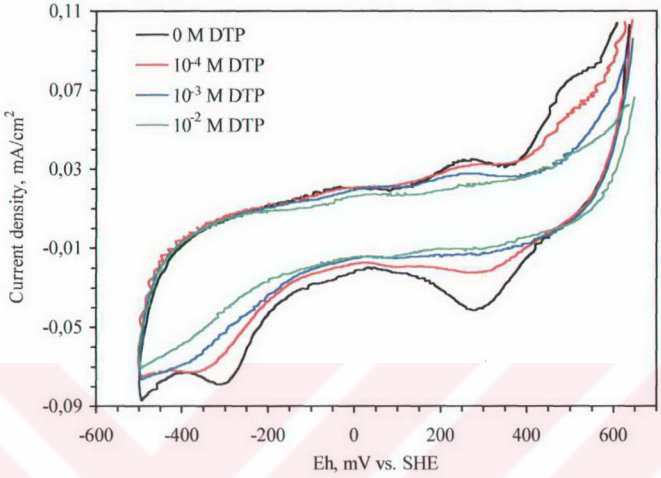

Figure 4.26. Cyclic voltammograms of chalcopyrite for 0 M, 10^{-4} M, 10^{-3} M and 10^{-2} M DTP (pH 6.97, v: 50 mV/s)

4.1.2.3 Cyclic Voltammograms of Chalcopyrite in the Presence of DTPI in pH 6.97

The cyclic voltammogram of chalcopyrite obtained in pH 6.97 buffer solution containing 10^{-4} M, 10^{-3} M and 10^{-2} M DTPI are given in Figures 4.27-4.29. The scan was applied between +650-500 mV for five cycles at 50 mV/s scan rate. As shown from figures, redox peaks did not appear in the presence of DTPI as compared with collectorless condition. On the contrary, there was an increase in current density at about –125 mV in cathodic and anodic directions. Also, current density started to increase negatively at about 200 mV in cathodic region. Last cycles of voltammograms presented in Figures 4.16 and 4.27-4.29 are given in Figure 4.30 to show the effect of DTPI concentration on chalcopyrite electrode. This figure shows that current density decreased and, anodic and cathodic peaks disappeared with an increase in collector concentration.

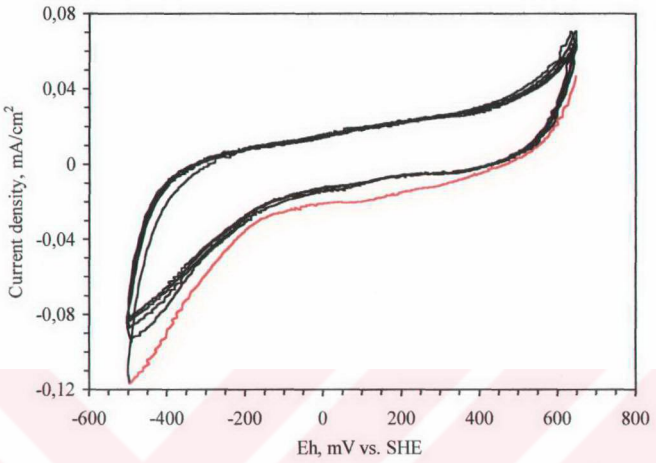

Figure 4.27. Cyclic voltammogram of chalcopyrite (pH 6.97, DTPI = 10^{-4} M, v = 50 mV/s)

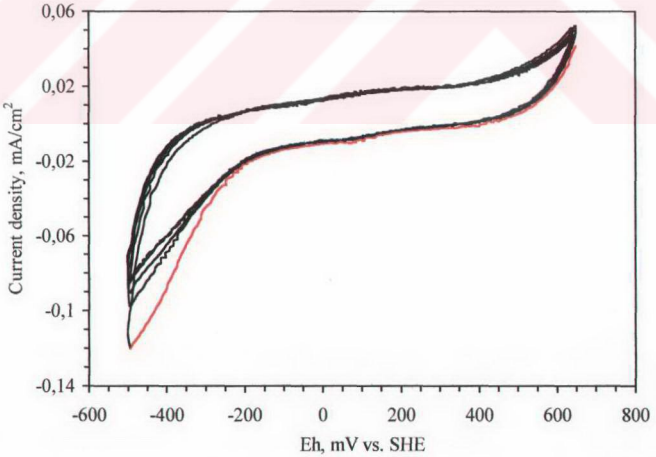

Figure 4.28. Cyclic voltammogram of chalcopyrite (pH 6.97, DTPI = 10^{-3} M, v = 50 mV/s)

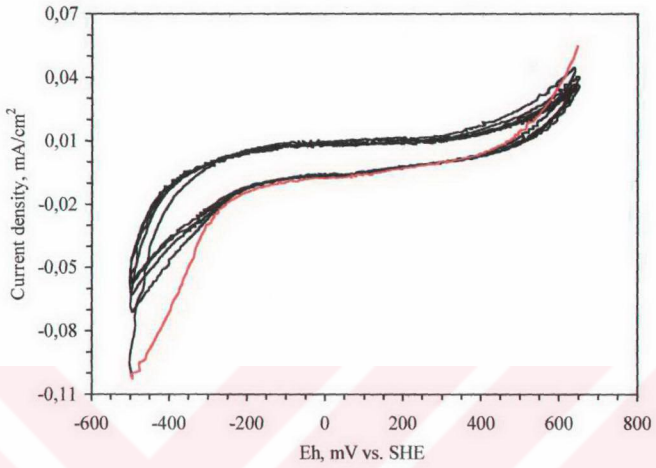

Figure 4.29. Cyclic voltammogram of chalcopyrite (pH 6.97, DTPI = 10^{-2} M, v = 50 mV/s)

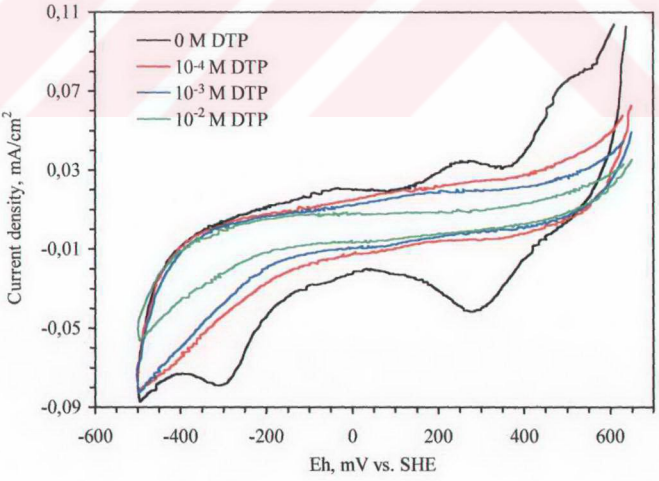

Figure 4.30. Cyclic voltammograms of chalcopyrite for 0 M, 10^{-4} M, 10^{-3} M and 10^{-2} M DTPI (pH 6.97, v: 50 mV/s)

4.1.3 pH 9.2

4.1.3.1 Cyclic Voltammograms of Chalcopyrite in Collectorless Condition in pH 9.2

An experiment was carried out with chalcopyrite electrode in pH 9.2 buffer solution and a cyclic voltammogram was obtained at 50 mV/s scan rate between +500 –500 mV pulp potential range (Figure 4.31). Five cycles were drawn between initial potential (500 mV) and reverse potential (-500 mV) to show the effect of cycling. Scanning was started at +500 mV in cathodic direction. Only one anodic peak at ~330 mV and a cathodic peak at ~ –270 mV appeared. In first cycle, cathodic peak was observed at lower current densities when compared with second cycle. Then, current density of peak K1 decreased slowly from second cycle to last one. Peak positions of anodic and cathodic peaks did not change with cycling. Meanwhile, current density of anodic peak (peak A1) decreased slowly with cycling.

A voltammogram was also measured at 50 mV/s scan rate by cycling from desired potentials (Figure 4.32). Scan was started at –300 mV in cathodic direction and voltammogram was obtained cutting the potential from 50 mV, 400 mV and 500 mV in anodic region and from –500 mV in cathodic region.

Current density increased with starting the scan initially in cathodic direction, however peak formation was not observed. In the second cycle turned back to cathodic region from 50 mV, peak did not still occur. When cycling from 400 mV to cathodic region, anodic and cathodic peaks formed. In the last cycle from 500 mV, no new peak formation was seen.

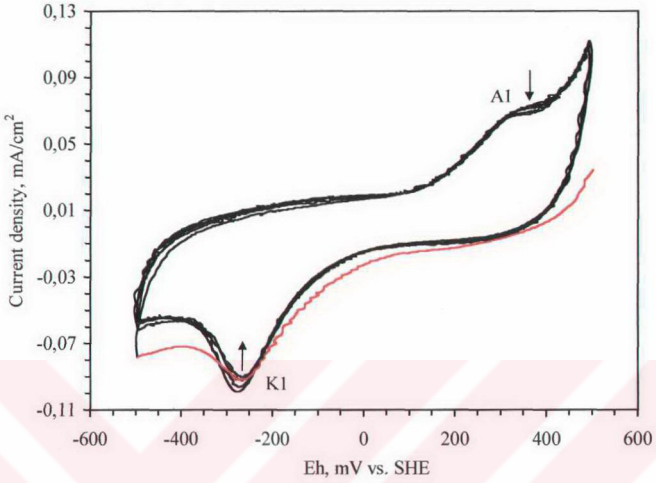

Figure 4.31. Cyclic voltammogram of chalcopyrite (pH 9.2, v = 50 mV/s)

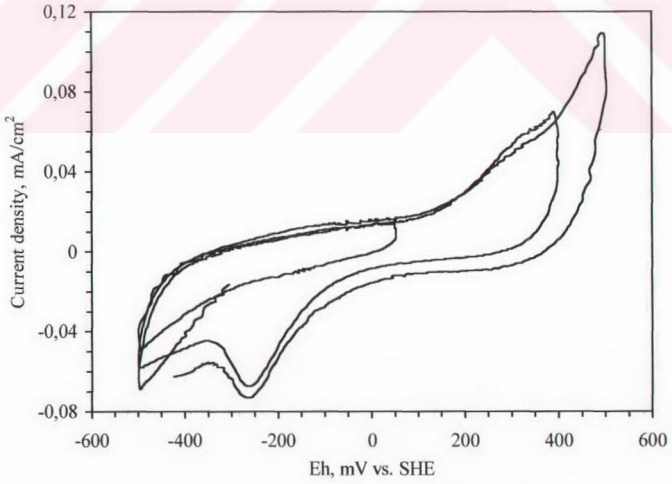

Figure 4.32. Controlled sweep voltammogram of chalcopyrite (pH 9.2, v = 50 mV/s)

Chalcopyrite voltammograms were also obtained at 10 mV/s and 20 mV/s scan rates with cycling the potential five times to show the effects of scan rate and number of cycles on peak potential and current density, (Figure 4.33-4.34). Peaks showed similar behaviour as compared with the peaks on the voltammogram performed at 50 mV/s scan rate.

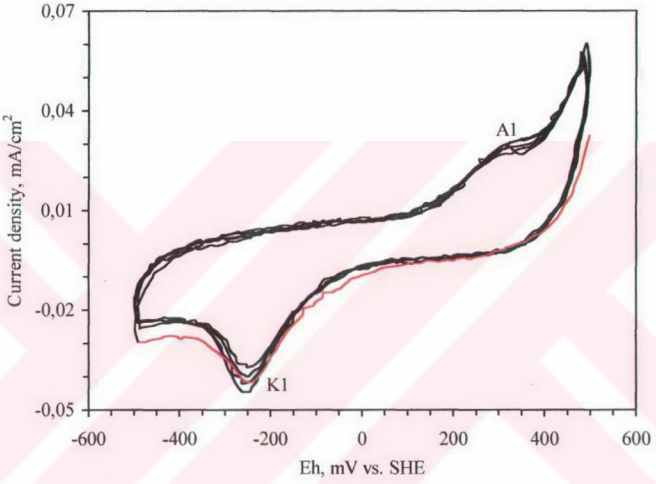

Figure 4.33. Cyclic voltammogram of chalcopyrite (pH 9,2, v = 20 mV/s)

The last cycles of Figures 4.31, 4.33 and 4.34 were given in Figure 4.35 to clarify the effects of scan rate on peak potential and peak current density. For this aim, Figures 4.36 and 4.37 were also drawn. As seen from Figures 4.35 and 4.36, formation potentials of anodic and cathodic peaks were shifted to more oxidising and more reducing potentials with increasing the scan rate, respectively. Moreover, current densities of peaks also changed with scan rate (Figure 4.37): Peaks occurred at higher current densities with the increased scan rates. There was almost a linear relationship between current density of anodic and cathodic peaks and square-root of scan rate.

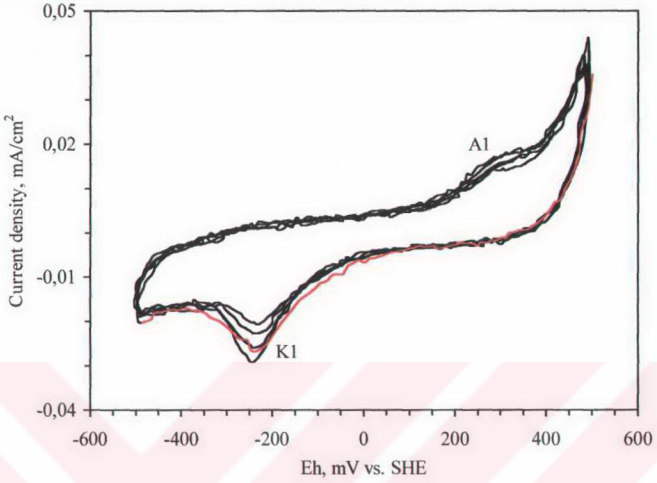

Figure 4.34. Cyclic voltammogram of chalcopyrite (pH 9,2, v = 10 mV/s)

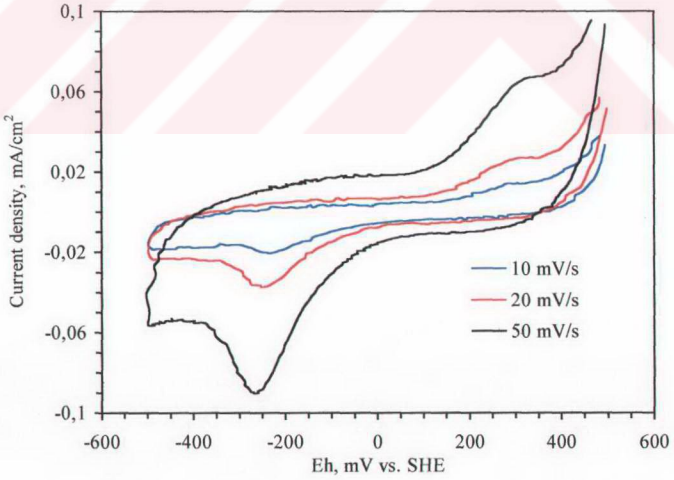

Figure 4.35. Cyclic voltammograms of chalcopyrite for different scan rates at pH 9.2

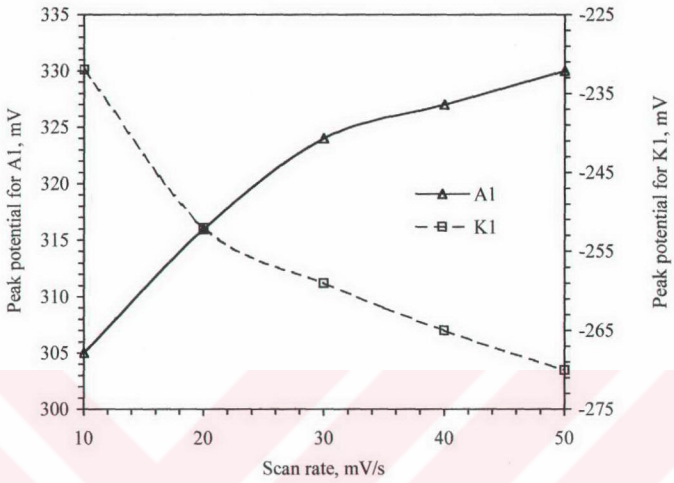

Figure 4.36. Relationship between formation potentials of peaks and scan rate

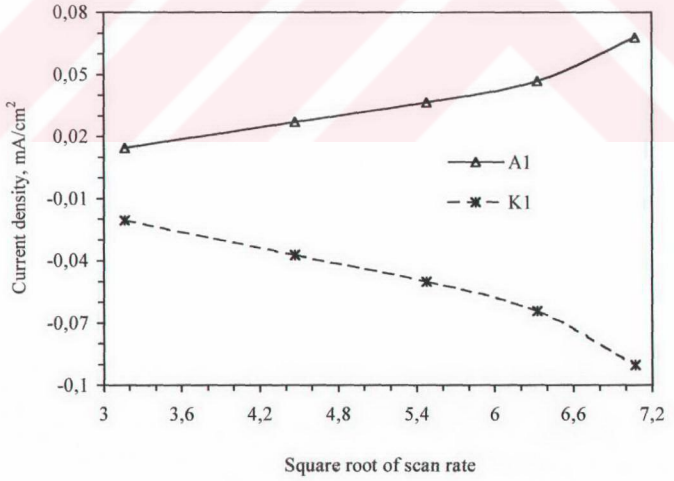

Figure 4.37. Relationship between current density of peaks and square-root of scan rate

4.1.3.2 Cyclic Voltammograms of Chalcopyrite in the Presence of DTP in pH 9.2

Cyclic voltammograms of chalcopyrite were measured in the presence of 10^{-4} M, 10^{-3} M and 10^{-2} M DTP (Figures 4.38-4.40). Electrode surface was swept between +500 –500 mV for five cycles with a scan rate of 50 mV/s. No new peak was observed on the voltammograms drawn in the presence of DTP as compared with collectorless condition. A slight reduction in the current density of redox peaks was seen with the increased collector concentration (Figure 4.41)

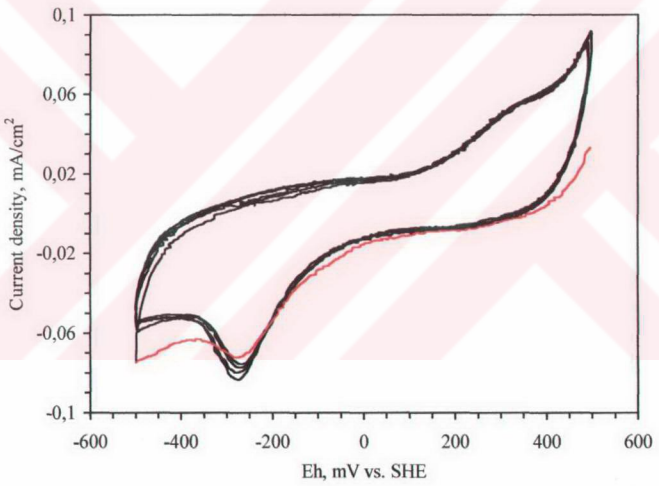

Figure 4.38. Cyclic voltammogram of chalcopyrite (pH 9.2, DTP = 10^{-4} M, v = 50 mV/s)

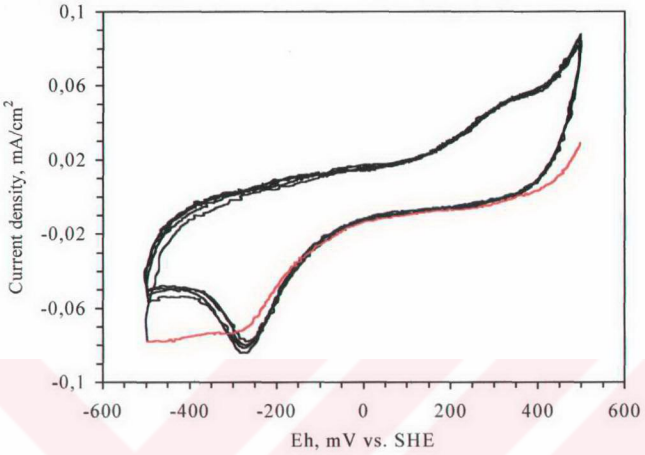

Figure 4.39. Cyclic voltammogram of chalcopyrite (pH 9.2, DTP = 10^{-3} M, v = 50 mV/s)

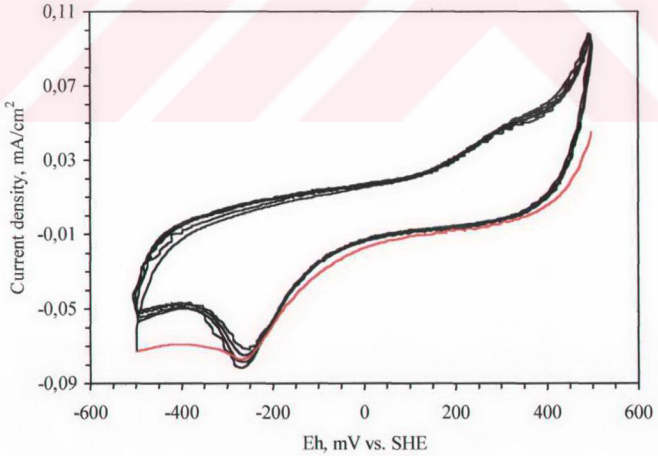

Figure 4.40. Cyclic voltammogram of chalcopyrite (pH 9.2, DTP = 10^{-2} M, v = 50 mV/s)

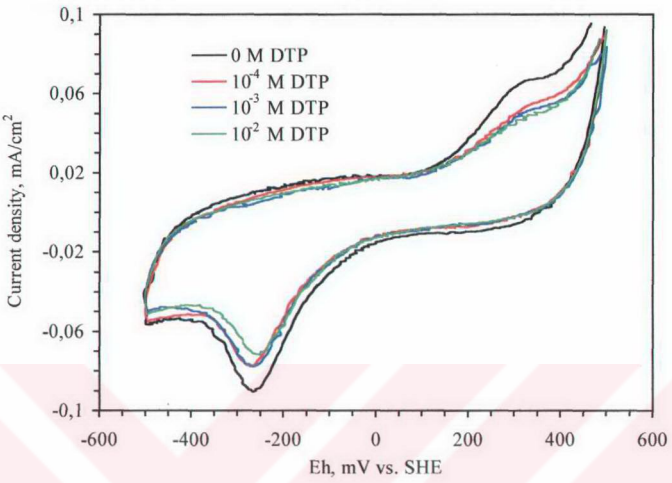

Figure 4.41. Cyclic voltammograms of chalcopyrite for 0 M, 10^{-4} M, 10^{-3} M and 10^{-2} M DTP (pH 9.2, v: 50 mV/s)

4.1.2.3 Cyclic Voltammograms of Chalcopyrite in the Presence of DTPI in pH 9.2

The cyclic voltammograms of chalcopyrite performed in pH 9.2 buffer solution containing 10^{-4} M, 10^{-3} M and 10^{-2} M DTPI are given in Figure 4.42-4.44. Electrode surface was scanned between +500 –500 mV for five cycles at 50 mV/s scan rate. No new peak was observed on the voltammograms drawn in the presence of DTPI as compared with collectorless condition (Figure 4.31). Current densities in first cycles of these three voltammograms were higher as compared with other cycles in cathodic region. With an increase in DTPI concentration, anodic peak disappears, cathodic peak shifted to more reducing potentials, and current density decreased. This was clearly demonstrated in Figure 4.45. This figure shows the last cycles of voltammograms presented in Figures 4.31 and 4.42-4.44 to display the effect of DTPI concentration on chalcopyrite electrode.

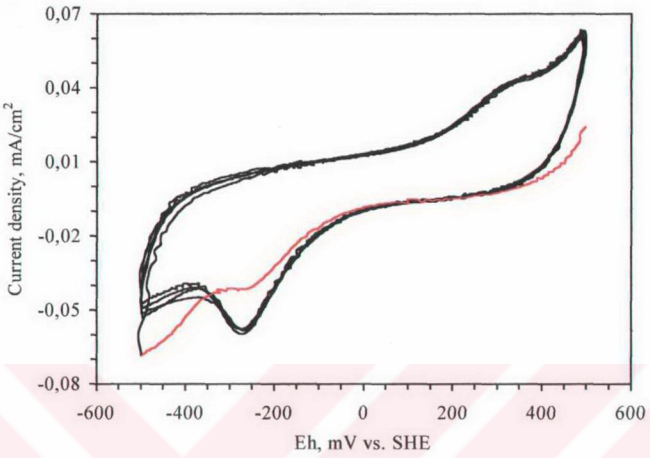

Figure 4.42. Cyclic voltammogram of chalcopyrite (pH 9.2, DTPI = 10^{-4} M, v = 50 mV/s)

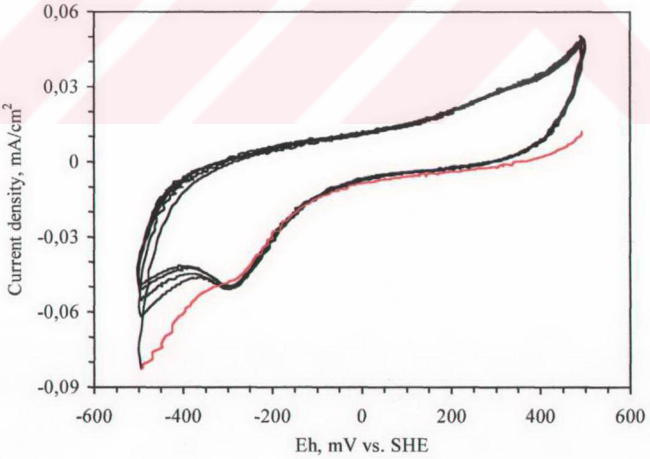

Figure 4.43. Cyclic voltammogram of chalcopyrite (pH 9.2, DTPI = 10^{-3} M, v = 50 mV/s)

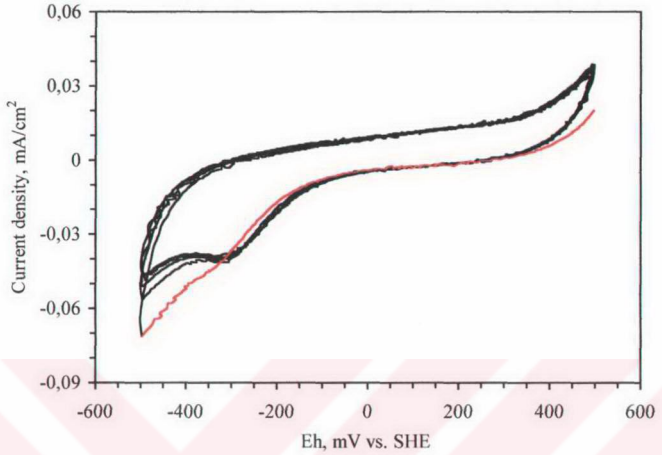

Figure 4.44. Cyclic voltammogram of chalcopyrite (pH 9.2, DTPI= 10^{-2} M, v = 50 mV/s)

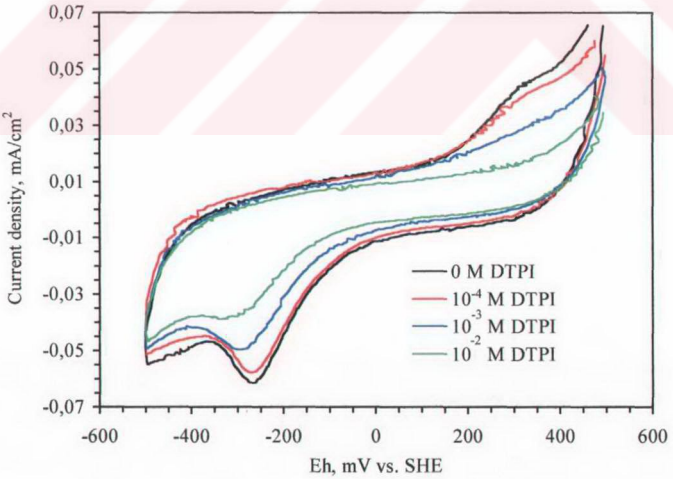

Figure 4.45. Cyclic voltammograms of chalcopyrite for different scan rates at pH 9.2 for 0 M, 10^{-4} M, 10^{-3} M and 10^{-2} M DTPI

4.1.4 pH 11

4.1.4.1 Cyclic Voltammograms of Chalcopyrite in Collectorless Condition in pH 11

Chalcopyrite voltammogram obtained in pH 11 buffer solution at 50 mV/s scan rate between +500 –500 mV pulp potential range is given in Figure 4.46. Potential was cycled five times between initial potential (500 mV) and reverse potential (-500 mV) to show the effect of cycling. Scanning was started at +500 mV in cathodic direction.

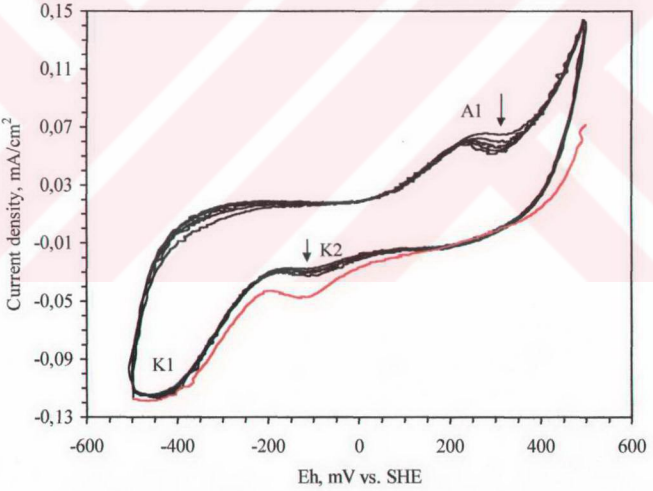

Figure 4.46. Cyclic voltammogram of chalcopyrite (pH 11, v = 50 mV/s)

Only one anodic (A1) and two cathodic (K1 and K2) peaks were appeared at ~240 mV (peak A1), ~ –460 mV (peak K1) and ~ –100 mV (peak K2). Peak K2 was observed at slightly cathodic potential in first cycle as compared with other cycles. Current densities and formation potentials of redox peaks did almost not

change with cycling. However, it should be also stated that current density of peak K2 increased very slowly while that of peak A1 decreased.

A cyclic voltammogram was also measured at 50 mV/s scan rate to determine which anodic peak is related with which cathodic peak (Figure 4.47). The scan was started at –200 mV in cathodic direction and controlled sweep voltammogram was measured cutting the potential from 0 mV, 300 mV and 500 mV in anodic region and from –500 mV in cathodic region in a sequence.

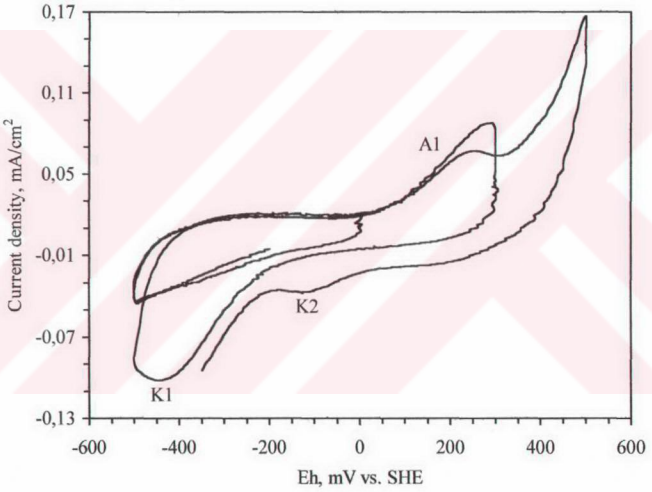

Figure 4.47. Controlled sweep voltammogram of chalcopyrite (pH 11, v = 50 mV/s)

Current density gradually increased with commencing the scan initially in cathodic direction. However, no peak formation occurred when cutting the potential from 0 mV. When potential sweep was reversed from 300 mV from anodic region, peak A1 occurred in anodic region and, in the reverse scan, it resulted in peak K1. In the last cycle, current density sharply increased above 300 mV in anodic region. In the reverse sweep, it caused the formation of peak K2 in

cathodic region. This means that this sharp increase in current density at highly oxidising potentials showed the formation of an anodic peak, and this peak resulted in the formation of second cathodic peak (K2).

Voltammograms were also drawn at 5 mV/s, 10 mV/s and 20 mV/s scan rates with cycling the potential five times to determine the effects of scan rate and number of cycles on the peak potential and peak current density, (Figures 4.48-4.49). New peak formation was not seen at lower scan rates. Redox peaks showed similar behaviour as compared with the peaks on the voltammogram drawn for 50 mV/s scan rate given in Figure 4.46.

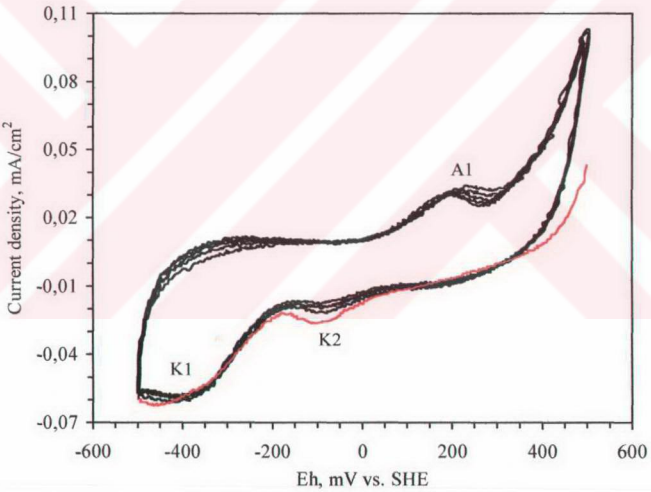

Figure 4.48. Cyclic voltammogram of chalcopyrite (pH 11, v = 20 mV/s)

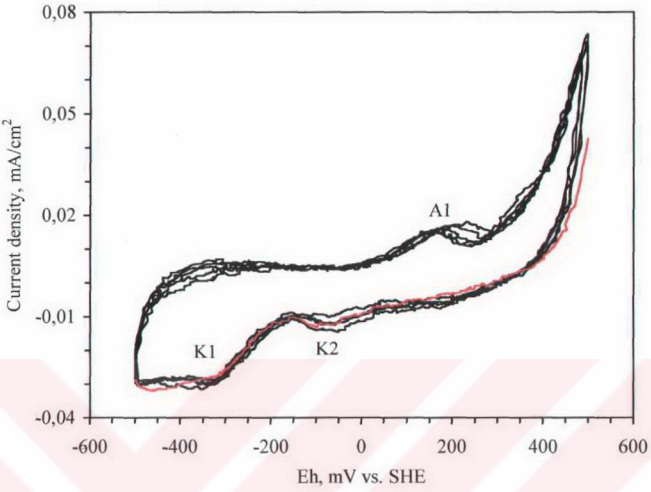

Figure 4.49. Cyclic voltammogram of chalcopyrite (pH 11, v = 10 mV/s)

The last cycles of voltammograms obtained at 50 mV/s, 20 mV/s and 10 mV/s scan rates given in Figures 4.46 and 4.48-4.49 were drawn in the same figure to determine which anodic peak was related to which cathodic peak (Figure 4.50). In addition, Figures 4.51 and 4.52 were also drawn to clarify the effects of scan rate on current densities and formation potentials of oxidation and reduction peaks, respectively. As shown from these figures, formation potential of peak A1 shifted to more reducing potentials at lower scan rates, while that of peak K1 shifted to more oxidising potentials. Formation potential of peak K2 did almost not change. All the peaks were appeared at lower current densities for smaller scan rates. The relationships between current densities and square-root of scan rates for all redox peaks were almost linear.

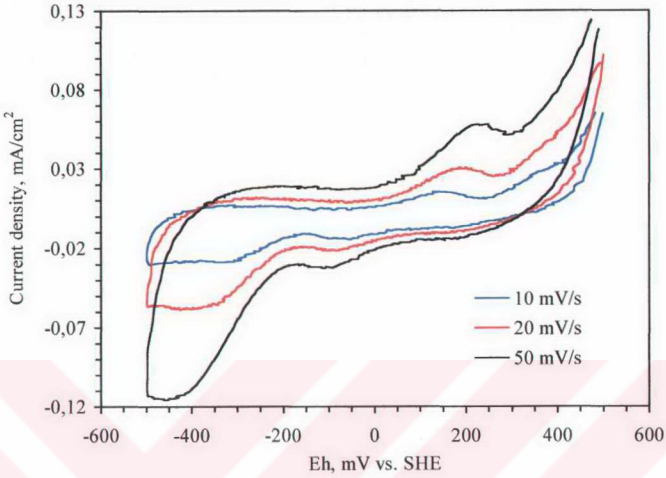

Figure 4.50. Cyclic voltammogram of chalcopyrite for different scan rates at pH 11

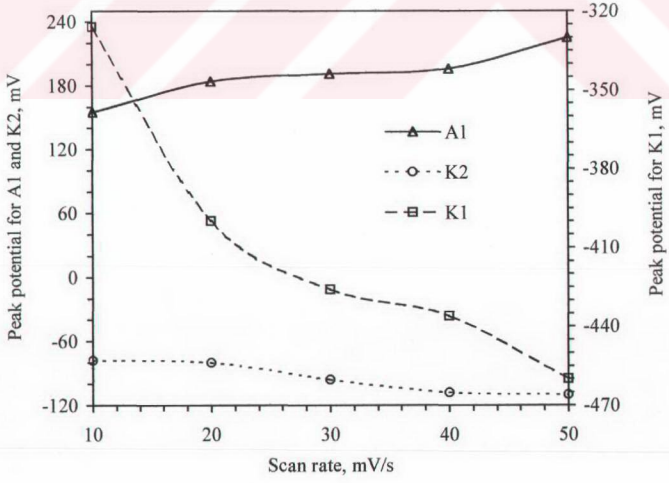

Figure 4.51. Relationship between formation potential of peaks and scan rate

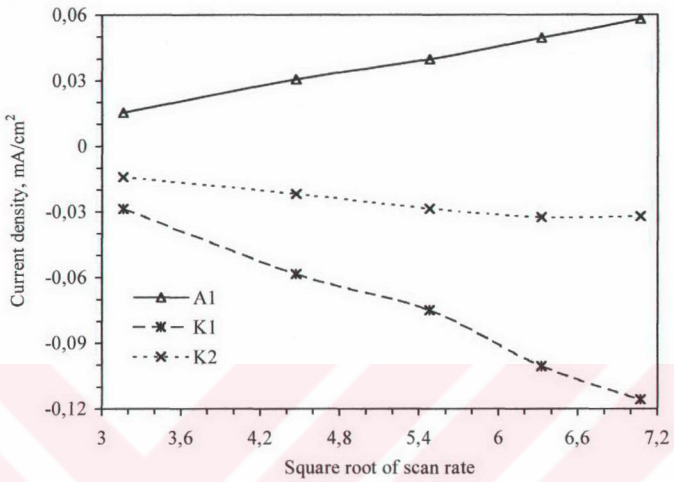

Figure 4.52. Relationship between current density of peaks and square-root of scan rate

4.1.4.2 Cyclic Voltammograms of Chalcopyrite in the Presence of DTP in pH 11

Cyclic voltammogram of chalcopyrite in the presence of 10^{-4} M, 10^{-3} M and 10^{-2} M DTP at pH 11 are given in Figures 4.53-4.55. Surface scan was applied between +500-500 mV for five cycles with a scan rate of 50 mV/s. A new peak was not observed on the voltammograms drawn in the presence of DTP in different concentrations as compared with collectorless condition (Figure 4.46). Figure 4.56 was also drawn to display the effects of DTP concentration on redox peaks: There were very small decreases in the current densities of redox peaks. Shifts in the formation potentials of redox peaks did not observed. Surface passivation did almost not occur for all three different collector concentrations.

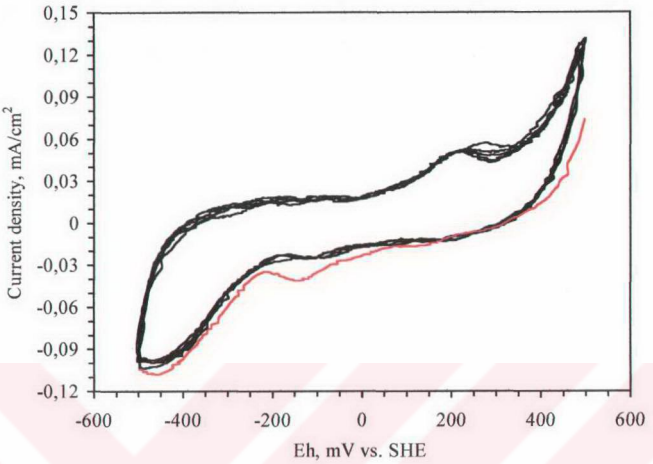

Figure 4.53. Cyclic voltammogram of chalcopyrite (pH 11, DTP = 10^{-4} M, v = 50 mV/s)

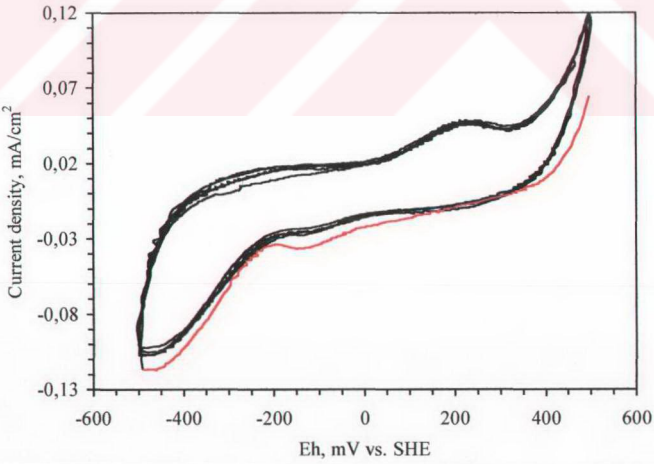

Figure 4.54. Cyclic voltammogram of chalcopyrite (pH 11, DTP = 10^{-3} M, v = 50 mV/s)

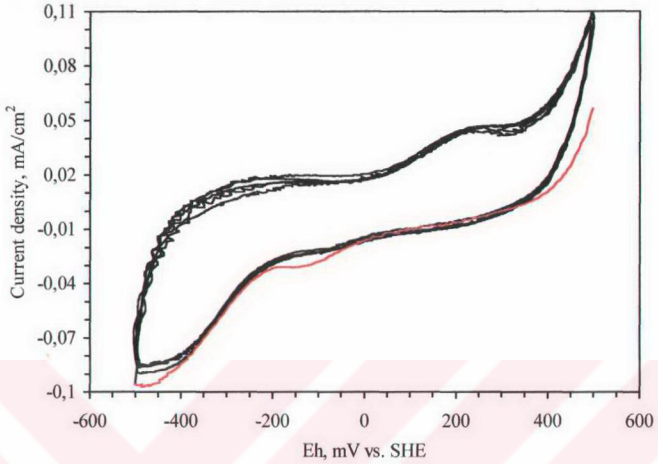

Figure 4.55. Cyclic voltammogram of chalcopyrite (pH 11, DTP = 10^{-2} M, v = 50 mV/s)

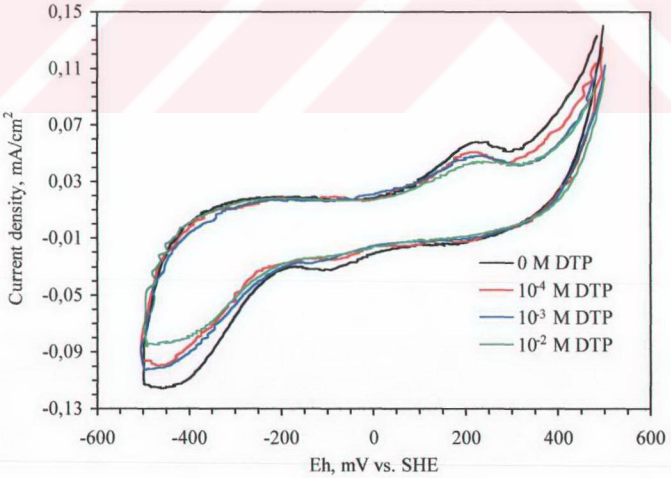

Figure 4.56. Cyclic voltammograms of chalcopyrite for 0 M, 10^{-4} M, 10^{-3} M and 10^{-2} M DTP (pH 11, v: 50 mV/s)

4.1.4.3 Cyclic Voltammograms of Chalcopyrite in the Presence of DTPI in pH 11

Chalcopyrite voltammograms were measured in pH 11 buffer solution containing 10^{-4} M, 10^{-3} M and 10^{-2} M DTPI to show the effects of collector concentration on mineral surface (Figures 4.57-4.59). Electrode surface was swept at 50 mV/s scan rate between +500 –500 mV for five cycles. No new peaks were observed on the voltammograms drawn in the presence of DTPI as compared with collectorless condition (Figure 4.46). Fifth cycles of voltammograms given in Figures 4.46 and 4.57-4.59 were drawn in the same figure to elucidate the effects of DTPI concentration on chalcopyrite surface (Figure 4.60): While current densities of peaks A1 and K1 decreased for higher collector concentration, peak K2 disappeared.

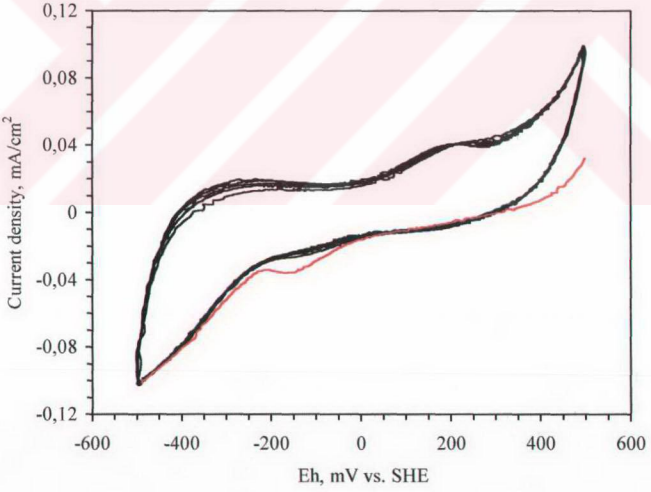

Figure 4.57. Cyclic voltammogram of chalcopyrite (pH 11, DTPI = 10^{-4} M, v = 50 mV/s)

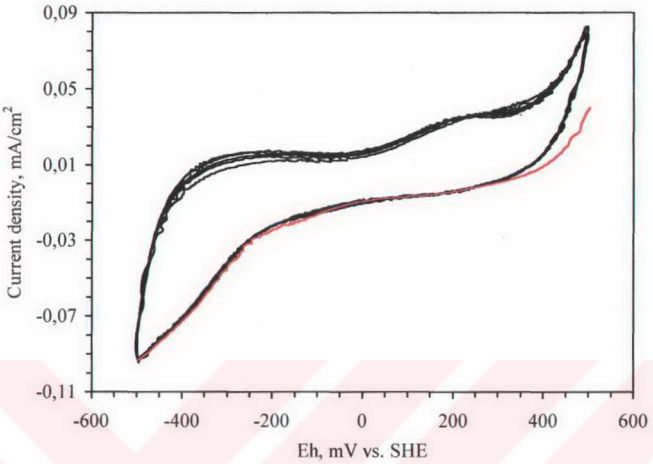

Figure 4.58. Cyclic voltammogram of chalcopyrite (pH 11, DTPI = 10^{-3} M, v = 50 mV/s)

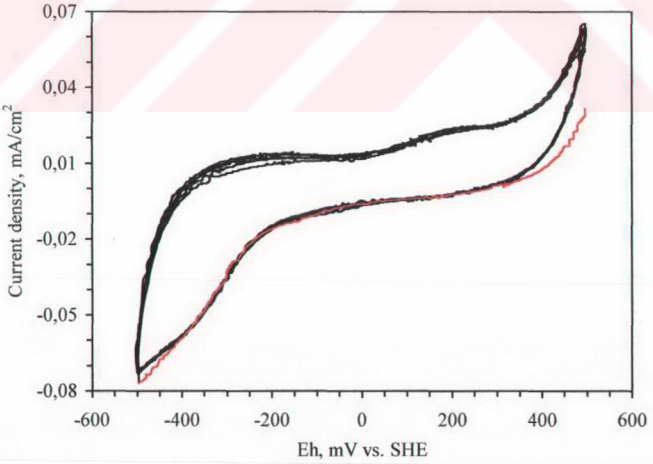

Figure 4.59. Cyclic voltammogram of chalcopyrite (pH 11, DTPI = 10^{-2} M, v = 50 mV/s)

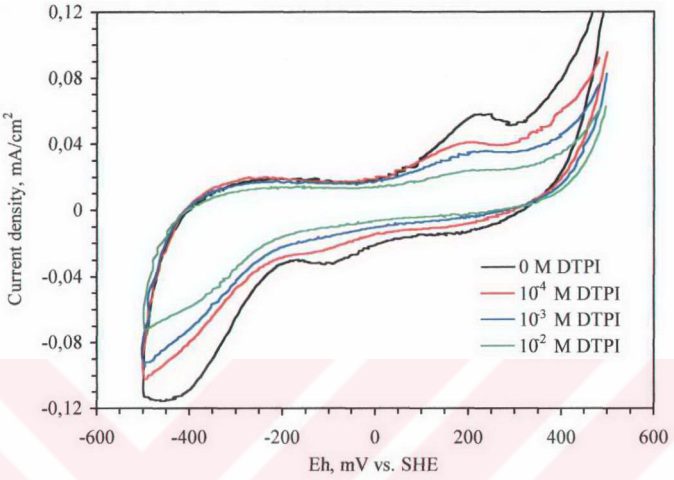

Figure 4.60. Cyclic voltammograms of chalcopyrite for 0 M, 10^{-4} M, 10^{-3} M and 10^{-2} M DTPI (pH 11, v: 50 mV/s)

4.2 DRIFT Study

DRIFT spectra of chalcopyrite sample were drawn to determine the surface species formed in the presence of DTP and DTPI. Finely ground chalcopyrite samples were polarised for 15 minutes at three different pulp potential values (-100 mV, 150 mV and 400 mV) and in four different deoxygenated buffer solutions (pH 4.67, pH 6.97, pH 9.2 and pH 11) for DRIFT study. In addition, as a reference, DRIFT spectra of monomers and dimers of DTP and DTPI were also mapped out. CuDTP and CuDTPI precipitates were obtained as products of reactions between Cu^{+2} and collector ions, and their spectra were drawn to find the peak positions of these compounds.

4.2.1 DRIFT Study with DTP

DRIFT spectrum of DTP is given in Figure 4.61.a. Peak positions of DTP spectrum are as follows in cm^{-1}: 2974, 2947, 2930, 2893, 2863, 1464, 1440, 1389, 1362, 1296, 1277, 1238, 1159, 1095, 1036, 1016, 943, 920, 802, 777, 746, 725, 706, 685, 646, 579 and 542.

As a reference, dimer of DTP was prepared and its spectrum was also obtained (Figure 4.61.b). Peak positions of $(DTP)_2$ were determined as follows in cm^{-1}: 2982, 2933, 2903, 2870, 1473, 1441, 1390, 1365, 1290, 1161, 1097, 1009, 970, 829, 799, 640, 503 and 496.

In highly oxidising potentials, when platinum and DTP are interacted and platinum surface is polarised in acid solution, dimer forms on platinum surface (Chander and Fuerstenau, 1974). Therefore, to confirm the dimer spectrum, platinum-powder was polarised at 750 mV in pH 4.67 buffer solution with DTP, and then DRIFT spectrum of powder was measured (Figure 4.61.c). Peak positions are as follows in cm^{-1}: 2978, 2927, 1466, 1450, 1389, 1290, 1215, 1159, 1099, 1016, 966, 824, 799, 646, 598 and 496.

In literature, it was pointed out that CuDTP precipitate forms in conformity with reactions 4.1 and 4.2 when DTP^- is interacted with Cu^{+2} ions (Shubov et al., 1976; Yordanov and Ranguelova, 2001; Yordanov et al., 1998). In addition, it was also mentioned that reaction 4.2 becomes slower when going from acid to alkaline condition (Goold and Finkelstein, 1972). That is to say, $Cu(DTP)_2$ predominantly forms in alkaline condition rather than CuDTP. Therefore, in slightly acid solution (pH 4.67), 10^{-2} M DTP solution was reacted with 10^{-2} M $CuSO_4.5H_2O$, and CuDTP precipitate was obtained. Precipitate was washed with distilled water five times and its DRIFT spectrum was also obtained (Figure 4.61.d). Peak positions are as follows in cm^{-1}: 2980, 2935, 2926, 2864, 1474, 1439, 1390, 1285, 1159, 1099, 1036, 1011, 964, 829, 787, 774, 642, 532 and 499.

$$2Cu^{+2} + 4DTP^{-} \rightleftharpoons 2Cu(DTP)_2 \qquad 4.1$$

$$2Cu(DTP)_2 \rightleftharpoons 2CuDTP + (DTP)_2 \qquad 4.2$$

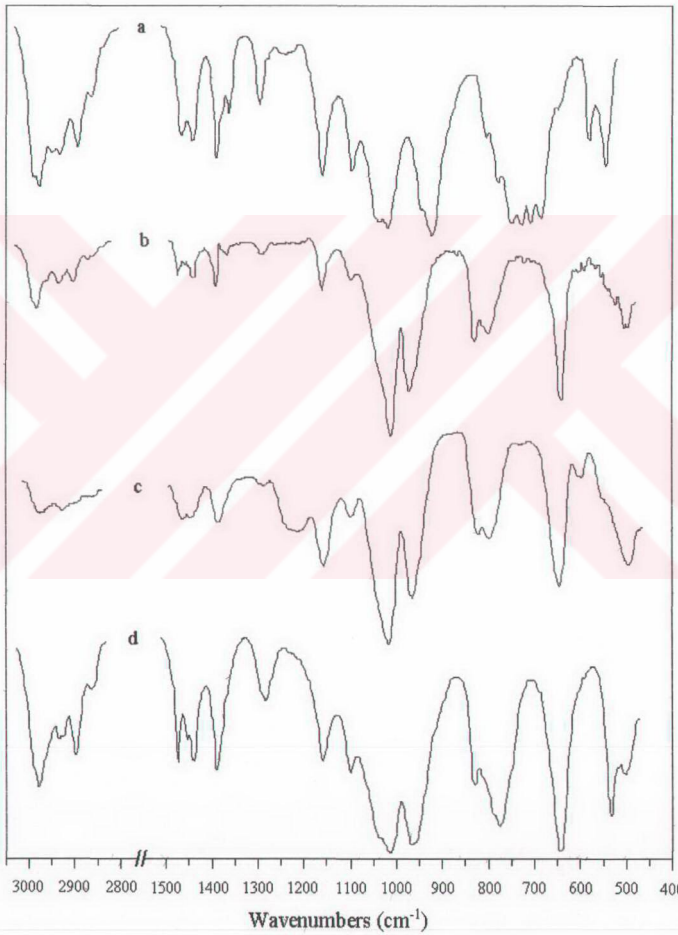

Figure 4.61. DRIFT spectra of a) DTP, b) $(DTP)_2$, c) Pt-powder polarised with 10^{-1} M DTP in pH 4.67 buffer at 750 mV, and d) Cu-DTP precipitate

Spectra were measured for chalcopyrite sample treated in acid solution (pH 4.67) at reducing (-100 mV), moderately oxidising (+150 mV) and highly oxidising (+400 mV) potentials to elucidate the effects of DTP on chalcopyrite and to interpret the surface compounds. For this aim, chalcopyrite was treated with 10^{-1} M DTP and then DRIFT spectra were drawn (Figure 4.62).

Especially in the spectrum for –100 mV, there are a lot of peaks between 1250-1500 cm^{-1}, but most of these are too weak to define as peaks. Peak positions are as follows:

–100 mV: 2957, 2872, 1460, 1436, 1389, 1369, 1292, 1256, 1158, 1101, 1018, 953, 839, 806, 756, 698, 619, 582, 517.

+150 mV: 2965, 2905, 2870, 1450, 1389, 1331, 1246, 1165, 1136, 1098, 1028, 960, 924, 841, 799, 695, 580, 546, 499.

+400 mV: 2965, 2875, 1458, 1388, 1325, 1159, 1099, 1016, 962, 831, 799, 716, 650, 613, 577, 520, 494

Spectra obtained from chalcopyrite samples interacted with 10^{-1} M DTP in pH 6.97 buffer solution are given in Figure 4.63. Peaks are very weak particularly in the spectrum of –100 mV (Figure 4.63.c). Peak intensities increase slowly at higher Eh values. Peak positions are as follows for each spectrum:

–100 mV: 2982, 2953, 2880, 1244, 1210, 1130, 1090, 1028, 963, 862, 814, 787, 746, 673, 601, 575, 549.

+150 mV: 2965, 2875, 1387, 1306, 1250, 1161, 1099, 1028, 959, 854, 806, 733, 645, 580, 546, 504.

+400 mV: 2974, 2880, 1454, 1396, 1339, 1300, 1240, 1103, 1018, 959, 870, 804, 765, 710, 665, 611, 580, 507.

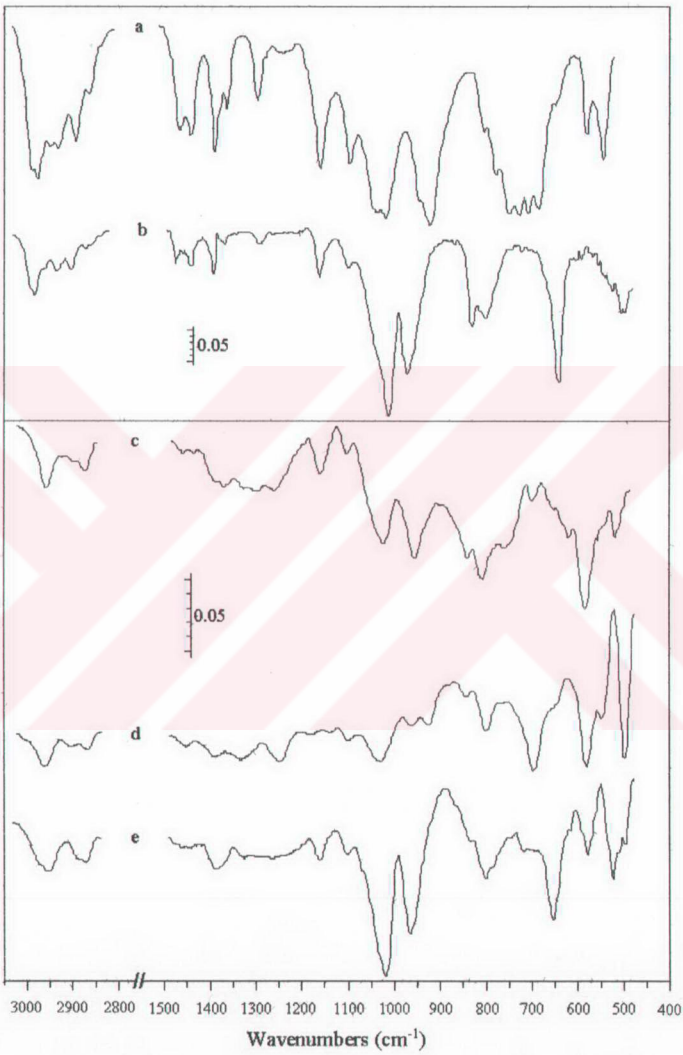

Figure 4.62. DRIFT spectra of chalcopyrite samples interacted with 10^{-1} M DTP in pH 4.67 buffer solution at c) –100 mV, d) +150 mV and e) +400 mV. Spectra of a) DTP and b) $(DTP)_2$ are given as references.

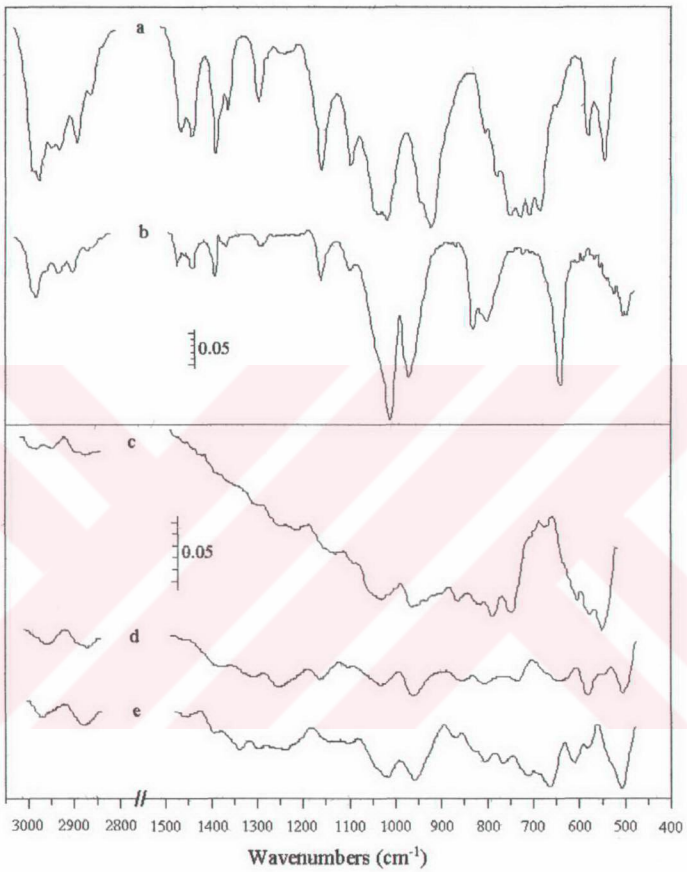

Figure 4.63. DRIFT spectra of chalcopyrite samples interacted with 10^{-1} M DTP in pH 6.97 buffer solution at c) –100 mV, d) +150 mV and e) +400 mV. Spectra of a) DTP and b) $(DTP)_2$ are given as references.

Figure 4.64 presents the spectra obtained from chalcopyrite samples reacted with 10^{-1} M DTP at –100 mV, +150 mV and +400 mV pulp potential values in pH 9.2 buffer solution. Peak positions in these spectra are determined as follows:

–100 mV: 2974, 2874, 1420, 1367, 1308, 1254, 1163, 1074, 1016, 953, 860, 795, 739, 670, 621, 584, 546, 501.

+150 mV: 2968, 2887, 2847, 1387, 1306, 1257, 1157, 1095, 1024, 955, 858, 783, 750, 694, 657, 623, 580, 546.

+400 mV: 2978, 2874, 1305, 1246, 1153, 1096, 1033, 953, 925, 864, 845, 791, 750, 681, 667, 611, 584, 553.

Chalcopyrite spectra obtained from samples reacted with 10^{-1} M DTP at –100 mV, +150 mV and +400 mV pulp potential values in pH 11 buffer solution are given in Figure 4.65. Peak positions in these spectra are found as follows:

–100 mV: 2978, 2887, 1458, 1392, 1300, 1257, 1161, 1099, 1022, 945, 850, 795, 764, 739, 694, 658, 621, 581, 507.

+150 mV: 2980, 2881, 1458, 1361, 1314, 1261, 1159, 1099, 1026, 954, 914, 857, 804, 762, 727, 671, 627, 575, 507.

+400 mV: 2976, 2874, 1460, 1421, 1385, 1304, 1256, 1161, 1099, 1020, 951, 891, 849, 803, 723, 696, 677, 630, 621, 584, 550, 509.

Figures 4.66-4.68 were presented below to demonstrate the effect of pH on the interaction between DTP and chalcopyrite. Peak positions of IR signals are given above. As shown from figures, maximum peak intensity is obtained at pH 4.67. It decreases sharply at 6.79 and, at higher pH values almost the same peak intensities were obtained.

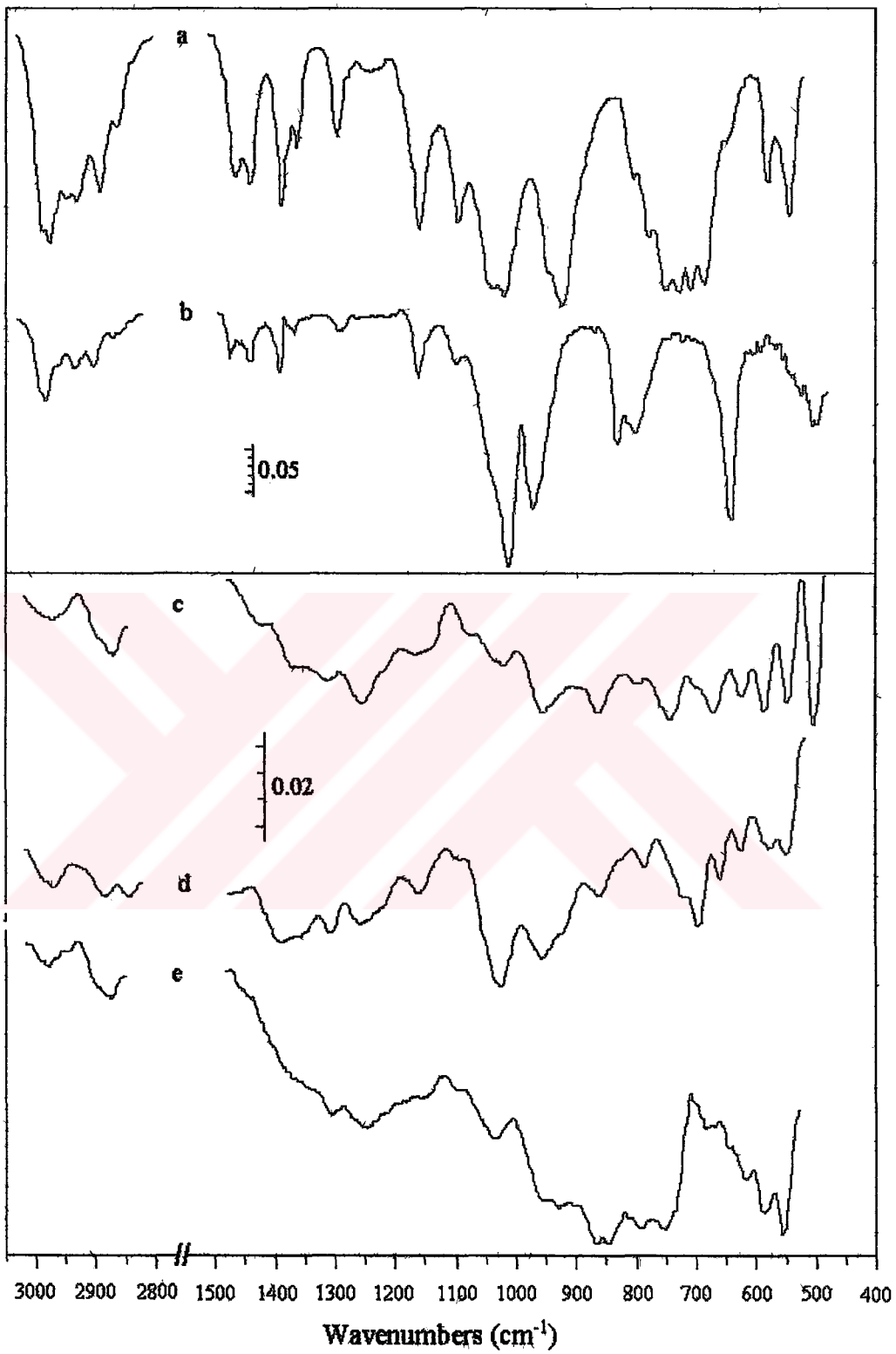

Figure 4.64. DRIFT spectra of chalcopyrite samples interacted with 10^{-1} M DTP in pH 9.2 buffer solution at c) –100 mV, d) +150 mV and e) +400 mV. Spectra of a) DTP and b) $(DTP)_2$ are given as references.

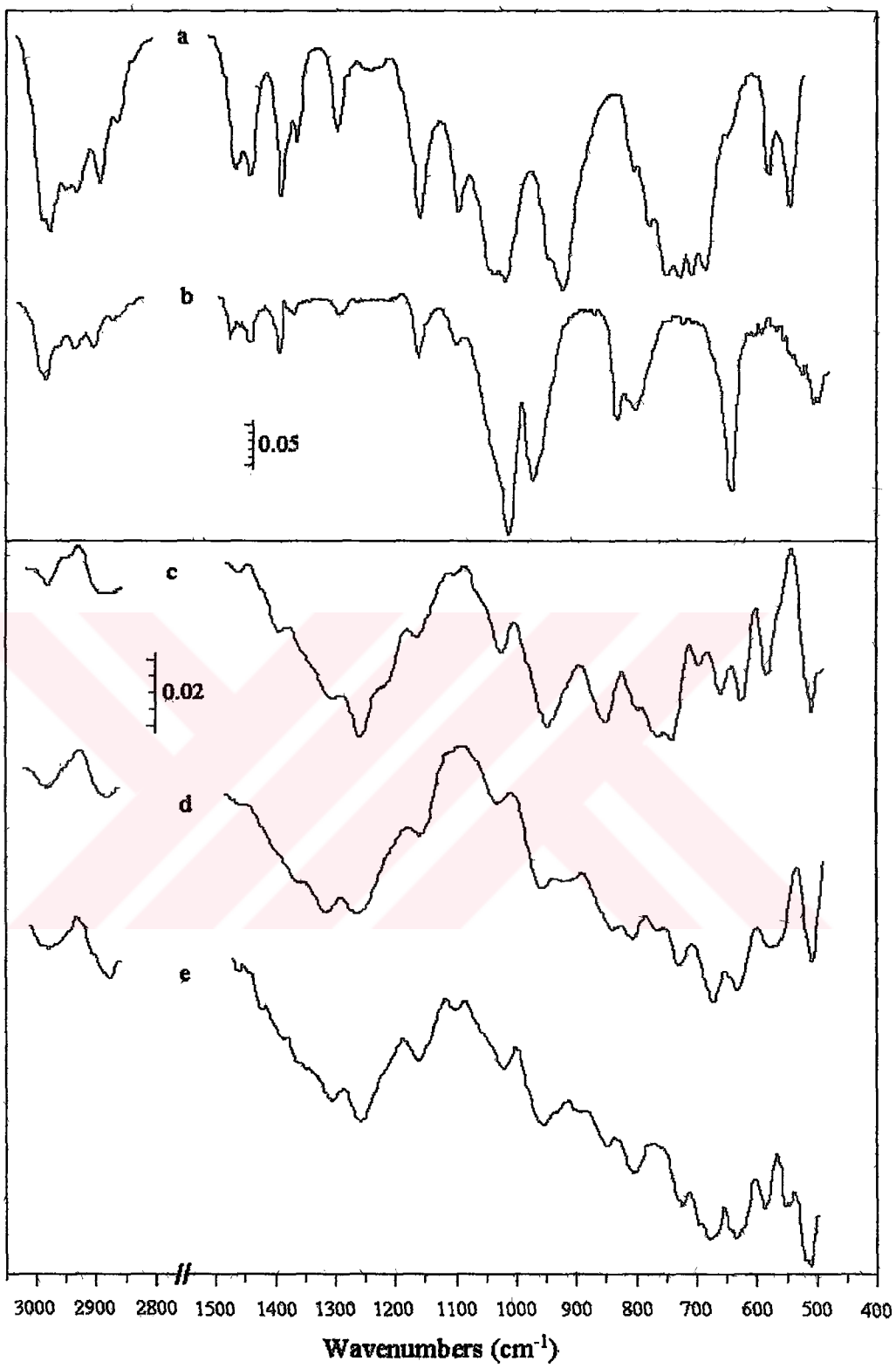

Figure 4.65. DRIFT spectra of chalcopyrite samples interacted with 10^{-1} M DTP in pH 11 buffer solution at c) –100 mV, d) +150 mV and e) +400 mV. Spectra of a) DTP and b) $(DTP)_2$ are given as references.

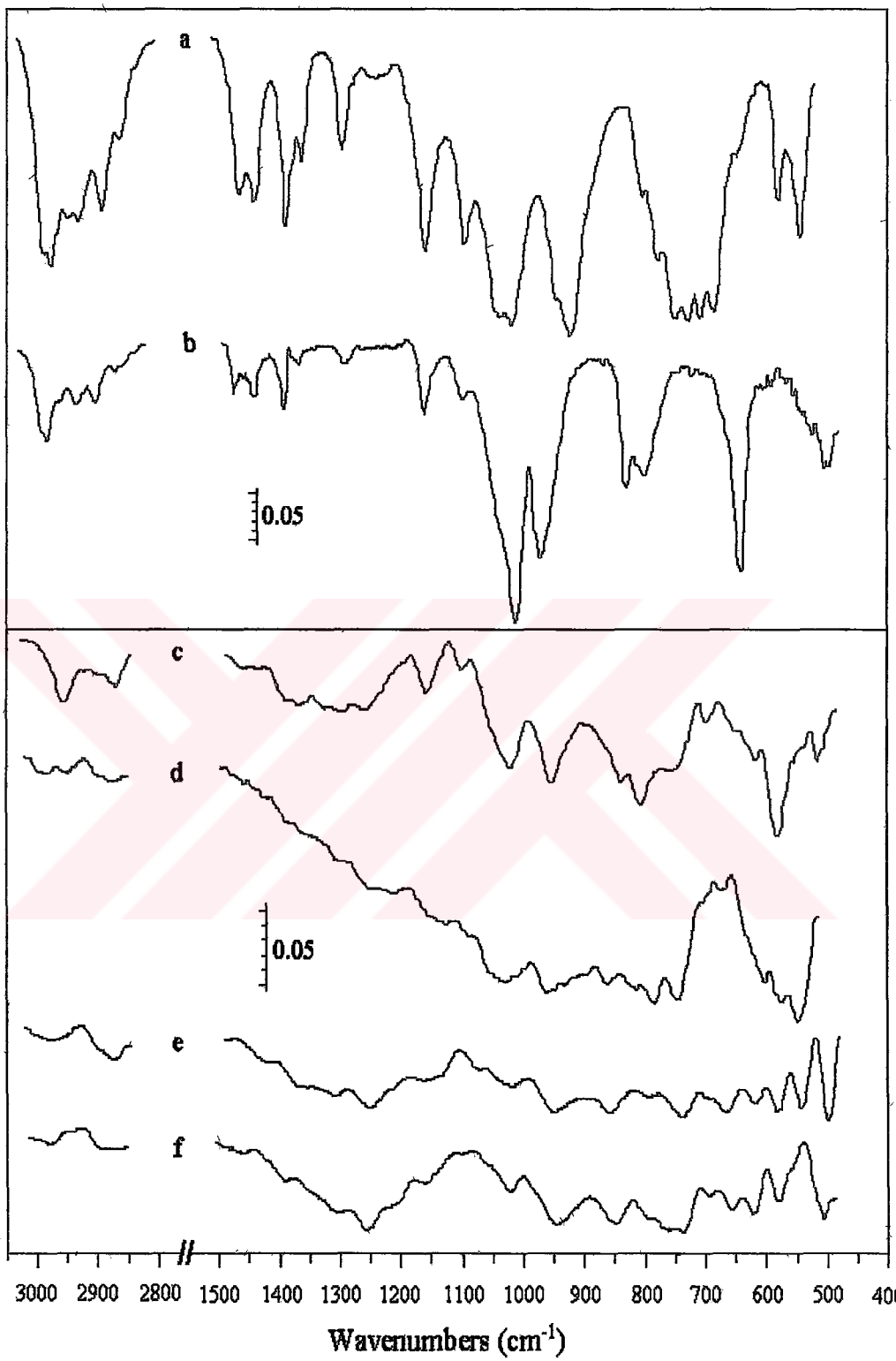

Figure 4.66. DRIFT spectra of chalcopyrite samples interacted with 10^{-1} M DTP at –100 mV in c) pH 4.67, d) pH 6.97, e) pH 9.2 and f) pH 11 buffer solutions. Spectra of a) DTP and b) $(DTP)_2$ are given as references.

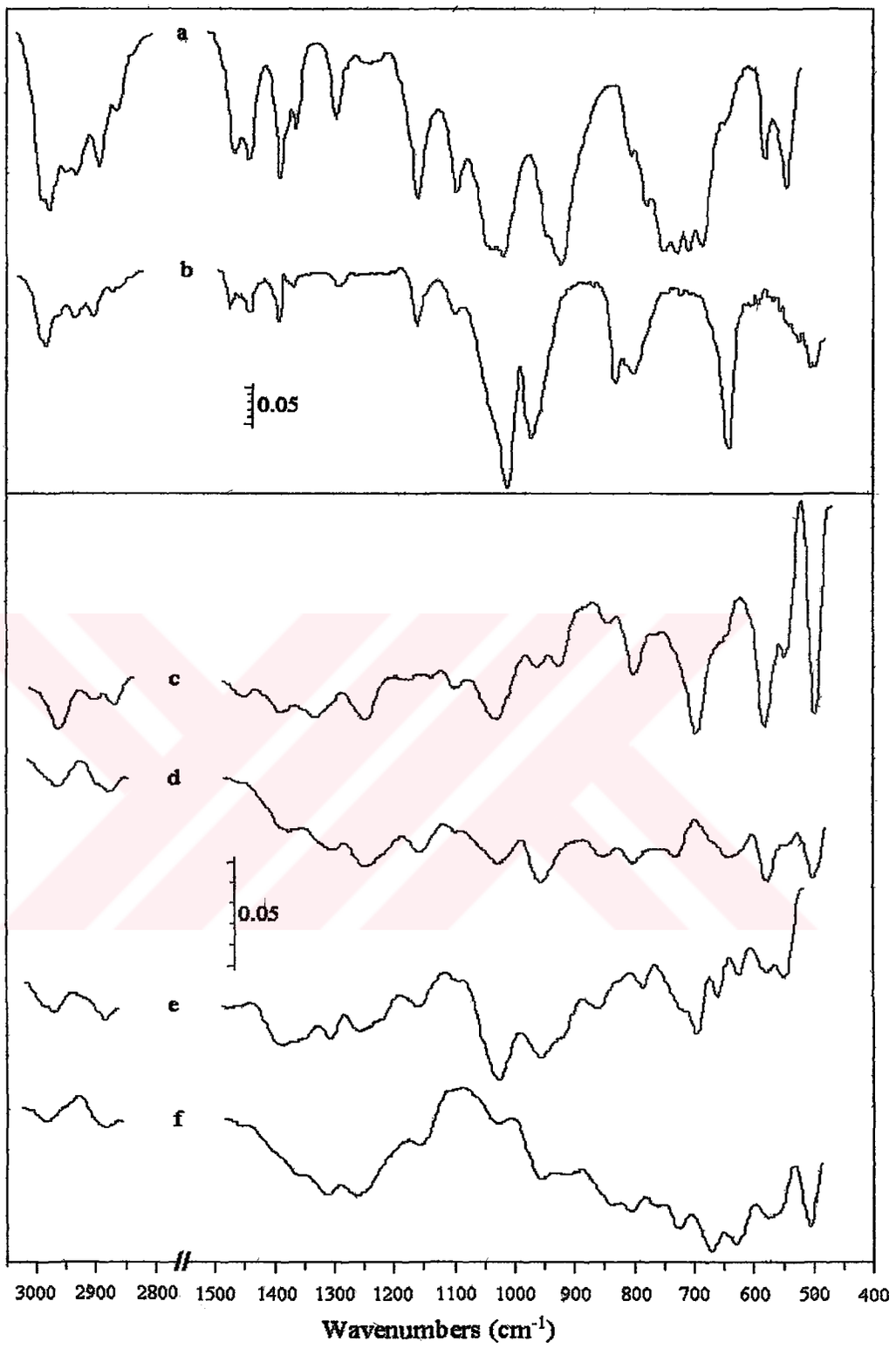

Figure 4.67. DRIFT spectra of chalcopyrite samples interacted with 10^{-1} M DTP at +150 mV in c) pH 4.67, d) pH 6.97, e) pH 9.2 and f) pH 11 buffer solutions. Spectra of a) DTP and b) $(DTP)_2$ are given as references.

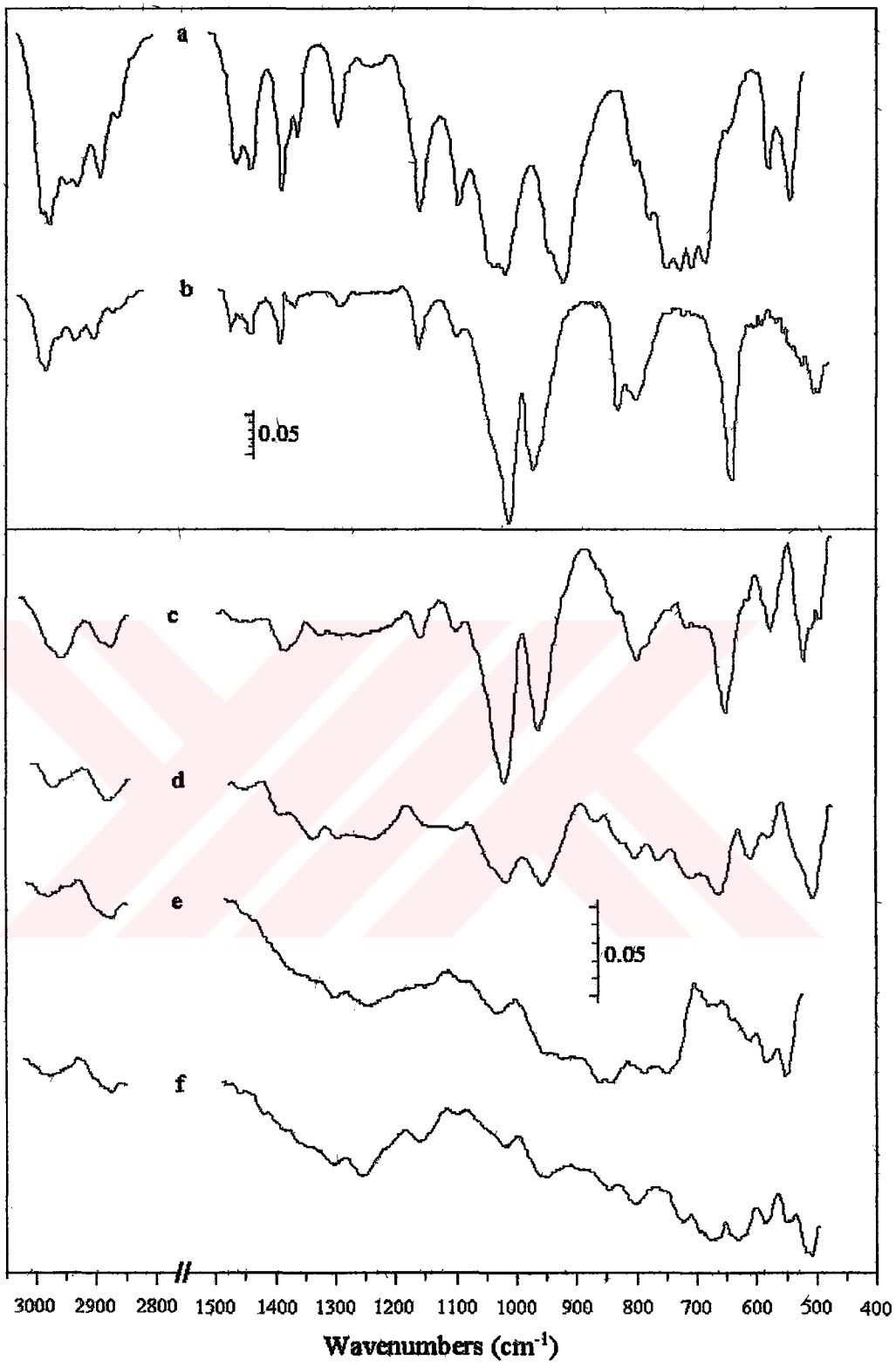

Figure 4.68. DRIFT spectra of chalcopyrite samples interacted with 10^{-1} M DTP at +400 mV in c) pH 4.67, d) pH 6.97, e) pH 9.2 and f) pH 11 buffer solutions. Spectra of a) DTP and b) $(DTP)_2$ are given as references.

4.2.2 DRIFT Study with DTPI

DRIFT spectrum of DTPI is given in Figure 4.69.a. Peak positions of DTPI spectrum are as follows in cm^{-1}: 2956, 2928, 2893, 2870, 1464, 1400, 1381, 1366, 1337, 1319, 1230, 1207, 1165, 1105, 1065, 1018, 949, 922, 843, 810, 761, 736, 712, 608, 528 and 520.

As a reference, dimer of DTPI was prepared and its spectrum was also obtained (Figure 4.69.b). Peak positions of $(DTPI)_2$ were determined as follows in cm^{-1}: 2957, 2930, 2906, 2868, 1462, 1390, 1367, 1337, 1317, 1240, 1207, 1163, 1105, 1063, 1055, 951, 924, 851, 818, 783, 748, 727, 596, 520, 505 and 490.

In highly oxidising potentials, when platinum and DTPI are interacted and platinum surface is polarised in acid solution, dimer forms on platinum surface (Hiçyılmaz et al., 2001). Therefore, to clearly identify the dimer spectrum, platinum-powder was polarised at 1250 mV in pH 4.67 buffer solution with DTPI, and then DRIFT spectrum of dried Pt-powder was obtained (Figure 4.69.c). Peak positions are as follows in cm^{-1}: 2957, 2928, 2903, 2870, 1463, 1391, 1373, 1337, 1240, 1211, 1163, 1107, 1063, 995, 951, 895, 845, 818, 786, 748, 714, 675, 596, 518, 483 and 469.

Similar to the case of DTP in section 4.2.1, CuDTPI precipitate forms according to reactions 4.3 and 4.4 when $DTPI^-$ is reacted with Cu^{+2} ions (Yordanov et al., 1983). However, reaction 4.4 may be slower and $Cu(DTPI)_2$ may form chiefly when going from acid to alkaline condition as in the case of DTP (Goold and Finkelstein, 1972). Hence, 10^{-2} M DTPI solution was interacted with 10^{-2} M $CuSO_4.5H_2O$, and CuDTPI precipitate was obtained in pH 4.67 buffer solution. Precipitate was washed with distilled water five times and its DRIFT spectrum was also obtained (Figure 4.69.d). Peak positions are as follows in cm^{-1}: 2957, 2929, 2908, 2893, 2868, 1462, 1393, 1381, 1366, 1337, 1319, 1238, 1207, 1165, 1105, 1065, 1020, 951, 924, 849, 818, 810, 793, 783, 750, 727, 714, 596, 579, 513 and 490.

$$2Cu^{+2} + 4DTPI^{-} \rightleftharpoons 2Cu(DTPI)_2 \qquad 4.3$$

$$2Cu(DTP)_2 \rightleftharpoons 2CuDTP + (DTP)_2 \qquad 4.4$$

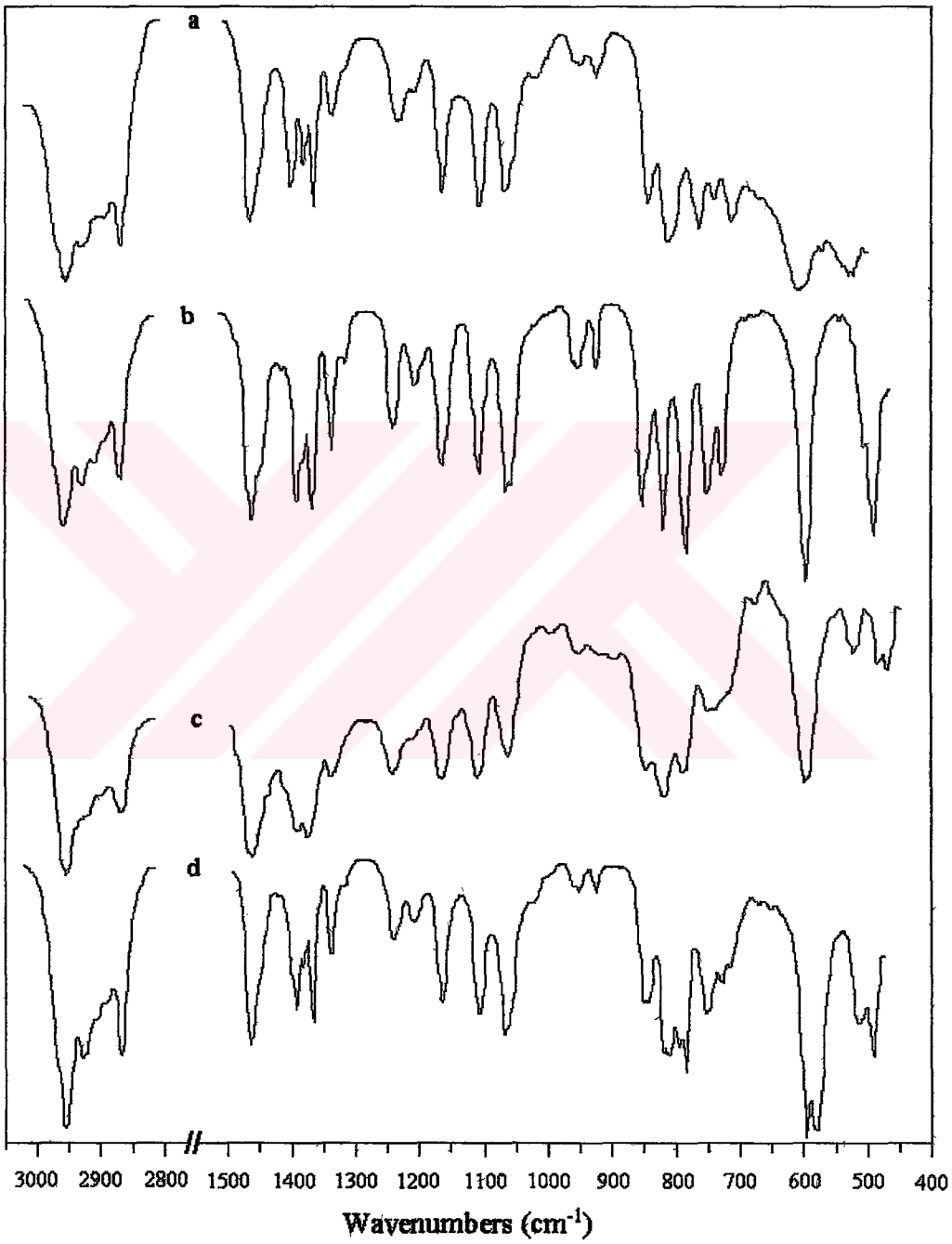

Figure 4.69. DRIFT spectra of a) DTPI, b) $(DTPI)_2$, c) Pt-powder polarised with 10^{-1} M DTPI in pH 4.67 buffer at 1250 mV, and d) Cu-DTPI precipitate

Chalcopyrite spectra were mapped out from polarised sample in acid solution (pH 4.67) at reducing (-100 mV), moderately oxidising (+150 mV) and highly oxidising (+400 mV) potentials to clarify the effects of DTPI on chalcopyrite and to interpret the surface compounds (Figure 4.70). For this purpose, chalcopyrite was treated with 10^{-1} M DTPI and then DRIFT spectra were measured. Peak intensities decrease by increasing the pulp potential. Peak positions are as follows:

–100 mV: 2957, 2903, 2870, 1462, 1392, 1371, 1338, 1240, 1165, 1107, 1063, 954, 916, 842, 810, 716, 679, 586, 513.

+150 mV: 2957, 2870, 1458, 1392, 1373, 1338, 1242, 1163, 1106, 1063, 1012, 954, 915, 845, 810, 713, 665, 586, 515.

+400 mV: 2957, 2898, 2870, 1458, 1392, 1371, 1337, 1298, 1242, 1163, 1107, 1065, 1022, 957, 920, 845, 810, 708, 675, 602, 586, 551, 534, 505, 488.

Chalcopyrite spectra obtained from samples prepared with 10^{-1} M DTPI in pH 6.97 buffer solution are given in Figure 4.71. Peak intensity did almost not change with Eh; only there is a small increase at higher Eh values. Peak positions are determined as follows:

–100 mV: 2957, 2870, 1460, 1388, 1371, 1338, 1242, 1211, 1165, 1107, 1063, 950, 918, 843, 812, 710, 667, 610, 585, 517, 494.

+150 mV: 2957, 2928, 2870, 1460, 1393, 1371, 1337, 1241, 1211, 1163, 1107, 1063, 957, 920, 845, 809, 729, 711, 698, 658, 640, 585, 509.

+400 mV: 2957, 2870, 1460, 1392, 1371, 1337, 1243, 1211, 1163, 1107, 1063, 957, 910, 845, 812, 710, 679, 655, 585, 520.

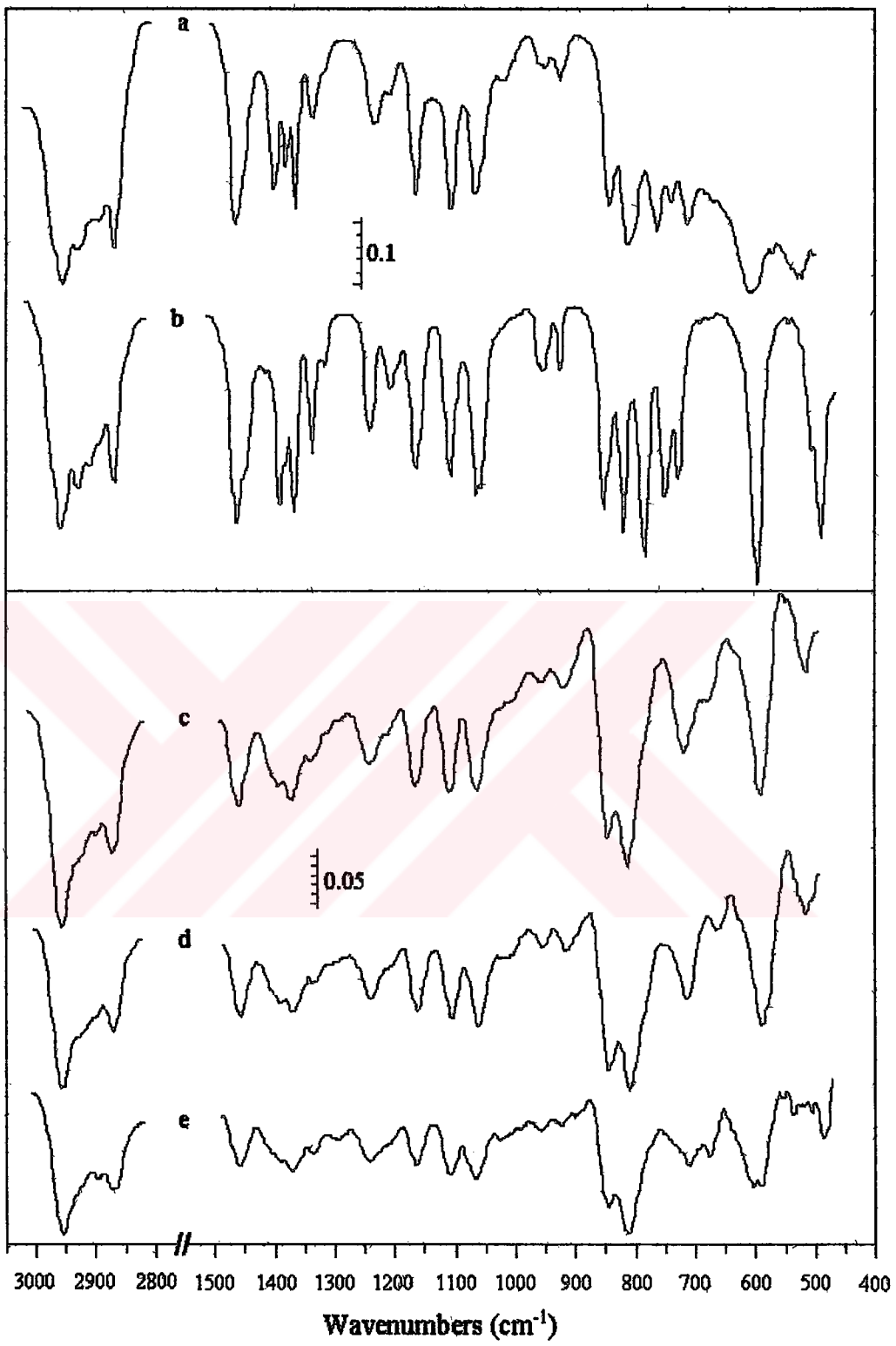

Figure 4.70. DRIFT spectra of chalcopyrite samples interacted with 10^{-1} M DTPI in pH 4.67 buffer solution at c) –100 mV, d) +150 mV and e) +400 mV. Spectra of a) DTPI and b) $(DTPI)_2$ are given as references.

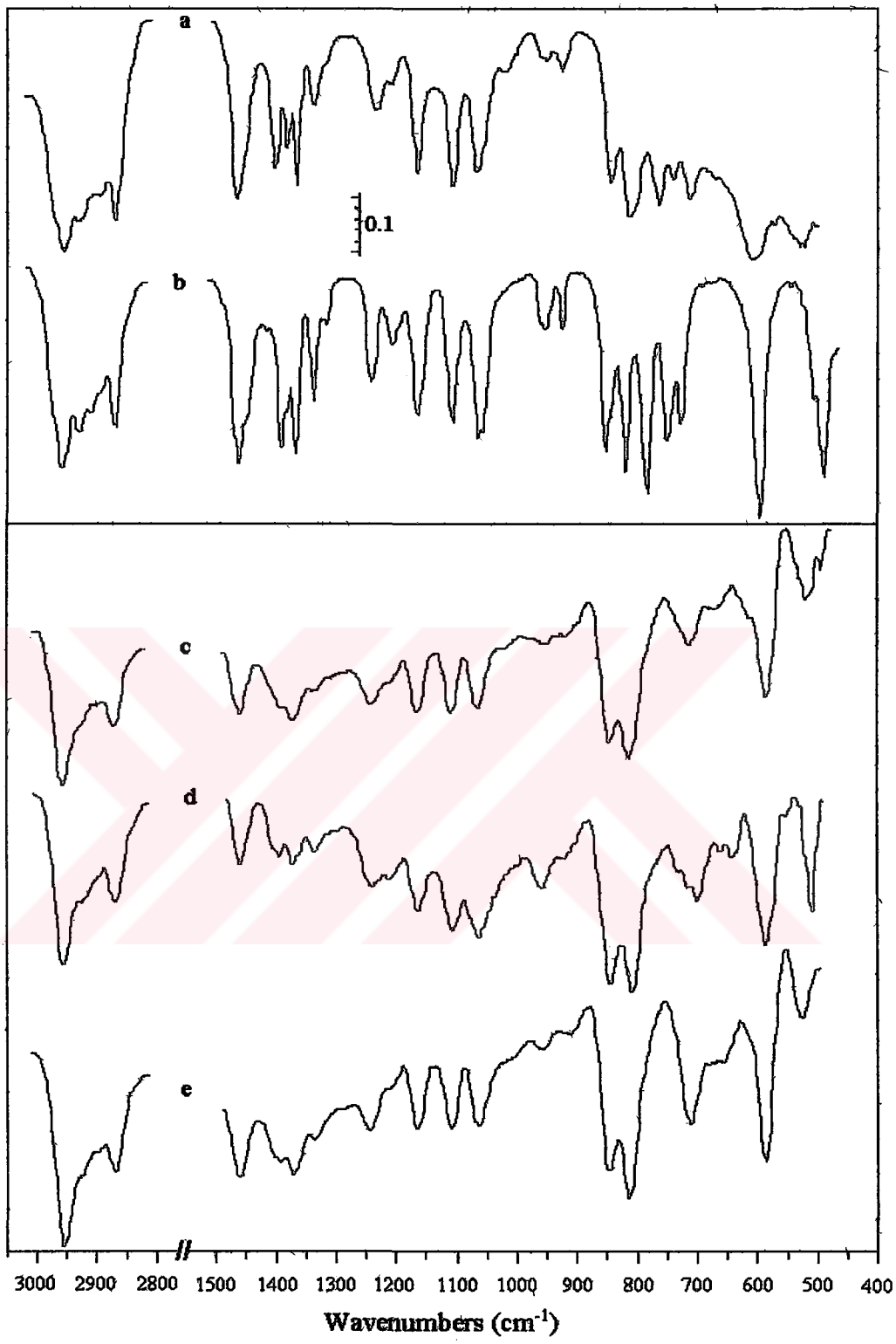

Figure 4.71. DRIFT spectra of chalcopyrite samples interacted with 10^{-1} M DTPI in pH 6.97 buffer solution at c) –100 mV, d) +150 mV and e) +400 mV. Spectra of a) DTPI and b) $(DTPI)_2$ are given as references.

Figure 4.72 presents the spectra obtained from chalcopyrite samples reacted with 10^{-1} M DTPI at –100 mV, +150 mV and +400 mV pulp potential values in pH 9.2 buffer solution. Peak positions in these spectra are determined as follows:

–100 mV: 2957, 2870, 1460, 1391, 1371, 1338, 1242, 1165, 1105, 1064, 1020, 958, 916, 845, 812, 706, 586, 515.

+150 mV: 2957, 2870, 1460, 1392, 1371, 1337, 1244, 1211, 1163, 1107, 1061, 1022, 932, 845, 812, 710, 681, 660, 625, 586, 548, 528, 494.

+400 mV: 2957, 2928, 2870, 1460, 1392, 1371, 1338, 1242, 1163, 1107, 1063, 945, 920, 845, 810, 710, 660, 612, 585, 538, 507, 494.

Chalcopyrite spectra obtained from samples reacted with 10^{-1} M DTPI at –100 mV, +150 mV and +400 mV pulp potential values in pH 11 buffer solution are given in Figure 4.73. Peak positions in these spectra are found as follows:

–100 mV: 2957, 2870, 1460, 1392, 1371, 1337, 1242, 1211, 1165, 1107, 1063, 1022, 947, 914, 845, 810, 713, 667, 581, 520.

+150 mV: 2957, 2870, 1459, 1390, 1371, 1337, 1242, 1195, 1163, 1105, 1064, 1020, 957, 920, 843, 810, 708, 673, 623, 579, 527, 514, 494, 482.

+400 mV: 2957, 2870, 1459, 1391, 1371, 1338, 1242, 1211, 1164, 1107, 1064, 1023, 959, 918, 842, 810, 710, 660, 613, 581, 543, 528, 513, 492.

For a clear identification of the effects of pH on the reaction between DTPI and chalcopyrite at certain pulp potential values, Figures 4.74-4.76 were given. These figures show that peak intensity decreased continuously by increasing the pulp pH. Peak positions of IR signals were given above.

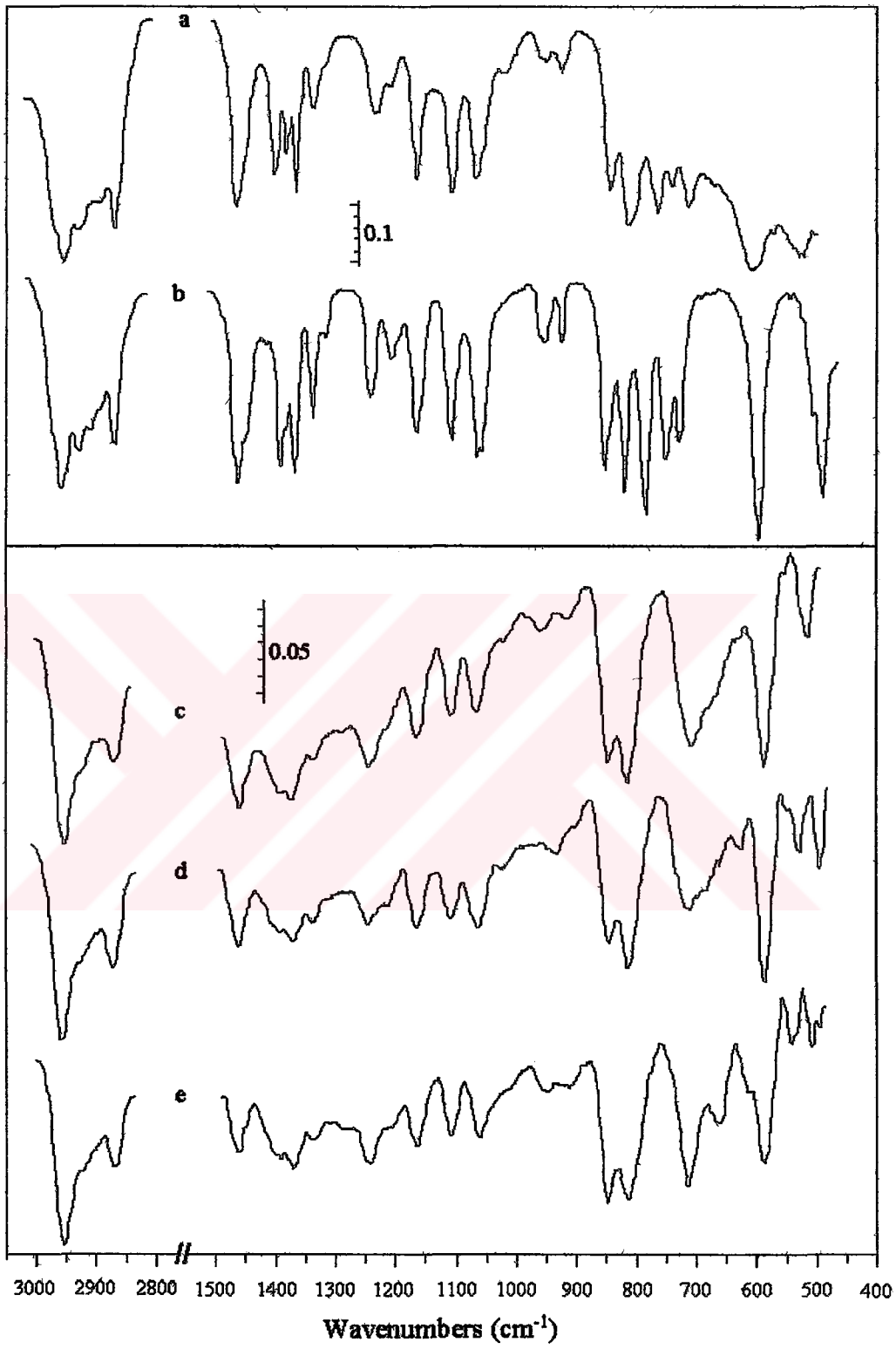

Figure 4.72. DRIFT spectra of chalcopyrite samples interacted with 10^{-1} M DTPI in pH 9.2 buffer solution at c) –100 mV, d) +150 mV and e) +400 mV. Spectra of a) DTPI and b) $(DTPI)_2$ are given as references.

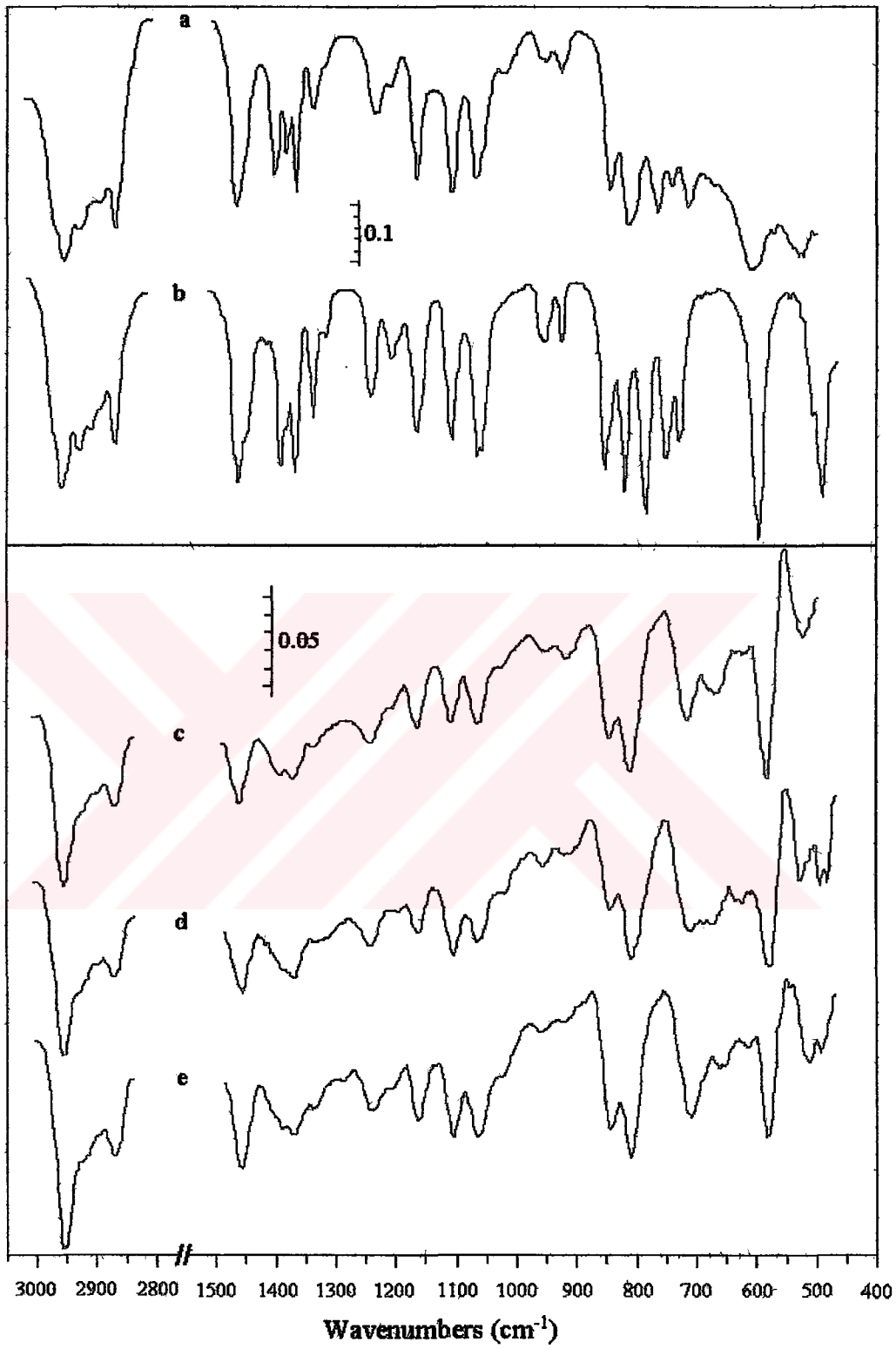

Figure 4.73. DRIFT spectra of chalcopyrite samples interacted with 10^{-1} M DTPI in pH 11 buffer solution at c) –100 mV, d) +150 mV and e) +400 mV. Spectra of a) DTPI and b) $(DTPI)_2$ are given as references.

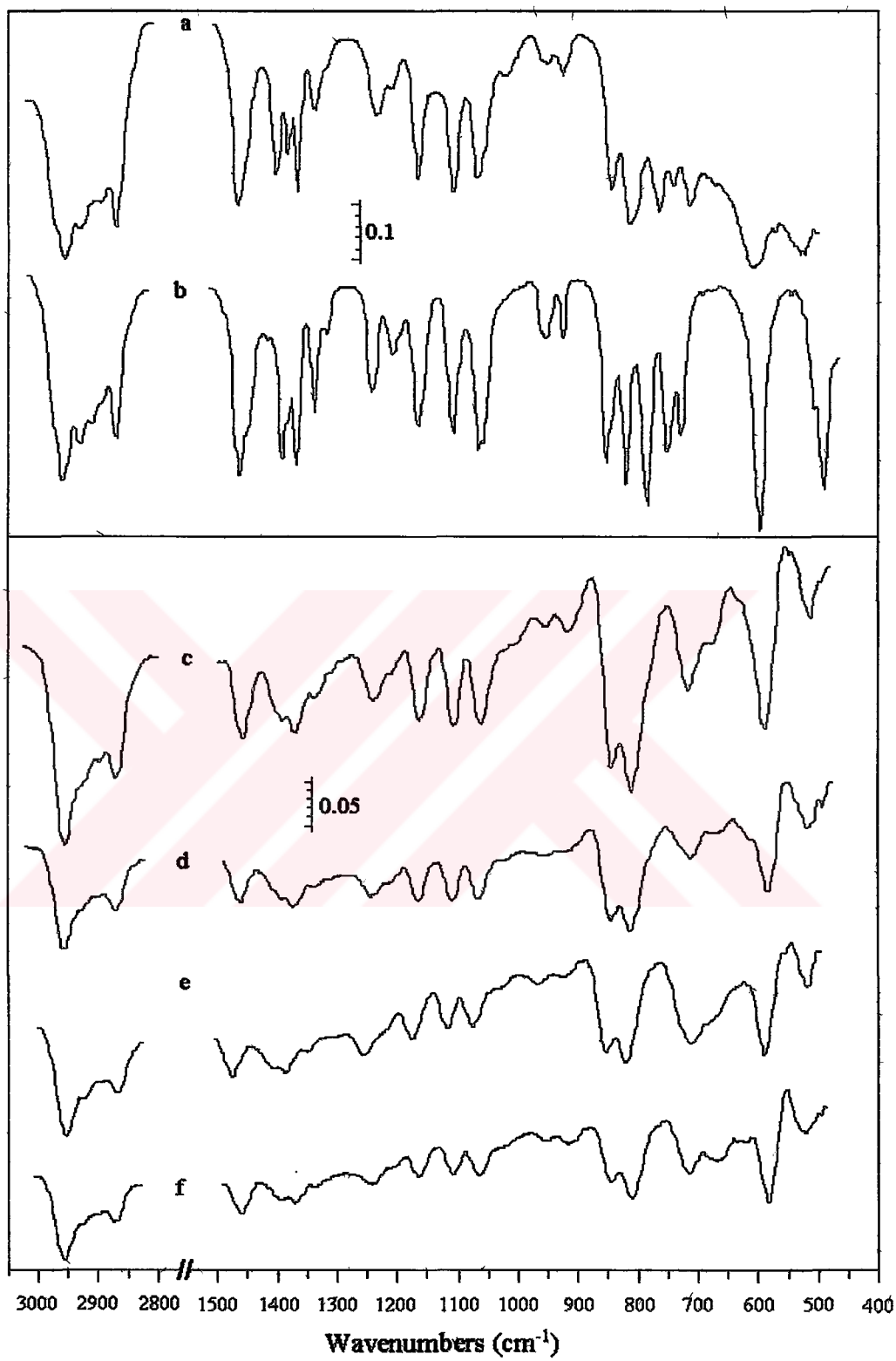

Figure 4.74. DRIFT spectra of chalcopyrite samples interacted with 10^{-1} M DTPI at –100 mV in c) pH 4.67, d) pH 6.97, e) pH 9.2 and f) pH 11 buffer solutions. Spectra of a) DTPI and b) $(DTPI)_2$ are given as references.

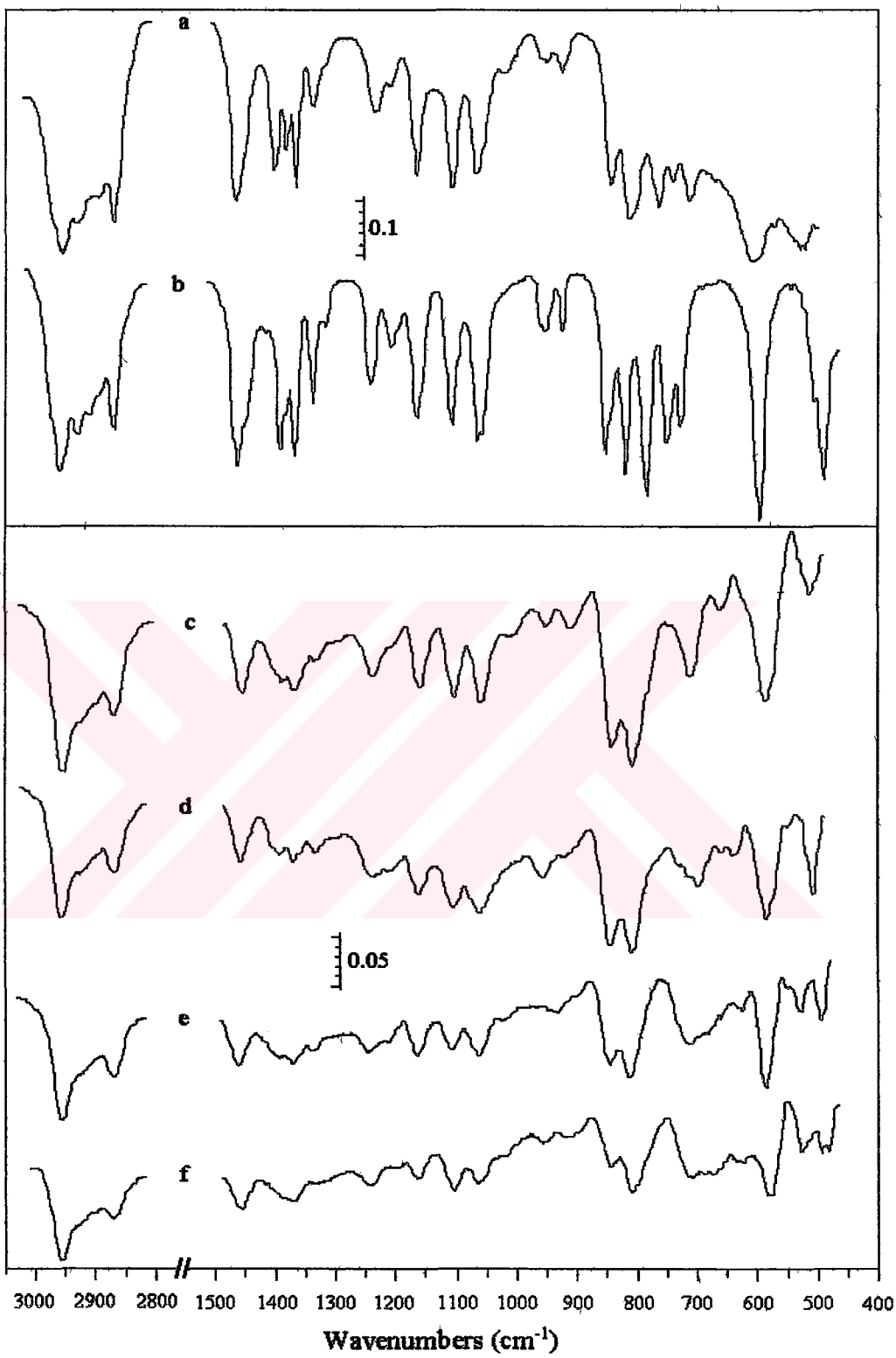

Figure 4.75. DRIFT spectra of chalcopyrite samples interacted with 10^{-1} M DTPI at +150 mV in c) pH 4.67, d) pH 6.97, e) pH 9.2 and f) pH 11 buffer solutions. Spectra of a) DTPI and b) $(DTPI)_2$ are given as references.

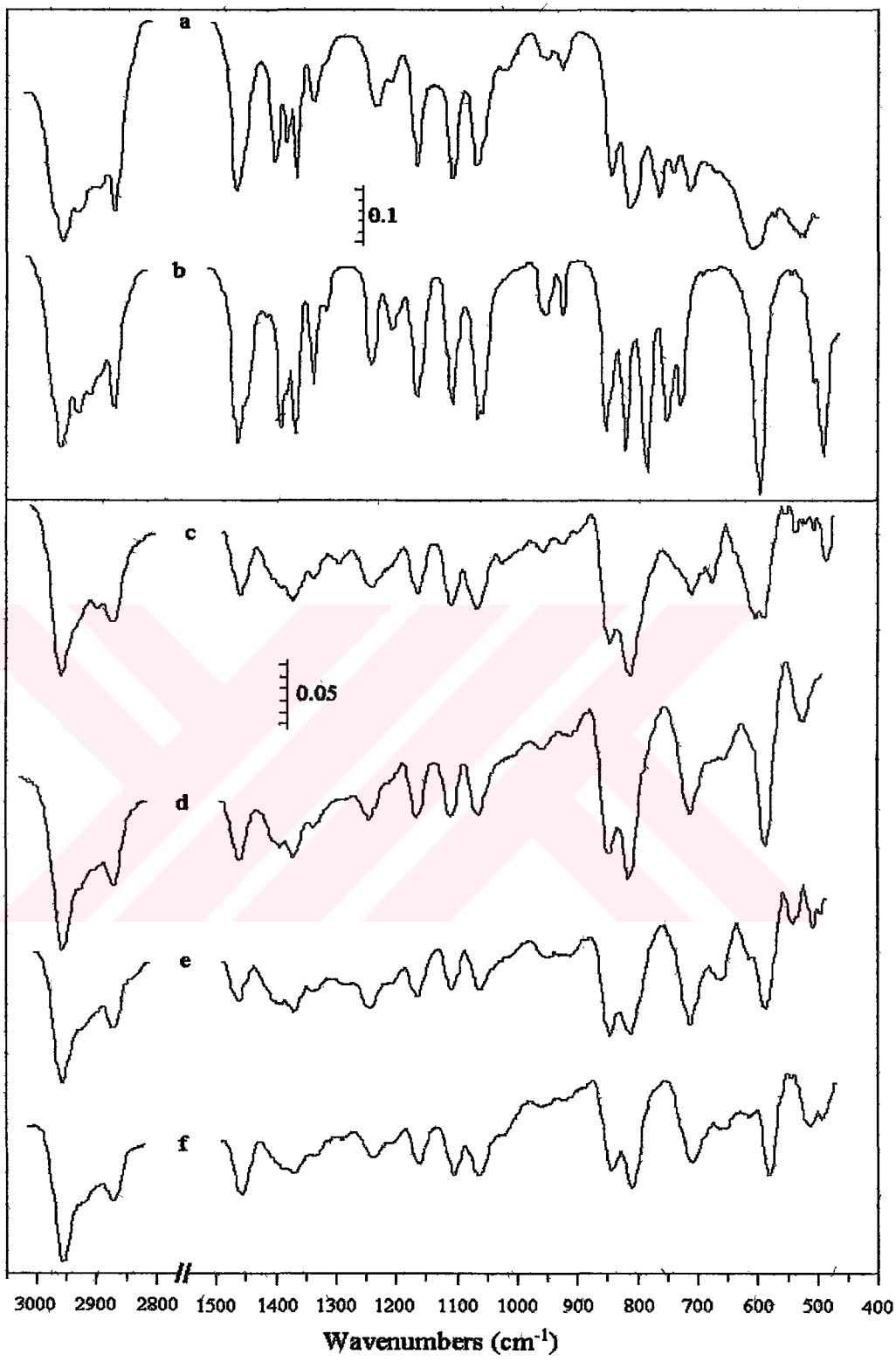

Figure 4.76. DRIFT spectra of chalcopyrite samples interacted with 10^{-1} M DTPI at +400 mV in c) pH 4.67, d) pH 6.97, e) pH 9.2 and f) pH 11 buffer solutions. Spectra of a) DTPI and b) $(DTPI)_2$ are given as references.

4.3 Flotation

Flotation studies were performed to determine the effect of pulp potential and pH value on chalcopyrite recovery. For this aim, flotation experiments were conducted in four different buffer solutions (pH 4.67, pH 6.97, pH 9.2 and pH 11) by polarising the mineral surface for 15 minutes at certain pulp potential values (-100 mV, 0 mV, 100 mV, 200 mV, 300 mV and 400 mV). These experiments were carried out in the absence and presence of DTP and DTPI.

Flotation experiments were made in oxygen-free condition to eliminate the oxidising effect of O_2 gas coming from air by intensive bubbling the pure nitrogen gas. A flowmeter was used to control the amount of flotation gas. So, at the beginning, gas flowrate was determined for certain flowmeter scales (28.5 ml/min, 35.5 ml/min, 59 ml/min and 112,5 ml/min for 50, 75, 100 and 150 scales of flowmeter, respectively).

A series of flotation experiments were performed to optimise the required flotation gas. In these experiments, closely sized cleaned quartz sample (-210+149 μm) was used. Since, quartz is a hydrophilic mineral, and it should not float up to an optimum gas flowrate. Flotation was applied by using distilled water for 10 minutes. If higher amount of gas is fed to modified Hallimond tube (flotation cell), quartz should be recovered in concentrate compartment due to entrainment. Figure 4.77 presents the experimental results made with quartz. While quartz recovery is low up to 35.5 ml/min, it increases gradually with an increase in gas flowrate. So, the amount of flotation gas was decided as 35.5 ml/min for the experiments with chalcopyrite.

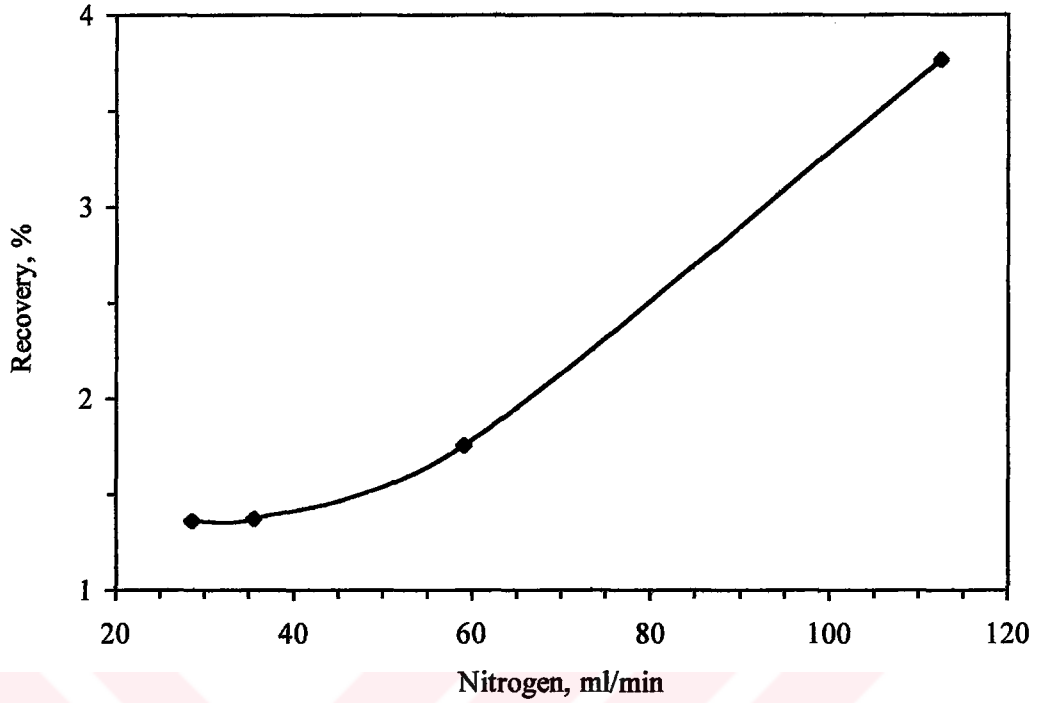

Figure 4.77. Change of quartz recovery with gas flowrate (Flotation time: 10 min; pH 5.5 (distilled water))

Experiments were also carried out to determine the flotation time. Chalcopyrite samples were floated in pH 9.2 buffer solution. Before each experiment, 15 minutes conditioning was applied. Results of these experiments are shown in Figure 4.78. Chalcopyrite recovery increases sharply up to 5 minute, then it increases gradually up to 10 minutes. Above 10 minutes, there is little increase in recovery. Hence, enough flotation time was decided as 10 minutes.

4.3.1 Flotation Studies in Collectorless Condition

Effect of pH on rest potential of chalcopyrite was investigated before collectorless flotation (Figure 4.79). The figure shows that rest potential of chalcopyrite almost linearly decreases with increasing the pulp pH value.

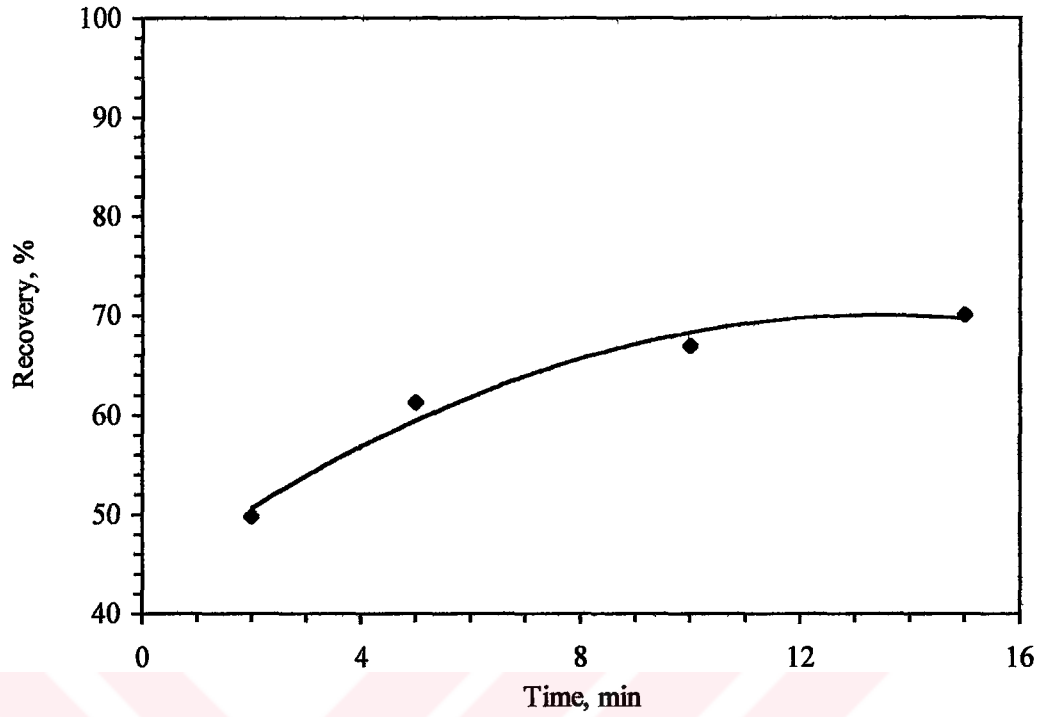

Figure 4.78. Flotation time vs. recovery relationship in collectorless condition at pH 9.2 (conditioning: 15 min)

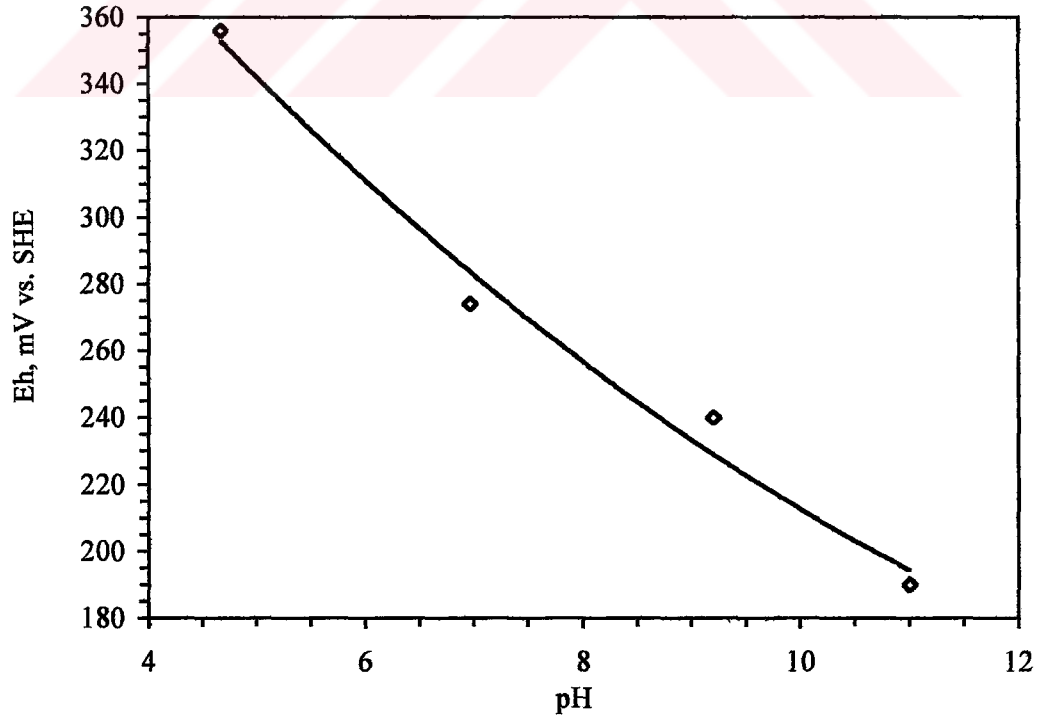

Figure 4.79. Rest potential change of chalcopyrite with respect to pulp pH

Chalcopyrite flotation was performed at different Eh and pH conditions (Figure 4.80). Before each experiment, 15 minutes conditioning (polarisation) was applied at certain potentials. Collectorless flotation experiments were repeated at least three times for all data obtained at certain Eh and pH conditions, and it was shown that results were reproducible with about 1.09 % standard deviation. Figure 4.80 shows that recovery did almost not change up to 0 mV. But, it sharply increased from 0 mV to 100 mV and then gradually decreased by increasing the pulp potential. Effect of Eh on chalcopyrite recovery was not so high in acid solution. On the other hand, recovery changed considerably with pulp potential at neutral and alkaline conditions. Chalcopyrite recovery reached its maximum value in acid solution and at moderately oxidising potentials. It decreased at higher pH values.

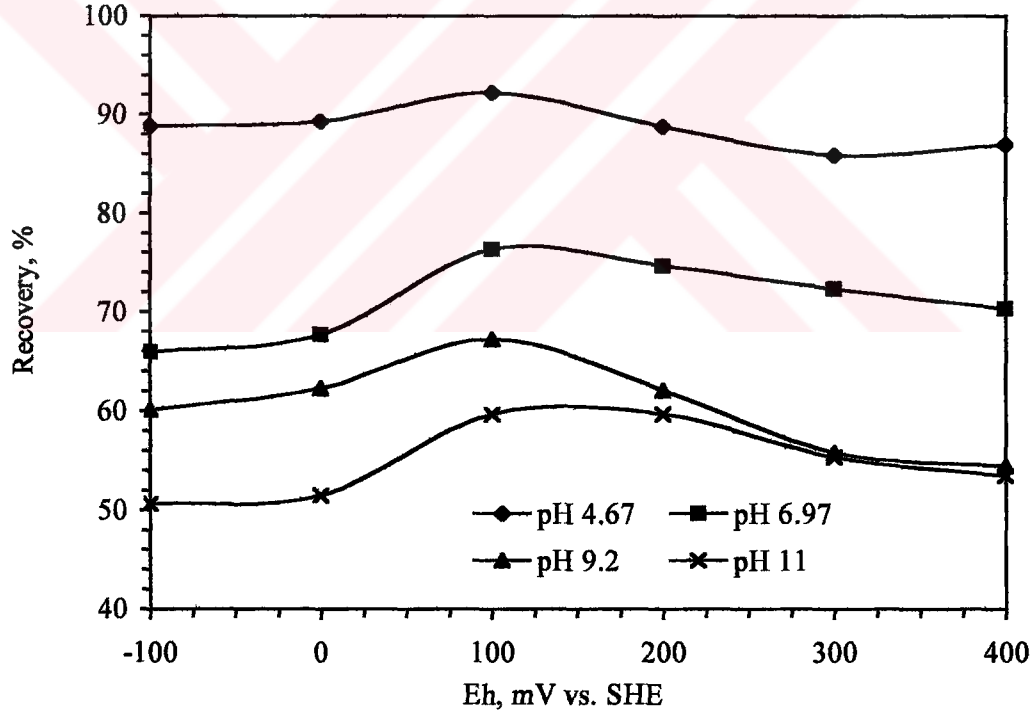

Figure 4.80. Pulp potential-recovery relationship in collectorless condition

For a clear demonstration of Eh-pH relationship, three-dimensional (Figure 4.81) relief map was drawn. As shown from this figure, highest recovery

can be obtained at moderately oxidising potentials (100-200 mV). Moreover, recovery increases sharply as pH went from alkaline to acid condition.

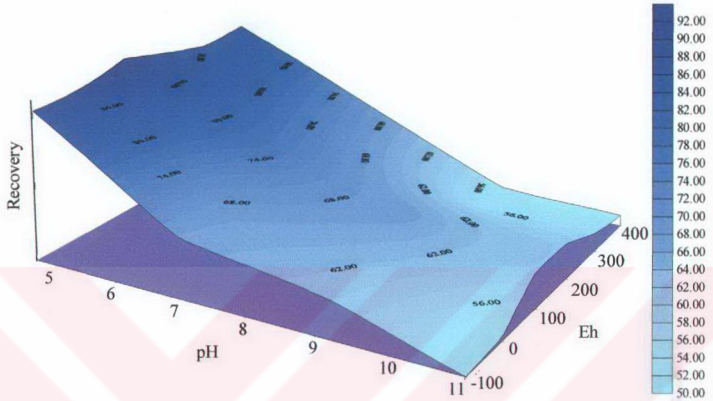

Figure 4.81. Three-dimensional relief map for collectorless flotation

4.3.2 Flotation Studies with DTP

Experiments were also made to clarify the effect of DTP on chalcopyrite at the same Eh and pH values applied in collectorless condition. Before each experiment, 15 minutes polarisation at certain Eh value was applied to satisfy the adsorption of collector on mineral surface. DTP induced flotation experiments were repeated at least three times for all data obtained at certain Eh and pH conditions, and it was shown that results were reproducible with about 0.73 % standard deviation.

At first, DTP amount used in flotation experiments was determined (Figure 4.82). Chalcopyrite recovery sharply increased up to 50 g/t collector dosage. Above this value, recovery did not increase appreciably with increasing DTP amount. Therefore, 50 g/t DTP was determined as optimum dosage for potential controlled flotation experiments.

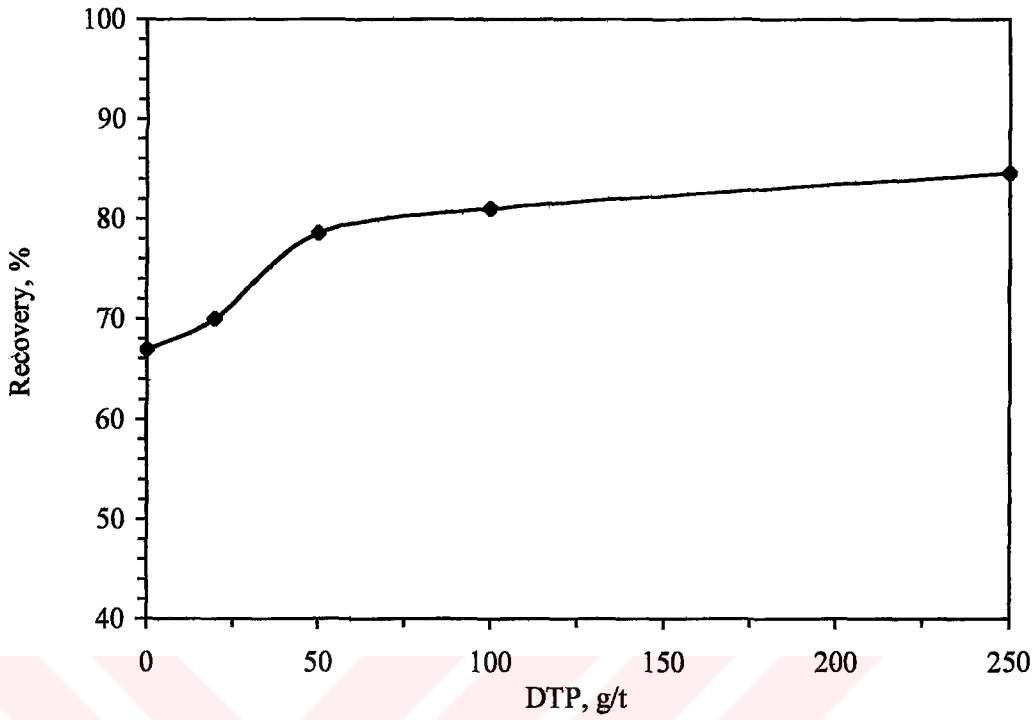

Figure 4.82. Effect of DTP amount on flotation recovery (conditioning 15 min; pH 9.2)

In addition, to demonstrate the effect of DTP on rest potential of chalcopyrite, pulp potential was measured during conditioning (Figure 4.83). Pulp potential decreased linearly with an increase in DTP amount. But, this decrease was not in considerable rate, because pulp potential decreased about 21 mV from 0 g/t DTP to 250 g/t DTP.

Figure 4.84 shows the results of Eh-recovery relationship for chalcopyrite flotation in the presence of 50 g/t DTP. Results for pH 4.67 and 6.97 were similar except that there was a small increase in recovery at moderately oxidising condition (100 mV) for pH 4.67 and a sharp decrease at highly oxidising condition (400 mV) for pH 6.97. In general, recovery increased up to 200-300 mV and then decreases. Maximum recovery values were obtained for pH 4.67 and decreased considerably with an increase in pH.

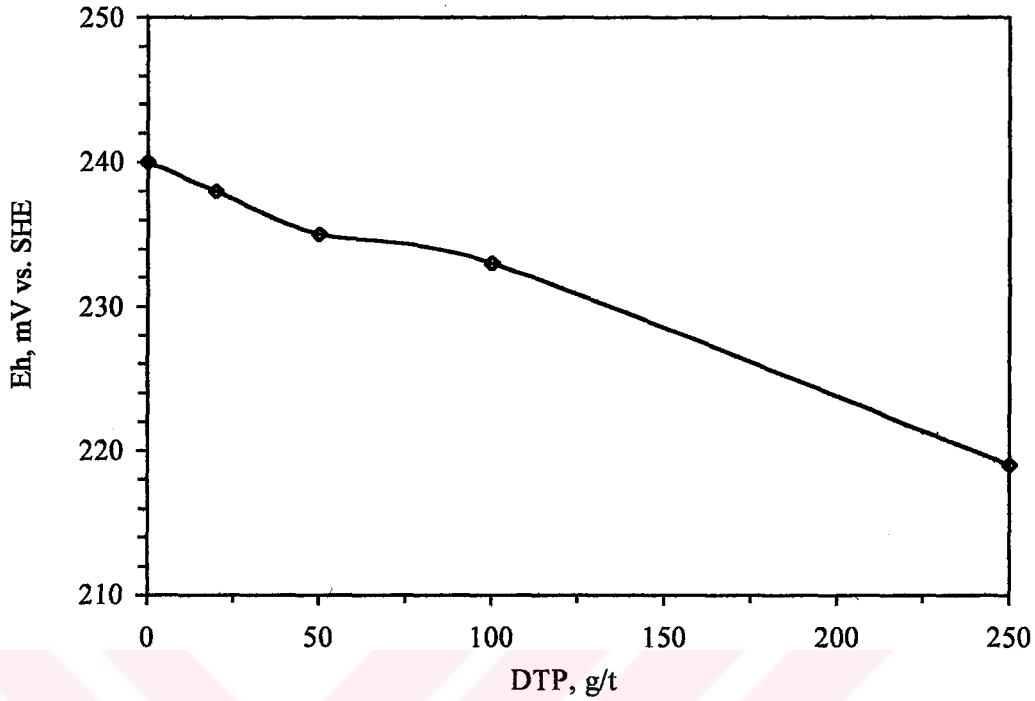

Figure 4.83. Effect of DTP amount on pulp potential (pH 9.2)

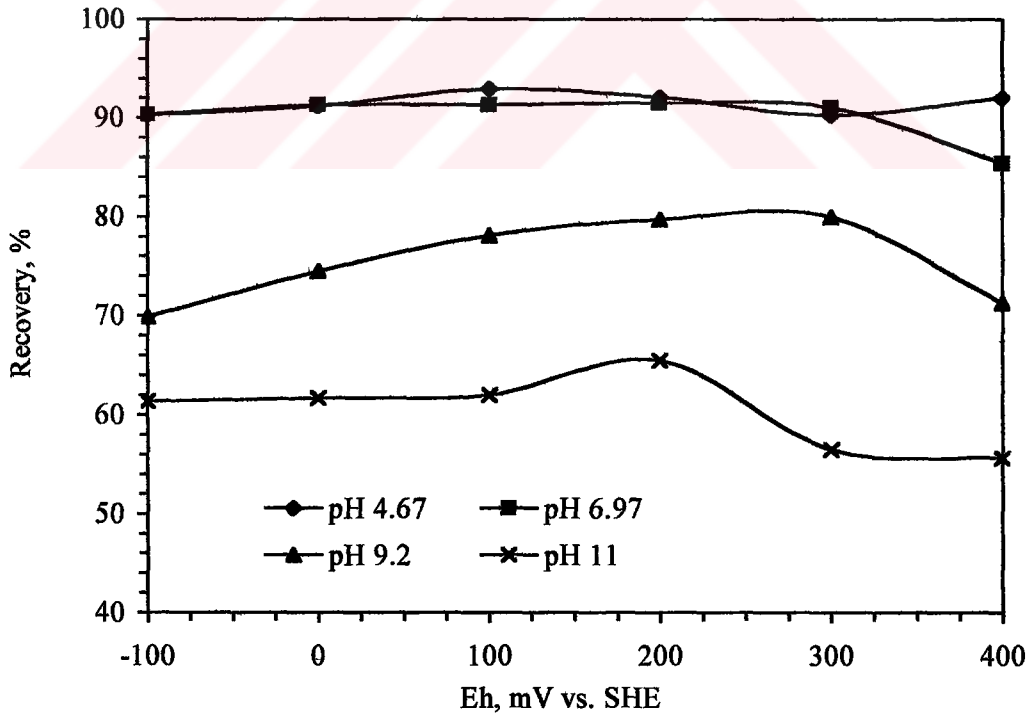

Figure 4.84. Pulp potential-recovery relationship in DTP (50 g/t) induced flotation

Three-dimensional (Figure 4.85) relief map was also drawn for a clear representation of Eh-pH relationship. This figure showed that highest recovery can be obtained at moderately oxidising potentials. Furthermore, there was a reasonable increase in chalcopyrite recovery as pH went from alkaline to acid condition.

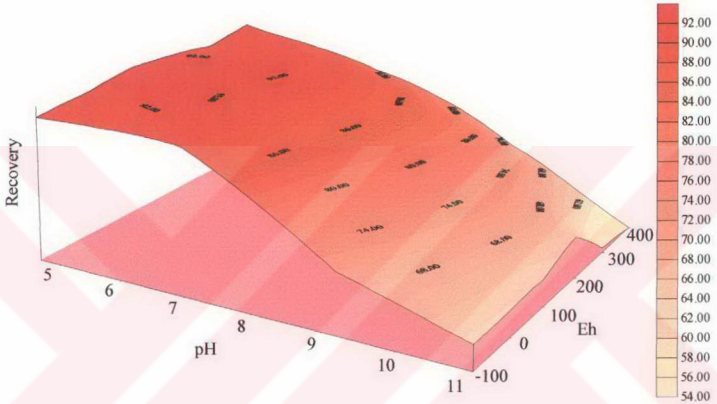

Figure 4.85. Three-dimensional relief map for DTP induced flotation

4.3.3 Flotation Studies with DTPI

Chalcopyrite flotation was performed with DTPI at different Eh and pH values to establish the effect of DTPI on chalcopyrite recovery at reducing, moderately oxidising and highly oxidising pulp potential values in acid, neutral and alkaline solutions. Before each experiment, chalcopyrite sample was polarised at certain potential for 15 minutes to satisfy the adsorption of collector on mineral surface at applied potential. DTPI induced flotation experiments were repeated at least three times for all data obtained at certain Eh and pH conditions, and it was shown that results were reproducible with about 0.91 % standard deviation.

DTPI amount used in potential controlled flotation experiments was determined as seen in Figure 4.86. Chalcopyrite recovery sharply increased up to 20 g/t collector dosage, and there was a small increase up to 50 g/t DTPI. Above this value, recovery did almost not change. So, 20 g/t DTPI was assumed as optimum dosage for potential controlled flotation experiments.

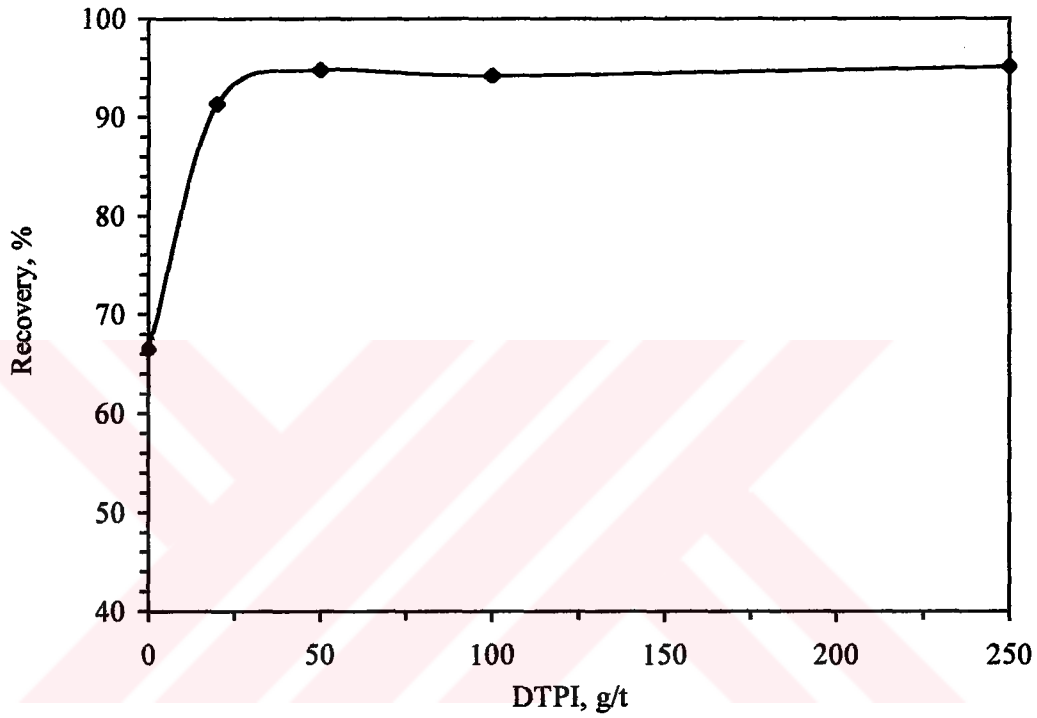

Figure 4.86. Effect of DTPI amount on flotation recovery (conditioning 15 min; pH 9.2)

Pulp potential was measured during conditioning to identify the effect of DTPI amount on rest potential of chalcopyrite, (Figure 4.87). Pulp potential did almost not change at lower dosages. Above 50g/t, it decreased about 19 mV up to 250 g/t DTPI concentration which was not in considerable rate.

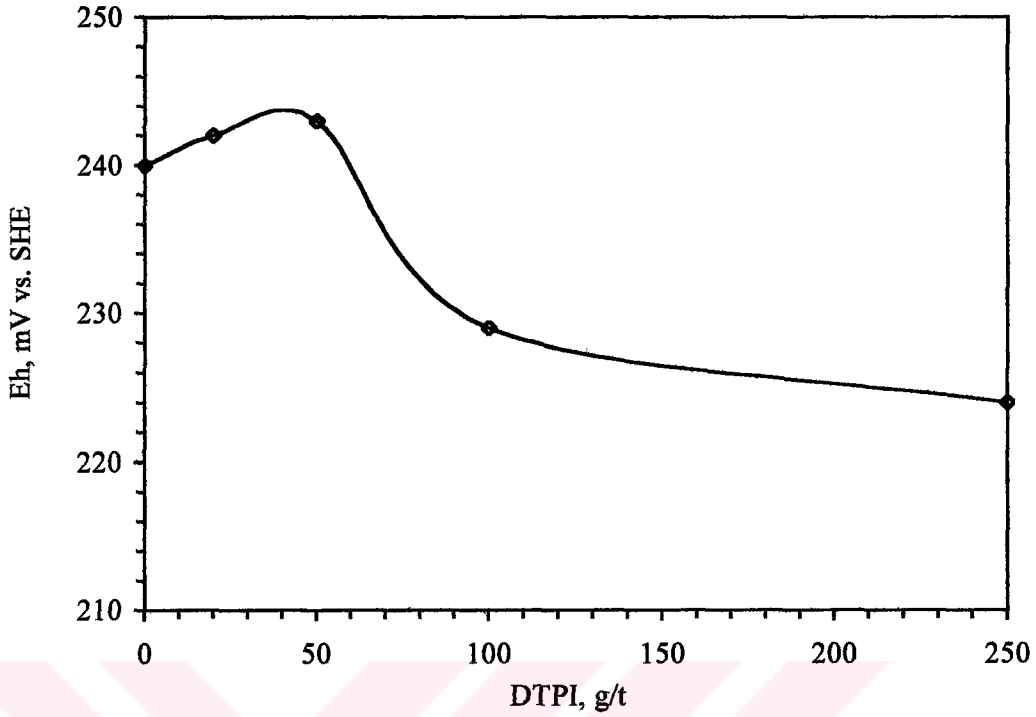

Figure 4.87. Effect of DTPI amount on pulp potential (pH 9.2)

Flotation experiments were carried out to determine the effect of pulp potential on chalcopyrite recovery for different pH values in the presence of 20 g/t DTPI (Figure 4.88). Results for pH 4.67 showed that collector concentration did almost not affect recovery for different pulp potential values, since recovery was anyway too high not to see the effect of pulp potential. Chalcopyrite recovery increased up to 100-200 mV and then decreased for pH 6.97, 9.2 and 11. In pH 11 buffer solution, this increase (up to 100 mV) was very sharp. Maximum recovery values were obtained for pH 4.67 and decreased considerably with an increase in pulp pH.

Three-dimensional (Figure 4.89) relief map was also drawn for a clear identification of the effect of Eh and pH on recovery of chalcopyrite. Figure 4.89 showed that highest recovery can be obtained at moderately oxidising potentials. In addition, at highly alkaline conditions, decrease in recovery was reasonably high for reducing and oxidising pulp potentials. Furthermore, recovery increased considerably as pH went from alkaline to acid condition.

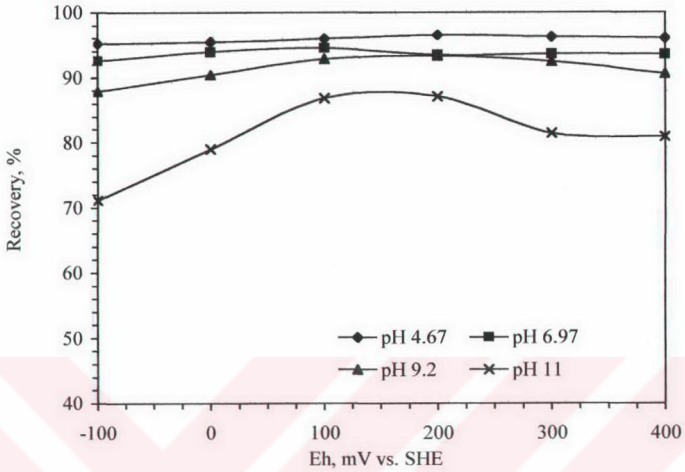

Figure 4.88. Pulp potential-recovery relationship in DTPI (20 g/t) induced flotation

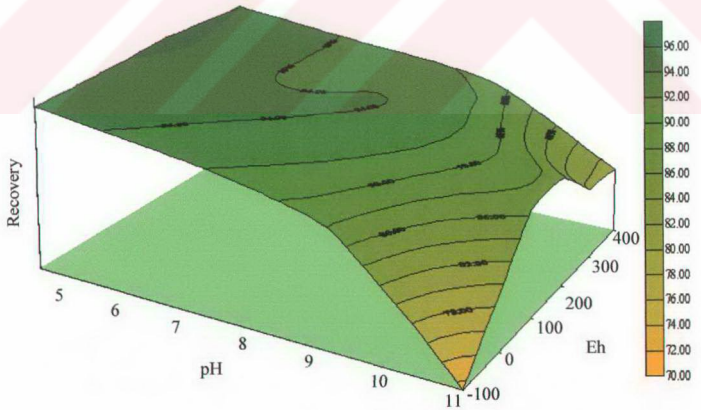

Figure 4.89. Three-dimensional relief map for DTPI induced flotation

4.3.4 Effect of Eh and pH on Flotation

Flotation results obtained in different buffer solutions in the presence and absence of DTP and DTPI are given in the same figures for each pH to clearly show the effect of collectors. Figure 4.90 presents the results for pH 4.67 buffer solution. When DTP was used as collector, there was a small increase in recovery as compared with collectorless condition. However, recovery increased considerably with DTPI. Recovery decreased progressively when increasing the pulp potential towards more oxidising values in collectorless condition and in the presence of DTP. But, this decrease can not be shown in the case of DTPI: Recovery was almost not affected from pulp potential.

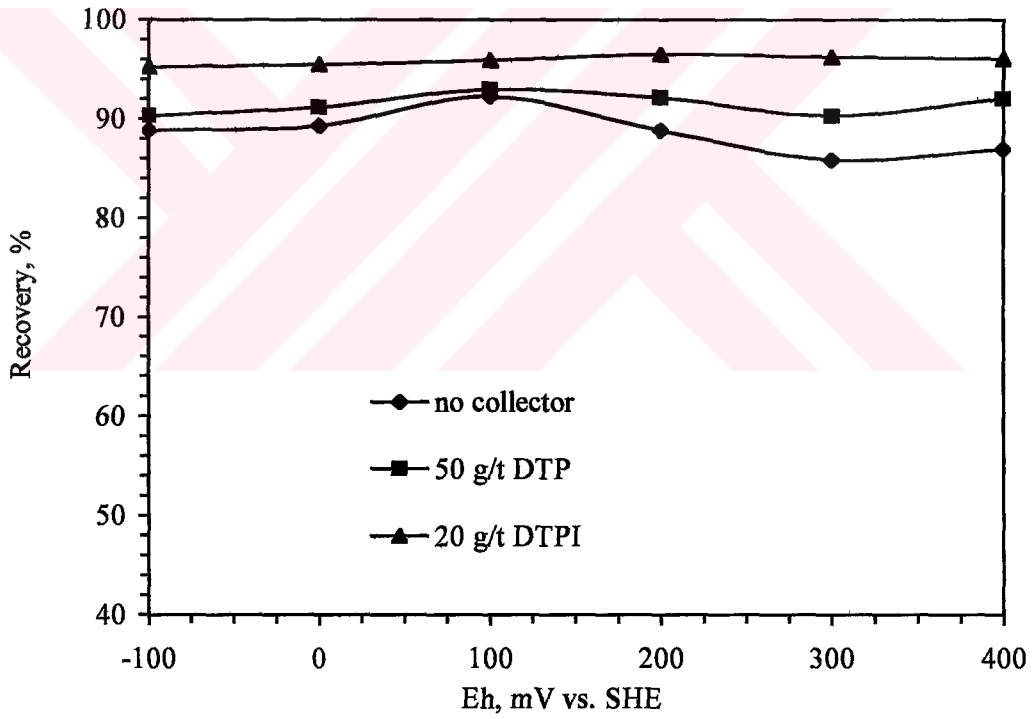

Figure 4.90. Effect of collectors on recovery in pH 4.67 buffer solution

Figure 4.91 represented that collectors significantly increased the chalcopyrite recovery in pH 6.97 buffer solution. Effect of DTP was similar to that of DTPI. Recoveries obtained by DTPI was about 2 % higher than those by DTP. Only, there was a considerable decrease at higher pulp potential values (400

mV) with DTP as compared with DTPI. Except this, recovery values did almost not change by pulp potential from –100 mV to 300 mV.

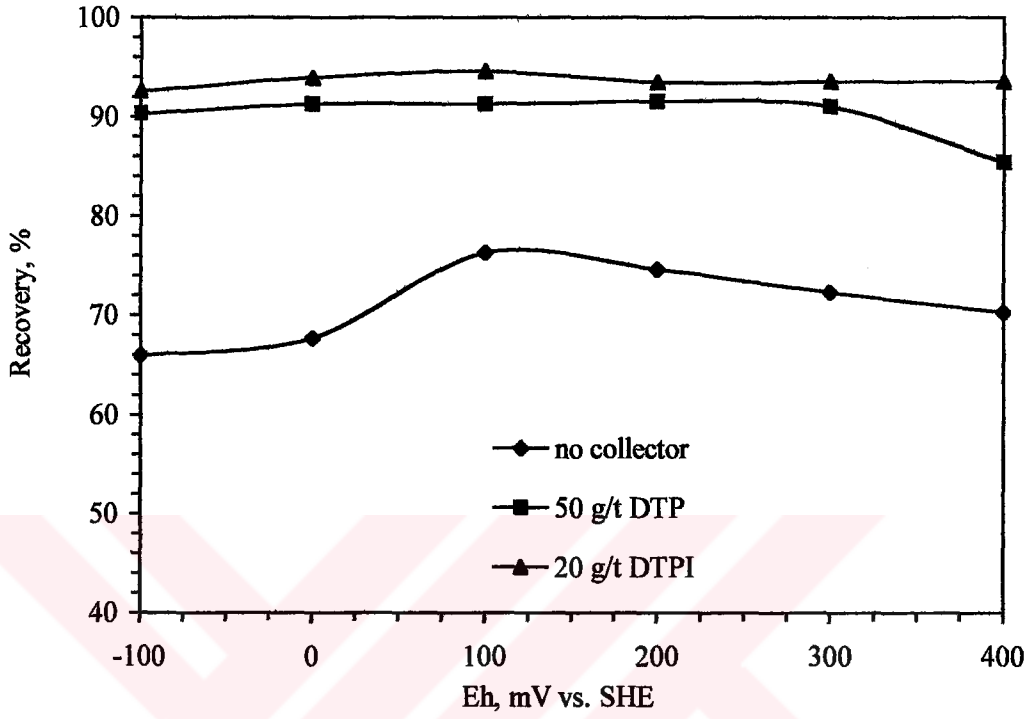

Figure 4.91. Effect of collectors on recovery in pH 6.97 buffer solution

In the case of pH 9.2, recovery was higher for DTPI than for DTP and for collectorless condition (Figure 4.92). DTP and DTPI followed similar trend; recovery increased up to 200-300 mV and then decreased up to 400 mV. On the other hand, it increased up to 100 mV and then gradually decreased as going to more oxidising potentials (400 mV) in collectorless condition.

Effect of DTP on chalcopyrite recovery was low as compared with collectorless condition in pH 11 buffer solution (Figure 4.93). However, DTPI resulted in an notable increase in recovery. Recovery followed similar trend for all three conditions: it increased up to moderately oxidising condition (100-200 mV) and then decreased with an increase in pulp potential to highly oxidising conditions (400 mV).

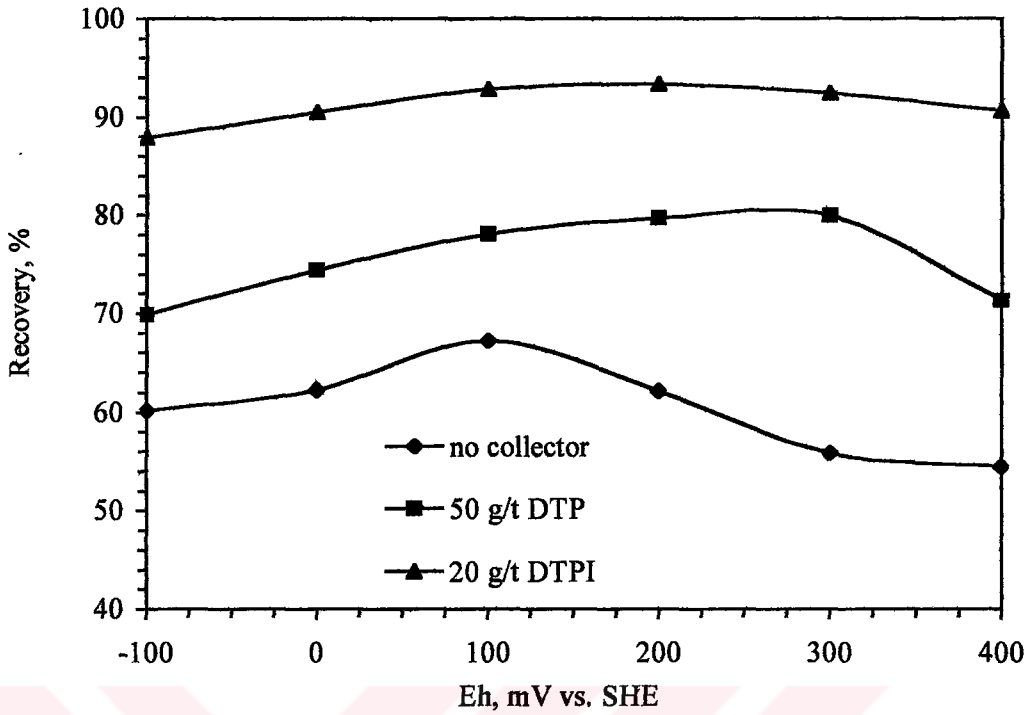

Figure 4.92. Effect of collectors on recovery in pH 9.2 buffer solution

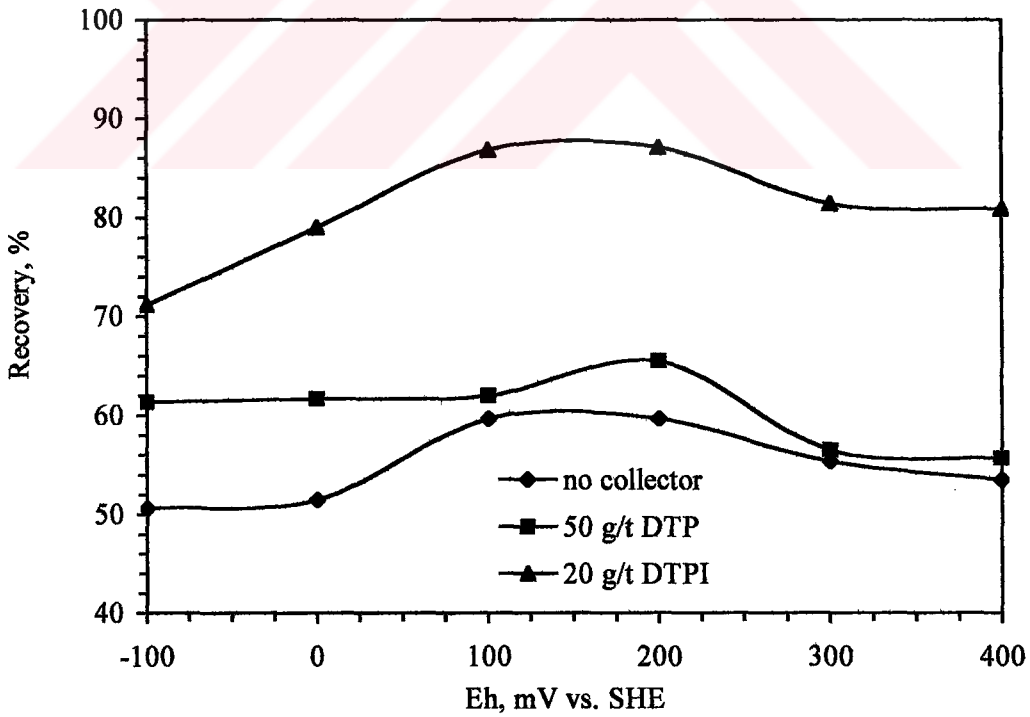

Figure 4.93. Effect of collectors on recovery in pH 11 buffer solution

CHAPTER 5

DISCUSSIONS

5.1 Cyclic Voltammetry

Sulphide minerals are, as mentioned before, semiconductors, and therefore, they can accept or donate electron in an aqueous solution. If a sulphide mineral donates electron, it will be oxidised according to reaction 5.1. If this reaction proceeds in reverse direction, mineral will accept electron and, so it will be reduced. During an electrochemical reaction, current density changes: If mineral donate electron, current density increases positively in anodic region and anodic oxidation occurs on mineral surface; if it accepts, current density increases negatively in cathodic region and cathodic reduction occurs.

$$MS \rightleftharpoons M^{+2} + S^{o} + 2e^{-} \qquad 5.1$$

Potential-current density diagram (voltammogram) is a tool for the determination of redox conditions of sulphide minerals, and it has been widely used in mineral processing. On a voltammogram, redox reactions can be seen, but they can not be defined without using theoretical values and other techniques, such as spectroscopy. However, surface passivation and reversibility of redox reactions can be determined, and surface composition of a mineral can be predicted by using voltammetry.

Cyclic voltammograms of chalcopyrite were drawn in the absence and presence of collector in different concentration to characterise the redox properties

of this mineral. Results were presented in Chapter 4. In this chapter, these results will be discussed.

5.1.1 pH 4.67

5.1.1.1 Cyclic Voltammetry Study in Collectorless Condition in pH 4.67

It can be seen from chalcopyrite voltammogram measured at 50 mV/s scan rate in slightly acid solution (Figure 4.1) that there are one cathodic and three anodic peaks. Anodic peaks formed at ~190 mV (A1), ~340 mV (A2) and ~550 mV (A3). Cathodic peak occurred at ~ –380 mV (K1). At lower scan rates (Figure 4.3-4.4), a new cathodic peak (K2) emerged starting at ~ 380 mV. This peak could not be seen in the voltammogram of 50 mV/s. This must be due to that kinetics of the reduction reaction resulting in peak K2 is slow and this reaction needs longer time periods to proceed.

Formation potentials of all redox peaks did almost not change with increasing the number of cycle at different scan rates. However, they changed at different scan rates as shown in Figure 4.6. Therefore, these redox peaks may be responsible for irreversible reactions. Because, for a reversible reaction, formation potential of a reaction should stay unchanged not only at increased number of cycles but also at various scan rates (Bott, 1999).

Current density of peak K1 decreased reasonably, while those of peaks A1 and A2 decreased very slightly with cycling except first cycle at all scan rates. This means that surface passivation occurred and electrode surface became electrochemically inactive. On the other hand, current density of A3 increased, since reaction responsible for this peak could not reach equilibrium, yet. In addition, current densities of redox peaks increased non-linearly with increasing

the scan rate (Figure 4.7). For a reversible reaction, current density should draw a line on a square-root of scan rate vs. current density diagram. So, it can be concluded that redox reactions occurring in pH 4.67 buffer solution between +650 –500 mV pulp potential range may not be fully reversible.

As shown in controlled sweep voltammogram (Figure 4.2), peak K1 was not observed in the first cycle. When cycling is progressed, peak A1 came into view and it resulted in the formation of peak K1 in the reverse scan. In the following cycles, current density of peak K1 continuously increased. For a reversible process, size of redox peaks should almost equal and, potentials of anodic and cathodic peaks should not be apart more than 0.0592/n V, where n shows the number of electron transferred in a reaction. This means that for a fully reversible process, potential difference between anodic and cathodic peaks should not exceeds 59.2 mV for one electron transfer. So, reaction (or reactions) resulting peaks A1 and K1 would not be fully reversible, since peaks A1 and K1 are far apart from each other and, size of peak K1 is greater and greater than that of peak A1.

Gómez et al. (1996) measured chalcopyrite voltammograms in highly acid solution (pH 2) between +200 –400 mV. They obtained a similar cathodic peak as compared with peak K1 and stated that proceeding the reactions 5.2 and 5.3 in reverse direction results in the formation of this peak in cathodic region. When H_2S concentration is assumed as 10^{-6} M, reactions 5.2 and 5.3 start to occur at –18 mV and 43 mV at pH 4.67, respectively.

$$Cu_2S_s + H_2S_{aq} \rightleftharpoons 2CuS_s + 2H^+_{aq} + 2e^- \qquad 5.2$$

$$Eh = E^\circ - 0.0592pH - 0.0296 \log a_{H_2S}$$

$$E^\circ = 0.081 \text{ Volt}$$

$$H_2S_{aq} \rightleftharpoons S_s^{\circ} + 2H_{aq}^{+} + 2e^{-} \qquad 5.3$$

$Eh = E^{\circ} - 0.0592pH - 0.0296 \log a_{H_2S}$

$E^{\circ} = 0.142$ Volt

Gardner and Woods (1979) also observed a cathodic peak on chalcopyrite voltammogram measured at pH 4.67 starting almost at the same potential (about –150 mV) with peak K1 in Figure 4.1. They proposed that this peak is the product of reaction 5.3.

In a different study (Lázaro et al., 1995), similar cathodic peak was obtained in acid leaching condition and it was concluded that this peak is the consequence of reaction 5.4 and 5.5. These reactions begin in cathodic direction at –34 mV and –45 mV for 10^{-6} M Fe^{+2} and 10^{-6} M H_2S in pH 4.67 solution, respectively. Standard formation potentials (E°) for reactions 5.2-5.5 were calculated from the free energy data of Latimer (1952), Garrels and Christs (1965) and Peters (1977).

$$Cu_5FeS_{4(s)} + 6H_2S_{aq} + 4Fe_{aq}^{+2} \rightleftharpoons 5CuFeS_{2(s)} + 12H_{aq}^{+} + 4e^{-} \qquad 5.4$$

$Eh = E^{\circ} - 0.1776pH - 0.0592 \log[Fe^{+2}] - 0.0888 \log a_{H_2S}$

$E^{\circ} = -0.093$ Volt

$$Cu_2S_s + 3H_2S_{aq} + 2Fe_{aq}^{+2} \rightleftharpoons 2CuFeS_{2(aq)} + 6H_{aq}^{+} + 2e^{-} \qquad 5.5$$

$Eh = E^{\circ} - 0.1776pH - 0.0592 \log[Fe^{+2}] - 0.0888 \log a_{H_2S}$

$E^{\circ} = -0.1032$ Volt

As shown on the controlled sweep voltammogram (Figure 4.2), peak K1 does not appear in the first sweep. However, current density sharply increases negatively showing that one (or more) of above reactions possibly proceeds in reverse direction to some extent. In the anodic scan, one (or more) of these reaction may result in the formation of peak A1. Size of peak K1 is larger than

peak A1. Therefore, it can be concluded that all reduced products were not re-oxidised in anodic scan.

Peak A2 would show the oxidation of chalcopyrite according to reaction 5.6 (Ekmekçi, 1995; Gardner and Woods, 1979). It has been established (Linge, 1976; Wadsworth, 1972) that iron is dissolved preferentially from chalcopyrite surface in acid solutions during oxidative leaching.

$$CuFeS_{2(aq)} \rightleftharpoons CuS_s + Fe^{+2}_{aq} + S^{\circ}_s + 2e^- \qquad 5.6$$

$Eh = E^{\circ} + 0.0296 \log[Fe^{+2}]$

$E^{\circ} = 0.293$ Volt

Reaction 5.6 initiate at 243 mV and 115 mV when Fe^{+2} ion concentration is accepted as 10^{-2} and 10^{-6} M at pH 4.67, respectively. This reaction may not be reversible, because peak A2 did not result in any cathodic peak formation in cathodic scan as shown in controlled sweep voltammogram (Figure 4.2). Only, it caused a reasonable increase in the current density of peak K1. This may be due to the reduction of S°, one of the oxidation products of chalcopyrite, to H_2S according to reaction 5.3 proceeding in reverse direction. HS^- formation is not expected at this pH and Eh (Figure 5.1).

CuS, the other oxidation product of reaction 5.6, oxidises at highly alkaline condition (reaction 5.7), and results in peak A3 in cyclic voltammogram (Gardner and Woods, 1979). Peak A3 caused the formation of peak K2 as shown in controlled sweep voltammogram (Figure 4.2). Peak K2 could not be observed clearly at 50 mV/s scan rate (Figure 4.1). It formed as a shoulder at 20 mV/s scan rate (Figure 4.3). Only, it drew a considerably sharp peak at 10 mV/s scan rate (Figure 4.4). Therefore, it can be commented that reversibility and kinetics of reaction 5.7 are low and, so, it needs longer time periods to proceeds in cathodic direction.

$$CuS_s \rightleftharpoons Cu^{+2}_{aq} + S^{\circ}_s + 2e^- \qquad 5.7$$

$Eh = E^{\circ} + 0.0296 \log[Cu^{+2}]$

$E^{\circ} = 0.59$ Volt

Reversible potential of reaction 5.7 changes with Cu^{+2} ion concentration: 531 mV and 412 mV for 10^{-2} M and 10^{-6} M Cu^{+2} ion concentration, respectively.

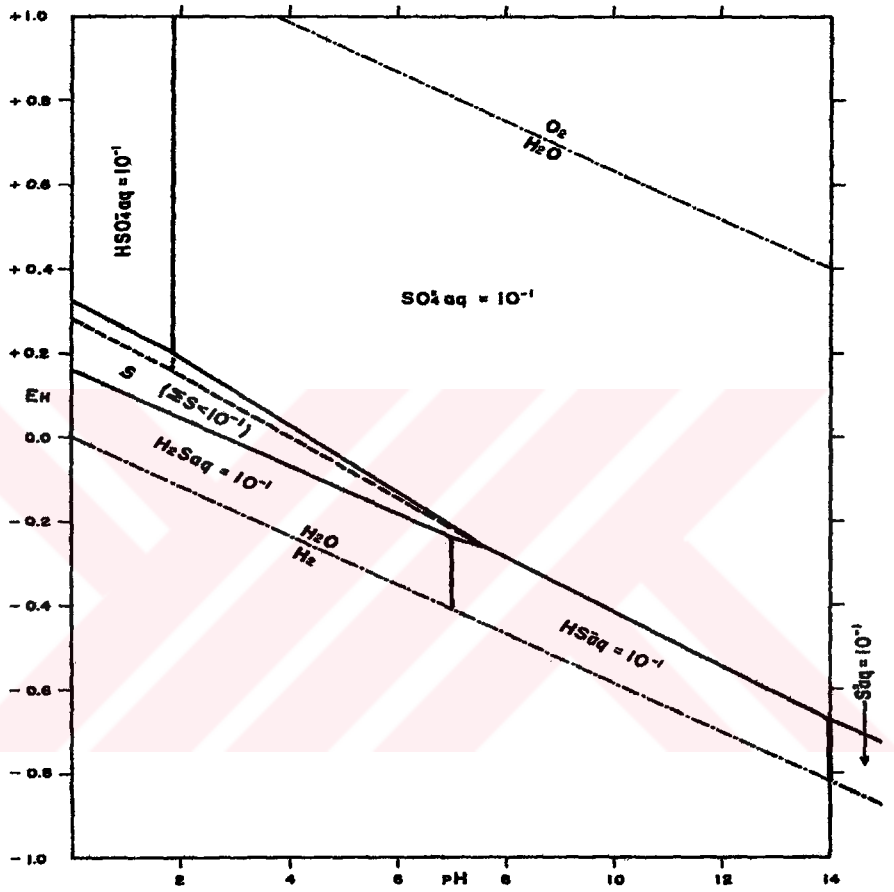

Figure 5.1. Equilibrium distribution of sulphur species in water at 25°C and 1 atmosphere total pressure for activity dissolved sulphide = 10^{-1}. Under these conditions, native sulphur is a stable phase. Dashed line indicates equal values of dissolved species within sulphur field. (Garrels and Christs, 1965)

S°, formed as products of reactions 5.6 and 5.7, is not stable at high Eh values. Because, thermodynamic considerations favour the formation of sulphate rather than sulphur (Figure 5.1). So, reaction 5.8 should proceed. However, oxidation of sulphides to sulphate generally exhibits a considerable degree of irreversibility (Peters, 1977) and S° can exist as a metastable phase.

$$S_s^\circ + 4H_2O \rightleftharpoons SO_4^{-2} + 8H_{aq}^+ + 6e^- \qquad 5.8$$

$$Eh = E^\circ + 0.0099 \log[SO_4^{-2}] - 0.0798pH$$

$$E^\circ = 0.357 \text{ Volt}$$

5.1.1.2 Cyclic Voltammetry Study in the Presence of DTP in pH 4.67

Chalcopyrite voltammograms were measured at various concentrations to explain the effect of DTP and its concentration on mineral surface (Figures 4.1 and 4.8-4.10). New peak formation was not observed on these voltammograms when compared with voltammograms measured in collectorless condition. However, current densities of redox peaks, seen in collectorless condition (Figure 4.1), decreased with increasing the collector concentration (Figure 4.11). Especially, current density of peak A3 decreased sharply with increasing the collector concentration. So, this implied that collector covered the mineral surface and prevented the electron transfer to some extent.

Collector adsorption possibly occurred by chemical mechanism, not by electrochemical mechanism. As a whole, this process is electrochemical in nature. Because, for collector adsorption, mineral surface should be oxidised (E) at first, and then collector react with metal ion (C) on the mineral surface; so, interaction between collector and mineral ions does not contain electron transfer. That is, collector adsorption may be employed with EC-mechanism. Kim (1995) explained the adsorption of DTPI on Ag-Au alloy with EC mechanism.

According to previous studies (Goold and Finkelstein, 1972; Grano et al., 1997a; Leppinen, 1991; Shubov et al., 1976; Yordanov et al., 1998), it is expected that chelating agent, DTP, reacts with Cu^{+2} ions to form CuDTP and $(DTP)_2$ on chalcopyrite surface as a result of reactions 5.9 and 5.10.

$$2Cu^{+2} + 4DTP^{-} \rightleftharpoons 2Cu(DTP)_2 \qquad 5.9$$

$$2Cu(DTP)_2 \rightleftharpoons 2CuDTP + (DTP)_2 \qquad 5.10$$

In addition, Chander and Fuerstenau (1974) studied on the interaction of platinum, copper and chalcocite with DTP. They observed the same anodic peak at about 0 mV on Pt, Cu and Cu_2S electrodes, and attributed to the formation of dithiophosphate radical (DTP^{o}) according to reaction 5.11. Woods (1971) observed a similar behaviour with copper and galena electrodes in xanthate solution.

$$DTP^{-} \rightleftharpoons DTP^{o} + e^{-} \qquad 5.11$$

On chalcopyrite voltammograms (Figure 4.8-4.10), such a peak can not be observed at 0 mV. However, DTP radical formation might have also formed during anodic scan, and its peak may not be distinguished due to larger intensities of peaks A1 and A2.

5.1.1.3 Cyclic Voltammetry Study in the Presence of DTPI in pH 4.67

Figures 4.1 and 4.12-4.14 show the chalcopyrite voltammograms measured at three different collector concentrations to explain the effect of DTPI and its concentration on mineral surface. Collector addition did not result in new peak formation. In contrast, current density of redox peaks decreased with increasing the collector concentration as compared with collectorless condition (Figure 4.15). Namely, surface coverage by DTPI occurred and electron transfer

was inhibited to some extent. In addition, current density sharply decreased in the first few cycles at highly reducing condition in cathodic scan. This may also be contributed to surface coverage.

Collector adsorption did not contain electron transfer. Because, as mentioned above, no new redox peak appeared on voltammograms in the presence of collector. Hence, it may occur by chemical mechanism. As in the case of DTP presented above, adsorption of DTPI may occur in two stage: 1) oxidation of mineral surface and dissolution of metal ions (Cu^{+2}) by electron transfer (E), and then 2) formation of Me-DTPI compound on mineral surface by chemical mechanism (C).

Yordanov et al. (1983) interacted Cu^{+2} and $DTPI^-$ ions to elucidate the reaction mechanism between them. They observed colour change of solution and then precipitate formation similar to DTP reported above. So they proposed the composition of $Cu(DTPI)_2$ and then formation of $CuDTPI+(DTPI)_2$ according to reactions 5.12 and 5.13.

$$2Cu^{+2} + 4DTPI^- \rightleftharpoons 2Cu(DTPI)_2 \qquad 5.12$$

$$2Cu(DTPI)_2 \rightleftharpoons 2CuDTPI + (DTPI)_2 \qquad 5.13$$

Hiçyılmaz et al. (2001) studied on the interaction between DTPI and platinum, pyrite, copper and Cu-activated pyrite by cyclic voltammetry technique. They could not observe any DTPI adsorption peak on platinum between +650 mV and –500 mV. In addition they proposed that DTPI adsorbed on pyrite, copper and Cu-activated pyrite possibly by chemical mechanism.

5.1.2 pH 6.97

5.1.2.1 Cyclic Voltammetry Study in Collectorless Condition in pH 6.97

Three anodic and three cathodic peaks appeared on cyclic voltammogram of chalcopyrite measured at 50 mV/s scan rate in pH 6.97 buffer solution (Figure 4.16): Anodic peaks reached their maximum peak potentials at ~ –30 mV (peakA1), ~270 mV (peak A2) and ~500 mV (peak A3). Those of cathodic peaks were ~ –315 mV (peak K1), ~100 mV (peak K2) and ~275 mV (peak K3). Peaks A1 and A2 could not be seen at 20 mV/s and 10 mV/s scan rates (Figure 4.18-4.19).

A sharp cathodic peak (peak K2) took shape at about 70 mV in the first cycle. It did not form with such a sharp shape in the following cycles. But, shoulder around 100 mV shows that this reaction proceeded in minor scale in cathodic region as compared with first cycle. Similar behaviour was also observed at 20 mV/s scan rate (Figure 4.18), whereas it disappeared at 10 mV/s scan rate (Figure 4.19).

Current density of redox peaks did almost not change except first cycle at 50 mV/s scan rate (Figure 4.16). Redox peaks behaved similarly at lower scan rates except small changes in peaks K1 and K3 (Figures 4.18-4.19). On the other hand, their current densities increased almost linearly with increasing the scan rate (Figure 4.22). Therefore, this may be commented as that redox peaks were responsible for reversible reactions. However, formation potentials of all redox peaks changed with changing scan rate showing irreversibility (Figure 4.21), although, they did almost not change with increasing the number of cycle for different scan rates (Figures 4.16, 4.18 and 4.19) as expected.

As shown in the controlled sweep voltammogram (Figure 4.17), formation of peak K1 resulted in peak A1 in anodic region. As long as the cycling proceeds, all anodic peaks contributed to increase the current density of peak K1. So, peak K1 did not show only the reduction of oxidation products of peak A1. In addition, Figure 17 shows that peak A3 resulted in the formation of peak K3, so the redox reaction initiating at this potential may be evaluated as a reversible reaction; but, large separation between them is an indicator for an irreversible process to some extent.

As pointed out above, peak K2 occurred sharply at about 70 mV in the first cycle. This peak possibly shows the reduction of surface oxides according to reaction 5.14 proceeding in reverse direction (Buckley et al., 1985). The standard formation potential for this reaction is 1.0568 V calculated from the free-energy data of Latimer (1952). A similar reduction peak was also obtained on pyrrhotite surface and the same reduction reaction was referred (Hamilton and Woods, 1981). This reaction initiates at 174 mV for 10^{-6} M Fe^{+2} concentration in pH 6.97 solution.

$$Fe^{+2}_{aq} + 3H_2O \rightleftharpoons Fe(OH)_{3(aq)} + 3H^{+}_{aq} + e^{-} \qquad 5.14$$

$Eh = E^{o} - 0.1776pH - 0.0592 \log[Fe^{+2}]$

$E^{o} = 1.0568$ Volt

As mentioned in chapter 3, electrode surface was polished and then washed with distilled water before immersing it into deoxygenated buffer solution for each electrochemical experiment. So, electrode surface oxidation possibly occurred during washing after polishing; since, such a sharp peak did not form in the following cycles. However, there is a shoulder around 100 mV indicating that reaction 5.14 continues in small scale in the following cycles.

Second anodic peak possibly shows the oxidation of chalcopyrite surface according reaction 5.15 (Gardner and Woods, 1979). From thermodynamic data, it can be calculated that this reaction begins at 134 mV at pH 6.97.

$$CuFeS_{2(s)} + 3H_2O \rightleftharpoons CuS_s + Fe(OH)_{3(s)} + S^\circ_s + 3H^+_{aq} + 3e^- \qquad 5.15$$

$Eh = E^\circ - 0.0592pH$

$E^\circ = 0.547$ Volt

Luttrell and Yoon (1984a) also investigated the oxidation of chalcopyrite treated in alkaline condition by XPS technique. In this study, however, the CuS component was found to be greater than the elemental sulphur whereas the reaction proposed by Gardner and Woods (1979) (reaction 5.15) should yield equal quantities of these products. Buckley and Woods (1984) studied the oxidation of chalcopyrite by XPS, too. They stated the formation of a sulphur rich copper sulphide of stoichiometry CuS_2. Moreover, they also pointed out that reversible potential of CuS_2 formation is close to that for reaction 5.15. Therefore, in neutral and alkaline solutions, CuS_2 or CuS may form on the mineral surface, and this can not be discriminated by cyclic voltammetry. Hence, evaluation was based on the CuS formation in neutral and alkaline solutions.

Peak A2 may be reversible to some extent. Reaction 5.15 forms a cathodic peak at about –40 mV in controlled sweep voltammogram (Figure 4.17). But, this peak can not clearly be observed on voltammogram measured at 50 mV/s, 20 mV/s and 10 mV/s scan rates (Figures 4.16 and 4.18-4.19) due to large and broad cathodic peaks. Reaction 5.15 may not be fully reversible. Because, it contributed to increase current density of peak K1.

CuS, product of chalcopyrite oxidation (reaction 5.15), oxidises at higher pulp potential values (peak A3):

$$CuS_s + H_2O \rightleftharpoons Cu(OH)_{2(s)} + S^\circ_s + 2H^+_{aq} + 2e^- \qquad 5.16$$

$Eh = E^\circ - 0.0592pH$

$E^\circ = 0.863$ Volt

Reaction 5.16 begins at 450 mV at pH 6.97. This reaction is reversible, because peak A3 results in peak K3 in cathodic scan.

S° emerging as products of reactions 5.15 and 5.16 is not stable at highly oxidising potentials (Figure 5.1), and it should oxidise in conformity with the reaction 5.8. Therefore, it can only found in a metastable phase.

In cathodic region, it is estimated that S° is reduced to H_2S and/or HS^- (peak K1) according to reactions 5.3 and 5.17 progressing in opposite direction, respectively. As a reaction product, H_2S and/or HS^- may form because pH 6.97 is between stability limits of them as shown in Figure 5.1. In anodic region, some of the reduced products of these reactions were re-oxidised (peak A1). In other words, this reaction is not fully reversible because size of peak K1 is larger and larger than peak A1.

$$HS^-_{aq} \rightleftharpoons S^\circ_s + H^+_{aq} + 2e^- \qquad 5.17$$

$Eh = E^\circ - 0.0296pH - 0.0296 \log[HS^-]$

$E^\circ = -0.06$ Volt

Reactions 5.3 and 5.17 start at –93 and –89 mV in cathodic region at pH 6.97, respectively, when H_2S and HS^- concentrations are assumed as 10^{-6} M. Therefore, it can not be possible by cyclic voltammetry to determine which one formed at pH 6.97, since their reversible potentials are almost equal

5.1.2.2 Cyclic Voltammetry Study in the Presence of DTP in pH 6.97

Electrochemical spectra of the chalcopyrite electrode drawn in pH 6.97 buffer solution containing 0 M, 10^{-4} M, 10^{-3} M and 10^{-2} M DTP are presented in Figures 4.16 and 4.23-4.25, respectively. Collector did not cause any new peak. However, the current densities of the redox peaks, observed in collectorless condition (Figure 4.1), decreased with increasing the collector concentration (Figure 4.11). So, this suggested that collector covered the mineral surface and prevented the electron transfer to some extent. It may be helpful to demonstrate

that the fall in current density at pH 6.97 is not so high when compared with that obtained at pH 4.67.

No new peak formation may be concluded that chemical mechanism gives rise to the formation of Cu-DTP chelate compound. Since, electrochemical interaction occurs with electron transfer and, hence, it produces new peak on voltammogram. For collector adsorption, at first, metal ion (Cu^{+2}) should dissolve preferentially from surface causing metal deficient surface, or it may be presents on electrode surface as anodic oxidation product (Chander and Fuerstenau, 1975). In conclusion, it may be summarised as follows: Metal ion accumulate on or near the mineral surface by electron transfer (E), and collector ions interact with them chemically (C). So, as a whole process, collector adsorption may be the consequence of EC-mechanism.

CuDTP formation is expected at pH 6.97 in consistent with the reactions 5.9-5.10 (Leppinen, 1991). However, reaction 5.10 becomes slower by the increase in collector concentration and pH (Finkelstein and Poling, 1977; Shubov et al., 1976). Furthermore, under metastable conditions, $Cu(DTP)_2$ can form only at higher electrode potentials (Fuerstenau, D.W., 1980). So, although CuDTP and $(DTP)_2$ formation on chalcopyrite surface was estimated at pH 6.97 buffer solution, $Cu(DTP)_2$ might also cause surface passivation. Type (or types) of the collector compound formed on mineral surface could not be identified by cyclic voltammetry.

5.1.2.3 Cyclic Voltammetry Study in the Presence of DTPI in pH 6.97

Figures 4.16 and 4.27-4.29 presents the chalcopyrite voltammograms obtained at various DTPI concentrations. Redox peaks obtained in collectorless condition did not appear in the presence of collector (Figure 4.30). A new peak was appeared in anodic scan starting at about –100 mV especially at 10^{-4} and 10^{-3} M DTPI concentrations as a shoulder. In cathodic scan, there was an increase in

current density negatively at the same potential. Woods (1971) observed a similar behaviour at copper and galena electrodes in xanthate solution. Chander and Fuerstenau (1974) also obtained a similar peak at about 0 mV at platinum, copper and chalcocite electrodes in DTP solution. If the analogy from the xanthate and dithiophosphate systems is carried over to the present system, this oxidation process is a one-electron charge transfer process:

$$DTPI^- \rightleftharpoons DTPI^\circ + e \qquad 5.18$$

Hiçyılmaz et al (2001) also studied on the adsorption of DTPI on platinum and copper electrodes. However, they did not observe such a peak around 0 mV.

In addition, current density increased negatively starting at about 180 mV in cathodic sweep. This possibly showed the reduction of $Fe(OH)_3$ in conformity with the reaction 5.14. However, rise in current density continued at lower Eh values. This meant that chalcopyrite surface oxidised in anodic scan (reaction 5.15) and its products were reduced in cathodic region.

Peak K3, obtained in collectorless condition, appeared as a small shoulder in 10^{-4} M DTPI solution, and disappeared at higher collector concentrations. Moreover, current density of peak A3 fell sharply in the presence of DTPI. So, this showed that collector coverage of surface prevented the oxidation of CuS at higher Eh values.

5.1.3 pH 9.2

5.1.3.1 Cyclic Voltammetry Study in Collectorless Condition in pH 9.2

In moderately alkaline condition, only one anodic and one cathodic peak occurred. In controlled sweep voltammogram (Figure 4.32), peak K1 did not form

in the first two cathodic scans. Cycling from 400 mV in anodic region produced anodic (A1) and cathodic (K1) peaks. This denoted that reaction eventuating peak A1 in anodic region was reversible and causes the formation of peak K1 in cathodic sweep.

Peak A1 showed the oxidation of chalcopyrite surface according to reaction 5.15. This reaction starts at 3 mV at pH 9.2. In addition, it resulted in peak K1 in cathodic scan showing that oxidation products were reduced in cathodic scan. Gardner and Woods (1979) and Pang and Chander (1990) obtained the same peaks and confirm this reversibility. However, for a fully reversible process, peak position should not change with scan rate, and peak separation does not exceed 0.0592/n, where n is the number of electron transferred in a reaction. It means that this reaction is irreversible to some extent. Since, potential difference between peaks was very high. Furthermore, formation potentials of peaks A1 and K1 were shifted to more reducing and more oxidising potentials at lower scan rates, respectively (Figure 4.36).

In addition, there is a new peak formation above 400 mV in anodic region. But, it did not initiate any new reduction peak in cathodic scan. This new emerging anodic peak possibly showed the oxidation of CuS according to reaction 5.16.

5.1.3.2 Cyclic Voltammetry Study in the Presence of DTP in pH 9.2

Figures 4.31 and 4.38-4.40 represents the cyclic voltammogram of chalcopyrite electrode in the presence of DTP. New peak formation was not appeared in the presence of collector. Only, current densities of redox peaks decreased slightly with increasing the collector concentration (Figure 4.41). However, current density decay was very small as compared with the voltammograms drawn at pH 4.67 and 6.97 (Figures 4.11 and 4.26). Therefore, it

may be concluded that adsorption density of DTP at pH 9.2 was lower than that at pH 4.67 and 6.97.

No new peak formation and current decay showed that DTP adsorbs chemically, not by electrochemically. Because, electrochemical adsorption cause new peak due to electron transfer. However, as a whole process, DTP adsorption may occur by electrochemical mechanism as mentioned in the previous sections: Dissolution of Cu^{+2} ions electrochemically, and formation of Cu-DTP compounds chemically according to reactions 5.9-5.10. Reaction 5.10 is very slow in alkaline condition (Chander and Fuerstenau, 1975; Finkelstein and Poling, 1977; Fuerstenau, D.W., 1980; Shubov et al., 1976;). Therefore, Cu-DTP compound of surface is likely $Cu(DTP)_2$. DTP may also be adsorbed on mineral surface by metathetic substitution mechanism, since in alkaline condition major surface products are oxides and hydroxides.

5.1.3.3 Cyclic Voltammetry Study in the Presence of DTPI in pH 9.2

Chalcopyrite voltammograms were given in Figures 4.31 and 4.42-4.44 for various DTPI concentrations. No new peak formed when collector was added. Nevertheless, current density of redox peaks decreased at higher collector concentration (Figure 4.45). This fall in current density showed the surface coverage of collector. As mentioned in the previous sections, this coverage did not form only by electrochemical mechanism. This may be due to EC-mechanism. Cyclic voltammetry studies did not give desired information to define type (or types) of Cu-DTPI compound formed on mineral surface. Hiçyılmaz et al (2001) also proposed that DTPI covered Cu-electrode surface and caused surface passivation. They could not obtain any identifiable peak between +650 mV and –500 mV on Pt voltammogram in the presence of DTPI.

5.1.4 pH 11

5.1.4.1 Cyclic Voltammetry Study in Collectorless Condition in pH 11

One anodic and two cathodic peaks came into view in highly alkaline condition (Figure 4.46). In controlled sweep voltammogram (Figure 4.47), no peak formation was observed in the first two cathodic scans. Cycling from 300 mV produced peak A1 in anodic region and peak K1 in cathodic region. This denoted that reaction eventuating peak A1 in anodic scan was reversible and caused the formation of peak K1 in cathodic sweep. When potential was cycled from 500 mV, a new anodic peak started to occur and, hence, current density sharply increased above 300 mV. It generates second cathodic peak (peak K2) in cathodic scan.

Current densities of redox peaks increased almost linearly with respect to square-root of scan rate (Figure 4.52) suggesting that redox peaks were reversible. However, though peak position of K2 did almost not change when scan rate was increased from 10 mV/s to 50 mV/s, those of peaks A1 and K1 shifted about 100 mV to more oxidising and more reducing potentials, respectively (Figures 4.50 and 4.51). Then, redox reaction resulting in peaks A1 and K1 should not be fully reversible, since they formed far apart from each other (more than 59 mV) and formation potentials of peaks A1 and K1 change with scan rate indicating that a slow electron transfer is involved (Cha and Park, 1996).

Further, it can be concluded that new anodic peak formed above 300 mV causes the peak K2, and reaction shaping these oxidation and reduction peaks is reversible. Even though, when small size of peak K2 and sharp increase in current density above 300 mV is taken into consideration, it can be commented that this reaction was not fully reversible and some of oxidised products are not reduced in cathodic scan.

Peak A1 possibly resulted from the oxidation of chalcopyrite surface with reaction 5.15 and peak K1 was responsible for the reduction of oxidised products deriving the reaction 5.15 in reverse direction. Increase in current density above 300 mV in anodic scan would be due to the oxidation of CuS according to reaction 5.16. This reaction proceeded in reverse direction in cathodic scan and produce peak K2.

5.1.4.2 Cyclic Voltammetry Study in the Presence of DTP in pH 11

Chalcopyrite voltammograms drawn at various DTP concentrations were given in Figures 4.46 and 4.53-4.55. No new peak formation was observed in the presence of collector. Current density of redox peaks decreased slowly with increasing the collector concentration (Figure 4.56). When compared with voltammograms measured at lower pH values (Figures 4.11, 4.26 and 4.41), current density decay was considerably low showing that adsorption density of collector on chalcopyrite surface at highly alkaline condition is low.

$Cu(DTP)_2$ formation is expected at highly alkaline condition (Finkelstein and Poling, 1977; Fuerstenau, 1980, D.W.; Shubov et al., 1976). However, this can not be confirmed by cyclic voltammetry due to no new peak formation belonging to $Cu(DTP)_2$.

5.1.4.3 Cyclic Voltammetry Study in the Presence of DTPI in pH 11

Cyclic voltammogram of chalcopyrite measured at various DTPI concentrations were given in Figures 4.46 and 4.57-4.59. New peak formation was not observed in the presence of DTPI. Even so, current density of redox peaks decreased with increasing the collector concentration (Figure 4.60). Hence, this means that DTPI adsorption on mineral surface performed and then electron transfer was prevented up to some extent due to surface coverage with collector.

Only at the highest collector concentrate (10^{-2} M DTPI), peak K2 disappeared. Besides this, other peaks can be distinguished. In contrast, at lower pH values (Figures 4.15, 4.30 and 4.45), redox peaks almost vanished and electron transfer was retarded. In conclusion, adsorption density decreased at higher pH values. Hiçyılmaz et al (2001) also obtained similar results and proposed that DTPI covered Cu-electrode surface and caused surface passivation. They could not obtain any identifiable peak between +650 mV and –500 mV on Pt voltammogram in the presence of DTPI.

Furthermore, when compared with dithiophosphate adsorption on chalcopyrite at pH 11 (Figure 4.56), DTPI covered the mineral surface more powerfully, and prevented the occurrence of redox peaks more. That is, DTP is weaker than DTPI as shown from voltammograms. Nevertheless, surface compounds can not be identified by cyclic voltammetry.

5.2 DRIFT Study

Surface chemistry is an important parameter in many aspects of mineral processing. In particular, an understanding of interaction mechanisms of different reagents with the mineral surface in an aqueous medium is of crucial importance in achieving the desired beneficiation by flotation. Infrared spectroscopy has found wide acceptance for characterising adsorption on mineral surfaces. An infrared spectrum represents a fingerprint of a sample with adsorption peaks that correspond to the frequencies of vibrations between the bonds of the atoms making up the mineral. Because, no two unique molecular structures produce the same infrared spectrum like a fingerprint. This makes infrared spectroscopy useful for identification of collector adsorption on mineral surfaces. However, when adsorption is low, this technique is not sufficiently sensitive.

DRIFT spectra of chalcopyrite were drawn to define the surface products formed in the presence of collector. Experiments were conducted at –100 mV, 150

mV and 400 mV pulp potential values in four different buffer solution having pH values of 4.67, 6.97, 9.2 and 11.

5.2.1 DRIFT Spectroscopy Study in the Presence of DTP

DRIFT spectrum of DTP was given in Figure 4.61.a. The IR bands observed between 3000-2800 cm^{-1} may be associated with the C-H vibrations of alkyl group. The IR bands between 1500-1250 cm^{-1} also belongs to C-H groups (Bellamy, 1975; Colthup et al., 1975; Drelich et al., 1998; Giesekke, 1983; Maslovsky, 1977; Meloan, 1963; Pouchert, 1981).

According to previous findings, the P-O-C group absorbs very strongly between 1100-1000 cm^{-1}. A second strong band appears between 1000-870 cm^{-1}. Also associated with the P-O-C group is a medium intensity band between 835-715 cm^{-1}. A weak but characteristic absorption also appears between 1190-1150 cm^{-1} (Colthup et al., 1975; Leppinen, 1991; Maege et al., 1998; Nakanishi and Solomon, 1977; Pouchert, 1981; Shishkov and Nikolov, 1972). Therefore, observed peaks between 1200-715 cm^{-1} were associated with P-O-C group.

Sulphur-phosphorus IR bands emerge below 720 cm^{-1}: IR bands observed at 706, 685, 646 and 579 cm^{-1} (Figure 4.61.a) would associated with P=S vibrations. On the other hand, peak appearing at 542 cm^{-1} belongs to P-S vibration (Leppinen, 1991; Nakanishi and Solomon, 1977; Shishkov and Nikolov, 1972; Van der Maas, 1972).

DRIFT spectrum of dimer of dithiophosphate is given in Figure 4.61.b. As compared with monomer spectrum of DTP (Figure 4.61.a), IR bands of dimer observed between 3000-2800 cm^{-1} and between 1500-1090 cm^{-1} almost coincide with those of monomer. However, their peak intensities are lower than those of monomer.

Split peak does not appear between 1050-1000cm^{-1} as in the case of monomer. Instead, there is a sharp peak at about 1009 cm^{-1}. Furthermore, the sharp peak of monomer observed at 920 cm^{-1} is shifted to 970 cm^{-1} in the spectrum of $(DTP)_2$. IR bands emerging between 835-720 cm^{-1} in the spectrum of monomer disappear. In place of them, two peaks form at 829 and 799 cm^{-1} in the dimer spectrum. These peaks belong to P-O-C group.

Considerable changes occur on the IR bands of sulphur-phosphorus: All of the P=S bands vanish and a sharp peak arise at 640 cm^{-1}. It is related to P=S vibrations (Leppinen, 1991). P-S band also expires. On behalf of, a broad peak forms reaching its maximum values at about 503-495 cm^{-1}. Colthup et al (1975) and Shishkov and Nikolov (1972) proposed that IR peaks observed between 520-470 cm^{-1} belong to S-S bands. Therefore, it can be concluded that characteristic peaks of $(DTP)_2$ can be written as 1009, 970, 829, 799, 640, 503 and 495 cm^{-1}.

DRIFT spectrum of platinum interacted with DTP at 750 mV was also obtained to confirm the peak positions of dimer (Figure 4.61.c). At this potential, it is expected that DTP adsorbs as $(DTP)_2$ on platinum surface according to reaction 5.19 (Chander and Fuerstenau, 1974; Kakovsky and Arashkevich, 1968):

$$2DTP^- \rightleftharpoons (DTP)_2 + 2e \qquad 5.19$$

$$Eh = E^\circ - 0.0592 \log[DTP^-]$$

$$E^\circ = 0.252 \text{ Volt}$$

DRIFT spectrum of Pt powder polarised with DTP almost coincides with that of dimer. There are additional peaks on Figure 4.61.c at 1215 and 598 cm^{-1}. These IR bands possibly belong to Pt and/or Pt-DTP compounds rather than $(DTP)_2$. As well, intensities of C-H vibration bands between 3000-2800 cm^{-1} are lower than those of $(DTP)_2$. This means that adsorption density of dithiophosphate is low on platinum powder surface.

Dithiophosphate may adsorb on chalcopyrite surface as $(DTP)_2$, CuDTP and/or $Cu(DTP)_2$. In addition, CuDTP+$(DTP)_2$ precipitate forms in accordance with reactions 5.9 and 5.10, when Cu^{+2} and DTP^- ions are interacted in acid solution as cited in literature. So, CuDTP precipitate was obtained to determine the IR bands of it. DRIFT spectrum of CuDTP is given in Figure 4.61.d. When compared with dimer spectrum (Figure 4.61.b), all the IR bands of $(DTP)_2$ appears on Figure 4.61.d. Of course, there are some differences from dimer spectrum: IR peaks between 1120-900 cm^{-1} and between 800-750 cm^{-1} more intense and broader than those obtained in $(DTP)_2$. There is a new sharp peak at 532 cm^{-1}. Moreover, C-H vibration bands between 3000-2800 cm^{-1} and between 1500-1250 cm^{-1} are more intense than those peaks of DTP and $(DTP)_2$ shown in Figures 4.61.a and 4.61.b, respectively. Hence, although peak intensities of C-H vibration bands may not be a characteristic property for identification of CuDTP, it can be determined by 532 cm^{-1} IR band on spectrum.

5.2.1.1 DRIFT Spectroscopy Study in the Presence of DTP in pH 4.67

DRIFT spectra of chalcopyrite were measured in the slightly acid solution (pH 4.67) at certain pulp potential values to elucidate the effects of Eh on collector adsorption on chalcopyrite surface and to determine the collector compound formed on mineral surface (Figure 4.62). Increase in pulp potential results in the increase in peak intensities.

C-H vibration peaks between 1500-1250 cm^{-1} almost disappeared on the spectrum of chalcopyrite mineral polarised at –100 mV pulp potential value (Figure 4.62.c). P-O-C bands obtained in dimer spectrum between 1200-900 cm^{-1} appear in Figure 4.62.c, but one of the major peaks formed at 953 cm^{-1}, neither at 920 cm^{-1} of monomer band nor at 970 cm^{-1} of dimer band. Shift in the peak position and weak C-H bands, band shape between 1050-900 cm^{-1}, and peak formation at 839 cm^{-1}, 806 cm^{-1} and 517 cm^{-1} IR bands may show that dimer formation occurred in conformity with reactions 5.11, 5.20 and/or 5.21. Hence,

dithiophosphate radical (DTP°) may also exist on the surface. Presence of DTP° in minor scale may also be supported by that broadness between 850-650 cm^{-1} and sharp band at 582 cm^{-1}. In contrast, P-S band at 542 cm^{-1} as in the case of DTP spectrum is not observed in this spectrum. Instead, there is a new peak formation at 517 cm^{-1}. In literature, IR band at 517 cm^{-1} was assigned to the S-S stretching mode (Bellamy, 1975), consequently showing the dimer formation. At this potential and pH, $Cu(DTP)_2$ formation is not expected. Further, absence of CuDTP peaks, weak $(DTP)_2$ and DTP° bands proposed that at this potential DTP adsorbed on chalcopyrite surface weakly.

$$2DTP^{\circ} \rightleftharpoons (DTP)_2 \qquad 5.20$$

$$DTP^{-} + DTP^{\circ} \rightleftharpoons (DTP)_2 + e^{-} \qquad 5.21$$

Chalcopyrite spectrum polarised at 150 mV is given in Figure 4.62.d. Similar to –100 mV, C-H bands also form weakly on the spectrum of 150 mV. Also, P-O-C peaks can not be observed clearly. A broad peak at 695 cm^{-1} and sharp peaks at 580 cm^{-1} and 499 cm^{-1} form. IR band of P-S bond is also observed at 546 cm^{-1} weakly.

Weak C-H and P-O-C band suggested that DTP concentration on chalcopyrite surface was in small scale. Broadness around 650 cm^{-1} and intense peak at 499 cm^{-1} might show dimer formation in minor scale. Furthermore, IR bands at 695 cm^{-1} and 580 cm^{-1} may be cited to DTP° formation. CuDTP did not form on mineral surface, because its characteristic IR band (532 cm^{-1}) was not seen on spectrum. $Cu(DTP)_2$ formation is also not expected in acid solution.

DRIFT spectrum of chalcopyrite sample polarised in 10^{-1} M DTP solution at 400 mV was represented in Figure 4.62.e. As compared with spectra measured for chalcopyrite conditioned with DTP at –100 mV and 150 mV, similar weak C-H peaks were obtained, however, peak intensities of P-O-C group for 400 mV are higher than those for –100 mV and 150 mV.

Weak C-H group, peak shape of P-O-C group especially between 1100-900 cm^{-1}, IR band formation at 831, 799, 650 and 494 cm^{-1} would be referred to dimer formation on mineral surface. In addition, there is a broad peak at 520 cm^{-1} starting at about 550 cm^{-1} possibly showing the CuDTP formation in accordance with the reactions 5.9-5.10, since IR band structure under 550 cm^{-1} resembled CuDTP spectrum. But, weak C-H group proposed that CuDTP might form on mineral surface in minor scale.

5.2.1.2 DRIFT Spectroscopy Study in the Presence of DTP in pH 6.97

Figure 4.63 shows the DRIFT spectra of chalcopyrite samples polarised with DTP measured in neutral solution (pH 6.97). As shown from figure, poor results were obtained: Peak intensities of IR bands were considerably low to evaluate and define surface compounds. Such poor results showed weak adsorption of DTP on chalcopyrite surface.

DRIFT spectra of chalcopyrite measured at –100 mV (Figure 4.63.c) and +150 mV (Figure 4.63.d) could not give any idea about collector adsorption. Only P-O-C bands, especially two sharp bands between 1100-900 cm^{-1}, were hardly distinguished showing surface coverage with DTP weakly. Peak intensities increased reasonably at higher Eh values: Figure 4.63.e presented the DRIFT spectrum of chalcopyrite polarised at 400 mV in pH 6.97 buffer solution. Especially P-O-C bands of this spectrum could be identified. When compared with reference spectra, dimer formation may be suggested at 400 mV, since this spectrum resembles the dimer spectrum. This suggestion would be supported with P-O-C, P=S and S-S bands observed between 1100-500 cm^{-1}.

5.2.1.3 DRIFT Spectroscopy Study in the Presence of DTP in pH 9.2

Chalcopyrite was treated with 10^{-1} M DTP in alkaline solution (pH 9.2) to obtain the DRIFT spectra of mineral polarised with collector to identify the adsorbed compound on mineral surface (Figure 4.64). Peak intensities are very low as compared with DRIFT spectra obtained in pH 4.67 and pH 6.97 buffer solution. Therefore, scale was shrunk for a clear demonstration.

When compared with the spectra of monomer and dimer, large differences were seen between them. It was thought that these differences came from surface oxidation rather than DTP adsorption. Hence, for comparison, chalcopyrite spectra polarised at reducing (Figure 5.2.a) and oxidising (Figure 5.2.b) potentials in collectorless condition were drawn. These spectra show that broadness between 1500-1100 cm^{-1} in Figures 4.64.c-e came from surface oxidation. On the other hand, this does not mean that collector had not adsorbed on chalcopyrite surface. Because, two important P-O-C peaks could be distinguished clearly between 1000-900 cm^{-1} in these spectra. They formed considerably sharper in Figure 4.64.d (polarised at 150 mV) as compared with others (Figures 4.64.c and 4.64.e). Although, it was stated in literature (Shubov et al., 1976) that $Cu(DTP)_2$ forms in alkaline condition on chalcopyrite surface, it could not be identified here possibly due to weak adsorption.

5.2.1.4 DRIFT Spectroscopy Study in the Presence of DTP in pH 11

DRIFT spectra of chalcopyrite were obtained in highly alkaline solution (pH 11) at –100 mV, +150 mV and +400 mV pulp potential values to clarify the effects of Eh on collector adsorption on mineral surface and to name the collector compounds formed on mineral surface (Figure 4.65). Similarity between DRIFT spectra of pH 11 and monomer and dimer is very low. Especially, there is a large and broad structure between 1500-1100 cm^{-1}. It was thought that such large differences should come from surface oxidation rather than DTP adsorption.

Indeed, such a structure formed more intensely as compared with the spectra measured in pH 9.2.

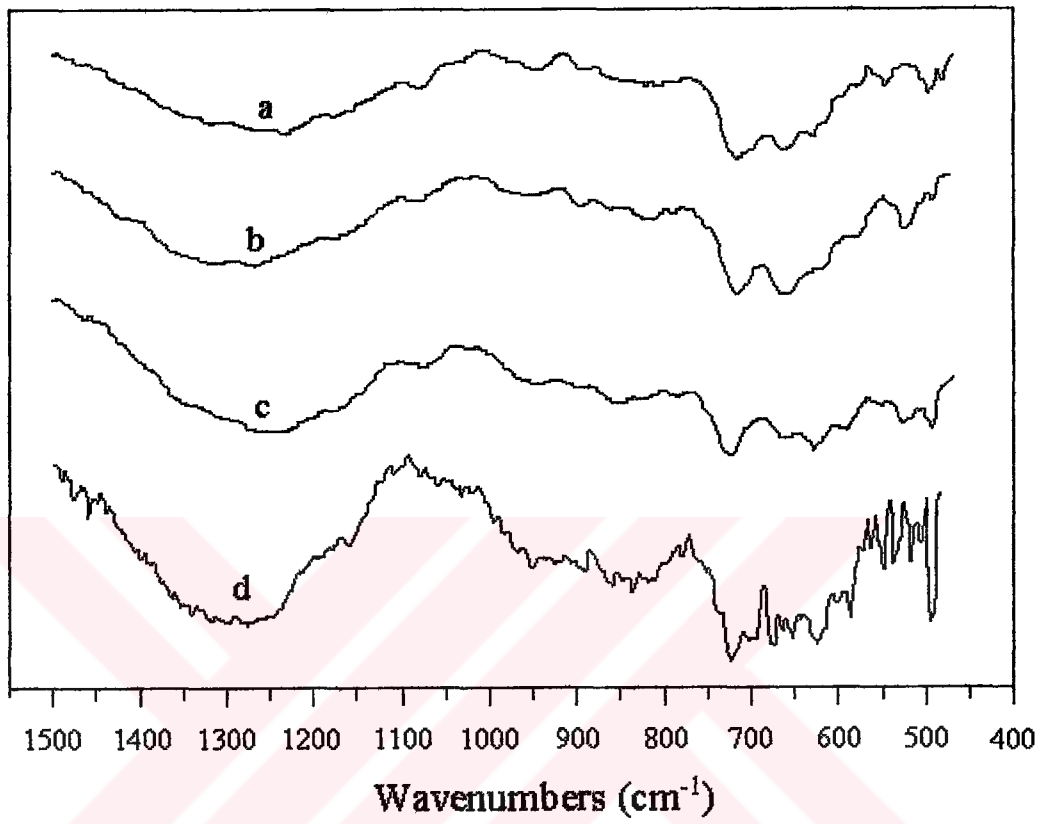

Figure 5.2. DRIFT spectra of chalcopyrite polarised in collectorless condition at a) –100 mV and b) +400 mV in pH 9.2 buffer solution and at c) –100 mV and d) +400 mV in pH 11 buffer solution.

Therefore, DRIFT spectra of chalcopyrite sample polarised at –100 mV (Figure 5.2.c) and 400 mV (Figure 5.2.d) in collectorless condition were measured to compare and clearly identify the surface compounds. These spectra showed that effect of DTP could not be seen at pH 11 due to intense oxidation on chalcopyrite surface. Hence, it can be concluded that heavy surface oxidation prevented collector adsorption.

5.2.1.5 Effect of Eh and pH on Chalcopyrite in the Presence of DTP

Above, DRIFT spectra of chalcopyrite mineral samples were analysed under the light of literature data. So, in this section, chalcopyrite spectra were evaluated according to IR band intensity. Because, peak intensity is an indicator for the amount of collector-mineral compounds formed.

Peak intensity observed on chalcopyrite spectra polarised with DTP increase with increasing the pulp potential at pH 4.67 (Figure 4.62) and pH 6.97 (Figure 4.63). This increase becomes reasonable at 400 mV. This means that maximum DTP adsorption occurs at oxidising conditions. However, effect of pulp potential can not be observed clearly in alkaline condition, especially at pH 11, due to heavy surface oxidation showing the reduced collector adsorption.

Figures 4.66-4.68 were also drawn to demonstrate the effect of pH on DTP adsorption in –100 mV, 150 mV and 400 mV pulp potential values, respectively. As shown from figures, maximum peak intensity is obtained from the sample polarised in pH 4.67 buffer solution, and then it sharply decreases in neutral solution. Observed peak intensities are almost the same in neutral and alkaline conditions. Leppinen (1991) also obtained such a result in an FTIR study on chalcopyrite-DTP interaction.

UV spectroscopy studies were also performed to identify the effect of pH on the adsorption of DTP on chalcopyrite surface quantitatively. Peak maximum for DTPI was found at 230 nm with an E_{max} = 3250 $mol^{-1}cm^{-1}$. Although, slight adsorption was observed with DRIFT data at pH 4.67, reproducible results could not be obtained in UV spectroscopy studies. Furthermore, DTP adsorption was not observed in alkaline condition (pH 11) like DRIFT results.

5.2.2 DRIFT Spectroscopy Study in the Presence of DTPI

DRIFT spectrum of DTPI is presented in Figure 4.69.a. IR bands found between 3000-2800 cm^{-1} and 1500-1300 cm^{-1} would be associated with the C-H vibrations of alkyl group (Bellamy, 1975; Drelich et al., 1998; Giesekke, 1983; Maslovsky, 1977; Meloan, 1963; Pouchert, 1981). The IR peaks observed between 1250-900 cm^{-1} may belong to isobutyl group of DTPI (Colthup et al., 1975; Pouchert, 1981).

Appearance of phosphorus-sulphur and phosphorous-carbon IR bands is expected below 900 cm^{-1}: Literature data proposed that P-C vibration peaks are anticipated at 850-650 cm^{-1} and 1320-1280 cm^{-1} (Bellamy, 1975; Colthup et al., 1975; Pouchert, 1981). So, it would be suggested that IR bands at 1319 cm^{-1}, 843 cm^{-1}, 810 cm^{-1}, 761 cm^{-1}, 736 cm^{-1} and 712 cm^{-1} are relevant to the P-C group. Sulphur-phosphorus IR bands emerge below 700 cm^{-1}: While 608 cm^{-1} is assumed to responsible for P=S bond, 528 cm^{-1} and 520 cm^{-1} bands would be associated with P-S vibrations (Basilio et al., 1992a; Colthup et al., 1975; Leppinen, 1991; Nakanishi and Solomon, 1977; Shishkov and Nikolov, 1972; van der Maas, 1972; Pouchert, 1981).

Figure 4.69.b presents the DRIFT spectrum of $(DTPI)_2$. When compared with DTPI spectrum (Figure 4.69.a), IR bands of monomer and dimer between 3000-2800 cm^{-1} and between 1500-900 cm^{-1} fit to each other except some differences: While 1381 cm^{-1} peak of monomer disappear, 1400 cm^{-1} and 1230 cm^{-1} bands of monomer are shifted to 1390 cm^{-1} and 1240 cm^{-1} in dimer spectrum, respectively. Also, 1065 cm^{-1} band of monomer split weakly to two peaks in $(DTPI)_2$ spectrum: 1063 cm^{-1} and 1055 cm^{-1}. P-C bands of $(DTPI)_2$ displace to higher wavenumbers.

There are important differences below 700 cm^{-1}: P=S band of monomer replaces from 608 cm^{-1} to 596 cm^{-1} in $(DTPI)_2$ spectrum. The other finding is that there is a sharp peak formation at 490 cm^{-1} and a small peak at 505 cm^{-1}. In

addition, an IR band is also observed as a shoulder at 520 cm^{-1}. 490 cm^{-1} and 505 cm^{-1} bands would be assigned to S-S bond (Colthup et al., 1975; Shishkov and Nikolov, 1972). It may be helpful to indicate that peak intensities of dimer are considerably higher than those of monomer. In conclusion, peak positions of P-C, P=S and S-S bands would be used to define $(DTPI)_2$.

To clearly identify and confirm the peak positions of $(DTPI)_2$ bands, a DRIFT spectrum was measured from platinum powder conducted with DTPI at 1250 mV (Figure 4.61.c). At this potential, it is expected that DTPI adsorbs as $(DTPI)_2$ on platinum surface according to reaction 5.22 (Hiçyılmaz et al., 2001):

$$2DTPI^- \rightleftharpoons (DTPI)_2 + 2e \qquad 5.22$$

Above 900 cm^{-1}, frequencies of IR bands of Pt powder polarised with DTPI almost coincides with those of dimer. However, intensities of these peaks are lower than those of dimer. P-C group does not split clearly as in the case of dimer, and shapes of P-C band resemble those of monomer. S-S bands are shifted to lower frequencies (483 cm^{-1} and 469 cm^{-1}). Further, P-S band forms at 518 cm^{-1}. These findings possibly showed that dimer formed in small scale on platinum surface. As well, similarity between spectra of monomer and platinum powder polarised with DTPI may be explained with accumulation of $DTPI^o$ on the surface consistent with the reaction 5.18.

Dithiophosphinate would react with chalcopyrite to form $(DTPI)_2$, CuDTPI and/or $Cu(DTPI)_2$. Similar to dithiophosphate, $Cu(DTPI)_2$ formation is expected only at high pH, Eh and collector concentration consistent with the reaction 5.12, and in acid solution CuDTPI+$(DTPI)_2$ formation is expected in conformity with the reaction 5.13 (Yordanov et al., 1983). Therefore, Cu^{+2} and $DTPI^-$ ions are reacted in acid solution to obtain CuDTPI+$(DTPI)_2$ precipitate as proposed by Yordanov et al (1983). DRIFT spectrum of this precipitate was drawn (Figure 4.69.d) to define the characteristic IR bands of CuDTPI. When compared with monomer and dimer spectra (Figures 4.69.a and 4.69.b), there are

two new IR bands, 581 cm^{-1} and 513 cm^{-1}, possibly showing the CuDTPI formation. Appearance of all $(DTPI)_2$ bands in Figure 4.69.d establishes the presence of $(DTPI)_2$ in the precipitate.

5.2.2.1 DRIFT Spectroscopy Study in the Presence of DTPI in pH 4.67

Chalcopyrite spectra were obtained in slightly acid solution at –100 mV, 150 mV and 400 mV pulp potential values to distinguish the effects of Eh on DTPI adsorption on chalcopyrite surface and to name the collector compound formed on mineral surface (Figure 4.62). Peak intensities decreased with increasing the pulp potential showing that the surface coverage of collector decreased at higher pulp potentials.

Similar IR bands were observed above 900 cm^{-1} on the spectrum of chalcopyrite mineral polarised at –100 mV pulp potential value as compared with monomer and dimer spectra of DTPI (Figure 4.70.c). However, there were considerable differences below 900 cm^{-1}. P-C band structure observed between 850-700 cm^{-1} changes reasonably. Splitting was not observed and only three peaks appeared between P-C group frequency range: two sharp peaks at 842 cm^{-1} and 810 cm^{-1}, and a small broad band at 716 cm^{-1}. Nevertheless, there is a bit similarity between P-C band structure of chalcopyrite polarised at –100 mV (Figure 4.70.c), platinum powder polarised with DTPI (Figure 4.69.c) and Cu-DTPI precipitate (Figure 4.69.d). The difference may come from lower peak intensities.

A new peak performed at 679 cm^{-1} like a shoulder. Such a peak also formed on platinum surface. This may be due to $DTPI^{\circ}$ formation (reaction 5.18). In addition, P=S band of –100 mV spectrum is broader than that of dimer. This finding would also support $DTPI^{\circ}$ formation.

Peak position of P=S band is 586 cm^{-1} between 608 cm^{-1} (DTPI band) and 581 cm^{-1} (CuDTPI band), and, as mentioned above, it has a broad band structure. Further, an IR band at 513 cm^{-1} was seen which may belong to CuDTPI formation. This peak might also show S-S bond. Since, S-S IR bands emerge between 520-470 cm^{-1} (Colthup et al., 1975; Shishkov and Nikolov, 1972). However, its lower intensity as compared with 490 cm^{-1} band of $(DTPI)_2$ made it difficult to define as dimer formation. In conclusion, it would be proposed that $(DTPI)_2$ formation may occur on chalcopyrite surface at reducing condition but amount of dimer precipitate on mineral surface should be very low. So, major DTPI compounds formed on the surface would be CuDTPI and/or $DTPI^o$.

Chalcopyrite spectrum polarised at 150 mV was given in Figure 4.70.d. Almost all IR bands of –100 mV spectrum were seen on the spectrum of 150 mV. 679 cm^{-1} band of reducing potential spectrum was shifted to 665 cm^{-1} and, it formed not as a shoulder but as a separate and sharp peak. So, it would show the DTPI adsorption on mineral surface powerfully as dithiophosphinate radical. It can not be related to CuDTPI, because such a peak was not observed on Cu-DTPI spectrum in Figure 4.69.d. 586 cm^{-1} and 515 cm^{-1} bands would show the CuDTPI adsorption on chalcopyrite surface.

DRIFT spectrum of chalcopyrite polarised in 10^{-1} M DTPI solution at +400 mV was presented in Figure 4.70.e. Almost all IR bands observed on the spectra of –100 mV and +150 mV can be seen on this figure. However, peak intensities of IR bands were low. In addition, there were two peaks at 602 cm^{-1} and 586 cm^{-1} possibly showing the $DTPI^o$ and CuDTPI formations, respectively. Further, 505 cm^{-1} may also belong to CuDTPI. 488 cm^{-1} band and broad structure around 600 cm^{-1} would show that major surface compound at oxidising potential is $(DTPI)_2$.

5.2.2.2 DRIFT Spectroscopy Study in the Presence of DTPI in pH 6.97

DRIFT spectra of chalcopyrite samples conditioned with DTPI measured in neutral solution (pH 6.97) was given in Figure 4.71. As shown from figure, there was a slight increase in peak intensity with pulp potential. Above 900 cm^{-1}, frequencies of IR bands on the spectra of chalcopyrite polarised at –100 mV (Figure 4.71.c), 150 mV (Figure 4.71.d) and 400 mV (Figure 4.71.e) show similarity as compared with monomer (Figure 4.71.a) and dimer (Figure 4.71.b) spectra of DTPI.

DRIFT spectrum of chalcopyrite polarised at –100 mV is given in Figure 4.71.c. There are considerable differences below 900 cm^{-1} when compared with monomer and dimer spectra. Especially, P-C band structure obtained between 850-700 cm^{-1} changed reasonably. Splitting was not observed and only three peaks emerged between P-C group frequency range: two sharp peaks at 843 cm^{-1} and 812 cm^{-1}, and a small broad band at 710 cm^{-1}. This may show collector adsorption on mineral surface. Presence of 667 cm^{-1} band and the small peak at 610 cm^{-1} possibly showed $DTPI^{o}$ accumulation on mineral surface. Moreover, 585 cm^{-1} and 517 cm^{-1} bands would imply that major surface compound was CuDTPI, while the peak at 494 cm^{-1} results from $(DTPI)_2$ generation on chalcopyrite surface.

Figure 4.71.d shows the DRIFT spectrum of chalcopyrite sample polarised at 150 mV. As it can be seen clearly, P-C band structure resembles P-C group frequency of –100 mV spectrum. Additionally, appearance of sharp IR peaks at 585 cm^{-1} and 509 cm^{-1} would show the surface accumulation of CuDTPI.

DRIFT spectrum of chalcopyrite polarised at 400 mV (Figure 4.71.e) displayed similar results as compared with the spectra obtained at moderately oxidising and reducing potentials. As in the case of others, major surface compound was possibly CuDTPI. Since, 585 cm^{-1} and 520 cm^{-1} IR bands would

show CuDTPI formation, although there was a small shift in the peak position of CuDTPI from 513 cm^{-1} (Figure 4.69.d) to 520 cm^{-1} (Figure 4.71.e).

5.2.2.3 DRIFT Spectroscopy Study in the Presence of DTPI in pH 9.2

Chalcopyrite was treated with 10^{-1} M DTPI at pH 9.2 to obtain the DRIFT spectra of mineral polarised with collector to determine the adsorbed compounds on mineral surface (Figure 4.72). As in the case of acid (pH 4.67) and neutral (pH 6.97) condition, above 900 cm^{-1}, frequencies of IR bands on chalcopyrite spectra polarised at –100 mV (Figure 4.72.c), 150 mV (Figure 4.72.d) and 400 mV (Figure 4.72.e) showed similarity when compared with monomer (Figure 4.72.a) and dimer (Figure 4.72.b) spectra of DTPI. Moreover, position of IR bands of P-C group was similar to each other.

Figure 4.72.c presented chalcopyrite spectrum for the sample polarised at reducing potential with 10^{-1} M DTPI. There were two sharp known peaks at the frequency of 586 cm^{-1} and 515 cm^{-1} as compared with Cu-DTPI spectrum (Figure 4.69.d). As pointed out before, these IR bands possibly showed the surface coverage of chalcopyrite with CuDTPI. Absence of any other different peak means that only CuDTPI would present on mineral surface.

Chalcopyrite spectrum of sample polarised with DTPI at 150 mV was given in Figure 4.72.d. Presence of 494 cm^{-1} band would offer $(DTPI)_2$ coverage of chalcopyrite surface. The IR band at 586 cm^{-1} might have revealed CuDTPI formation. But, 513 cm^{-1} peak of CuDTPI is not observed. Instead, there were two new peaks: A small peak at 548 cm^{-1} as a shoulder and a sharp peak at 528 cm^{-1}. In addition, a new peak formation was also observed at 625 cm^{-1}. These peaks were not indicators of $(DTPI)_2$ (Figure 4.69.b) and CuDTPI (Figure 4.69.d). Therefore, they would belong to $Cu(DTPI)_2$.

Figure 4.72.e display DRIFT spectrum of chalcopyrite polarised with DTPI at 400 mV. 660 cm^{-1} and 612 cm^{-1} IR bands may show DTPI° formation. There was a small peak at 494 cm^{-1} which would belong to $(DTPI)_2$. But, as compared with dimer spectrum, peak size indicated that amount of dimer accumulation is very low. The peaks observed at 585 cm^{-1} and 507 cm^{-1} would show CuDTPI formation. Further, the broad IR band at 538 cm^{-1} should be the signal of $Cu(DTPI)_2$, since such a peak did not appear at dimer (Figure 4.69.b) and Cu-DTPI (Figure 4.69.d) spectra.

5.2.2.4 DRIFT Spectroscopy Study in the Presence of DTPI in pH 11

DRIFT spectra of chalcopyrite were obtained at pH 11 by polarising the sample with DTPI at –100 mV, +150 mV and +400 mV pulp potential values to elucidate the effects of pulp potential on DTPI adsorption and to define the collector compounds formed on mineral surface (Figure 4.73). Frequencies of IR bands observed at different potentials at pH 11 above 700 cm^{-1} almost coincide with peak positions observed at pH 4.67, 6.97 and 9.2. Surface adsorption peaks appear below 700 cm^{-1}.

DRIFT spectrum of chalcopyrite polarised at reducing condition was given in Figure 4.73.c. IR band of 667 cm^{-1} would be responsible for DTPI° formation on chalcopyrite surface. Furthermore, there were two sharp peaks at 581 cm^{-1} and 520 cm^{-1} possibly demonstrating the CuDTPI coverage of surface. Dimer formation was not observed in reducing condition.

Chalcopyrite spectrum of sample (Figure 4.73.d) polarised with DTPI at 150 mV displayed a bit differences from the spectrum of reducing condition. Similarly, 673 cm^{-1} band may be a sign for the presence of DTPI° on mineral surface. 494 cm^{-1} and 479 cm^{-1} bands would belongs to $(DTPI)_2$ formation. Presence of 527 cm^{-1} peak would show $Cu(DTPI)_2$. Since, such a peak was not observed on dimer (Figure 4.69.b) and Cu-DTPI (Figure 4.69.d) spectra.

Moreover, presence of CuDTPI may also be stated on mineral surface. Because, the sharp band at 579 cm^{-1} and the small band at 514 as a shoulder would show CuDTPI accumulation in minor amounts. In conclusion, it may be proposed that $(DTPI)_2$ and $Cu(DTPI)_2$ were main surface products at moderately oxidising potentials at pH 11.

Figure 4.73.e showed DRIFT spectrum of chalcopyrite polarised at 400 mV with 10^{-1} M DTPI. 660 cm^{-1} and 613 cm^{-1} IR bands may show $DTPI^{o}$ formation. Presence of 492 cm^{-1} IR band on the spectrum would be attributed to dimer formation. As mentioned above, 581 cm^{-1} and 513 cm^{-1} peaks would belong to CuDTPI, so it may indicate that CuDTPI form on mineral surface at 400 mV in highly alkaline condition. Occurrence of 528 cm^{-1} peak as a shoulder and the small IR band at 543 cm^{-1} was possibly responsible for $Cu(DTPI)_2$ formation in small amounts on chalcopyrite.

5.2.2.5 Effect of Eh and pH on Chalcopyrite in the Presence of DTPI

DRIFT spectra of chalcopyrite samples were assessed in accordance with the IR band intensity. Because, peak intensity shows the amount of DTPI-mineral compounds formed.

Peak intensity of chalcopyrite spectra polarised with 10^{-1} M DTPI in slightly acid condition reasonably decreased with increasing the pulp potential (Figure 4.70). On the other hand, in the case of neutral (pH 6.97) (Figure 4.71) and alkaline conditions (pH 9.2 and pH 11) (Figures 4.72-4.73), effect of pulp potential may not be taken into account: Peak intensities increased in pH 6.97 and 9.2 very slowly while they decrease in pH 11 buffer solution.

To elucidate the effect of pH on chalcopyrite-DTPI interaction on the basis of peak intensities, Figures 4.74-4.76 were drawn for –100 mV, 150 mV and 400 mV pulp potential values, respectively. As shown from figures, maximum peak

intensity is obtained from the sample polarised in pH 4.67 buffer solution, and then it decreases in neutral and alkaline conditions. When compared with DTP spectra, IR bands of DTPI-chalcopyrite spectra can be clearly distinguished proving that DTPI is a more powerful collector for chalcopyrite than DTP (Gorken et al., 1992; Kim, 1995; Klimpel, 1999; Nagaraj and Avotins, 1988).

UV spectroscopy studies were also performed to identify the effect of pH on the adsorption of DTPI on chalcopyrite surface quantitatively. Peak maximum for DTPI was found at 236 nm with an E_{max} = 6300 $mol^{-1}cm^{-1}$. Chalcopyrite was polarised for 15 minutes at 150 mV in 20 ml $1.71x10^{-4}$ M DTPI buffer solution. In slightly acid solution (pH 4.67), about 27 % decrease in DTPI concentration of solution was observed after polarisation, whereas it was obtained as 13 % in alkaline condition (pH 11).

5.3 Flotation Study

Flotation behaviour of sulphide minerals is strongly dependent on pulp potential due to semiconducting property of them (Fornasiero et al., 1996; Trahar, 1983). Hence, a great advantage is gained when electrochemical techniques are combined with wetting methods such as modified Hallimond tube flotation to study flotation systems (Gardner and Woods, 1979; Chander, 1988; Chander and Fuerstenau, 1974, 1975). Electrochemical techniques can be used to control the oxidation state of sulphide minerals and to determine the nature and amount of surface species. The wetting techniques of contact angle and flotation measurements can be used to determine hydrophobicity of the surface.

In the previous sections of this chapter, surface compounds were established by using voltammetric and spectroscopic techniques. This section dealt with the demonstration of the effect of these surface compounds on flotation behaviour of chalcopyrite.

5.3.1 Collectorless Flotation

Figure 4.80 presents the pulp potential vs. recovery relationship in collectorless condition. Highest chalcopyrite recoveries were obtained at mildly oxidising potentials (~100 mV) and at lowest pH values (pH 4.67).

Results of flotation experiments performed in slightly acid solution showed that chalcopyrite recovery was almost not affected by pulp potential. Only there was a small decrease at oxidising potentials, which may be due to SO_4^{-2} formation according to reaction 5.8.

Iron preferentially dissolves from chalcopyrite surface in acid solution (Grano et al., 1997a, b; Kelsall et al., 1992; Linge, 1976; Wadsworth, 1972). Fairthorne et al. (1997) stated that the concentration of iron species determined in solution is greater than that of copper. Adsorption and/or precipitation of iron ions as hydroxide is not expected in acid solution (Buckley et al., 1985; Gardner and Woods, 1979; Gómez et al. 1996; Ralston, 1991) and, therefore, concentration of hydrophobic surface species, such as CuS and S°, increases in accordance to preferential dissolution of metal ions. As depicted in the voltammetry section above, major surface compounds are CuS and S° in acid solution. Hence, reasonably high chalcopyrite recovery was obtained due to abundance of hydrophobic surface species in acid solution. Due to slow oxidation reaction of S° to SO_4^{-2} (Peters, 1977), a small decrease should also be expected at oxidising potentials.

In the neutral solution, chalcopyrite recovery decreased considerably: approximately 15 % as compared with the results obtained in slightly acid solution. It should be due to the precipitation of metal oxides/hydroxides, especially iron hydroxides. Since, coverage of the chalcopyrite surface with hydrophilic metal hydroxides increases with pH (Fairthorne, et al., 1997). Increase in recovery at mildly oxidising potentials would be dealt with the concomitant exposure of iron-deficient, sulphur-rich layers. Voltammetric study (Figure 4.16 and reaction 5.15) proposed the CuS, S° and $Fe(OH)_3$ formation at slightly

oxidising potentials, Although S° formation was also expected at highly oxidising potentials (reaction 5.16), chalcopyrite recovery decreased possibly due to intense coverage of mineral surface by metal hydroxides ($Cu(OH)_2$ and $Fe(OH)_3$) with increasing pulp potential.

Similar results were also observed in alkaline condition (pH 9.2 and pH 11): Recovery increased up to slightly oxidising potentials and then decreased at higher potentials. Higher recovery at mildly oxidising potentials was possibly due to elemental sulphur rich surface (reaction 5.15). Lower recovery at reducing potentials may be due to unoxidised mineral surface. Many researchers obtained similar results and concluded that slight surface oxidation of sulphides was essential for flotation (Finkelstein et al., 1975; Gardner and Woods, 1979; Heyes and Trahar, 1977; Trahar, 1983; etc.). Lower recovery was also obtained at highly oxidising potentials possibly due to hydrophilic metal hydroxides (Fairthorne et al., 1997; Rao et al., 1992; Senior and Trahar, 1991). Decrease in chalcopyrite recovery with an increase in pulp pH shows the heavier surface coating of metal hydroxides at higher pH values (Chander, 1991; Fairthorne et al., 1997; Kocabağ and Smith, 1989; Luttrell and Yoon, 1984a, b; Ruonala et al., 1997).

5.3.2 DTP Induced Flotation

DTP induced flotation experiments were conducted to determine the effect of Eh, pH and surface composition on chalcopyrite recovery (Figure 4.84). As stated above, DTP-chalcopyrite interaction was investigated with cyclic voltammetry and DRIFT spectroscopy. Under the light of these investigations, DTP induced flotation of chalcopyrite were commented.

Chalcopyrite recovery does almost not change with pulp potential in slightly acid solution (Figure 4.84). When collectorless flotation is taken into account (Figure 4.90), it can be seen that there is a small increase in recovery. The reason of the increase in recovery could not be identified clearly by cyclic

voltammetry: DTP caused surface passivation, but did not initiate new peak (Figures 4.8-4.10). On the other hand, DRIFT spectra gave valuable information (Figure 4.62): IR signals showed that dimer formation weakly on mineral surface resulted in a slight increase (~2 %) in recovery as compared with collectorless condition. Besides dimer, dithiophosphate radical (DTP°) adsorption in reducing and moderately oxidising potentials and CuDTP formation at highly oxidising potentials (+400 mV) were also proposed to explain this small increase by DRIFT results.

In neutral solution (pH 6.97), significantly high recovery was obtained with respect to collectorless condition (Figure 4.91). In neutral and alkaline conditions, there is always a competition between metal hydroxides and collector ions to cover mineral surface. Therefore, flotation recovery is a good indicator for activity of these ions. DTP induced flotation results obtained in pH 6.97 buffer solution shows that coverage of chalcopyrite surface with hydrophilic species is not so heavy, and then collector was able to adsorb on mineral surface. At reducing and mildly oxidising potentials, almost the same results were obtained as compared with acid solution (Figure 4.84). However, there is a noticeable decrease at oxidising potentials (400 mV), which may be due to heavy surface oxidation. Because, accumulation of hydrophilic species on chalcopyrite surface increases at higher pulp pH and oxidising potentials (Fairthorne, et al., 1997; Gardner and Woods, 1979; Buckley et al., 1985).

Cyclic voltammograms of chalcopyrite measured in neutral solution (Figures 4.23-4.25) confirms the adsorption of DTP on mineral surface. Yet, collector compounds could not be defined by voltammetry. They could not also be identified by DRIFT spectra clearly (Figure 4.63): At reducing and mildly oxidising potentials, weak collector adsorption was determined, but any surface compound could not be estimated with a few data not to make a mistake. At 400 mV reasonably intense IR signals were obtained possibly showing the dimer formation. In contrast to DRIFT results, flotation recovery almost did not decrease up to 300 mV and then slowly decreased. Although dimer adsorption increases at

highly oxidising potentials, which were expected to increase flotation recovery, recovery decreased due possibly to the increase in the surface activity of hydrophilic compounds.

Flotation recovery significantly decreased in pH 9.2 buffer solution concerning the results obtained in acid and neutral solutions (Figure 4.84). Since, as stated above, surface concentration of metal hydroxides increase at higher pH values (Fairthorne, et al., 1997; Gardner and Woods, 1979; Buckley et al., 1985). Though, DTP would be able to reasonably improve chalcopyrite recovery (Figure 4.92). Chalcopyrite voltammograms (Figures 4.38-4.40) shows that adsorption density of DTP is low at alkaline condition with regard to the results obtained at pH 4.67 and pH 6.97. These voltammograms did not give any idea about hydrophobic DTP species formed on mineral surface. Heavy oxidation was also observed on DRIFT spectra (Figures 4.64 and 5.2a,b). Therefore, hydrophobic DTP species could not be defined. DTP could be observed on chalcopyrite surface polarised at reducing and mildly oxidising potentials. Lowest peak intensity was observed at highly oxidising potential (400 mV) proving that hydrophilic metal oxides/hydroxides were major surface compounds. Eh-recovery curve is in conformity with this result.

Decrease in chalcopyrite recovery is very high in pH 11 buffer solution regarding with the results obtained at lower pH values (Figure 4.84). This shows the heavy surface oxidation. Only, a small improvement in chalcopyrite recovery was satisfied at reducing and moderately oxidising potential when compared with results obtained in collectorless condition (Figure 4.93). DTP did almost not result in surface passivation as shown from voltammograms and no new peak is observed (Figures 4.53-4.55). Further, DRIFT spectra could not be evaluated due to heavy oxidation (Figure 4.65).

5.3.3 DTPI Induced Flotation

Flotation experiments were performed with DTPI to elucidate the effect of pulp potential, pH and collector compounds on the hydrophobicity of chalcopyrite. Surface composition was clarified with cyclic voltammetry and DRIFT studies.

Pulp potential does not affect chalcopyrite recovery in pH 4.67 buffer solution (Figure 4.88). On the other hand, DTPI causes significant increase in recovery concerning the collectorless flotation (Figure 4.90). To demonstrate the reasons of such increase, cyclic voltammetry and DRIFT spectroscopy experiments were made. No new peak formation is not observed on voltammograms (Figures 4.12-4.14), but collector addition results in surface passivation which indicates the surface coverage of chalcopyrite with DTPI. However, DTPI species formed on mineral surface can not be defined by cyclic voltammetry. Identifying information was obtained from DRIFT study: One of the hydrophobic species in slightly acid solution would be DTPI°. In reducing condition, CuDTPI and/or DTPI° formation was predicted causing surface hydrophobicity. Major surface compounds are DTPI° in mildly oxidising potentials and $(DTPI)_2$ at higher potentials. Recovery values show that DTPI adsorbs on chalcopyrite powerfully.

High flotation response is also observed in neutral buffer solution (Figure 4.88). Similar to the results obtained in acid buffer, effect of pulp potential on chalcopyrite recovery can not be seen clearly. However, high recovery results show that DTPI adsorb effectively on chalcopyrite surface in neutral solution. Cyclic voltammetry did not demonstrate the surface compounds. Instead, surface compounds were determined by DRIFT study: Major surface compound is CuDTPI under neutral condition.

A small decrease is seen on chalcopyrite recovery at pH 9.2 (Figure 4.88) when compared with the results obtained in slightly acid and neutral conditions.

At this pH, maximum recovery was obtained at moderately oxidising potentials. Surface passivation occurs in the presence of DTPI, but no new peak formed. Therefore, Cu-DTPI compounds could not be determined by cyclic voltammetry. DRIFT study proposed that CuDTPI be formed at reducing potentials. $(DTPI)_2$+$Cu(DTPI)_2$ formation was predicted from IR-signals at moderately oxidising potentials while $Cu(DTPI)_2$+CuDTPI accumulation was estimated at highly oxidising potentials.

Chalcopyrite recovery decreased considerably in pH 11 buffer solution especially at reducing and highly oxidising potentials concerning with the results obtained in lower pH values (Figure 4.88). However, it was reasonably high at moderately oxidising potentials. Surface passivation observed on voltammograms shows that collector was adsorbed on mineral surface. On the other hand, DRIFT study suggests that CuDTPI adsorption occurs at reducing potentials, while $(DTPI)_2$, CuDTPI and $Cu(DTPI)_2$ form on chalcopyrite surface at oxidising potentials.

5.3.4 Effect of Eh and pH on Flotation

Effect of collectors on the flotability of chalcopyrite was investigated comparatively in this section. In general, at all pH values studied, maximum recovery was obtained at moderately oxidising potentials, and flotability was noticeably low at reducing and highly oxidising potentials.

High recovery was obtained in collectorless condition in slightly acid solution due to iron deficient surface (Figure 4.90). Therefore, effect of collectors was low either in the presence of DTP and DTPI. On the other hand, the highest recovery was obtained with DTPI. In addition, pulp potential did almost not affect chalcopyrite recovery. However, the general trend in the presence of DTP was similar to collectorless condition: Recovery increased up to moderately oxidising potentials and then decreased.

Chalcopyrite recovery decreased reasonably in neutral condition possibly due to surface coverage by hydrophilic iron hydroxides (Fairthorne, et al., 1997). However, collectors resulted in considerable improvement (Figure 4.94). As stated above, there is a competition between hydrophilic species and collector compounds in neutral and alkaline conditions. Therefore, results showed that collectors overcame the adverse effects of hydrophilic species.

Decrease in recovery in alkaline solutions (pH 9.2 and pH 11) was expected in collectorless condition due to heavy oxidation (Fairthorne, et al., 1997). Therefore, collector was used to improve it. Figures 4.92 and 4.93 showed that positive effect of DTP on chalcopyrite recovery sharply decreased with pH whereas DTPI gave better result. Therefore, it would be proposed that DTPI adsorbed on chalcopyrite and results in better flotation response that DTP as stated in literature (Gorken et al., 1992; Klimpel, 1999).

CHAPTER 6

CONCLUSIONS AND RECOMMENDATIONS

In the light of cyclic voltammetry, DRIFT spectroscopy and microflotation tests with chalcopyrite, following conclusions and recommendations were given.

6.1 Conclusions

1. a) Cyclic voltammetry tests performed in pH 4.67 buffer solution showed that redox reactions occurring on chalcopyrite surface were not fully reversible possibly due to preferential dissolution of iron.

   b) In neutral and alkaline solutions, redox peaks observed on chalcopyrite voltammograms were not fully reversible possibly due to irreversible surface coverage by iron-hydroxides.

   c) DTP and DTPI did not give any identifiable peak in cyclic voltammetry study. Only, they caused surface passivation. Voltammetry tests showed that adsorption density of collectors on chalcopyrite surface decreased with increasing the pulp pH. Especially, effect of DTP on surface passivation was very low in alkaline solutions.

2. a) In slightly acid solution, DTP adsorbed weakly on chalcopyrite surface. DRIFT spectra suggested that major surface compound was adsorbed dithiophosphate (DTP^o) in reducing and moderately oxidising potentials. At highly oxidising potentials, $(DTP)_2$ and CuDTP formation may occur.

b) In neutral and alkaline conditions, metal hydroxides covered chalcopyrite surface dominantly and DTP adsorption was restricted due to presence of hydrophilic oxides/hydroxides on mineral surface. Therefore, hydrophobic species formed on chalcopyrite surface could not be defined.

c) DRIFT spectra propose that CuDTPI and/or $DTPI^o$ cover the chalcopyrite surface in slightly acid solution at reducing and moderately oxidising potentials. However, at highly oxidising potentials, $(DTPI)_2$ would be the major surface compound. Lower peak intensities at higher pulp potentials explain the reduced adsorption density of DTPI.

d) In neutral pH, DRIFT spectra proposed that CuDTPI formed on chalcopyrite surface.

e) It was found from DRIFT spectroscopy that DTPI would adsorb on chalcopyrite surface as CuDTPI at reducing potentials, $Cu(DTPI)_2$ and/or $(DTPI)_2$ at oxidising potentials in pH 9.2 buffer solution.

f) In pH 11 buffer solution, CuDTPI formation would be expected at reducing potentials according to DRIFT spectroscopy. On the other hand, major surface compounds are possibly $(DTPI)_2$ and/or $Cu(DTPI)_2$ at oxidising potentials. CuDTPI may also form at oxidising potentials.

3. a) Maximum chalcopyrite recovery was obtained in moderately oxidising potentials (100-300 mV) in the presence and absence of DTP and DTPI: Lower recovery at highly oxidising potentials would be due to hydrophilic surface species, while it was possibly due to unoxidised mineral surface at reducing potentials. Effect of Eh on recovery decreased at lower pH: In slightly acid solution, Eh did almost not affect recovery.

b) In collectorless condition, recovery reached its maximum value in slightly acid solution due to preferential dissolution of iron and then formation of iron-deficient, S^{o}-rich chalcopyrite surface. It decreased with increasing the pulp pH because of surface coverage by hydrophilic metal hydroxides.

c) DTP resulted in a bit improvement on recovery in slightly acid solution as compared with collectorless flotation. Since, recovery is already reasonably high in collectorless condition. In neutral condition, DTP caused a considerable increase in recovery. This means that DTP can overcome adverse effect of hydrophilic species. But, its collecting property decreased sharply in alkaline condition. That is, heavy surface coating by hydrophilic species prevented collector adsorption. Voltammetry and DRIFT spectroscopy results confirmed this finding.

d) Recovery was almost not affected by Eh up to pH 9.2 in DTPI induced condition. Its effect could only be seen in pH 11. DTPI displayed better results than DTP. This confirmed that DTPI is more powerful collector than DTP.

6.2 Recommendations

- Surface species were tried to be defined in different conditions by using cyclic voltammetry and DRIFT spectroscopy methods. To confirm the findings listed above, additional tests by applying different methods (such as X-ray Photoelectron Spectroscopy, Secondary Ion Mass Spectroscopy, Auger Electron Spectroscopy, Electron Spin Resonance, etc.) may be helpful.

- In this thesis, DTP and DTPI, selective collectors for chalcopyrite, were examined. Different new collectors may also be studied to determine the better collector for chalcopyrite.

- Chalcopyrite generally occurs with other sulphides in nature. Therefore, for industrial application, electrochemistry of complex ore should also be investigated due to galvanic interaction.

REFERENCES

Alexiev, V., Iliev, V.I. and Yordanov, N.D., 1984. "An EPR study of bis(organodithiocarbonato) copper(II) complex", *J. Molecular Struc.*, V.114, pp.441-444.

Allison, S.A., Goold, L.A., Nicol, M.J. and Granville, A., 1972. "A Determination of the Products of Reaction between various Sulphide Minerals and Aqueous Xanthate Solution, and a Correlation of the Products With Electrode Rest Potentials", *Met. Trans.*, Vol. 3, pp. 2613.

Aplan, F.F. and Chander, S., 1987. "Collectors for Sulfide Mineral Flotation", Reagents in Mineral Technology, Somasundaran, P. and Moudgil, B.M. (Eds.), Marcel Dekker, Inc., New York, pp. 335-369.

Arbiter, N., Cooper, H., Fuerstenau, M.C., Harris, C.C., Kuhn, M.C., Miller, J.D. and Yap, R.F., 1985. "Flotation", SME Mineral Processing Handbook, Weiss, N.L. (Ed.), AIME, New York, USA, Vol.1, pp.5.1-5.109.

Arbiter, N., Fujii, U., Hansen, B. and Raja, A., 1975. "Surface properties of Hydrophobic Solids", Advances in Interfacial Phenomena of Particulate/Solution/Gas Systems: Applications to Flotation Research, Somasundaran, P. and Grieves, R.P. (Eds.), American Institute of Chemical Engineers, Symposium Series, Vol. 71, No. 150, pp.

Arbiter, N. and Gebhardt, J.E., 1992. "Requirements for Industrial Collectorless Flotation of Sulphide Minerals", Proc. Third Int. Symp. on Electrochemistry in Mineral and Metal Processing III, Woods, R. and Richardson, P.E. (Eds.), The Electrochemical Society, Inc., pp.1-13.

Aslan, A., 2002. Kompleks Sülfürlü Cevherlerde Minerallerin Flotasyon Davranımına Elektrokimyasal Parametrelerin Etkileri, Hacettepe Üniversitesi Fen Bilimleri Enstitüsü, Doktora Tezi, 225 p.

Bahena, G., González, I. And Arce, E.M., 2000. "A comparative study of electrochemical behavior of chalcopyrite, chalcocyte and bornite in sulfuric acid solution", Fifth International Symposium on Electrochemistry In Mineral and Metal Processing, The Electrochemical Society, Inc., Toronto, Ontario, Canada.

Basilio, C.I., Kim, D.S., Yoon, R.-H. and Nagaraj, D.R., 1992a. "Studies on the use of monothiophosphates for precious metals flotation", *Minerals Eng.*, V.5, No.3-5, pp.397-409.

Basilio, C.I., Kim, D.S., Yoon, R.-H. Leppinen, J.O. and Nagaraj, D.R., 1992b. "Interaction of thiophosphinate collectors with precious metals", SME-AIME Annual Meeting, Phoenix, Arizona, Preprint No.92-174.

Basilio, C., Pritzker, M.D., Yoon, R.-H., 1985. "Thermodynamics, electrochemistry and flotation of the chalcocite-potassium ethyl xanthate system", 114th SME/AIME Annual Meeting, New York, N.Y., Preprint No.85-86.

Basilio, C.I., Yoon, R.-H., Nagaraj, D.R. and Lee, J., 1991. SME-AIME Annual Meeting, Denver, Colorado, Preprint No.91-171.

Baulsir, C.F. and Tague Jr., T.J., 2002. Introduction to Diffuse Reflectance Infrared Fourier Transform Spectroscopy, Technical Note, Spectra-Tech, Inc., 4 p.

Bellamy, L.J., 1975. The Infra-red Spectra of Complex Molecules, Chapman and Hall, London, Third Edition, 433 p.

Berglund, G. and Forssberg, K.S.E., 1987. "Pulp Chemistry Measurements in Sulphide Mineral Flotation", *Erzmetall*, Vol. 40, No. 4, pp. 189-195.

Biegler, T. and Horne, M.D., 1985. "The Electrochemistry of Surface Oxidation of Chalcopyrite", Proc. Int. Symp. on Electrochemistry and Metal Processing, The Electrochemical Society, Inc., pp. 321-343.

Bott, A.W., 1999. "Characterisation of Chemical Reactions Coupled to Electron Transfer Reactions Using Cyclic Voltammetry", *Current Separations*, Vol. 18, No. 1, pp. 9-16.

Bozkurt, V., Xu, Z. and Finch, J.A., "Pentlandite/Pyrrhotite Interaction and Xanthate Adsorption", *Int. J. Miner. Process.*, V.52, pp.203-214.

Brinen, J.S., Greenhouse, S., Nagaraj, D.R. and Lee, J., 1993. "SIMS and SIMS Imaging Studies of Adsorbed Dialkyl Dithiophosphates on PbS Crystal Surface", *Int. J. Miner. Process.*, V.38, pp.93-109.

de Bruyn, P.L. and Agar, G.E. 1962. "Surface Chemistry of Flotation", Froth Flotation: 50th Anniversary Volume, Fuerstenau, D.W., (Ed.), The American Institute of Mining, Metallurgical, and Petroleum Engineers, Inc., New York, pp.91-138.

Buckley, A.N., Hamilton I.C. and Woods, R., 1985. "Investigation of The Surface Oxidation of Sulphide Minerals by Linear Potential Sweep Voltammetry and X-Ray Photoelectron Spectroscopy", Flotation of Sulphide Minerals, Forssberg, K.S.E. (Ed.), Elsevier, Amsterdam, pp.41-60.

Buckley, A. and Woods, R., 1982. "Investigation of the Surface Oxidation of Sulphide Minerals via ESCA and Electrochemical Techniques", Interfacial Phenomena in Mineral Processing, Yarar, B. and Spattiswood, D.S. (Eds.), Engineering Foundation, pp.1-17.

Buckley, A.N. and Woods, R., 1984. "An X-Ray Photoelectron Spectroscopic Study of the Oxidation of Chalcopyrite", *Aust. J. Chem.*, Vol. 37, pp. 2403-2413

Buckley, A.N. and Woods, R., 1992. "Underpotential Deposition of Dithiophosphate on Chalcocite", *J. of Electroanal. Chem.*, Vol. 357, pp. 387-405.

Buckley, A.N. and Woods, R., 1995. "Identifying chemisorption in the interaction of thiol collectors with sulfide minerals by XPS: Adsorption of xanthate on silver and silver sulfide", *Colloids Surf. A*, V.104, pp.295-305.

Cases, J.M., Mielczarski, J.A., de Donato, P., Mielczarski, E., Kongolo, M., BarrJs, O., Alnot, M. and Ehrhardt, J.J., 1997. "Relationship between Surface Composition and Flotation Behaviour of Chalcopyrite Prepared under Different Conditions", Proceedings of the XX International Mineral Processing Congress, Aachen, 21-26 September, pp. 477-489.

Cha, D.K. and Park, S.M., 1996. "Strong Oxidants for Organic Waste Destruction from Oxidation of Manganese Hydroxide", Proceedings of the HSRC/WERC Joint Conference on the Environment, Erickson, L.E., Tillison, D.L., Grand, S.C. and McDonald, J.P. (Eds.), May 21-23, New Mexico, pp. 1-11.

Chander, S., 1988. "Electrochemistry of Sulphide Mineral Flotation", *Minerals Metall. Process.*, pp. 105-113.

Chander, S., 1991. "Electrochemistry of Sulfide Flotation: Growth Characteristics of Surface Coatings and Their Properties, with Special Reference to Chalcopyrite and Pyrite", *Int. J. Miner. Process.*, Vol. 33, pp. 121-134.

Chander, S., 1999. "Fundamentals of Sulfide Mineral Flotation", Advances in Flotation Technology, Proceedings of a Symposium held at the Annual SME Meeting, Parekh, B.K. and Miller, J.D. (Eds.), Society of Mining, Metallurgy, and Exploration, Inc., pp.129-145.

Chander, S. and Briceno, A., 1987. "Kinetics of Pyrite Oxidation", *Minerals Metall. Process.*, pp.171-176

Chander, S. and Fuerstenau, D.W., 1974. "The Effect of Potassium Diethyldithiophosphate on the Electrochemical Properties of Platinum, Copper and Copper Sulfide in Aqueous Solutions", *Electroanal. Chem. Interf. Electrochem.*, Vol. 56, pp. 217-247.

Chander, S. and Fuerstenau, D.W., 1975. "Electrochemical Reaction Control of Contact Angles on Copper and Synthetic Chalcocite in Aqueous K-Diethyl Dithiophosphate Solutions", *Int. J. Miner. Process.*, V. 2, pp. 333-352.

Chander, S, Wie, J.M. and Fuerstenau, D.W., 1975. "On the Native Floatability and Surface Properties of Naturally Hydrophobic Solids", Advances in Interfacial Phenomena of Particulate/Solution/Gas Systems: Applications to Flotation Research, Somasundaran, P. and Grieves, R.P. (Eds.), American Institute of Chemical Engineers, Symposium Series, Vol. 71, No. 150, pp. 183-188.

Cheng, X. and Iwasaki, I., 1992. "Effect of chalcopyrite and pyrrhotite interaction on flotation separation", *Minerals Metall. Process.*, pp.73-79.

Colthup, N.B., Daly, L.H. and Wiberley, S.E., 1975. Introduction to Infrared and Raman Spectroscopy, Academic Press, New York, N.Y., Second Edition, 523 p.

Crozier, R.D., 1978. "Processing of copper sulphide ores: Froth flotation reagents, a review, *Min. Mag.*, V.138, pp.332-339.

Crozier, R.D., 1984. "Plant Reagents Part 1: Changing Patterns in the Supply of Flotation Reagents", *Min. Magazine*, pp.202-213.

Dennen, W.H., 1959. Principles of Mineralogy, Ronald Press, New York.

Drelich, J., Lu, Y., Chen, L., Miller, J.D. and Guruswamy, S., 1998. "FTIR Internal Reflection Spectroscopy Studies of the Effect of pH on Adsorption of Oleate/Oleic Acid at the Surface of a TiO_2 Thin Film Deposited on a Ge Single Crystal", Applied Surface Science, V.125, pp.236-244.

Ekmekçi, Z., 1995. Toplayıcısız Kalkopirit-Pirit Flotasyonunda Galvanik Etkileşimin Rolü, Hacettepe Üniversitesi Fen Bilimleri Enstitüsü, Doktora Tezi, 185 p.

Ekmekçi, Z. and Demirel, H., 1997. "Collectorless Flotation of Chalcopyrite and Pyrite: Influence of Pulp Potential, pH and Galvanic Contact", Proc. 20th International Mineral Processing Congress, Aachen, pp.77-85.

Ekmekçi, Z. and Demirel, H. 1998. "Collectorless Flotation of Murgul (Turkey) Copper Ore", *Trans. IMM*, V.107, pp.C76-C81.

Fairthorne, G., Fornasiero, D. and Ralston, J., 1997. "Effect of Oxidation on the Collectorless Flotation of Chalcopyrite", *Int. J. Miner. Process.*, Vol. 49, pp. 31-48.

Finkelstein, N.P., Allison, S.A., Lovell, V.M. and Stewart, B.V., 1975. "Natural and induced hydrophobicity in sulphide mineral systems", Advances in Interfacial Phenomena of Particulate/Solution/Gas Systems: Application to Flotation Research, Somasundaran, P. and Grieves, R.G. (Eds.), Am. Inst. Chem. Eng., Symp. Ser. No.150, V.71, pp.165-175.

Finkelstein, N.P. and Poling, G.W., 1977. "The Role of Dithiolates in the Flotation of Sulphide Minerals", *Miner. Sci. Eng.*, V.9, No.4, 177-197

Fornasiero, D., Fairthorne, G. and Ralston, J., 1996. The Interaction of Butyl Ethoxycarbonyl Thiourea with Sulphide Minerals", Proc. Int. Symp. on Electrochemistry in Mineral and Metal Processing, Woods, R., Doyle, F. and Richardson, P.R. (Eds.), The Electrochemical Society, Inc., Pennington, NJ, pp. 61-71.

Forssberg, K.S.E., Antii, B. and Palsson, B.I., 1984. "Computer-assisted calculations of thermodynamic equilibria in the chalcopyrite-ethyl xanthate system", Reagents in the Mineral Industry, Institute of Mining and Metallurgy, London, pp.251-264.

Fuerstenau, D.W., 1980. "Thermodynamics of Sulfide Mineral Flotation Systems", US Bureau of Mines Information Circular, 8818, pp.35-61.

Fuerstenau, M.C., 1980. "Thiol Collector Adsorption Processes", US Bureau of Mines Information Circular, 8818, pp.7-23.

Fuerstenau, D.W., 1999. "The Froth Flotation Century", Advances in Flotation Technology, Proceedings of a Symposium Held at the Annual SME Meeting, Parekh, B.K. and Miller, J.D. (Eds.), March 1-3, Society for Mining, Metallurgy, and Exploration, Inc., Denver, Colorado, pp.3-21.

Fuerstenau, M.C., 1999. "Froth Flotation: The First Ninety Years", Advances in Flotation Technology, Proceedings of a Symposium Held at the Annual SME Meeting, Parekh, B.K. and Miller, J.D. (Eds.), March 1-3, Society for Mining, Metallurgy, and Exploration, Inc., Denver, Colorado, pp. xi-xxxiii.

Fuerstenau, D.W. and Hanson, J.S., 1991. "The electrochemical and flotation behaviour of chalcocite and mixed oxide/sulphide ores", *Int. J. Miner., Process.*, V.33, pp.33-47.

Fuerstenau, D.W., Herrera-Urbina, R. and McGlashan, D.W., 2000. "Studies on the applicability of chelating agents as universal collectors for copper minerals", *Int. J. Miner. Process.*, V.58, pp.15-33.

Fuerstenau, M.C., Huiatt, J.L. and Kuhn, M.C., 1971. "Dithiophosphate vs. xanthate flotation of chalcocite and pyrite", *Trans SME/AIME*, V.250, pp.227-231.

Fuerstenau, M.C., Kuhn, M.C. and Elgillani, D.A., 1968. "The role of dixanthogen in xanthate flotation of pyrite", *Trans. SME/AIME*, V.241, pp.148.

Fuerstenau, D.W., Metzger, P.H. and Seele, G.D., 1957. "How to Use This Modified Hallimond Tube for Better Flotation Testing", *Eng. Min. J.*, V.158, No.3, pp.93-95.

Fuerstenau, D.W. and Pradip, 1984. "Mineral flotation with hydroxamate collectors", Reagents in the Mineral Industry, Jones, M.J. and Oblatt, R. (Eds.), The Institute of Mining and Metallurgy, London, pp.161-168.

Gardner, J.R. and Woods, R., 1977. "An electrochemical investigation of contact angle and of flotation in the presence of alkyl xanthates II: Galena and pyrite surfaces", *Aust. J. Chem.*, V.30, pp.981-991.

Gardner, J.R. and Woods, R., 1979. "An electrochemical investigation of the natural floatability of chalcopyrite", *Int. J. Miner. Process.*, Vol. 6, pp. 1-16.

Garrels, R.M. and Christ. C.L., 1965. Solutions, Minerals and Equilibria, Harper and Row, New York, 450 p.

Gaudin, A.M., 1927. Flotation Mechanism: A Discussion of the Functions of Flotation Reagents, AIME Technical Publication, No. 4, 27 p.

Gaudin, A.M., 1974. "The Role of Oxygen in Flotation", *J. Colloids Interf. Sci.*, Vol. 47, No. 2, pp. 309-314.

Gaudin, A.M., Dewey, F., Duncan, W.E., Johnson, R.A. and Tangel, Jr.D.F., 1934. "Reactions of Xanthate with Sulphide Minerals", *Trans. SME/AIME*, Vol.112, pp.319-347.

Gebhardt, J.E. and Shedd, K.B., 1988. "Effect of Solution Composition on Redox Potentials of Platinum and Sulphide Mineral Electrodes", Proc. Symp. on Electrochemistry in Mineral and Metal Processing II, Richardson, P.E. and Woods, R. (Eds.), The Electrochemical Society, Atlanta, May 15-20, pp. 84-100.

Giesekke, E.W., 1983. "A Review of Spectroscopic Techniques Applied to the Study of Interactions between Minerals and Reagents in Flotation Systems", *Int. J. Miner. Process.*, V.11, pp.19-56.

Gómez, C., Figueroa, M., Muñoz, J., Blázquez, M.L. and Ballester, A., 1996. "Electrochemistry of Chalcopyrite", *Hydrometallurgy*, V. 43, pp. 331-344

Goold, L.A. and Finkelstein, N.P., 1972. The reaction of sulphide minerals with thiol compounds, National Institute for Metallurgy, Report No. 1439, 9 p.

Gorken, A., Nagaraj, D.R. Riccio, P., 1992. "The role of pulp redox potentials and modifiers in complex sulphide flotation with dithiophosphinates", Proc. Int. Symp. on Electrochemistry in Mineral and Metal Processing III, Woods, R. and Richardson, P.E. (Eds.), The Electrochemical Society, Inc., Pennington, pp.17.

Grano, S.R, Cnossen, H., Skinner, W., Prestidge, C.A. and Ralston, J., 1997a. "Surface modifications in the chalcopyrite-sulphite ion system II: Dithiophosphate collector adsorption study", *Int. J. Miner. Process.*, V.50, pp.27-45.

Grano, S.R., Sollaart, M., Skinner, W., Prestidge, C.A. and Ralston, J., 1997b. "Surface modifications in the chalcopyrite-sulphite ion system. I. Collectorless flotation, XPS and dissolution study", *Int. J. Miner. Process.*, V.50, pp.1-26.

Griffin, L., Johnson, N.W., Koch, D.F.A., Ramprakash, Y. and Woods, R., 1992. "Voltammetric Determination of Surface Species on Sulphide Minerals in Flotation Pulps", Proc. of the Third Int. Symp. on Electrochemistry in Mineral and Metal Processing III, Woods, R. and Richardson P.E. (Eds.), The Electrochemical Society, Inc., USA, pp. 159-167.

Hamilton, I.C. and Woods, R., 1981. "An investigation go surface oxidation of pyrite and pyrrhotite by linear sweep voltammetry", *J. Electroanal. Chem.*, V.118, pp.327-343.

Hamilton, I.C. and Woods, R., 1984. "A Voltammetric Study of the Surface Oxidation of Sulphide Minerals", Proceedings of International Symposium on Electrochemistry in Mineral and Metal Processing, Richardson, P.R., Srinivasan, S.S. and Woods, R. (Eds.), The Electrochemical Society, Inc., Pennington, NJ, pp. 259-285.

Hayes and Ralston, 1988. "The Collectorless Flotation and Separation of Sulphide Minerals by Eh Control", *Int. J. Miner. Process.*, Vol. 23, pp. 55-84.

Hepel, T. and Pomianowski, A., 1977. "Diagrams of Electrochemical Equilibria of the System Copper-KEX-Water at 25 °C", *Int. J. Miner. Process.* V.4, pp.345-361.

Heyes, G.W. and Trahar, 1977. "Natural Floatability of Chalcopyrite", *Int. J. Miner. Process.*, Vol. 4, pp. 317-344

Hiçyılmaz, C., Ekmekçi, Z., Gökağaç, G. and Altun, N.E., 2001. Fosfin Türü Kollektörlerin Pirit ile Etkileşiminin Elektrokimyasal Olarak İncelenmesi, Orta Doğu Teknik Üniversitesi Araştırma Fonu Projesi, AFP No. 2000-03-05-01, Ankara, 35 p.

Hill, A.C., 1969. *J. Sci. Food. Agric.*, V.20, p.4.

Hochstetler, S.E. and Wightman, R.M., 1998. "Detection of Secretion with Electrochemical Methods", Electrophysiology, French, R.J. (Ed.), Biophysical Society, Bethesda, MD, pp. 1-49.

Janetski, N.D., Woodburn, S.I. and Woods, R., 1977. "An electrochemical investigation of pyrite flotation and depression", Int. J. Miner. Proc., V.4, pp.227-239.

Jones, M.H. and Woodcock, J.T., 1978a. "Evaluation of Ion-Selective Electrode for Control of Sodium Sulphide Additions During Laboratory Flotation of Oxidised Ores", *Trans. IMM*, Vol. 87, pp. C99-C106.

Jones, M.H. and Woodcock, J.T., 1978b. "Optimisation and Control of Laboratory Sulphidisation of Oxidised Copper Ores with an Ion-Selective Electrode", Proceedings of the Australasian Institute for Mining and Metallurgy, No. 266, pp. 11-19.

Jones, M.H. and Woodcock, J.T., 1979. "Control of Laboratory Sulphidisation with a Sulphide Ion Selective Electrode before Flotation of Oxidised Lead-Zinc-Silver Dump Material", *Int. J. Miner. Process.*, Vol. 6, pp. 17-30.

Kakovskii, I.A. and Arashkevich, V.M., 1968. "The Study of the Properties of Organic Disulfides", VIII. International Mineral Processing Congress, Leningrad, pp.1-10.

Kakovskii, I.A., Stepanov, B.A., Ryazantseva, O.F. and Serebryakova, N.V., 1959. "The redox potentials of dithiophosphates", Russian J. Physical Chem., V.33, No.8, pp.178-183.

Kelsall, G.H., England, K.E.R., Vaughan, D.J. and Yin, Q., 1992. "Electrochemical Oxidation of Chalcopyrite in Alkaline Solutions", Proc.Third Int. Symp. on Electrochemistry in Mineral and Metal Processing III, Woods, R. and Richardson, P.E. (Eds.), The Electrochemical Society, Inc., pp.318-341.

Kim, D.S., 1995. "Studies on the interaction of alkyl thiophosphinate with precious metals", *Bull. Korean Chem. Soc.*, Vol. 16, No. 4, pp. 321-325.

Klauber, C., Parker, A., van Bronswijk, W. and Watling, H., 2001. "Sulphur speciation of leached chalcopyrite surfaces as determined by X-ray photoelectron spectroscopy", *Int. J. Miner. Process.*, Vol. 62, pp. 65-94.

Klimpel, R.R., 1999. "A Review of Sulfide Mineral Collector Practice", Advances in Flotation Technique, Parekh, B.K. and Miller, J.D. (Eds.), Proceedings of a Symposium Held at the Annual SME Meeting, March 1-3, Denver, Colorado, USA, pp.115-127.

Kocabağ, D., 1983. The Oleophilicity/Hydrophobicity of Galena and Pyrite in Two-Liquid Flotation, Ph.D. Thesis, Department of Mineral Resources Engineering, University of London, 212 p.

Kocabağ, D., 1992. "Sülfür Cevherlerinin Flotasyonu 1: Sülfür Minerallerinin Özellikleri ve Flotasyona Etkileri", *Madencilik*, Vol. 31, No. 3, pp. 33-49.

Kocabağ, D., 1994. "Redox Effects on the Flotation of Sulphide Minerals", Progress in Mineral Processing Technology, Demirel, H. and Ersayın, S. (Eds.), Balkema, Rotterdam, pp.105-111.

Kocabağ, D. and Smith, M., 1989. "Kalkopiritin Kollektörsüz Flotasyonunun İki Sıvı Flotasyonu ile İncelenmesi: Öğütme Ortamı ve pH'nın Etkisi", Türkiye Madencilik Bilimsel ve Teknik 11. Kongresi, TMMOB Maden Mühendisleri Odası Yayını, Ankara, pp.433-447.

Kounaves, P.S., 1997. "Voltammetric Techniques", Handbook of Instrumental Techniques for Analytical Chemistry, Settle, F.A. (Ed.), Prentice Hall, Virginia, pp. 709-725.

Kowal, A. and Pomianowski, A., 1973. "Cyclic Voltammetry of Ethyl Xanthate on a Natural Copper Sulphide Electrode", *Electroanal. Chem. Interf. Electrochem.*, Vol. 46, pp.411-420.

Laajalehto, K., Kartio, I. And Suoninen, E., 1997. "XPS and SR-XPS Techniques Applied to Sulphide Mineral Surfaces", *Int. J. Miner. Process.*, V.51, pp.163-170.

Labonté, G. and Finch, J.A., 1990. "Behaviour of Redox Electrodes during Flotation and Relationship to Mineral Flotabilities", *Minerals Metall. Process.*, pp.106-109.

Latimer, W.M., 1952. The Oxidation States of the Elements and their Potentials in Aqueous Solutions, Prentice Hall, Inc., New York, Second Edition, 395 p.

Lázaro, I., Martínez-Medina, N., Rodríguez, I., Arce, E. and González, I., 1995. "The use of carbon paste electrodes with non-conducting binder for the study of minerals: Chalcopyrite", *Hydrometallurgy*, V. 38, pp. 277-287.

Leja, J, 1982. Surface Chemistry of Froth Flotation, Plenum Press, New York, 758 p.

Leppinen, J., 1991. FTIR and Flotation Investigations of Adsorption of Diethydithiophosphate on Sulfide Minerals, Technical Research Centre of Finland, Research Report No:726, 23 p.

Leppinen, J., Basilio, C.I. and Yoon, R.-H., 1988. "Spectroelectrochemical study of ethyl xanthate adsorption on sulphide minerals", Proc. Int. Symp. on Electrochemistry in Mineral and Metal Processing II, Richardson, P.E. and Woods, R. (Eds.), The Electrochemical Society, Inc., Pennington, pp.49-65.

Linge, H.G., 1976. "A study of chalcopyrite dissolution in acid ferric nitrate by potentiometric titration", *Hydrometallurgy*, V.2, pp.51-64.

Luttrell, G.H. and Yoon, R.-H., 1984a. "Surface Studies of the Collectorless Flotation of Chalcopyrite", *Colloids Surf.*, pp. Vol. 12, pp. 239-254.

Luttrell, G.H. and Yoon, R.-H., 1984b. The Collectorless Flotation of Chalcopyrite Ores Using Sodium Sulfide", Int.J.Min.Proc., V.13, pp.271-283.

Maege, I., Jaenhne, E., Henke, A., Adler, H.-J.P., Bram, C., Jung, C. and Stratmann, M., 1998. "Self-Assembling Adhesion Promoters for Corrosion Resistant Metal Polymer Interfaces", *Progress in Organic Coatings*, V.34, pp.1-12.

Majima, H. and Takeda, M., 1968. "Electrochemical studies of the xanthate-dixanthogen system on pyrite", *Trans. SME/AIME*, V.241, pp.431-436.

Malghan, S.G., 1986. "Role of Sodium Sulphide in the Flotation of Oxidised Copper, Lead, and Zinc Ores", *Minerals Metall. Process.*, Vol. 3, pp. 158-163.

Marabini, A.M., Contini, G. and Cozza, C., 1993. "Surface spectroscopic techniques applied to the study of mineral processing", *Int. J. Miner. Process.*, V.38, pp.1-20.

Marabini, A.M. and Cozza, C., 1988. "A new technique for determining mineral-reagent chemical interaction products by transmission IR spectroscopy: Cerussite-xanthate system", *Colloids Surf.*, V.33, pp.35-41.

Maslovsky, E.Jr., 1977. Vibrational Spectra of Organometallic Compounds, John Wiley and Sons, New York, 528 p.

Matabishi, M.K., Handfield-Jones, R. and Akdoğan, G., 2000. "Effect of Electrochemical Environment on Collectorless Flotation of Some Sulphide Minerals", Mineral Processing on the Verge of the 21st Century, Proceedings of the 8th International Mineral Processing Symposium, Özbayoğlu, G., Hoşten, Ç., Atalay, M.Ü., Hiçyılmaz, C. and Arol, A.İ. (Eds.), 16-18 October, Antalya/Turkey, pp. 211-214.

Meloan, C.E., 1963. Elementary Infrared Spectroscopy, The Macmillan Company, New York, 193 p.

Mingione, P.A., 1990. "Use of AEROPHINE® 3418A Promoter for Sulphide Minerals Flotation" American Cyanamid Company, Paper No. 26, pp.485-508.

Nagaraj, D.R. and Avotnis, P.V., 1988. "Developments of new sulfide and precious metals collectors", Proceedings of the II International Mineral Processing Symposium, Aytekin, Y. (Ed.), İzmir, Turkey, pp.399-410.

Nagaraj, D.R. and Somasundaran, P., 1981. "Chelating agents as collector in flotation: Oximescopper minerals systems", *Min. Eng.*, V.33, No.9, pp.1351-1357.

Nakanishi, K. and Solomon, P.H., 1977. Infrared Absorption Spectroscopy, Holden-Day, Inc., San Francisco, USA, 287 p.

Natarajan, K.A. and Iwasaki, I., 1970. "Behaviour of Platinum Electrodes as Redox Potential Indicators in Some Systems of Metallurgical Interest", *Transactions SME/AIME*, Vol. 247, pp. 317-324.

Natarjan, K.A. and Iwaaasaki, I., 1972. "Eh-pH Response of Nobel Metal and Sulfide Mineral Electrodes", *Trans. SME/AIME*, Vol. 252, pp. 437-438.

Natarjan, K.A. and Iwaaasaki, I., 1973a. "Effects of Poisoning of Pt-Electrodes on Eh Measurements", *Trans. SME/AIME*, V.254, pp.22-28.

Natarjan, K.A. and Iwasaki, I., 1973b. "Practical Implications of Eh Measurements in Sulphide Flotation Circuits", *Trans. SME/AIME*, Vol. 254, pp. 323-328.

Natarjan, K.A. and Iwasaki, I., 1974. "Eh Measurements in Hydrometallurgical Systems", *Minerals Sci. Eng.*, Vol. 6, No. 1, pp. 35-44

Nicholson, R.S. and Shain, I., 1964. "Theory of stationary electrode polarography", *Anal. Chem.*, V.36, No.4, pp.706-723.

O'Dell, C.S., Dooley, R.K., Walker, G.W., Richardson, P.E., 1984. " Chemical and electrochemical reactions in the chalcocite-xanthate system", Proc. Int. Symp. Electrochemistry in Mineral and Metal Processing, Richardson, P.E., Srinivasan, S. and Woods, R. (Eds.), The Electrochem. Soc., Pennington, N.J., PV-10, pp.81-95.

O'Dell, C.S., Walker, G.W. and Richardson, P.E., 1986. "Electrochemistry of the chalcocite-xanthate system", *J. Appl. Electrochem.*, V.16, pp.544-554.

Palsson, B.I. and Forssberg, K.S.E., 1988. "Computer-assisted calculations of thermodynamic equilibria in the galena-ethyl xanthate system", *Int. J. Miner. Process.*, V.23, pp.93-121.

Palsson, B.I. and Forssberg, K.S.E., 1989. "Computer-assisted calculations of thermodynamic equilibria in sphalerite-ethyl xanthate system", *Int. J. Miner. Process.*, V.26, pp.223-258.

Pang, J. and Chander, S., 1990. "Oxidation and Wetting Behaviour of Chalcopyrite in the Absence and Presence of Xanthates", *Minerals Metall. Process.*, pp.149-155.

Pang, J. and Chander, S., 1993. "Properties of Surface Films on Chalcopyrite and Pyrite and Their Influences in Flotation", XVIII. International Mineral Processing Congress, Sydney, 23-28 May, pp.669-677.

Persson, P. and Malmensten, B., 1991. "Interactions between sulfide minerals and alkylxanthate ions, Part 5: A vibration spectroscopic study of the interactions between chalcocite, synthetic copper(I) sulfide, acanthite and synthetic silver(I) sulfide, and ethylxanthate ions in aqueous and acetone solutions", *Colloids Surf.*, V.59, pp.279-292.

Persson, I., Persson, P., Valli, M., Fözö, S. and Malmensten, B., 1991. "Reactions on Sulphide Mineral Surfaces in Connection with Xanthate Flotation Studied by Diffuse Reflectance FTIR Spectroscopy, Atomic Absorption Spectrophotometry and Calorimetry", *Int. J. Miner. Process.*, V.33, pp.67-81.

Peters, E., 1977. "Electrochemistry of sulphide minerals", Trends in Electro-Chemistry, Bockris, J.O'M., Rand, D.A.J. and Welch, B.J. (Eds.), Plenum Press, New York, N.Y., pp.167-290.

Peters, E., 1984. "Electrochemical mechanism for decomposing sulphide minerals", Proc. Int. Symp. on Electrochemistry in Mineral and Metal Processing, Richardson, P.E., Srinivasan, S. and Woods, R. (Eds.), The Electrochemical Society, Pennington, N.J., V.10, pp.343-361.

Piantadosi, C., Jasieniak, M., Skinner, W.M. and Smart, R.St.C., 2000. "Statistical comparison of surface species in flotation concentrates and tails from TOF-SIMS evidence", *Minerals Eng.*, Vol. 13, No. 13, pp. 1377-1394.

Plaksin, I.N., Shafeyev, R.S. and Chanturia, V.A., 1968. "Relation between Energy Structure of Mineral Crystals and Their Flotation Properties", Proceedings of 8th International Mineral Processing Congress, Leningrad, pp. 1-8.

Pouchert, C.J., 1981. The Aldrich Library of Infrared Spectra, Aldrich Chemical Company, Inc., Wisconsin, USA, Third Edition, 1873 p.

Pourbaix, M., 1963. Atlas of Electrochemical Equilibria, Gauthiers-Villars, Paris.

Pritzker, M.D. and Yoon, R.-H., 1984 ."Thermodynamic Calculations on Sulfide Flotation Systems, I. Galena-Ethyl Xanthate System in the Absence of Metastable Species", *Int. J. Miner. Process.*, V. 12, pp. 95-125.

Pritzker, M.D. and Yoon, R.-H., 1987. "Thermodynamic Calculations on Sulfide Flotation Systems, II. Comparisons with Electochemical Experiments on the Galena-Ethyl Xanthate System", *Int. J. Miner. Process.*, V. 20, pp. 267-290.

Pritzker, M.D., Yoon, R.H., Basilio, C. and Choi, W.Z., 1985. "Solution and Flotation Chemistry of Sulfide Minerals", *Canadian Metall. Quarterly*, Vol.24, No.1, pp27-38

Ralston, J., 1991. "Eh and its Consequences in Sulphide Mineral Flotation", *Minerals Eng.*, Vol. 4, No. 7-11, pp. 859-878.

Rand, D.A.J. and Woods, R., 1984. "Eh Measurement in Sulphide Mineral Slurries", *Int. J. Miner. Process.*, Vol. 13, pp. 29-42.

Rao, S.R., Labonté, G. and Finch, J.A., 1992. "Electrochemistry in the Plant", Innovations in Flotation Technology, Mavros, P. and Matis, K.A. (Eds.), Kluwer Academic, pp. 203-223.

Ravitz, S.F. and Porter, R.R., 1933. Oxygen Free Flotation I: Flotation of Galena in Absence of Oxygen, AIME Technical Publication, No: 513, USA, 17 p.

Richardson, P.E. and O'Dell, C.S., 1985. "Semiconducting characteristics of galena electrodes: Relationship to mineral flotation", *J. Electrochem. Soc.*, V.132, pp.1350-1356.

Richardson, P.E., Stout, J.V., Proctor, C.L. and Walker, G.W., 1984. "Electrochemical flotation of sulphides: chalcocite-ethyl xanthate interactions", *Int. J. Miner. Process.*, V.12, pp.73-93.

Rickelton, W.A., 1998. "The removal of cadmium impurities from cobalt-nickel solutions by precipitation with sodium diisobutyldithiophosphinate", *Hydrometallurgy*, V.50, pp.339-344.

Rogers, J., 1962. "Principles of Sulfide Mineral Flotation", Froth Flotation: 50th Anniversary Volume, Fuerstenau, D.W. (Ed.), The American Institute of Mining, Metallurgical, and Petroleum Engineers, Inc., New York, pp.139-169.

Rudzinski, W., Echegoyen, L. and Jobin, J., 1980. *J. Agric. Food Chem.*, V.28, p.469.

Ruonala, M., Heimala, S. and Jounela, S., 1997. "Different Aspects of Using Electochemical Potential Measurement in Mineral Processing", *Int. J. Miner. Process.*, V.51, pp.97-110.

Salamy, S.G. and Nixon, J.C., 1953. "The application of electrochemical methods to flotation research", Recent Developments in Mineral Dressing, Institute of Mining and Metallurgy, London, pp.503-516.

Sato, M., 1960."Oxidation of Sulphide Ore Bodies II: Oxidation Mechanisms of Sulphide Minerals at 25°C", *Econ. Geo.*, Vol. 55, pp. 1202-1231.

Senior, G.D. and Trahar, W.J., 1991. "The influence of metal hydroxides and collector on the flotation of chalcopyrite", *Int. J. Miner. Process.*, V.33, pp.321-341.

Shishkov, A.N., and Nikolov, N.K., 1972. "Infrared spectra of some bis(dialkoxy- and diaryloxyphosphino-thioyl) disulfides", *Nauch. Tr., Plovdivski Univ., Mat., Fiz., Khim., Biol.*, V.10, No.3, pp.87-95.

Shubov, L.Ya., Zalesnik, I.B. and Mitrofanov, S.I., 1976. "Mechanism of hydrophobization of chalcopyrite during the flotation with dithiophosphates", *Tsvetn. Met.*, V.4, pp.82-86.

Smith, F.G., 1942. "Variations in the Properties of Pyrite", *American Miner. J., Miner. Soc. America*, Vol. 27, No. 1, pp. 1-19.

Sturrock, P.E. and Barringer, G.E., 1998. "Supersensitive Analytical Detection by Voltammetry", *American Lab.*, pp.21-24.

Suoninen, E., Laajalehto, K., Kartio, I., Heimala, S. and Jounela, S., 1992. "Surface layer structure of sulfide mineral treated in thiol collector solutions", Proc. The Third Int. Symp. on Electrochemistry in Mineral and Metal Processing III, Woods, R. and Richardson, P.E. (Eds.), pp.259-268.

Sutherland, K.L. and Wark, I.W., 1955. Principles of Flotation, Australasian Institute of Mining and Metallurgy, Melbourne, 489 p.

Taggart, A.F., Taylor, T.C. and Knoll, A.F., 1930. "Chemical Reactions in Flotation", *Trans. SME/AIME*, Vol. 87, pp. 217-260.

Talonen, P., Rastas, J. and Lepinen, J.O., 1991. "In situ FTIR study of ethyl xanthate on gold, silver and copper electrodes under controlled potential", *Surf. Interface Anal.*, V.17, pp.669-674.

Termes, S.C. and Richardson, P.E., 1996. "Application of FT-IR spectroscopy for in situ studies of sphalerite with aqueous solutions of potassium ethylxanthate and with diethyldixanthogen", *Int. J. Miner. Process.*, V.18, pp.167-178.

ThermoNicolet, 2002. NICOLET'S Introduction to FT-IR, ThermoNicolet Instrument Corporation, Inc., http://www.thermo.com/eThermo/CMA/PDFs/ Articles/articlesFiles_12268.pdf, 7 p.

Thomas, M.T., Peterson, D.A., Hartley, J.N. and Freeman, H.D., 1982. "Application of Surface Spectroscopies to Interfacial Problems in Mineral Processing", Interfacial Phenomena in Mineral Processing, Yarar, B. and Spattiswood, D.S. (Eds.), Engineering Foundation, pp.33-61.

Tipman, R.N. and Leja, J., 1975. "Reactivity of xanthate and dixanthogen in aqueous solutions of different pH", *Colloid Polym. Sci.*, V.253, No.1, pp.4-10.

Tolun, R., 1987. "Chemistry of Sulphide Mineral Flotation", Mineral Processing Design, Yarar, B. and Dogan, Z.M. (Eds.), NATO ASI Series, Series E: Applied Sciences-No.122, Martinus Nijhoff Publishers, Boston, pp.37-75.

Trahar, W.J., 1983. "A Laboratory Study of the Influence of Sodium Sulphide and Oxygen on the Collectorless Flotation of Chalcopyrite", *Int. J. Miner. Process.*, Vol. 11, pp. 57-74.

Trahar, W.J., 1984. "The Influence of Pulp Potential in Sulphide Flotation", Principles of Mineral Flotation, The Wark Symposium, Jones, M.H. and Woodcock, J.T. (Eds.), The Australasian Institute of Mining and Metallurgy, Victoria, Australia, pp.117-135.

Valli, M., Manlmensten, B. and Persson I., 1994. "A Vibrational Spectroscopic Study of the Interaction between some Sulphide Minerals and O,O-Diethyl Dithiophosphate Ions in Aqueous Solution", *Colloids Surf. A*, Vol. 83, pp. 227-236.

Van der Maas, J.H., 1972. Basic Infrared Spectroscopy, Heyden and Son Ltd., London, Second Edition, 110 p.

Wadsworth, M.E., 1972. "Advances in the leaching of sulphide minerals", *Min. Sci. Eng.*, V.4, No.4, pp.36-47.

Wang, X., Forssberg, K.S.E. and Bolin, N.J., 1989. "Thermodynamic calculations on iron-containing sulphide mineral flotation systems, I. The stability of iron-xanthate", *Int. J. Miner. Process.*, V.27, pp.1-19.

Wark, I.W., 1938. Principles of Flotation, Australasian Institute of Mining and Metallurgy, Melbourne, 346 p.

Wark, I.W. and Cox, A.B., 1934. "Principles of Flotation I: An Experimental Study of the Effect of Xanthates on Contact Angles at Mineral Surfaces", *Trans. SME/AIME*, Vol.112, pp. 189-244.

Winer, G. and Woods, R., 1973. "The relation of collector redox potential to flotation efficiency: Monothiocarbonates", *Sep. Sci.*, V.8, No.2, pp.261-267.

Woods, R., 1971. "The Oxidation of Ethyl Xanthate on Platinum, Gold, Copper, and Galena Electrodes: Relation to the Mechanism of Mineral Flotation", *J. Phy. Chem.*, Vol. 75, pp. 354-362.

Woods, R., 1984. "Electrochemistry of Sulphide Flotation", Principles of Mineral Flotation, The Wark Symposium, Jones, M.H. and Woodcock, J.T. (Eds.), The Australasian Institute of Mining and Metallurgy, Victoria, Australia, pp.91-115.

Woods, R., 1987. "Flotation of Sulphide Minerals", Reagents in Mineral Technology, Somasundaran, P. and Moudgil, B.M. (Eds.), Marcel Dekker, New York, NY, pp. 39-78.

Woods, R., 1996. "Chemisorption of thiols on metal and metal sulphides", Modern Aspects of Electrochemistry, Bockris, J.O'M., Conway, B.E. and White, R.E. (Eds.), Plenum Press, New York, No.29, pp. 401-453.

Woods, R., Basilio, C.I., Kim, D.S. and Yoon, R.-H., 1992. "Ethyl xanthate chemisorption isotherms and Eh-pH diagrams for the silver+water+ethyl xanthate system", *J. Electroanal. Chem.*, V.328, pp.179-194.

Woods, R., Chen, Z. and Yoon, R.-H., 1997. "Isotherms for the chemisorption of ethyl xanthate on lead", *Int. J. Miner. Process.*, V.50, pp.47-52.

Woods, R., Hope, G.A. and Watling, K., 2000. "Surface enhanced Raman scattering spectroscopic studies of the adsorption of flotation collectors", *Minerals Eng.*, V.13, No.4, pp.345-356.

Woods, R., Kim, D.S., Basilio, C.I. and Yoon, R.-H., 1995. "A Spectroscopic Study of Chemisorption of Ethyl Xanthate on Gold", *Colloids Surf. A*, V.94, pp.67-74.

Woods, R., Young, C.A. and Yoon, R.H., 1990. "Ethyl Xanthate Chemisorption Isotherms and Eh-pH Diagrams for the Copper/Water/Xanthate and Chalcocite/Water/Xanthate Systems", *Int. J. Miner. Procc.*, V.30, pp.17-33.

Yoon, R.-H., 1981. "Collectorless Flotation of Chalcopyrite and Sphalerite Ores Using Sodium Sulphide", *Int. J. Miner. Process.*, Vol. 8, pp. 31-48.

Yoon, R.-H. and Basilio, C.I., 1993. "Adsorption of Thiol Collectors on Sulphide Minerals and Precious Metals: A New Perspective", XVIII International Mineral Processing Congress, Sydney, 23-28 May, pp.611-617.

Yordanov, N.D., 1997. *Trans. Met. Chem.*, V.22, p.200.

Yordanov, N.D., Alexiev, V., Macicek, J., Glowiak, T. and Russell, D., 1983. *Transition Met. Chem.*, V.8, p.257.

Yordanov, N.D., Antov, L. and Grampp, G., 1998. "Stopped-flow spectrophotometric study on the reactions between copper(II) ions and some dithiophosphates", *Inorganic Chimica Acta*, V.272, pp.291-294.

Yordanov, N.D. and Ranguelova, K., 2001. "Effects of solute-coordinating solvent interactions and temperature on the EPR and electronic spectra of bis(dithiophosphato)copper(II)", *Spectrochimica Acta Part A*, 10 p.

Yordanov, N.D. and Velcheva, C.R., 1990. *Acad. Bulg. Sci.*, V.43, p.57.

Zachwieja, J.B., McCarron, J.J., Walker, G.W. and Buckley, A.N., 1989. "Correlation between the Surface Composition and Collectorless Flotation of Chalcopyrite", *J. Colloids Interf. Sci.*, Vol. 132, No. 2, pp. 462-468.

Zhang, Q., Rao., S.R. and Finch, J.A., 1993. "Basic studies on the bulk precipitates formed from iron salt and xanthate solutions", XVIII International Mineral Processing Congress, 23-28 May, Sydney, pp.979-983.

Zhou, R. and Chander, S., 1991. "Comparison of Gold, Platinum and Sulphide Ion Selective Electrodes as Sensor for Eh Measurement in Sulfide Solutions", *Minerals Metall. Process.*, pp.91-96.

APPENDICES

APPENDIX A

SCANNING ELECTRON MICROSCOPY RESULT

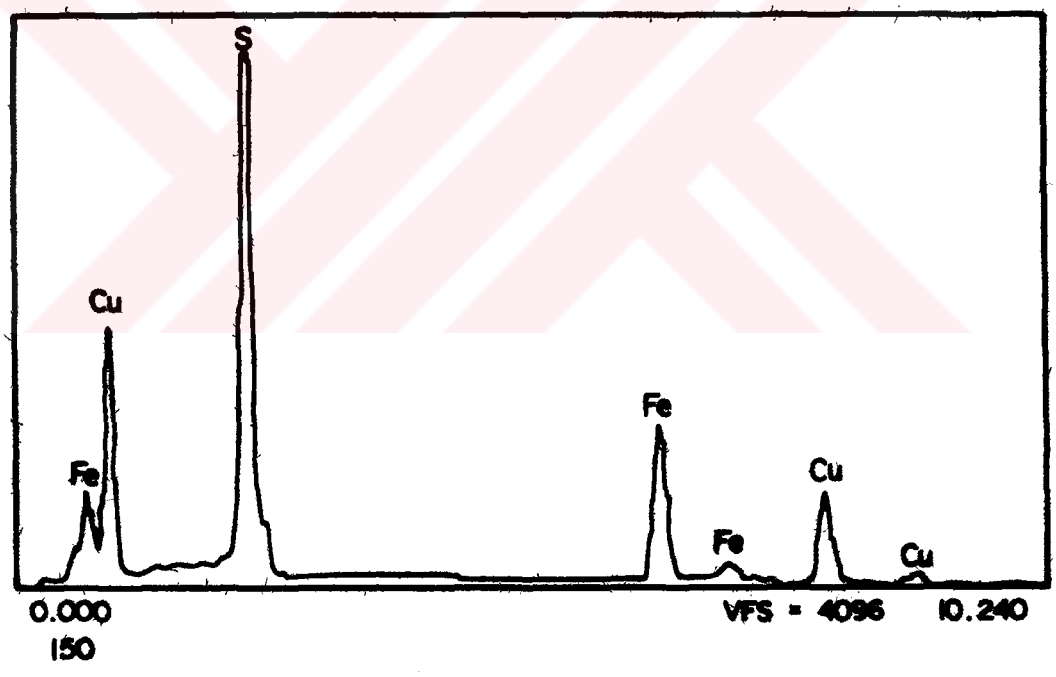

Figure A1. Scanning electron microscopy spectrum of highly mineralised chalcopyrite rock specimen

APPENDIX B

NUCLEAR MAGNETIC RESONANCE SPECTROSCOPY RESULTS

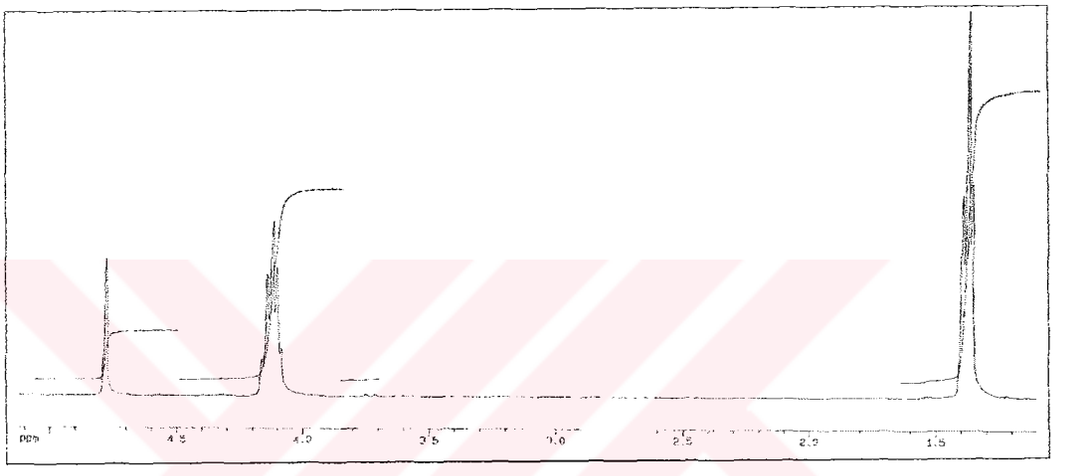

Figure B1. ^{1}H NMR spectrum of DTP (Solvent: Deuterated Water)

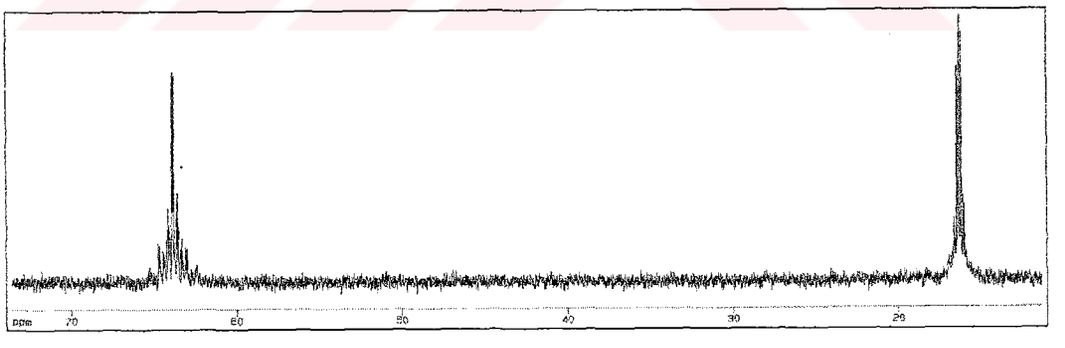

Figure B2. ^{14}C NMR spectrum of DTP (Solvent: Deuterated Water)

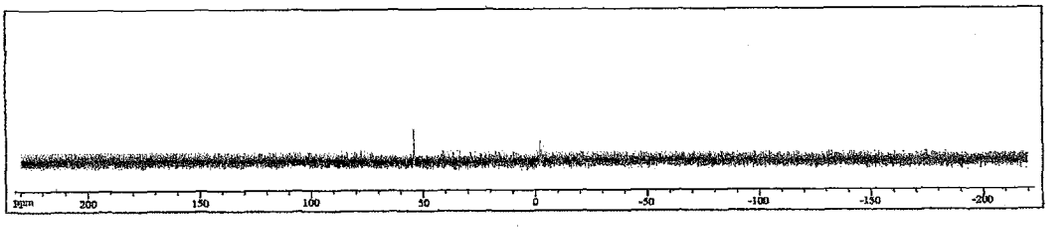

Figure B3. ^{31}P NMR spectrum of DTP (Solvent: Chloroform)

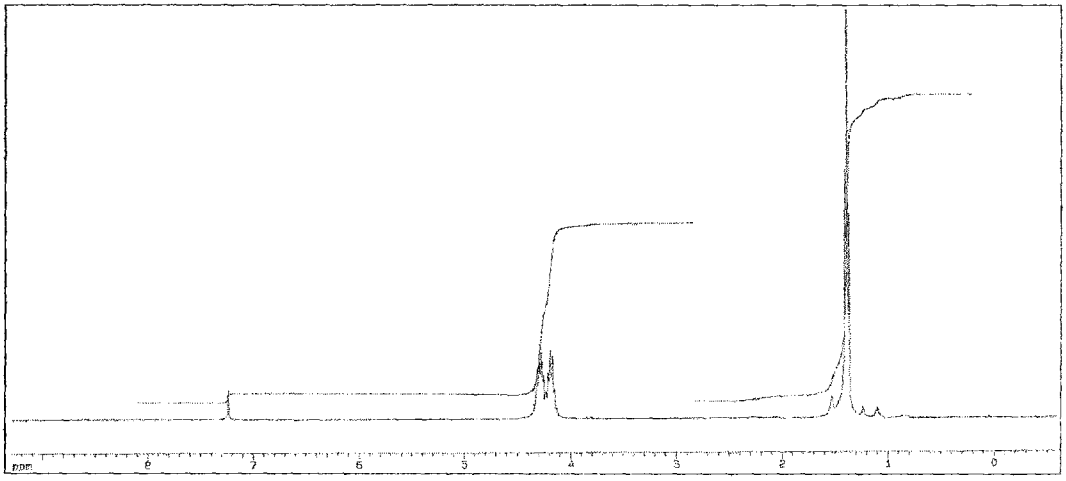

Figure B4. ^{1}H NMR spectrum of $(DTP)_2$ (Solvent: Chloroform)

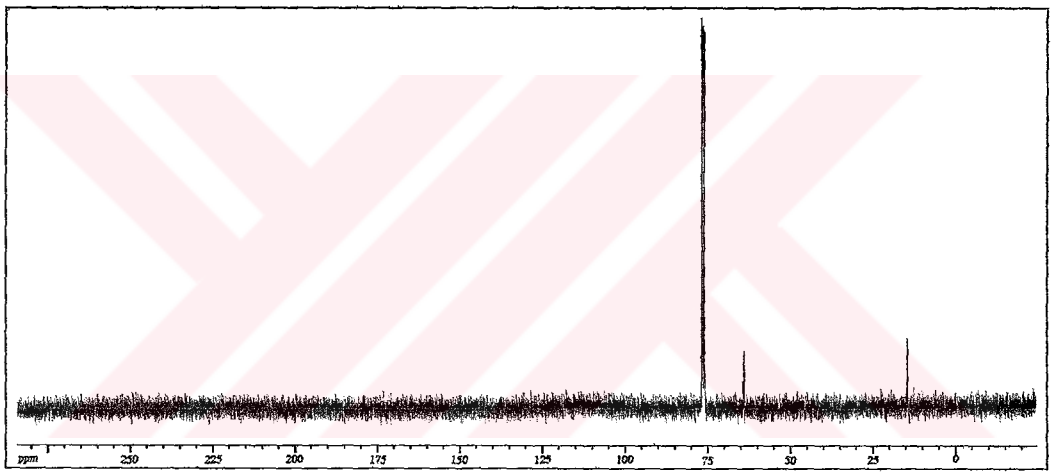

Figure B5. ^{14}C NMR spectrum of $(DTP)_2$ (Solvent: Chloroform)

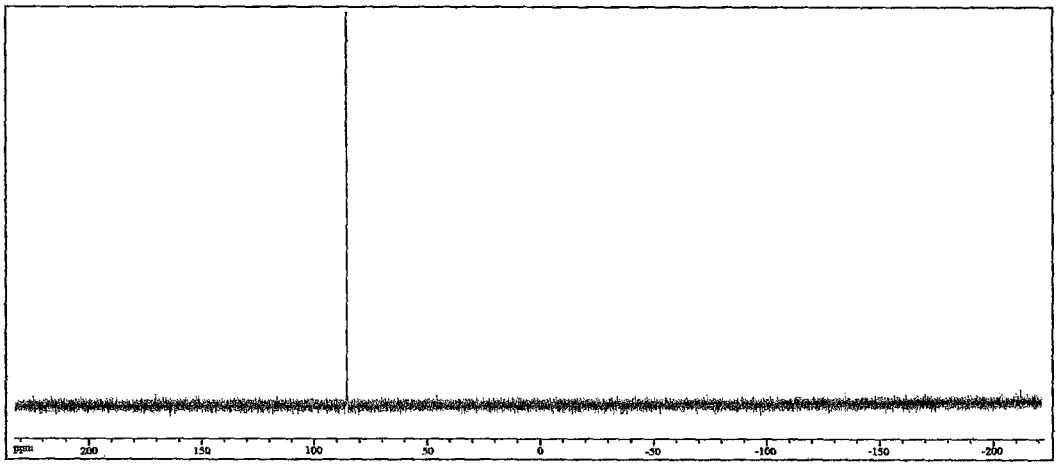

Figure B6. ^{31}P NMR spectrum of $(DTP)_2$ (Solvent: Chloroform)

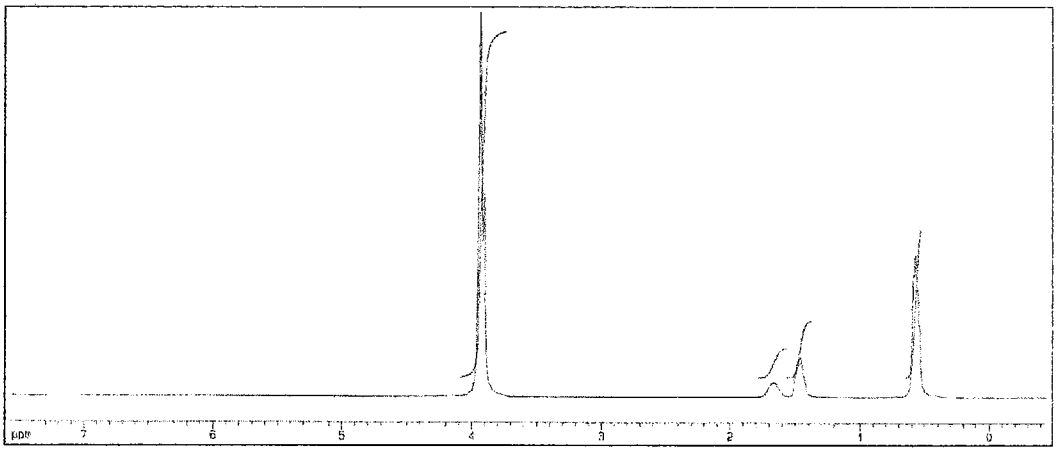

Figure B7. ^{1}H NMR spectrum of DTPI (Solvent: Chloroform)

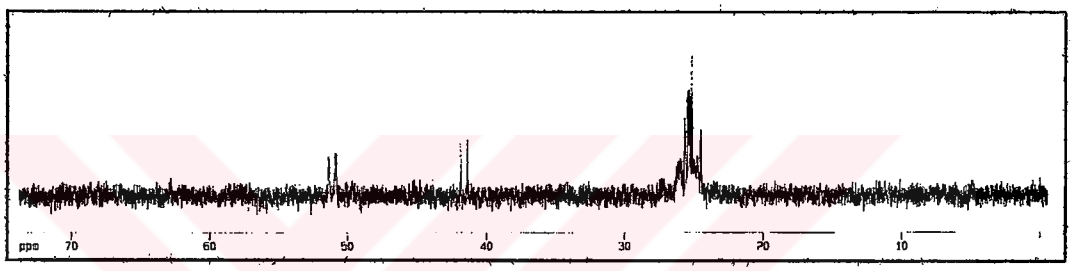

Figure B8. ^{14}C NMR spectrum of DTPI (Solvent: Chloroform)

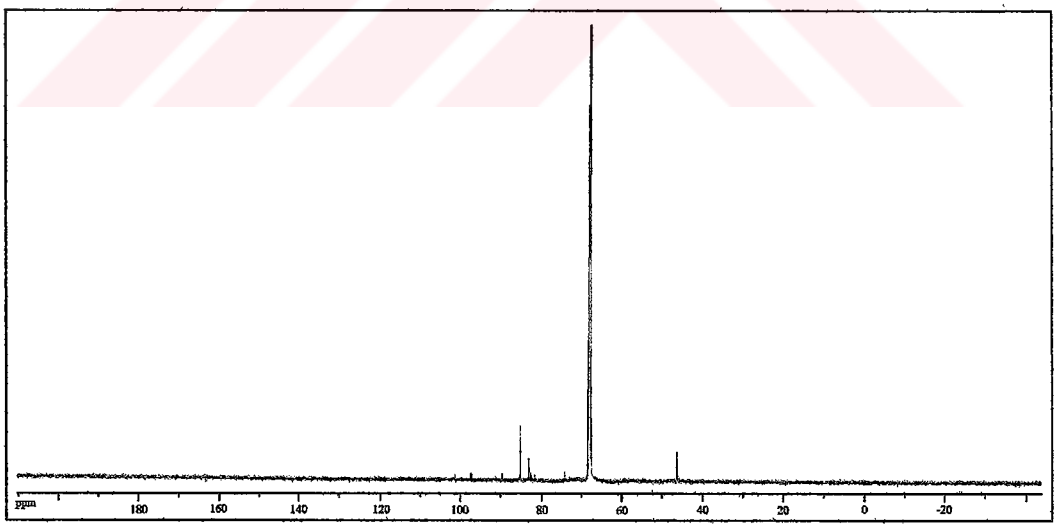

Figure B9. ^{31}P NMR spectrum of DTPI (Solvent: Chloroform)

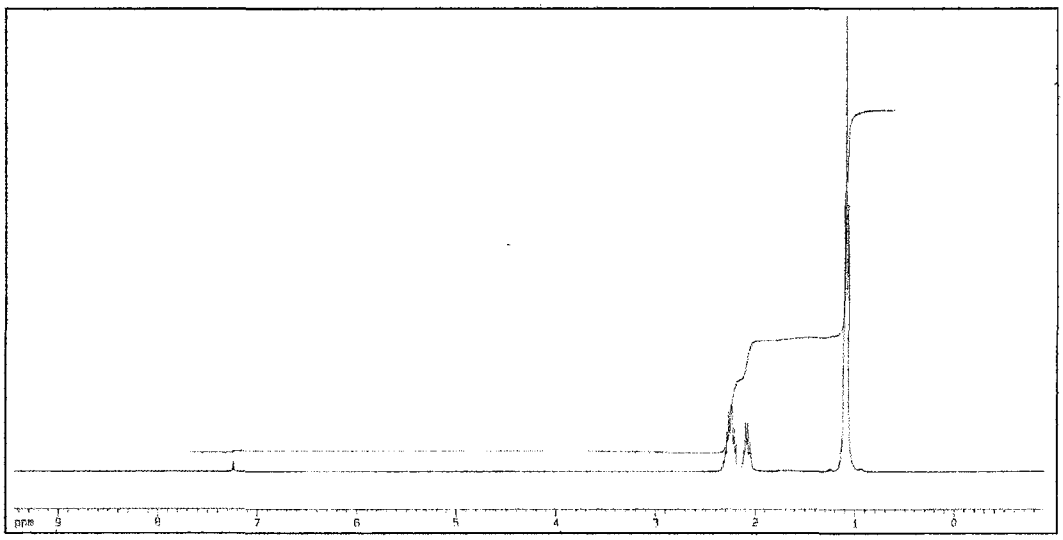

Figure B10. ^{1}H NMR spectrum of $(DTPI)_2$ (Solvent: Chloroform)

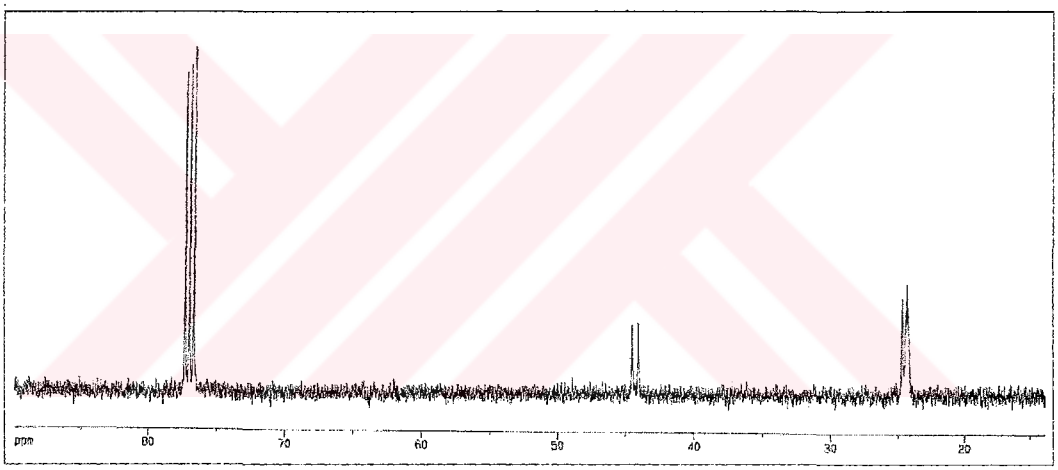

Figure B11. ^{14}C NMR spectrum of $(DTPI)_2$ (Solvent: Chloroform)

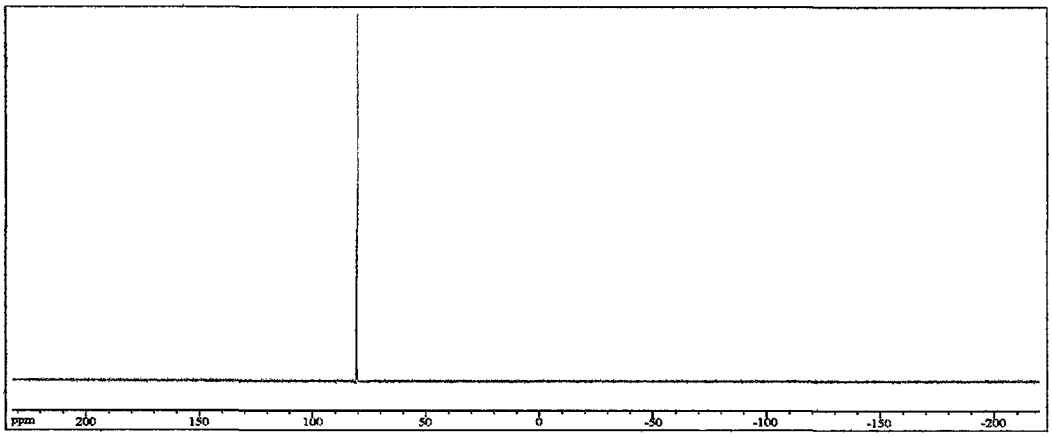

Figure B12. ^{31}P NMR spectrum of $(DTPI)_2$ (Solvent: Chloroform)

VITA

Taki GÜLER was born in Sivas on August 5, 1969. He received his B.S. and M.Sc. degrees from Mining Engineering Department of Middle East Technical University in July 1993 and July 1997. He worked in Cumhuriyet University Divriği Vocational School For Higher Education as an instructor from 1994 to February 2000. Then, he worked in Cumhuriyet University Metallurgical Engineering Department as a research assistant from February 2000 to November 2000. Since then, he has been working as a research assistant in Mining Engineering Department, Middle East Technical University.

He is a member of Chambers of Mining Engineers of Turkey and Mineral Processing Society. His research interests are flotation and electrochemistry of sulphide flotation. He has 4 paper written in English.